

RECEIVED
4/15/98

ORIGINAL



Final Report

**Remote Controlled Near Surface/Surface UXO
Detection System**

ESTCP Project Number 9525

March 1998

Contents

1. Assessment of the SAIC Remote Controlled Uxo Detection Project.
2. SAIC Final Report.
3. Yuma Proving Ground Test Record.

ASSESSMENT OF THE SAIC REMOTE CONTROLLED UXO DETECTION
PROJECT

NIGHT VISION ELECTRONIC SENSORS DIRECTORATE
MARCH 17, 1997

CONTENTS

1.0	Background.....
2.0	Purpose.....
3.0	Programmatics.....
3.1	Schedule.....
3.2	Funding.....
4.0	System Description.....
5.0	Test.....
5.1	Test Description.....
5.2	Test Results.....
6.0	Demonstration.....
6.1	Demonstration Description.....
6.2	Demonstration Results.....
7.0	Conclusions.....

1.0 Background. Unexploded ordnance (UXO) is one of the most serious and prevalent environmental problems at DoD facilities. This includes active sites and test ranges as well as Formerly Used Defense Sites (FUDS) and BRAC sites. Recent studies have shown that ordnance components are the second most frequently occurring contaminant at army sites and were reported at almost 20% of the 1100 army sites surveyed. This UXO must be detected, located, and removed in order to restore the locations to a safe condition, specifically at the near surface for future use to farm livestock or as a wildlife refuge. Current techniques for UXO remediation are very slow and labor intensive, involving hand held detectors and probes and the removal or detonation of munitions by individual EOD personnel. Some locations cannot be remediated by these techniques as the ubiquitous presence of UXO prevents human operators access to the sites. The system under development addresses the need to detect surface and near surface UXO. These munitions are either on the surface or covered up by twelve inches of soil, dust, or natural debris.

The Environmental Security Technology Certification Program (ESTCP) provided funds to NVESD for the development and demonstration of the Remote Controlled Surface/ Near Surface UXO Detector. This project incorporates three sensors into a remote controlled ground-based platform for the detection, location, and verification of surface and near surface UXO. The prime contractor is SAIC, San Diego, CA.

The UXO detector consists of a Schiebel metal detector array, a thermal neutron activation (TNA) sensor, and video cameras. The metal detector is used to detect and locate any amount of metal on or near the surface (within a 12 inch depth), and the TNA is used to confirm the detection of UXO by sensing the nitrogen content of the explosive in the UXO.

2.0 Purpose. The purpose of this project is to develop and demonstrate a system which can detect and confirm the presence of an explosive UXO in the surface/ near surface of soil. The ability to verify the presence of the explosive provides a unique advantage to the operator by reducing the number of interrogations of false alarms. Reducing the number of false alarms obviously leads to the reduction of time, cost, and frustration of the clearance crew. Also, the ability to remotely control the system reduces the opportunities for harm of the crew. Therefore, the system was fabricated, tested, improved, and demonstrated during the period of performance.

3.0 Programmatic. ESTCP provided funds to NVESD for the development and demonstration of the Remote Controlled Surface/ Near Surface UXO Detector. This project will incorporate three sensors into a remote controlled ground-based platform for the detection, location, and verification of surface and near surface UXO. The prime contractor is SAIC, San Diego, CA. The TNA is provided and supported by SAIC, Santa Clara, CA. The Institute for Defense Analyses (IDA) provided test planning and data analysis support.

Schedule. The contract to SAIC was awarded thru the Office of Special Technology (OST) and technically managed at the Night Vision Electronic Sensors Directorate

4.0 System Description. The Surface-Near Surface UXO Detector is a remotely controlled system for unexploded ordnance detection and verification. The system is comprised of the following subsystems.

Tele-Operated Vehicle. The vehicle chassis and remote control were supplied by Robotech of Calgary, Alberta, Canada. The Robotech vehicle is based on a Melroe Bobcat 773, which is diesel powered and uses skid steering. There are two degrees of freedom on the boom which supports the sensors, lifting and tilting. Both motions must be used in a coordinated way to correctly position the TNA sensor. All vehicle functions are controlled from a single operator using twin, dual axis, self-centering joysticks. These joysticks effect proportional control of vehicle speed/direction and boom lift/tilt operations.

Schiebel Metal Detector Array. The primary sensor is the one meter Schielbel coil induction array. The array has eight transmitting and receiving coils which are powered from an electronics unit housed in a standard 19" enclosure. This array is rigidly encased in fiberglass, and is operated flush to the ground. The resolution of the sensor is ten inches due to the coil spacing. The 12 bit digitized signal is recorded with respect to position using the encoder, compass, and GPS location information.

The operator is critical in the first step of discriminating between false alarms and potential detections. The operator determines if the response is a detection by inspecting the intensity of the signal and the shape of the response as well. Also, if the system has scanned a large area for the operator to select targets to investigate with the TNA, the operator will select a number of targets considering a preconceived density of targets, false alarms, and associated area size.

Thermal Neutron Activation Sensor. The system incorporates a thermal neutron activation (TNA) sensor as a secondary or confirmatory sensor to make definite target identification of the buried object that was triggered the Schielbel metal detector. The TNA sensor employs prompt gamma neutron activation in a single compact sensor with a single low intensity isotopic neutron source. The sensor detects nitrogen specific to high explosives. The configuration of the nuclear sensor assembly is made compact with a 20 microgram isotopic Cf-252 source and twelve NaI(Tl) gamma-ray detectors. The sensor weight is about 350 lbs. After the operator positions the TNA head over the suspicious spot on the ground, the sensor is activated and the signals are analyzed. Depending on the size of the target, the analysis may take from tow to fifteen minutes. The decision is made in real time by thresholding the average of the 8 detector outputs (Yuma test) or the average 12 detector outputs (Socorro test); post processing was also conducted by the logical "or" combination of these outputs with a threshold obtained from the average of the maximum three adjacent detectors.

Vision System. The visible camera, which is the primary camera for vehicle and sensor positioning, is a PANASONIC GP-US502 high resolution color camera. This camera features a 1/2" format and 3 CCDs to obtain a horizontal resolution if 700 TV lines. The

camera is mounted to a pan/tilt mechanism on the tele-robotic vehicle. The pan/tilt mechanism has the ability to slew at 15 deg/sec in both degrees of freedom with a 45 lb. payload.

Navigation System. The navigation system is comprised of a wheel encoder, a differential GPS, and a digital compass. The encoder is intended to provide short range accuracy (order of one inch). It allows one to display images of the metal detector signals and to control the motion of the vehicle in positioning the TNA over a detected target. The differential GPS is intended to provide long range accuracy (order of one meter or less). It allows one to display a symbol of the vehicle in a navigation window and to record the position of detected targets. This display of the trajectory of the vehicle in the navigation window, expanded to a proper scale, is useful to the operator in insuring complete coverage of the site. The stored measured vehicle locations can be curve fitted in post processing to provide better estimates of the vehicle path and to verify coverage of an area.

The differential GPS consists of an Ashtech Super C/A (Model SCA12) receiver, with 12 independent channels, and a DCI FM receiver which acquires and passes on to the Ashtech the differential corrections in RTCM format. The Ashtech unit is configured to make code-phase (not carrier-phase) measurements, and can provide latitude and longitude updates once every second. Communication between the Ashtech GPS and the on-board computer is by RS-232. In addition, the SCA-12 can provide other information that can be used to assess the accuracy of the measurements. Differential corrections must be supplied to the Ashtech GPS in RTCM 104 format. Another Ashtech receiver, placed at a known location, generates the differential corrections.

The digital compass (Model TCM2 by Precision Navigation, Inc.) provides the heading of the vehicle and is accurate to a tenth of a degree. The TCM2 combines a three-axis magnetometer and a two-axis tilt sensor. The tilt sensor allows the microprocessor in the compass to internally correct the compass indications for tilt. The digital compass is needed to plot the symbol of the vehicle in the correct orientation and is also used to calculate the coordinates of a detection (because the GPS antenna, of which latitude and longitude are determined, is not located at the same position as the detector, either Schiebel coil or TNA unit).

Target Marking. A target marking system is mounted on the translation stage which also supports the TNA. The system consists of an automated spray paint can which is remotely triggered by the operator when a target is located.

Operator Control Station. The operator control station for the system consists of two electronic enclosures and a remote control joystick box for vehicle control. One of these enclosures contains two RF video receivers, operating a 1720 MHz and 1810 MHz, and a standard video monitor used to display the standard video images. The second enclosure

contains the operator console consisting of a computer, RF data modem, color display, keyboard and mouse.

5.0 Test. The test of the UXO detection system occurred 17-23 June 1996. The purpose of the test was to assess its capability to detect unexploded ordnance typically found in the first foot of soil. Specifically, the system detection parameters were determined with respect to size and shape of target, orientation, explosive content of target, burial depth, and elapsed time of detection. The sensors were tested individually and in parallel; the system was not integrated at this point. The tests included blind tests, data collection, and other demonstrations designed to verify the robotic and verification capabilities of the detection system.

5.1 Test Description.

Test Site. The test site was located at the New Mexico Tech Energetic Materials Research and Testing Center in Socorro, NM. Two types of terrain were used for the test. One area was off road with uneven terrain. The second area was a smooth, unimproved road surface. Socorro, NM, has an arid environment with an average annual rainfall of 9.35 inches.

- a. A Calibration Test: where all information about the emplaced ordnance was released to the contractor.
- b. A Data Collection Test: where the contractor was given information about the location of the emplaced ordnance/ clutter, but not the depth, orientation, and type of target.
- c. A Blind Test: where the contractor was not given any information about the ordnance/ clutter present.

The blind test was designed to permit an objective evaluation by the government of the capabilities of different subsystems. Accordingly, the blind test, both in the one-dimensional lanes and in the two-dimensional field, consisted of two parts. Part A was carried out with the metal detector and robotic vehicle only (no TNA), and was conducted remotely. Its purpose was to localize and mark the metal detections as the targets were detected. Part B was carried out with the TNA module to test its verification capabilities on the detections found by the metal detector. Since the test in the two-dimensional field was significantly different due to the terrain and approach over the older one-dimensional lane mode of testing, the metal detector scanned the entire area first for part A, and the operator afterwards analyzed the map of metal detector returns and determined which spots to return to with the TNA for part B.

The data collection effort was designed to establish a controlled experiment to verify the blind test data. The results of the data collection was a file which provides data to determine detection limits vs. orientation, burial depth, explosive content, elapsed time, and type of target.

Calibration areas were setup with targets at each depth found in the test areas. The purpose of the calibration areas were for the contractor to familiarize themselves with the response of the system from the targets and with the background characteristics.

Target List. The targets were ordnance with the appropriate fuze or devices removed for safety reasons. The types of targets are representative of the size and amount of explosive of those targets found typically in the first foot of soil.

QTY	NAME	TYPE	EXPLOSIVE CONTENT	NITROGEN CONTENT	TYPICAL DEPTH
20	M56A3	20mm HE round	10.7 g H-761 plus 38.9 g propellant	(3.53 g)+	surface-3"
40	M789	30mm HEDP projectile	22 g Type PBXN-5	(7.26 g)	surface-3"
20	Simulant	Cylinder	100g C4	34 g	
20	Simulant	Cylinder	200g C4	68 g	
20	M49A5	60mm mortar	.79 lb. (359 g) Comp B	111.1 g	surface-12"
40	M393A2	105mm HEP-T projectile	4.4 lb. Comp B	1.34 lb. (609.3 g)	surface-12"

Table 1. Ordnance information

Clutter was buried in order to verify the TNA's ability to distinguish between actual UXO and metallic clutter; the test site was naturally free of metallic debris. The clutter was the above targets with no explosive inside the shell.

Each UXO type was buried at burial depths according to the Table 2. Burial depths were measured to the surface of the center of the ordnance item.

NAME	TYPE	BURIAL DEPTHS
M56A3	20mm HE round	flush, 1", 2", 3"
M789	30mm HEDP projectile	flush, 1", 3"
Simulant	100g simulant	flush, 2", 3", 6"
Simulant	200g simulant	2", 6", 12"
M49A5	60mm mortar	2", 6", 12"
M393A2	105mm HEP-T projectile	2", 6", 12"

Table 2. Ordnance burial depths

5.2 Test Results. The following table is the results from the blind tests collectively from lanes 1-7. "PD MD" was the probability of detection of the metal detector alone with the expectation of the metal detector to locate the target within 12". "PD TNA" is the probability of detection for the TNA alone and only considers the targets, which the metal detector detected as well as located close enough for the TNA to investigate, i.e. 6". The probability for the system was not included because the system was tested, by testing the individual sensors. Also, no false alarm data for the metal detector was included because the area was very pristine with no naturally occurring alarms. The PFA TNA was the false alarms calculated using the clutter objects, which were buried for this purpose.

TYPE	PD MD within 12"	PD TNA within 6"
20mm	11/11	1/4
30mm	11/11	4/7
100g	10/10	4/7
200S	11/11	1/6
60mm	9/9	0/7
105mm	18/18	5/8
OVERALL	70/70	15/39
PFA TNA	3/26	

6.0 Demonstration. The demonstration of the UXO detection system occurred 4-15 November 1996. The purpose of the demonstration was to demonstrate the capability of the integrated system to detect unexploded ordnance typically found in the first foot of soil. The system detection parameters were again determined with respect to size and shape of target, orientation, explosive content of target, burial depth, elapsed time of detection, and speed over which the system has passed over the target. The critical test issues included the following:

1. What is the present performance and limits of the system in terms of probability of detection and false alarm rates?
2. Does the TNA reliably detect within the range of 22 g to 2.5 lb of explosive? At which burial depths? At which orientation?
3. How much time does the TNA require to reliably make a detection decision?
4. Which method of operation should the remote system be operated: scan and search or stop and go?

5. Current estimates indicate that the TNA requires the object of interest to be within four inches of the center of the sensor head. Does the metal detector locate the object accurately enough for the TNA to be useful?

6. Is the system capable of completely covering the site without gaps in coverage?

The demonstration included blind tests and data collection designed to determine and confirm the robotic and verification capabilities of the detection system.

6.1 Demonstration Description.

Test Site. The test site was located at the Yuma Proving Grounds (YPG), AZ. The terrain is flat with small undulations. The soil has a desert pavement on the top surface with soft sand underneath the hard surface. YPG has an arid environment with an average annual rainfall of 3.80 inches. The site had been used as a test range for decades, so the amount of metallic debris, or false alarms for the metal detector, was dense.

Methodology. Again, the test consists of three sections:

- a. A Calibration Test: where all information about the emplaced ordnance is released to the contractor.
- b. A Data Collection Test: where the contractor is given information about the location of the emplaced ordnance/ clutter, but not the depth, orientation, and type of target.
- c. A Blind Test: where the contractor is not given any information about the ordnance/ clutter present.

The blind test is designed to permit an objective evaluation by the government of the capabilities of the entire system. One-dimensional lanes and two dimensional areas were setup for the blind test. The original plan was to use the stop and confirm method for the one-dimensional lanes and one of the two dimensional areas, and the scan and confirm method for the other two dimensional area. After trying the stop and confirm on the first lane, that method was determined inefficient due to the high density of naturally occurring false alarms for the metal detector. Accordingly, the approach to the blind test for the other 3 lanes and one two-dimensional field was to first scan and collect data on the area with the metal detector. Then determine potential target locations off-line, and return to those locations with the TNA to verify the presence of a target or false alarm.

The data collection effort, which was in coordination with the blind test, was designed to establish a controlled experiment to verify the blind test data. The results of the data collection were a file, which provides data to determine detection limits vs. orientation, burial depth, explosive content, elapsed time, type of target, and speed over which the system passed over the target.

Calibration areas were setup with targets at each depth found in the test areas. The purpose of the calibration areas was for the contractor to familiarize themselves with the response of the system from the targets and with the background characteristics.

Target List. The targets were ordnance with the appropriate fuze or devices removed for safety reasons. The types of targets are representative of the size and amount of explosive of those targets typically found in the first foot of soil.

QTY	NAME	TYPE	EXPLOSIVE CONTENT	NITROGEN CONTENT	TYPICAL DEPTH
10	M56A3	20mm round	10.7 g H-761	(3.53 g)	surface-3"
40	M789	30mm HEDP projectile	22 g Type PBXN-5	7.9 g	surface-3"
20	Simulant	Cylinder	100g C4	34 g	surface-6"
20	M822	40mm projectile	120 g Octol	39.6 g	
20	Simulant	Cylinder 8"X1"	200g C4	68 g	
20	Simulant	Cylinder 6"X1-1/2"	200g C4	68 g	
40	M49A5	60mm mortar	0.79 lb (359 g) Comp B	111.1 g	surface-12"
50	M821	81mm mortar	1.6 lb RDX/TNT		surface-12"
20	Simulant	Cylinder 6"X5"	2.5 lb C4	0.83 lb. (378.3 g)	
10	M393A2	105mm HEP-T projectile	4.4 lb Comp B	1.34 lb. (609.3 g)	surface-6"

Table 3. Ordnance information

Clutter was not buried due to the high density of metallic debris.

Each UXO type was buried at burial depths according to the Table 2. Burial depths are measured to the surface of the center of the ordnance item.

NAME	TYPE	BURIAL DEPTH
M56A3	20mm round	flush, 1"
M789	30mm HEDP projectile	flush, 1", 3"
Simulant	100g Cylinder	flush, 1", 2", 6", 12"
M822	40mm projectile	flush, 2", 6"
Simulant	200g Cylinder 6"X1-1/2"	2", 6", 12"
Simulant	200g Cylinder 8"X1"	2", 6", 12"
M49A5	60mm mortar	2", 6"
M821	81mm mortar	2", 6", 12"
Simulant	2.5 lb Cylinder	2", 6", 12"
M393A2	105mm HEP-T projectile	2", 6", 12"

Table 4. Ordnance burial depths

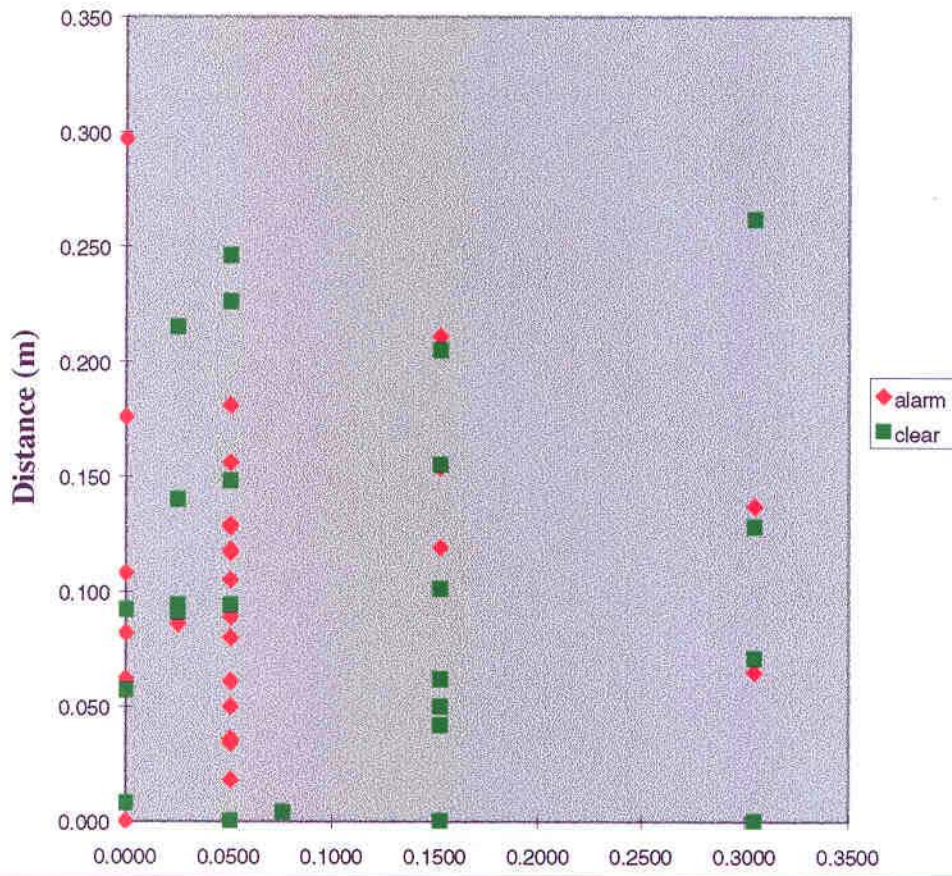
6.2 Demonstration Results.

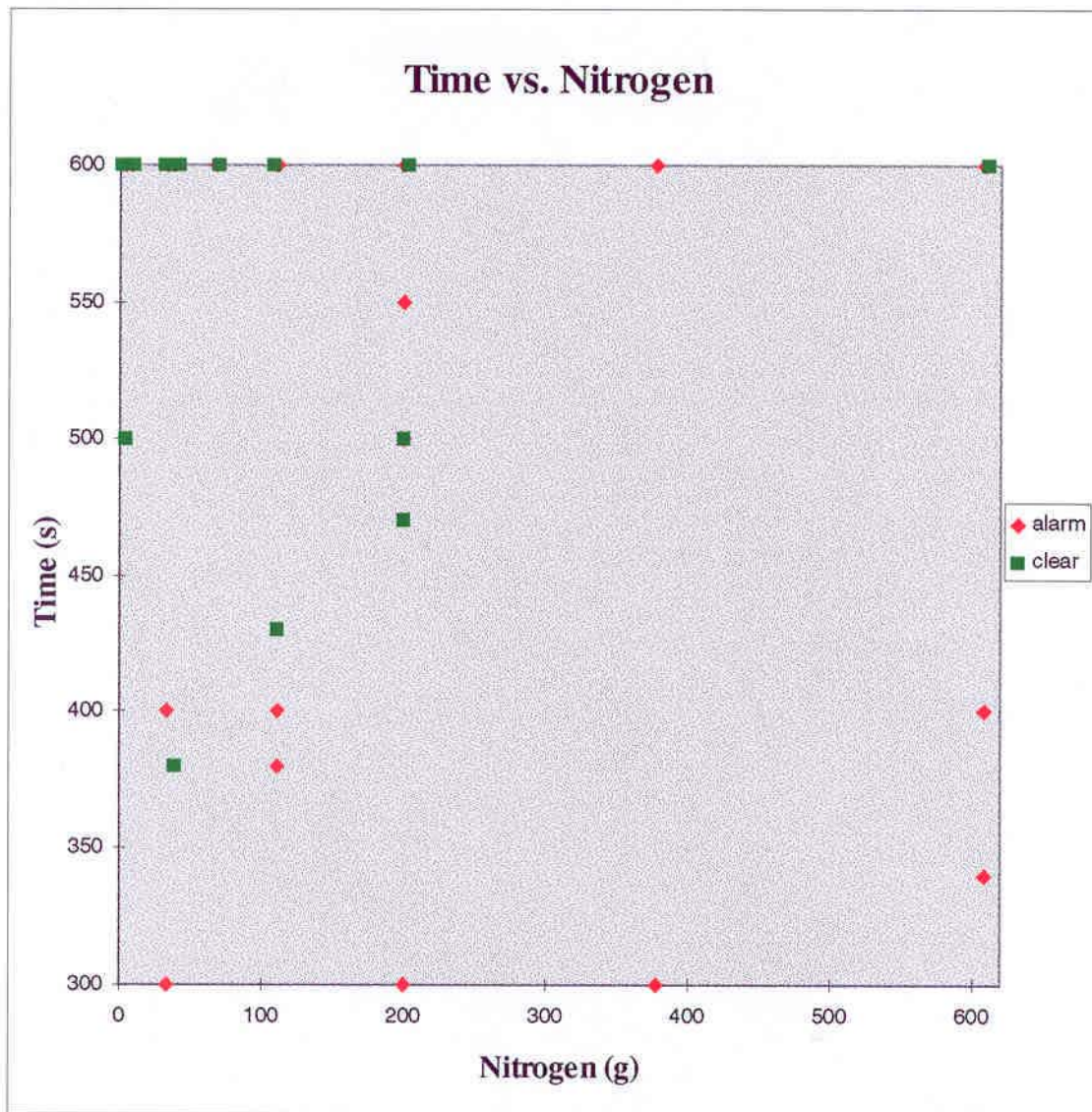
The following table is the results from the blind tests collectively from lanes 1-4 and area 1. "PD System" represents the combined effort of the metal detector and TNA working as a system with the expectation of being able to mark the target within 6". "PD MD" was the probability of detection of the metal detector alone with the expectation of the metal detector to locate the target within 12". "PD TNA" is the probability of detection for the TNA alone and only considers the targets, which the metal detector detected as well as located close enough for the TNA to investigate, i.e. 6". In order to understand the capabilities of the TNA to detect the targets, analysis of this data was performed with respect to type, depth, distance, and explosive content of the targets, and the following graphs represent the analysis.

TYPE	PD SYSTEM	PD MD within 12"	PD TNA within 6'	POST PROCESSED ALL OFFSETS
20mm	1/5	3/5	1/3	1/3
30mm	3/11	3/6	3/7	3/7
(30mm)	0/3	3/7	-	-
((30mm))	0/1	3/8	-	-
100g	4/10	3/9	4/6	6/7
40mm	2/9	3/10	2/6	4/6
200S	2/8	3/11	2/3	4/4
200L	1/6	3/12	1/3	3/4
60mm	6/16	3/13	6/6	6/8
81mm	6/14	3/14	6/9	7/10
2.5lb	2/2	3/15	2/2	3/3
105mm	5/6	3/16	5/6	6/6
OVERALL	32/91	3/17	32/51	43/58
FAR SYSTEM (/sq.m)	19/2860			
FAR MD (/sq.m)	19/2861			
PFA TNA	19/2862			

In order to understand the capabilities of the TNA to detect the targets, analysis of this data was performed with respect to type, depth, distance, and explosive content of the targets, and the following graphs represent the analysis.

Distance vs. Depth





7.0 Conclusions. An integrated system was demonstrated but its capabilities are not completely understood. The following conclusions can be made about the system:

1) It has not been logically and methodically determined what the best TNA sensor should be. An in-depth study to determine the best detector type, detector size, quantity of detectors, and best source needs to be conducted. The systematic errors within the system need to be calculated on a consistent system in order for the background subtracting methods to work more efficiently. A statistically significant data collection and complementary blind test needs to be conducted with variance of the target burial depth, distance, and nitrogen amount. The soil variation needs to be measured in order to determine its effect on the performance and robustness of the TNA.

2) There is a need for a more accurate GPS in order for the system to accurately locate the detections. The accuracy is critical for the TNA to verify the detection from the metal detector due to the TNA's footprint of 12" diameter.

3) A wider metal detector array is critical for complete coverage of the site as well as reduction of time required to scan an area.

4) The system requires a more robust radio design which can handle environmental conditions as well as ranges of 1 km or more.

**REMOTE CONTROLLED
SURFACE/NEAR SURFACE
UXO DETECTOR**

Final Technical Report

Submitted to:

OFFICE OF SPECIAL TECHNOLOGY

10530 Riverview Road
Ft. Washington, MD 20744

Contract No. DAAD05-93-D-7019

Submitted by:

Science Applications International Corporation

4161 Campus Point Court
San Diego, California 92121

June 1997 (Rev.)

Table of Contents

1. Introduction and Summary	1-1
2. Requirements	2-1
2.1 Contractual Requirements	2-1
2.2 Top Level System Requirements	2-2
2.3 Top Level Subsystem Requirements	2-3
3. Vehicular Platform	3-1
3.1 Description of the Hardware	3-1
3.2 Performance.....	3-2
4. Data and Video Communications	4-1
4.1 Description of the Hardware	4-1
4.2 Performance.....	4-1
5. Metal Detector Array	5-1
5.1 Description of the Hardware	5-1
5.2 Performance on UXO.....	5-2
6. TNA Sensor	6-1
6.1 TNA Optimization	6-4
6.2 Signal Processing	6-4
6.3 Field Test Results from the OCDT Program	6-7
6.4 Stabilization	6-9
6.5 System Improvement.....	6-9
6.6 Sources of Errors.....	6-12
7. Navigation and Mapping	7-1
7.1 Overview	7-1
7.2 Systems of Coordinates and Transformations	7-1
7.3 Implementation	7-5
7.4 Performance.....	7-7

8. Control Station and Software	8-1
8.1 Control Station	8-1
8.2 Software	8-1
9. Socorro Test.....	9-1
9.1 Description of the Site.....	9-1
9.2 Description of the Ordnance.....	9-1
9.3 Summary of Data Acquisition.....	9-3
9.4 Coordinate Systems.....	9-7
9.5 Metal Detector Results.....	9-9
9.6 TNA Results	9-17
9.7 Main Conclusions From Socorro Test	9-23
10. Yuma Test.....	10-1
10.1 Description of the Site.....	10-1
10.2 Description of the Ordnance.....	10-1
10.3 Summary of Data Acquisition.....	10-3
10.4 Coordinate System	10-4
10.5 Metal Detector Results.....	10-7
10.6 TNA Results	10-12
10.7 Main Conclusions From Yuma Test.....	10-28
11. Conclusions.....	11-1

1. INTRODUCTION AND SUMMARY

This final report describes the work carried out under two phases of a project sponsored by the Environmental Security Technology Certification Program (ESTCP) to develop and test a system for the detection of shallow buried unexploded ordnance. The project was monitored by NVESD, Fort Belvoir, VA and by the Office of Special Technology.

Unexploded ordnance (UXO) is one of the most serious and prevalent environmental problems at DoD facilities. Recent studies have shown that ordnance components are the second most frequently occurring contaminant at Army sites and were reported at almost 20% of the 100 Army sites surveyed. This UXO must be detected, located, and removed in order to restore the location to a safe condition. Current techniques for UXO remediation are very slow and labor intensive, involving hand-held detectors and probes and the removal or detonation of munitions by individual EOD personnel. Some locations cannot be remediated by these techniques as the ubiquitous presence of UXO prevents human operators access to the sites. The system developed and demonstrated under this project addresses the need to detect surface and near-surface UXO. These munitions are either on the surface or covered up by a few inches of soil, dust or natural debris.

The approach is to first detect the UXO using a metal detector array (primary sensor), and then make use of a verification sensor (Thermal Neutron Analyzer or TNA). Both sensors are supported by a remotely-controlled vehicle whose position can be monitored through differential GPS.

This project has benefited from the experience acquired under a larger demining project that resulted in the development of the Vehicular Mine Detection Testbed (VMDT) system and in tests conducted at Fort A.P. Hill, VA, in November 1995. The VMDT was a fast prototyping effort in which many subsystems were brought together in a very short time. Subsequently, a large part of the VMDT system was made available to this program. Under Phase 1 of the program, the following actions were taken:

Upgrading and reutilization of the VMDT platform. The Robotech vehicle, on which the VMDT was based, underwent repair work at the manufacturer's facility and was then brought back to the SAIC facility in San Diego, CA.

Acquisition of a metal detector array. A new primary sensor was acquired and tested using conventional (that is non remotely controlled) vehicles.

Development of navigation and mapping capabilities. The navigational tools chosen (GPS, compass, encoder) have proven to be sufficiently accurate to provide maps of the metal detector signal. Accordingly, this area received more attention than originally contemplated, and a differential base station system was procured.

Implementation of TNA gain stabilization. The tests on the VMDT indicated that gain variations due to temperature changes and other factors were a major source of concern. Accordingly, action was taken to develop and implement an automatic gain correction scheme.

Preparation for tests on two-dimensional areas. Previous tests of similar systems on mine targets were often conducted using one-dimensional lanes. Development of the system and preparation of the test plans emphasized the use of two-dimensional test areas.

Under Phase 2 of the program the following actions were taken:

Test at Socorro, NM, and data analysis. The metal detector and the TNA were tested as separate systems using a variety of vehicular platforms.

Modification of hardware and software. Several changes were made to improve the precision of positioning, the two sensors were integrated on the Robotech platform, the Robotech control itself was made more robust, and the number of individual detectors in the TNA sensor was increased from 8 to 12.

Test at Yuma, AZ, and data analysis. The metal detector and the TNA were operated as an integrated system from a common location.

Section 2 discusses the requirements for the system and subsystems, as they are derived from the statement of work and from the goals of the project.

Section 3 describes the vehicular platform, the problems encountered, and the corrective actions taken. In a similar way, Section 4 describes problems and solutions related to the communication equipment used. Section 5 describes the metal detector array and results obtained from UXO targets. The verification sensor (Thermal Neutron Analyzer or TNA) is discussed in Section 6. Navigation and mapping have been given a strong emphasis in the project and are described in Section 7. The control station and the software are described in Section 8. Section 9 describes the activities and the results from the test conducted at Socorro, NM, in June 1996. In a similar way, section 10 describes activities and results from the final test conducted at Yuma, AZ, in October-November 1996.

Finally, conclusions and recommendations for additional work are contained in Section 11.

2. REQUIREMENTS

The Remote Controlled Surface Near/Surface UXO Detector is a system which includes a group of sensors mounted on a teleoperated vehicle and is designed to detect surface and near surface unexploded ordnance. The system was tested on Government test areas at Socorro, NM and Yuma, AZ in the early summer and fall of 1996. This section describes the perceived top level system and subsystem requirements that flow from the contractual Statement of Work and which evolved based on discussions and clarifications with the program COTR. SAIC's recent experience with the Vehicular Mine Detection Testbed (VMDT) and the process of preparation of the Socorro test plan also had a bearing on the refinement of the requirements. Most of the requirements have been met. In the following discussion, notes are made when significant deviations from the requirements were present in the actual implementation.

2.1 CONTRACTUAL REQUIREMENTS

The contract Statement of Work (SOW), Requirements, Section 3, explicitly identifies an integrated system containing certain hardware. This hardware includes, but is not limited to:

- Robotic Vehicle
- Metal Detector Array
- TNA Sensor
- Global Positioning System
- TV Camera

The tasks listed in Section 4 of the SOW further identify additional hardware/software specifications, including:

- A mine marking system must be included.
- Robotic vehicle is to be an all-terrain vehicle, powered by an internal combustion engine.
- Metal detector is to be based on eddy currents and must be capable of detecting gram quantities of metal.
- TNA sensor is to be CF-252 based.
- The control station should include a computer system, video display, RF data communication, vehicle control functions.

The performance requirements for the hardware come largely from the performance goals for the system. Although these goals are not explicitly defined in the contract, discussions and clarifications with the program COTR as well as the preparation of the test plans have resulted in a broad consensus as to what the goals should be.

After the VMDT tests at Fort A. P. Hill, SAIC requested to be able to use the major subsystems of the VMDT for use on the UXO program. In January 1996 the US Army agreed to transfer all but the metal detector to the UXO program as Government Furnished Property (GFE). In that way, many of the hardware choices have been made. However, there are differences in the UXO and the mine detection missions and not all of the VMDT GFE performed up to expectations during the field tests. Thus, it is important to identify the key top level requirements both at the system and subsystem level.

2.2 TOP LEVEL SYSTEM REQUIREMENTS

The main objective of the project is to carry out tests intended to assess the performance of the detection technologies in a field situation. Accordingly, the requirements for the entire system are closely connected to, and take into consideration, the tests that will be carried out. Some of the requirements, such as for data logging and monitoring of the data stream, are determined more by this assessment goal than by the operational necessity of a fully developed system derived from this effort. Since one of the sensors (TNA) is, in its present state of development, relatively large and heavy, one of the requirements is for the system to be able to carry the TNA to the positions where a verification of explosive presence is wanted.

2.2.1 Detection Targets

The definition of unexploded ordnance is broad, including mines, shells, bombs, etc. The range of sizes is also broad, as is the range of burial depths. In general, a system is judged better the smaller and deeper the UXO it can detect at an acceptable false alarm rate. The tests to be carried out with the system will have a selection of UXO buried at or near the surface.

2.2.2 Test Areas and Surfaces

Both one-dimensional lanes and two-dimensional areas are to be used in the field tests. In most cases, the roughness of the test surfaces will have the characteristics of the natural soil of the test locations. The surface may be scrapped or graded on some of the test areas.

2.2.3 Burial Depths

Burial depths are specified in the test plans so that the maximum depth for near surface is 12 inches (30 cm). Different UXO shell orientations will be used. Information on typical orientation and burial depth is available from the JPG test report and references therein.

2.2.4 Forward Advance Speed and Detection Times

There is no specified forward advance speed, but one of the metrics of the field test will be to determine how fast the system can detect all the detectable UXOs. The UXO clearance mission is interpreted to mean that the highest priority is given to a high probability of detection and that the time for detection (or confirmation in the case of the TNA) is secondary.

SAIC had originally set a goal of 1 to 2 km/hr when scanning with the metal detector array. Complete coverage of a 100 m × 100 m area, using a one meter array, was anticipated to take no more than six hours (accounting for turns and overlap). Based on the results from the VMDT, a maximum of 5 minutes was initially budgeted for confirmation with the TNA sensor. As part of the investigation, the time to confirm various size shells was to be determined. The results from the Yuma test indicated that the above values were too optimistic. In reality it took six hours to scan a 50 m × 50 m area, and the average time for TNA verification was 10 minutes. The longer time for the scan was due to an underestimate of the time needed to turn and reposition the vehicle, and to unanticipated interruptions.

2.2.5 Environmental

The UXO detector must be capable of testing in the ambient conditions of San Diego/Santa Clara as well as the test areas at Socorro, NM and Yuma, AZ. The temperatures expected could range from over 100 deg F in direct sun to below freezing. Due to time constraints, the electronics and signal processing system is primarily Commercial Off The Shelf (COTS) and not ruggedized for extreme temperatures. Accordingly, a safe estimate of the allowable temperature range for the tests is 20 deg F to 110 deg F. The system should be operable in the rain.

2.3 TOP LEVEL SUBSYSTEM REQUIREMENTS

The main requirement is that each subsystem be tested individually to the point that sufficient knowledge on its reliability and performance is available before it is integrated into the system.

2.3.1 Remotely-Controlled Vehicle

The remotely-controlled vehicle needs to be capable of supporting the weight of the UXO sensors and their associated local signal processing and communication systems. It must be capable of a controlled slow speed (order of 1 km/hr) without jerks, as well as a faster speed (about 5 km/hr) for transfers while not collecting data. The vehicle must provide at least 1.2 kW electrical power for the sensors and signal processing equipment (an external on-board generator may be used). The vehicle used is a Melroe Bobcat 773 which was made telerobotic by Robotech of Calgary, Canada.

The sensors are mounted on a mechanical interface plate adapted from a Bobcat tool plate. The remote Robotech controls, coupled with the visible cameras must allow the operator to lower the metal detector array or the TNA sensor semi-independently, but not simultaneously. This motion is accomplished with a combination of the lift and tilt controls.

The metal detector array is lowered to be in contact or near contact with the ground. The TNA is to be lowered to a ground standoff distance of around 1-2 inches (at the center) with a known accuracy of ± 0.25 inches. The TNA must be level with the ground so that the side to side difference in standoff is no more than 1 inch. The TNA should not be allowed to "hit" the ground (it is somewhat fragile and could break).

The remotely-controlled vehicle must be capable of being moved slowly forward or backwards and positioned to an accuracy of ± 5 cm. It must be capable of 4 hour operation between refueling and must be able to go for 8 hours per day operation without maintenance.

2.3.2 Metal Detector Array

The metal detector array must be capable of sensing the metal content of buried UXO, and to provide some indication of the size of the UXO. The metal detector array for the UXO system must contain eight independent coils and must cover a one meter swath in front of the vehicle. The display of the metal detector signals must allow the operator to identify the centroid of the UXO to an accuracy of ± 10 cm. This information is to be used both for marking and for positioning of the TNA detector.

amount of pan and tilt are used, is to assist in the remote positioning of the sensors. A third purpose is to look into other directions to observe interesting features. This should be allowable, with the vehicle stopped, by using the full pan and tilt capabilities of the camera mount.

The control and sensor data must be transmitted to and from the vehicle computer via a bi-directional VHF radio link. The goal for communication range is one mile line of sight, with no interference.

2.3.5 Navigation and Mapping

The system shall include a near real time differential GPS system, with submeter positioning accuracy, and an electronic compass. Near real time is intended to mean one position determination per second, or faster. Position, velocity, and tracking information from the GPS receiver, and orientation from the compass should be transmitted over the radio link.

The differential corrections for the GPS, in RTCM 104 format, can be either from an FM station (if available) or from a specially installed base station.

The positional and orientation information is to be used to:

- Display a map, in near real time, of the metal detector signals.
- Record the coordinates of observed targets.
- Navigate the vehicle back to a previously observed target.
- Insure complete coverage of the test area.
- Assist in positioning the system for marking.
- Assist in positioning of the TNA sensor over a target for verification of explosive presence.

The system should also contain a wheel encoder which is used for displaying the metal detector signal over a short range (order of meters). The encoder itself can be very accurate (order of mm), however the ultimate accuracy depends on the interaction of the wheel with the terrain (possibility of wheel slippage).

2.3.6 UXO Marking System

The system should contain means for leaving a semi-permanent indication of a suspect indication on the ground. The primary goal is to mark exactly on top of the desired location, with an accuracy of ± 10 cm. If marking exactly on top of the target is not achievable, a fallback position is to mark at a different location, provided that the displacement vector (offset components) is estimated and recorded.

The target marking material should be non-hazardous.

The metal detector array support must be durable enough to withstand being dragged over the test ground for the approximately one month of testing and calibration. All metal detector cables should function without deterioration in the rain.

2.3.3 TNA Sensor

The TNA sensor is the secondary sensor and must be capable of confirming the presence of the high explosive in surface and near surface buried UXO. The time for making this determination was initially set as a goal to be less than five minutes, and it was later increased to 10 minutes. The TNA sensor should be "fail-safe", that is, if it is not capable of confirmation, it must not "clear". The sensor must move transverse to the direction of vehicle motion to the suspect location indicated by the metal sensor (the positioning along the direction of motion is done through the movement of the teleoperated vehicle).

The following requirements are flowed down to the TNA sensor:

- The TNA sensor includes the neutron source, detectors, and signal processing system.
- The system shall contain 8 7.5 cm x 7.5 cm NaI detectors or larger (the number of detectors was increased to 12 after the Socorro test).
- The source/detector configuration should be such that pulse pair pileup is not significant in the region around the 10.8 MeV nitrogen line.
- The TNA sensor must be automatically self calibrating.
- Cold startup and initialization should take no longer than one hour with a goal of 20 minutes.
- TNA should be self diagnosing and fail gracefully (it should remain operable if one or more detector channels are not functioning).
- The sensor should be optimized for detection of minimal amounts of high explosives.
- The TNA should function in soils with moisture contents from dry to 25% moisture.
- The weight of the sensor should not exceed 350 lb.
- The neutron source must be loadable in an easy and safe way.

The following are requirements for the TNA positioning device:

- The TNA positioning device should be capable of positioning the TNA sensor to a given position to an accuracy of 0.5 inches.
- The positioner shall include devices to indicate the standoff of the TNA to an accuracy of ± 0.25 inches, and a tilt of ± 0.5 inches relative to the middle of the sensor.
- The weight of the sensor, supports, and positioning mechanism should not exceed 700 lb.

2.3.4 Video and Data Communications

A color video camera with zoom capabilities is to be mounted on a support providing pan and tilt capabilities. The primary purpose of the video camera is to provide the operator with a real time view of the area in front of the vehicle, so as to allow safe driving of the vehicle (when the vehicle is moving the camera must always point to the front). A secondary purpose, for which zoom and a moderate

2.3.7 Control Station and Software

The system is to contain a control station to allow for:

- Teleoperation of the robotic vehicle
- Pan, tilt, and zoom of the cameras
- Identification of the target position using real-time feedback from metal detector array
- Positioning of the TNA sensor over a suspect UXO target
- Interpretation of the TNA indication
- Positioning and remote activation of the target marking system
- Sensor and system diagnosis
- Start up and calibration of sensors
- Visualization and logging of the sensor signals

The control station is to contain a computer, radio communication equipment, and a minimum of two monitors, one to display the video signal from the camera and one to display the interaction with the computer.

3. VEHICULAR PLATFORM

3.1 DESCRIPTION OF THE HARDWARE

The vehicle chassis and remote control were supplied by Robotech of Calgary, Alberta, Canada. The Robotech vehicle is based on a Melroe Bobcat 773, which is diesel powered and uses skid steering. The manual controls have been modified with electric servovalves. These valves are controlled by a microprocessor-based control system. The operator's control station communicates with the vehicle controller over a radio frequency link with a nominal one mile line of sight capability.

All vehicle functions are controlled from a single operator using twin, dual axis, self-centering joysticks. These joysticks effect proportional control of vehicle/speed direction and boom lift/tilt operations. In addition, thumb controlled "rocker" switches, located at the top of the joysticks, are used to control functions requiring higher degrees of precision.

There are two degrees of freedom on the boom which supports the sensors, lifting and tilting. Both motions must be used in a coordinated way to correctly position the TNA sensor.

The following are fail-safe features designed to ensure safety and virtually eliminate the potential for damage through any reason other than misuse or operator error:

- Vehicle warning lights flash and audible alarm sounds for ten seconds before the engine can be started. The alarm sounds continuously when the vehicle is backing up.
- The parking brake is automatically engaged when the engine is turned off. It must be manually disengaged.
- The control console can be locked out with a key to prevent unauthorized use.
- Radio signals are interrogated continuously to ensure valid input. In the event that radio signal is lost, the Robotech vehicle will shut down.
- Unique radio frequencies are used. In the unlikely event that a second transmitter on the same frequency should enter the vehicle's range, the Robotech vehicle will shut down rather than respond to erroneous signals.
- Emergency shut down buttons are located on both the control console and the Robotech vehicle itself.

The vehicle has a lift capacity of 1300 pounds with 40 horsepower.

3.2 PERFORMANCE

The selection of the Robotech vehicle was mostly determined by the need to carry the TNA sensor, which weighs in excess of 350 lb. While the vehicle has more than the minimum power required to handle such a load, it is designed mostly for heavy excavating operations. In some instances, during the VMDT operation, it appeared that the precision and smoothness required to position the TNA sensor was not available with the original Robotech system.

The problems were mostly with control and software. Accordingly, the vehicle was shipped back to the manufacturer in Canada, where a number of modifications were made both to the hydraulic valves and to the software. Because of these upgrades, better positioning performance was attained during the Socorro and Yuma tests. Apart from a control problem encountered at Socorro, which was due to the high temperatures during the test (the problem was later solved by moving a control enclosure outside the vehicle), the upgrades resulted in smoother operation and better positioning performance.

4. DATA AND VIDEO COMMUNICATIONS

4.1 DESCRIPTION OF THE HARDWARE

Communications play an important role in the system. Data and video links exist between the vehicle and the control station. For the data, four separate RF communication links are implemented on the system. The first link is integral to the Robotech vehicle control system and is used exclusively for speed and direction changes and for varying the height and tilt of the boom. The link is implemented through a pair of 2 W, 462.5 MHz modems manufactured by Motorola.

The second link carries all the sensor data. The data are transmitted to and from the vehicle computer via a bi-directional, 2 W, VHF data radio link, with frequency selected at 415 MHz. The protocol for this data link was developed specifically for this system.

The third data link is between the TNA computer on the vehicle and the TNA controller. It is implemented through a pair of spread-spectrum transceivers manufactured by Freewave Technologies, Inc. The modems have an output power of 0.3 W and operate in the range 902-928 MHz. The specifications for this type of modem indicate that it can be operated at distances up to 20 miles.

The fourth link is between the vehicle mounted GPS receiver and the base station which provides the differential corrections. This link is implemented through a pair of RFM96W modems, manufactured by Pacific Crest Corporation. The modems have an RS-232 compatible interface configurable for 150 to 9600 baud operation. The power is 2 W and the selected frequency is 425 MHz. Optionally, one can also receive differential corrections from an FM station associated with DCI (Differential Corrections Incorporated), if one is within the range of such a station.

Video output from the visible camera is sent to an RF transmitter located in an enclosed electronics bay on the vehicle. The video signal is transmitted at 1720 MHz to the operator console for display on a monitor. The visible camera is a Panasonic GP-US502 high resolution color camera. This camera features a 1/2 in. format, and 3 CCDs to obtain a horizontal resolution of 700 TV lines. This camera provides the resolution and color registration necessary for this application, and is the primary observation and control camera for the sensor positioning.

4.2 PERFORMANCE

In the first stages of the VMDT, some problems were encountered with remote data transmission. One was short range and the other was occasional interference from other sources. The first problem was due to the low power (10 mw) of a modem type that had otherwise outstanding characteristics. We transitioned to higher power RF modems, fully expecting to operate at a range of about one mile. However, we had some occasional problems with the Pacific Crest modems, when the ranges were of the order of three hundred meters.

The second problem is more difficult to predict, and depends on the actual environment in which the equipment is operated. All modems used contained error correction schemes which should substantially reduce the effect of interference. In general, the system seemed to operate better in the morning than in the afternoon, and occasional communication drops were seen to depend on the orientation. By far, the best performance was obtained with the spread spectrum modems.

5. METAL DETECTOR ARRAY

5.1 DESCRIPTION OF THE HARDWARE

The primary sensor is a one meter metal detector induction array manufactured by Schiebel Systems Ltd. of Nepean, Ontario, Canada. The sensor is a modular system consisting of an electronic unit and an array of induction coils. The array has eight partially overlapping transmitting and receiving coils which are rigidly embedded in fiberglass.

Transmitter pulses are generated in the electronic unit and applied in sequence to the transmitting coils in the array. The pulses radiated from the search head create eddy currents in nearby metal objects. The eddy currents create a secondary field, which induces a current in the respective receiving coil in the array. The induced current is amplified, processed, and digitized in the electronics unit to provide a detection signal for further signal processing and display.

The electronic unit is housed in a half size rack enclosure and contains individual circuit cards which are interconnected by means of a backplane circuit card. The electronics unit also contains a microprocessor and communicates serially with the computer at 19,200 baud. The Transmit/Receive (T/R) card handles eight individual search heads located in the array. The card contains the pulse generators, the output amplifiers, the receiving circuits, and the ADC (analog to digital converter). The 12 bit ADC converts the analog signals from the coils to digitized signals within the range 0-4095. The T/R card also contains self-check circuits for each individual search head to check malfunction, open loop or short circuit.

The Power Supply card transforms the supplied on-board voltage (12-23 V DC) into the required system voltages. Commands are available for resetting, starting the pulsed mode, calibrating, and other functions. A software package running under Windows is also available from Schiebel. The software controls the array and can be used to collect and display data. Our approach, however, has been to use the low level commands to the array and to write our own software which, in addition to the metal detector, controls the other sensors and functions of the system. This approach provides a software package which is more tailored to the application.

The metal detector array has been tested extensively using conventional vehicles, both by itself and in conjunction with navigational elements such as GPS, compass, and encoder. Both semi-rigid mounting and support with flexible straps have been tested. On the Robotech vehicle, we used the flexible strap mount for the Socorro test. We then realized that this was affecting the marking and positioning accuracy and used the semi-rigid mounting in the Yuma test.

There are no sensitivity adjustments on the Schiebel detector. The only control allowed to the operator is to calibrate. When a calibration is performed, the signals from all the coils are adjusted slightly below the middle of the dynamic range (about 1500-1600 out of 4095). We perform the calibration by lifting the detector up in the air, so that it will be away from metal in the ground.

5.2 PERFORMANCE ON UXO

The Schiebel metal detector array is very sensitive, and can detect small amounts of metal. The array was primarily intended for detecting mines, even minimum metal mines, and is perhaps too sensitive for UXO work. The signals from the large UXO targets buried near the surface easily saturate the array, and large signals are obtained from clutter as well.

The main problem with the array during the Yuma test was not sensitivity, but the difficulty of separating signals from real targets from clutter buried near the surface. Figures 5.1 through 5.10 show the shape of the peaks from the eight coils in the metal detector array for each of the ten targets in the calibration lane at Yuma Proving Ground (see Section 10). The ordinate in each figure is the value of the digitized signal from each coil (between 0 and 4095) and the abscissa is the position in meters as given by the wheel encoder. The following observations can be made:

- The depth of these targets is rather shallow, only two targets (105 mm and 81 mm) were buried at 6 in., and the rest were at 2 in. or less.
- In addition to the large, saturated, positive peak, all the targets show a negative peak, which in some cases also saturates at the lower limit of the ADC converter.
- Some of the figures (for example 5.5, 5.7, and 5.8) show the effect of clutter near the targets.

During the Yuma test, the selection of targets to be further investigated with the TNA sensor was done looking at shapes like the ones in Figures 5.1 through 5.10. Unfortunately, the selection was influenced by the lack of data for targets buried at lower depths and by the (wrong) assumption that all targets would provide signals similar to the ones illustrated here.

The data indicate that a correlation exists between the observed shapes of the peaks and the ordnance type. Figure 5.11 shows the width of the saturated part of the peak versus the cubic root of the mass of explosive (taken as a rough indicator of a linear dimension of the UXO target). This is a rough correlation, since it does not take into account neither depth, nor the behavior of the signal from each coil.

Obviously, there is a substantial amount of information contained in the signal traces from the metal detector coils. The traces may have sudden variations due to the non uniform scan of the detector over the targets (the array is dragged and may bump up and down). We believe that the metal detector array could be utilized to discriminate against clutter. In order to do this, one should first make the scans more uniform, and, second, learn to analyze the peaks against an expanded data base. This analysis approach is not new. In fact, it was used successfully with the Geonics EM61 electromagnetic detector during the Jefferson Proving Ground tests, and resulted in improved detection probability and lowered false alarm rates.

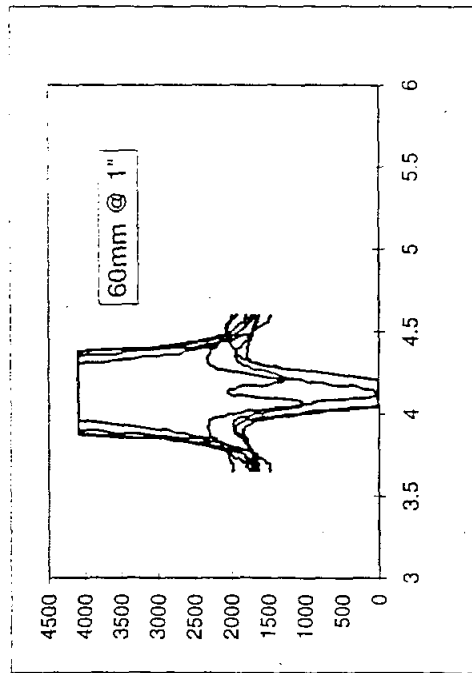


Figure 5.1. Peak Shape for 60 mm UXO at 1" Depth.

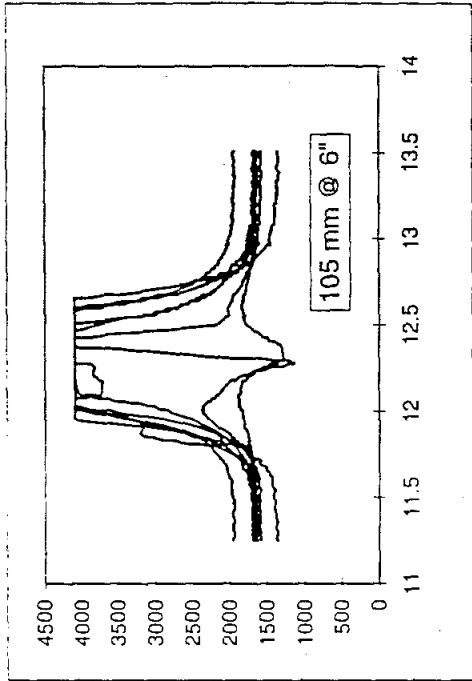


Figure 5.2. Peak Shape for 105 mm UXO at 6" Depth.

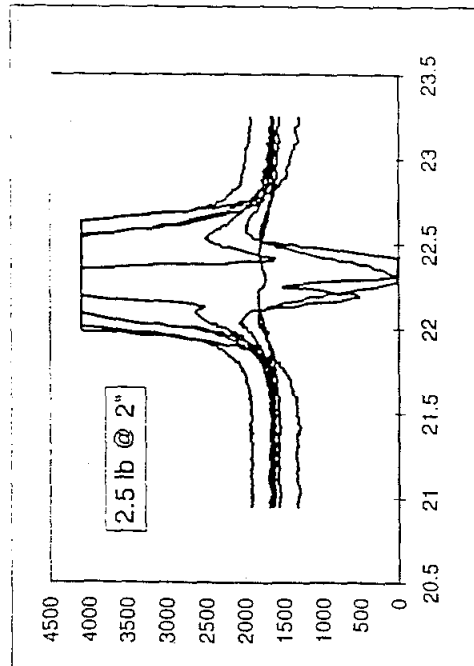


Figure 5.3. Peak Shape for 2.5 lb Simulant at 2" Depth.

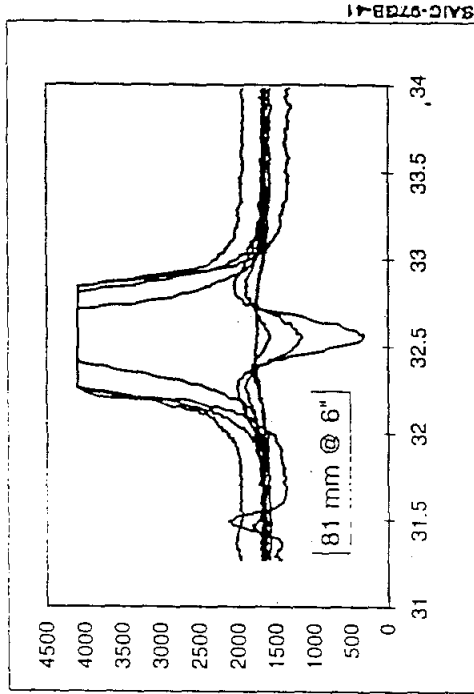


Figure 5.4. Peak Shape for 81 mm UXO at 6" Depth.

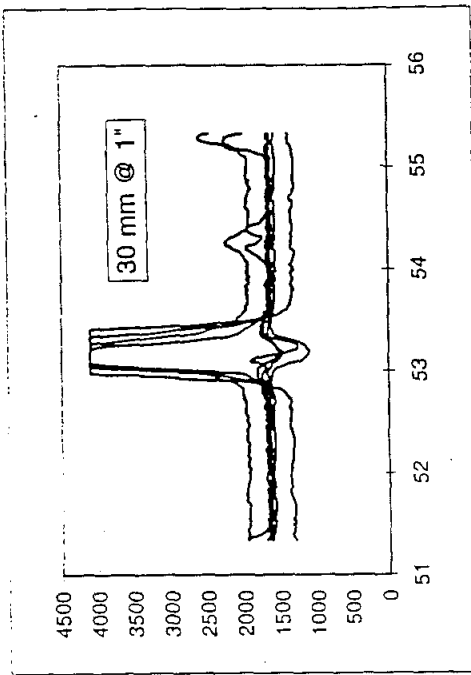


Figure 5.6. Peak Shape for 30 mm UXO at 1" Depth.

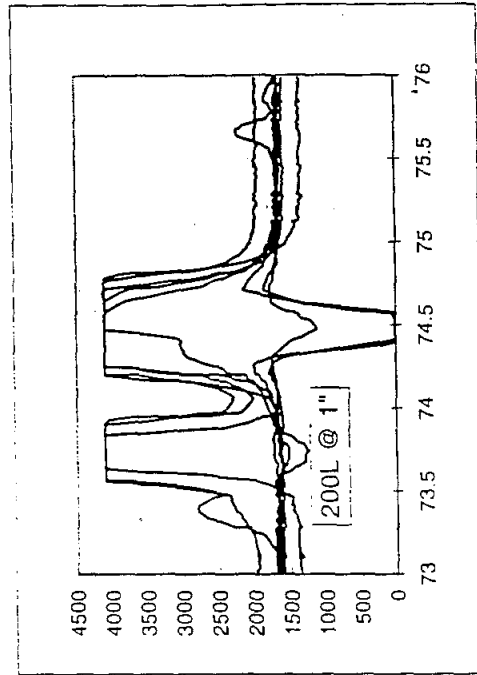


Figure 5.8. Peak Shape for 200 g L UXO at 1" Depth.

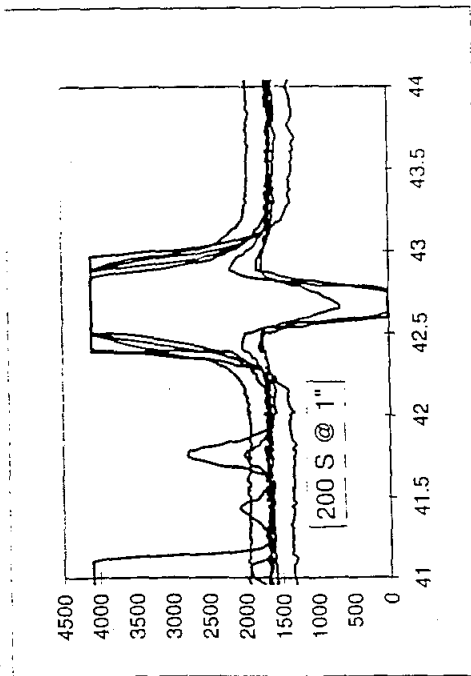


Figure 5.5. Peak Shape for 200 g S Simulant at 1" Depth.

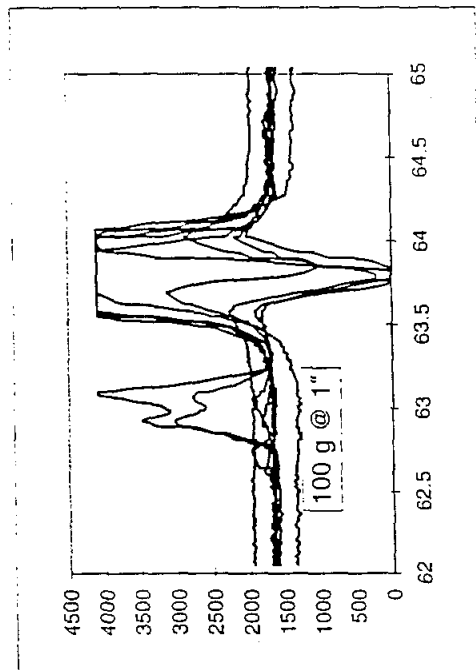


Figure 5.7. Peak Shape for 100 g Simulant at 1" Depth.

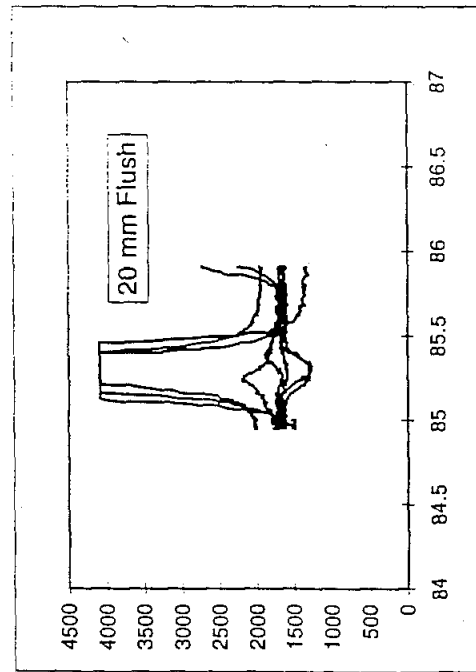


Figure 5.9. Peak Shape for 200 mm UXO Flush with the Surface.

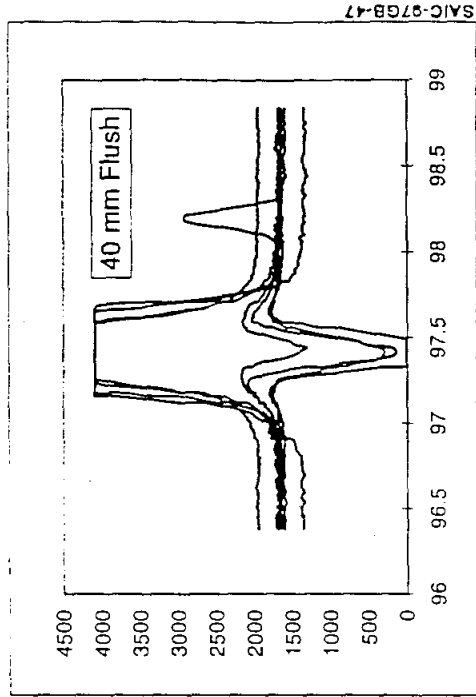


Figure 5.10. Peak Shape for 40 mm UXO Flush with the Surface.

SAIC-97GB-47

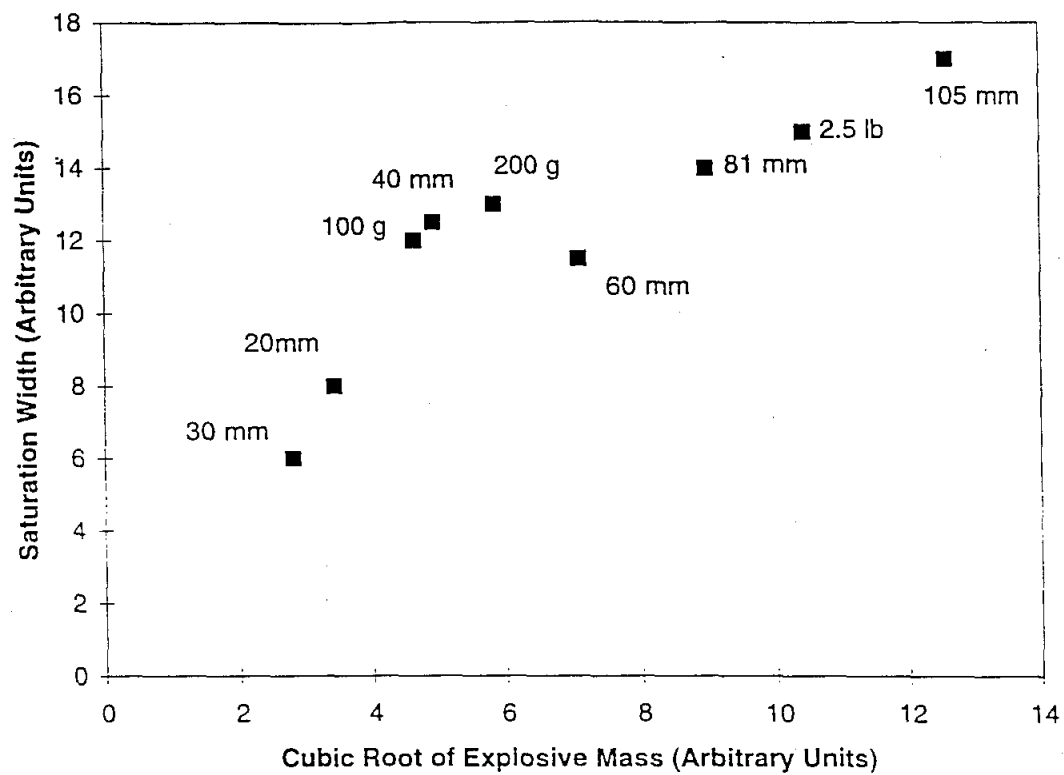


Figure 5.11. Peak width versus UXO Size.

6. TNA SENSOR

The role of the Thermal Neutron Analysis (TNA) sensor is to confirm the presence of explosives that accompany the metal detected by the Schiebel metal detector. In this sense the TNA is a secondary detector. The TNA measures high densities of nitrogen which is unique to modern high explosives. Figure 6.1 shows the basic principle of the TNA detection of buried explosives. An isotopic ^{252}Cf source emits neutrons which are slowed down (or moderated) within the sensor module before they penetrate the ground. Gamma-ray detectors measure the spectrum of the neutron capture gamma rays from the elemental ingredients of the buried objects and surrounding soil. Figure 6.2 compares typical TNA spectra from a buried mine and soil. The capture gamma ray from nitrogen at 10.8 MeV is characteristic of the nitrogen present in high explosives in mines and UXO. The TNA spectrum also yields spectral information from silicon, iron and other soil constituents. The neutron detectors measure the back-scattered thermalized neutrons and give a largely independent measure of the hydrogen content.

Previous versions of the TNA sensor were investigated as a possible application for tactical countermine (Multisensor Fusion for Vehicle Mounted Mine Detection, DARPA). In that mission, short detection time was a primary requirement and this necessitated the use of large neutron sources and many detectors. In fact the sensor weighed around 4000 lb. For UXO and mine detection for cleanup purposes, the time requirements were not critical, thus opening a number of options for the source size and sensor sensitivity trade-offs. For the UXO program, an initial attempt was made to reduce the weight of the TNA sensor to less than 500 lb. (a weight budget dictated by the chosen tele-robotic vehicle) and to make it sensitive to small quantities of explosives. Previous to the start of the program, simulation studies on this optimization were carried out. The first part of the present program, described in section 6.1, was aimed at confirming that a reduced sized system was sensitive to small explosive quantities. Experimental studies carried out in the laboratory confirmed that the desired sensitivity was achievable.

The second study conducted under the present program was on background (or noise) reduction. This was an experimental program carried out using both laboratory and field data. The goal was to reduce interfering spectral contributions to the nitrogen region of the capture gamma ray spectrum. These contributions arose from a variety of sources. This work is described in Section 6.2.

The optimized design was used as the basis for construction of a field prototype TNA sensor for the Government's Operational Capabilities Demonstration Test (OCDT) for detection of buried mines for humanitarian purposes (Vehicular Mine Detection Testbed, CECOM RDEC NVESD, Contract DAAB12-95-C-0030). The OCDT culminated in successful field tests of a prototype compact TNA sensor during November 1995. Some of the results of that field testing relevant to the present UXO detection program are described in Section 6.3

After the field tests of the TNA sensor under the OCDT, the need for automated stabilization of the TNA sensor gain was recognized. This led to the adaptation of existing software to determine the position of peaks of known energy in the capture gamma ray spectrum and the use of these positions to determine appropriate positions of the regions of the spectra used in the signal processing. This work is described in Section 6.4.

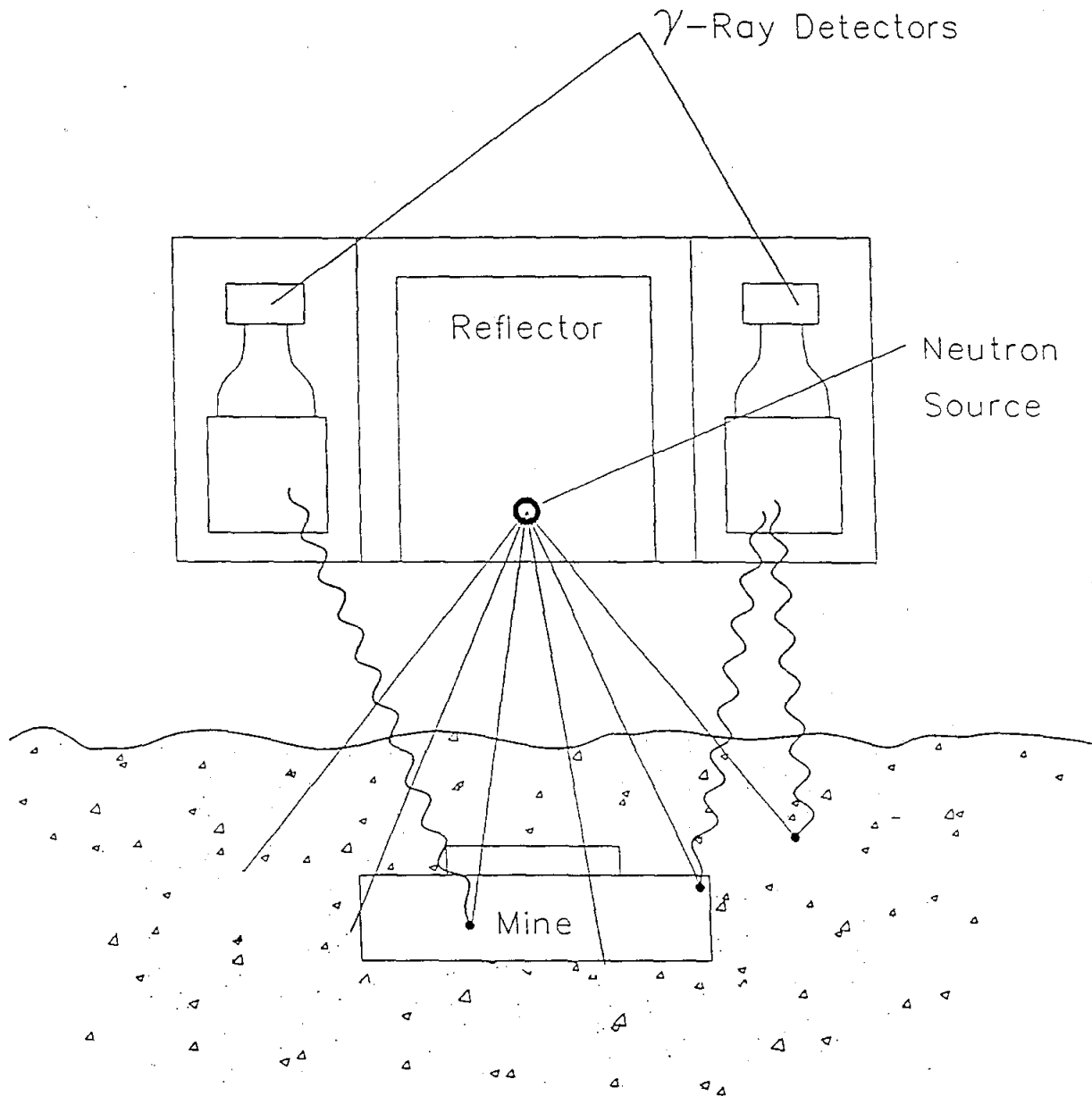


Figure 6.1 Principle of TNA for detection of buried explosives.

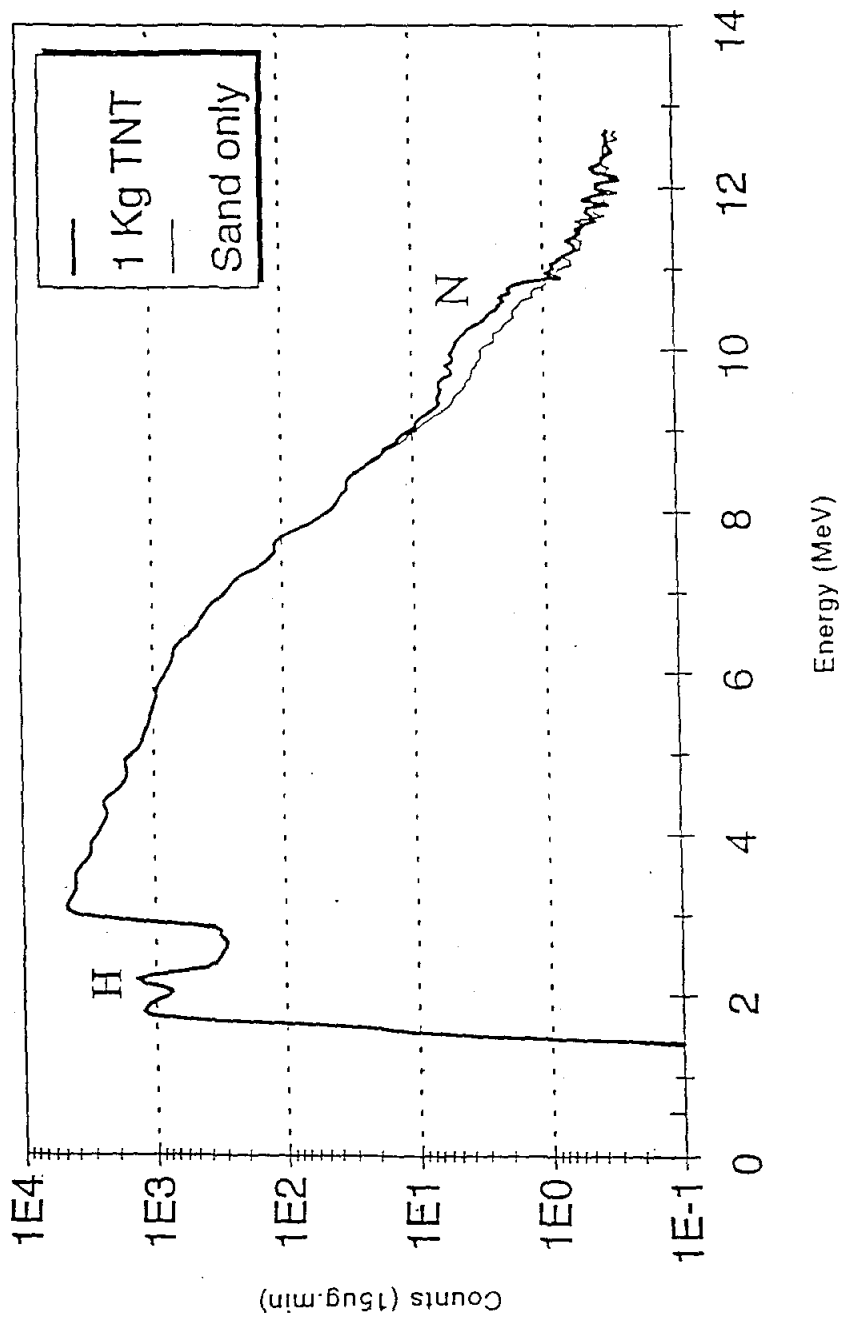


Figure 6.2 Capture neutron spectrum from TNA showing unique signal from nitrogen and hydrogen in an explosive.

6.1 TNA OPTIMIZATION

Prior to the start of the present program, simulation studies conducted by SAIC indicated that a moderator size of around 12 in. was appropriate for use with 3 in. x 3 in. NaI(Tl) detectors and a 20 mg ^{252}Cf source. Although the larger explosives would be self moderating, it was necessary to pre-moderate the neutrons to maximize the sensitivity to the smallest quantity of explosive. A bench top version of the TNA sensor was set up in the laboratory, and measurements made to confirm sensitivity and test the on-line data acquisition code.

TNA imaging code, that takes net counts from the eight detectors in the system and creates an image indicative of the mine position and quantity of explosive, was implemented as part of the real-time data code. In order to create this image, it was necessary to obtain the system response to a simulant in various locations. A 550 gram of 90% melamine was used in this mapping. The surface of the test bed of sand was divided into a 5 x 5 grid of 3 in. x 3 in. squares. The melamine simulant was placed at these grid locations and static measurements were performed with good statistical precision. The counts from these measurements were then background corrected and used to create a detector response matrix to predict the location of the mine in a two dimensional grid. To test this imaging code, measurements were taken using the 550 gram sample in various positions in the grid, the response matrix was applied to the net counts from these measurements and the results plotted. Figure 6.3a shows the sample placed in the center of the grid, where the response of all the detectors is symmetric. Figure 6.3b shows the sample at one edge of the grid. This code was incorporated in the operator station for the TNA used in the OCDT.

6.2 SIGNAL PROCESSING

Using the data from measurements in the laboratory and in the field under the OCDT program, a signal processing algorithm was developed for reducing noise in the nitrogen signal. This algorithm, called the spectral correlation method (SCM), was developed by SAIC for noise reduction in medium resolution spectral data.

The background in the nitrogen region come from neutron capture in silicon (10.6 MeV), pulse pile up, fast neutron capture in the NaI(Tl) detector and cosmic rays. Pileup occurs when two or more gamma rays, whose combined energies fall in the nitrogen region, impact the detector within the resolving time of the electronics. In some cases the tail of elements such as chromium (9.7 MeV) may result in a background contribution.

Using the SCM, the unwanted signal in the nitrogen region of the spectrum was "nulled out". Figure 6.4 shows the results of applying this technique to signals from eighteen different kinds of ground. The top curve is the gross signal from the nitrogen region and the lower curve is the net nitrogen signal with no explosive present for these ground types. The net signal fluctuates around zero, as would be expected. This technique was tested with the field data from the OCDT taken at Fort A.P. Hill as described below. The same method was used for the Socorro and Yuma field tests.

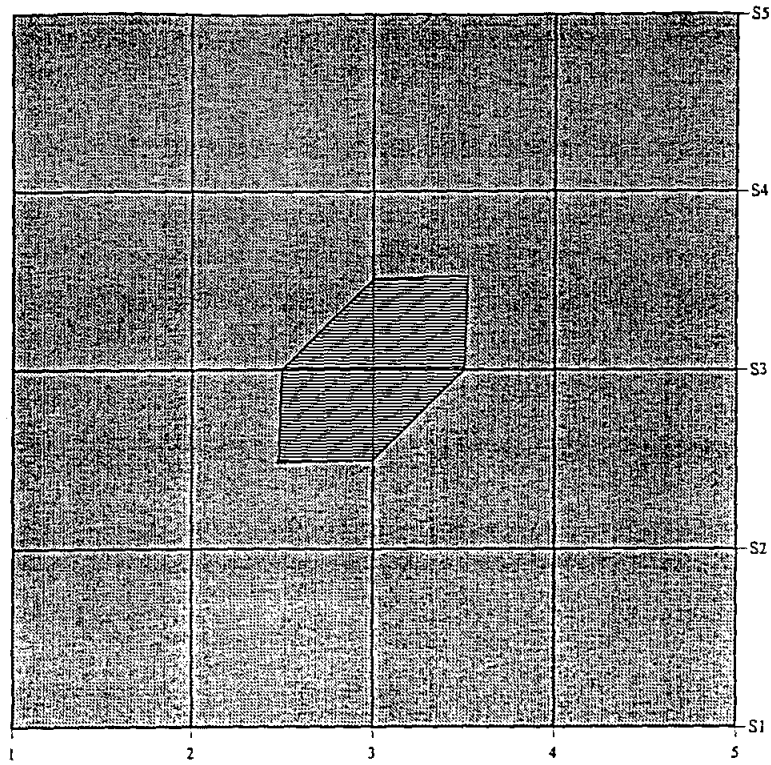


Figure 6.3a TNA image of a 550gm simulant at the center of a response grid.

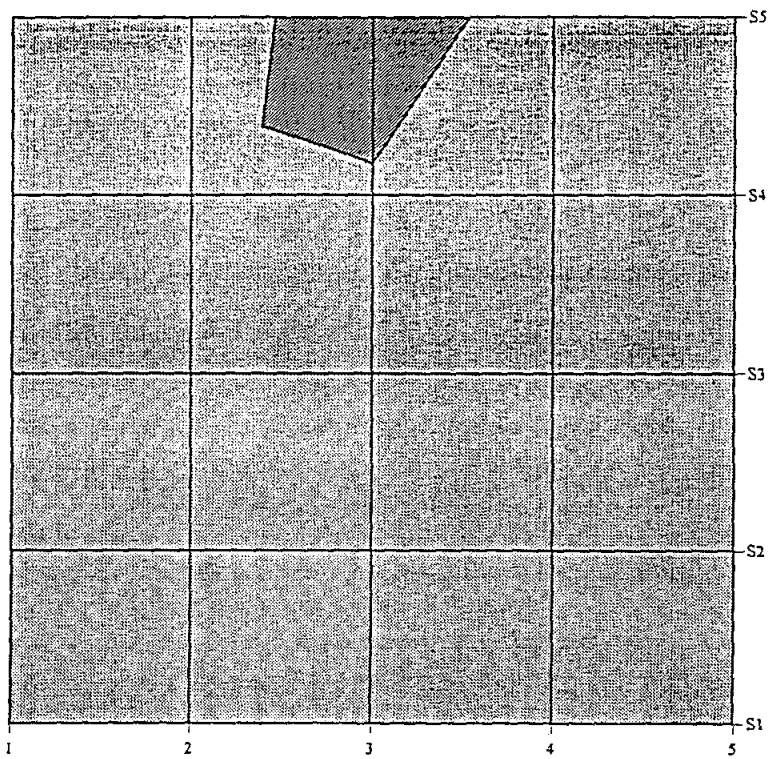


Figure 6.3b TNA image of a 550gm simulant at the edge of a response grid.

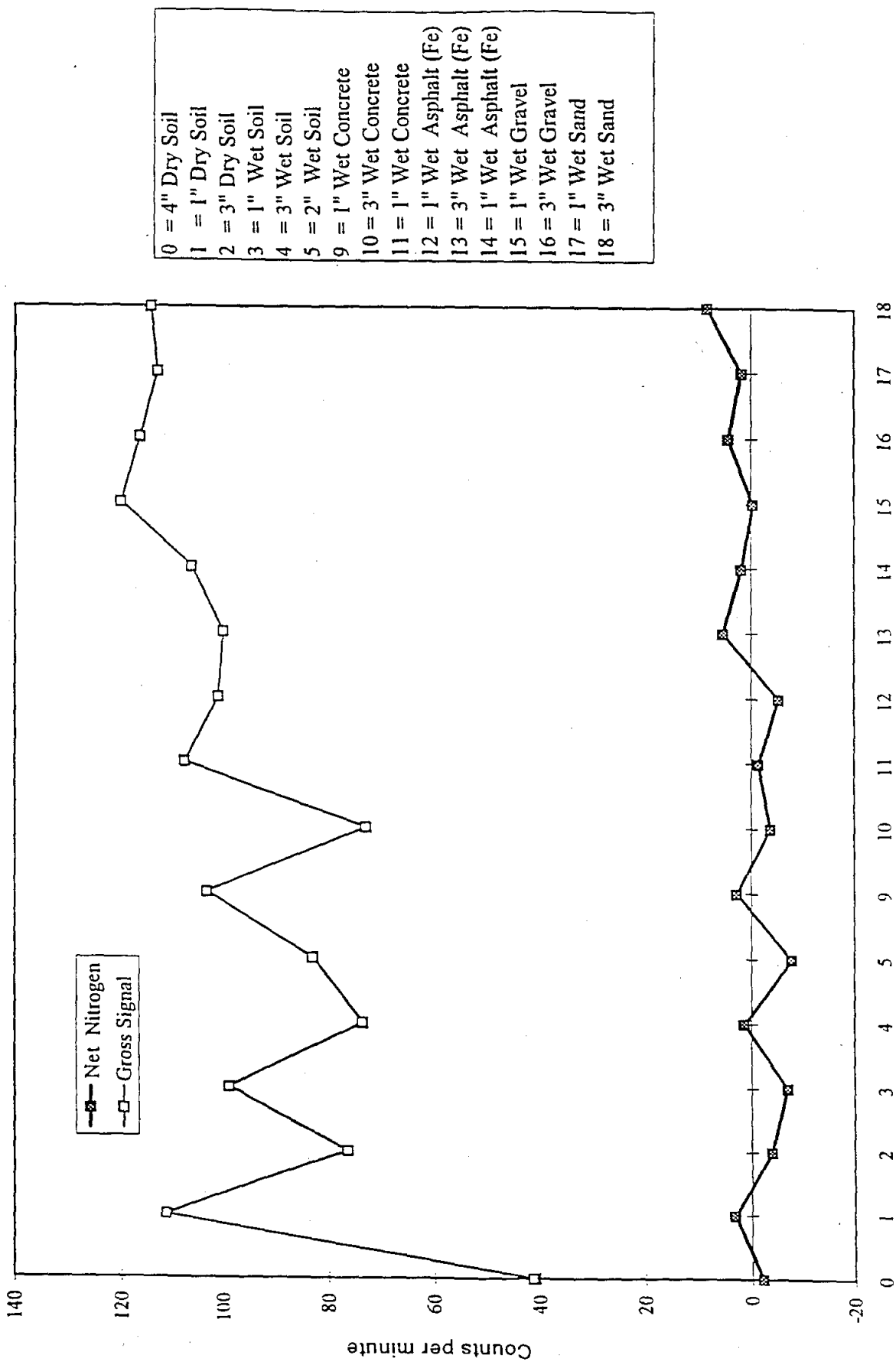


Figure 6.4 TNA "noise" reduction. Signal processing "nulls out" signal in nitrogen region of spectrum as shown for eighteen different ground types.

6.3 FIELD TEST RESULTS FROM THE OCDT PROGRAM

During the OCDT, a prototype TNA sensor was mounted on a multi-sensor remotely-controlled vehicle. The TNA sensor was used as a secondary sensor to confirm the presence of a mine or clearing metal detections from a 2 meter flexible Schiebel metal detector array. During the actual test period, the TNA sensor demonstrated that it was able to image buried anti-tank and large anti-personnel mines.

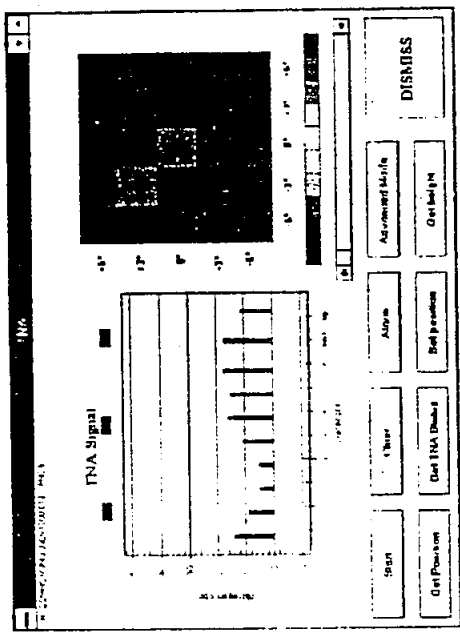
In most cases the TNA sensor was allowed a time budget of 5 minutes to form an image. On the paved road, tests were conducted to establish a minimum detection time, which was less than 1 minute for anti-tank mines. These results are discussed below.

Table 6.1 summarizes the detection capabilities of the TNA in the tests. Overall, the TNA showed its ability to act as a confirmatory sensor, and as a primary sensor on paved roads for interrogating filled pot holes.

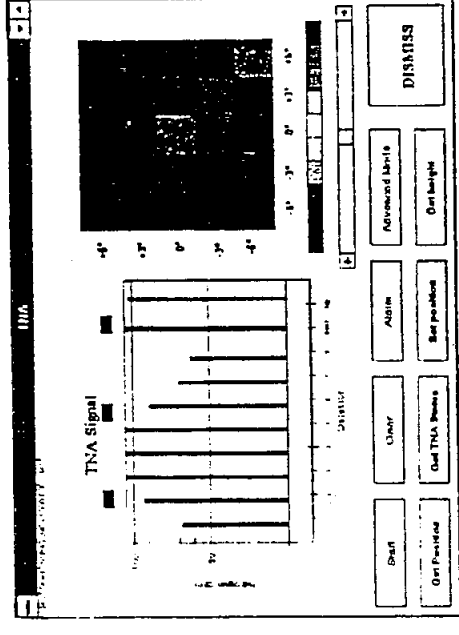
Table 6.1 TNA Sensor Mine Detection Results

MINE	MINE TYPE	EXPLOSIVE/QTY.	TNA
M15	Anti-tank mines - metal	RDX/15.4 lb.	Detectable
TMD44	Anti-tank mines - metal	TNT Dynamite	Detectable
TM62	Anti-tank mines - metal	HE/15.4 lb.	Detectable
M19	Anti-tank mines - plastic	Comp B/20 lb.	Detectable
VS2.2	Anti-tank mines - plastic	Comp B/4.7 lb.	Detectable
VS1.6	Anti-tank mines - plastic	HE/4.1 lb.	Detectable
PMD6	Anti-personnel mines - large, metal	TNT/0.44 lb.	Detectable
M14	Anti-personnel mines - small, minimum metal	Tetryl/0.06 lb.	Below demonstrated level of sensitivity
TS50	Anti-personnel mines - small, minimum metal	T4/0.11 lb.	Marginal (detected once)
VS50	Anti-personnel mines - small, minimum metal	RDX/0.095 lb.	Below demonstrated level of sensitivity

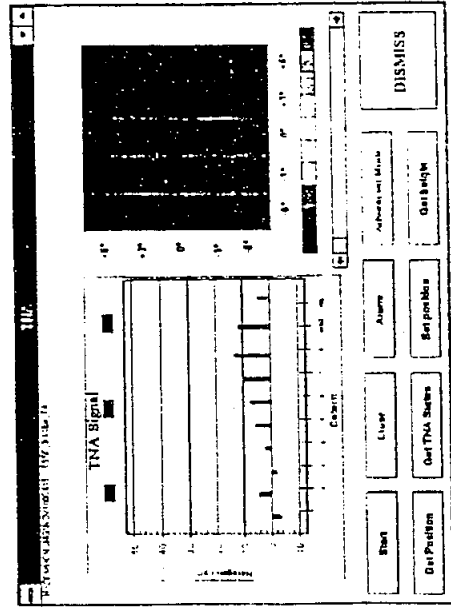
The TNA data was recorded as a set of eight detector responses from which a TNA image of the mine was produced. Based on suggestions that arose during the field tests, the individual detector response was added to the TNA image screen for the post processed data. In addition, two "features" indicative of the presence of a mine were added, namely the average signal in all detectors and the highest average signal in three adjacent detectors. Figure 6.5a shows TNA images of four buried mines. In the image of the largest of the mines, the M15 (lower right), individual detector response is shown in the first eight bar graphs; in this image detectors 3, 4 and 5 are off the display scale. The ninth bar graph



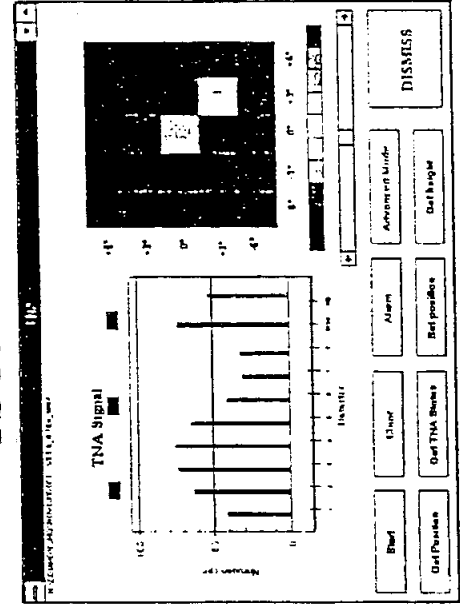
PMD6



M15 - in soil

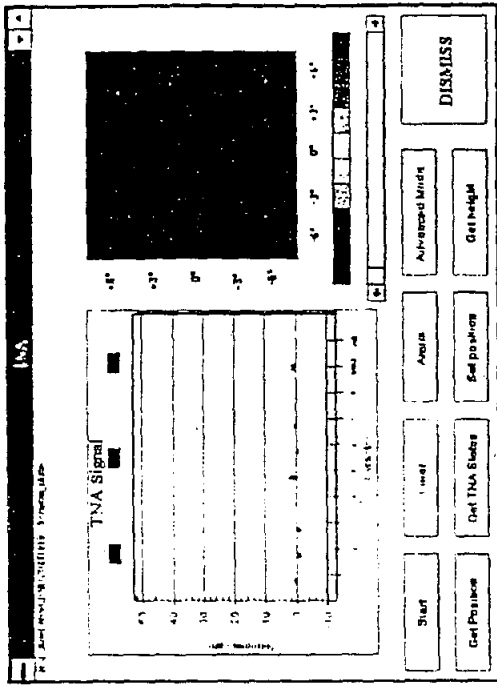


TS 50

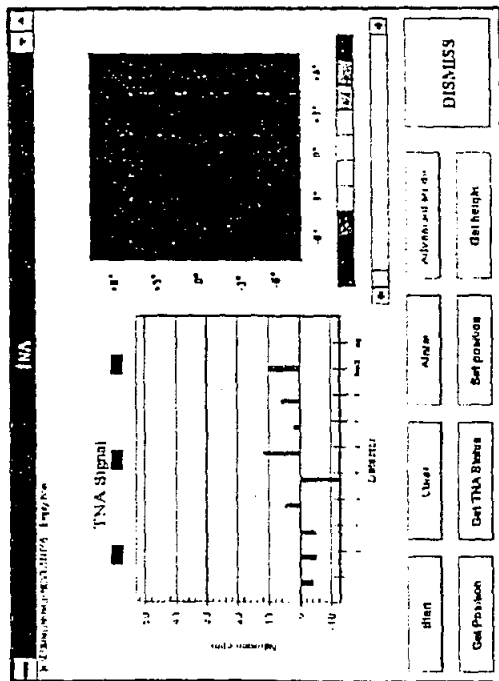


VS1.6

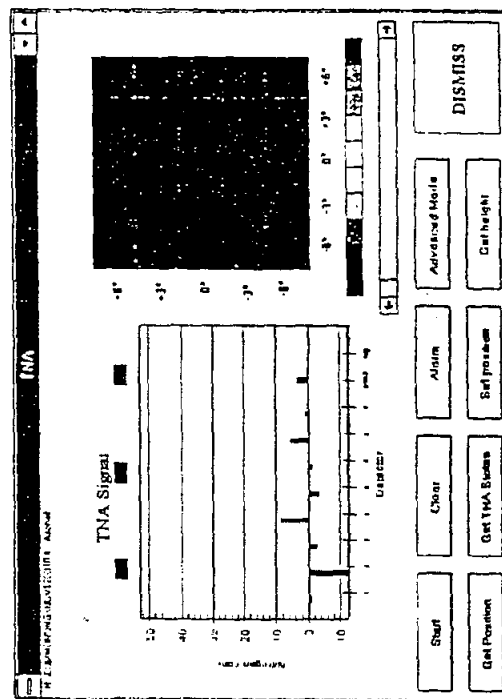
Figure 6.5a TNA operator screens for various sizes of buried mines.



Schiebel Clutter Alarm - soil



Concrete Road



Asphalt Road

Figure 6.5b TNA operator screens showing null response to different ground types.

is the average signal of the highest three adjacent detectors (also off scale) and the tenth bar graph is the average of all detectors. The image on the right is a spatial representation of the mine position under the TNA sensor. The front of the TNA sensor is to the right of the image.

The TNA images for other buried mines, a small anti-personnel mine (TS50), a larger anti-personnel mine (PMD6), and a small and large anti-tank mines (VS1.6 and M15) are also shown in Figure 6.5a. These data were taken in the various test areas and will be described below. When properly calibrated the TNA was insensitive to the various ground compositions of the test areas and metal clutter. Figure 6.5b shows the TNA sensor response to the concrete road, the asphalt road and metal clutter buried in soil (which alarmed the metal detector array), when no mine is present, demonstrating that the TNA is insensitive to ground surface and clutter.

6.4 STABILIZATION

During field tests of the TNA sensor on the VMDT platform, it was recognized that automatic gain stabilization was required for extended operations. The need of calibration can be observed in Figure 6.6. The solid curve shows the temperature as a function of time and the curve with symbols shows the position of the 10.8 MeV peak. The variation of the peak centroid as a function of temperature requires the implementation of stabilization or automatic energy calibration.

A software package was developed and tested which used the known peak positions of various capture gamma ray lines in the spectra to determine the gain function. This function was then used to determine the position of the nitrogen region and other regions of the spectra for signal processing.

An overnight test was run to quantify the stability of the system. The standard deviation of the NET Nitrogen signal, and the error in energy calibration were looked at as a measure of the system's stability. The test consisted of a static test with sand, a 40 mm and 81 mm shells. The system was calibrated, then set to calibrate itself every 10 minutes. At the end of each 10 minute calibration cycle, the system performed an energy calibration, and reported various parameters to a log file. The log file was then analyzed to determine the quality of stabilization. Additional tests were carried out in the field tests in Socorro and Yuma showing that the stabilization was able to correct for energy drifts.

6.5 SYSTEM IMPROVEMENT

Various system modifications were identified with the experience gained during the Socorro test to improve the performance of the TNA sensor:

- Increase of number of detectors from 8 to 12
- Improved shielding
- Increase of source strength

Detector 1

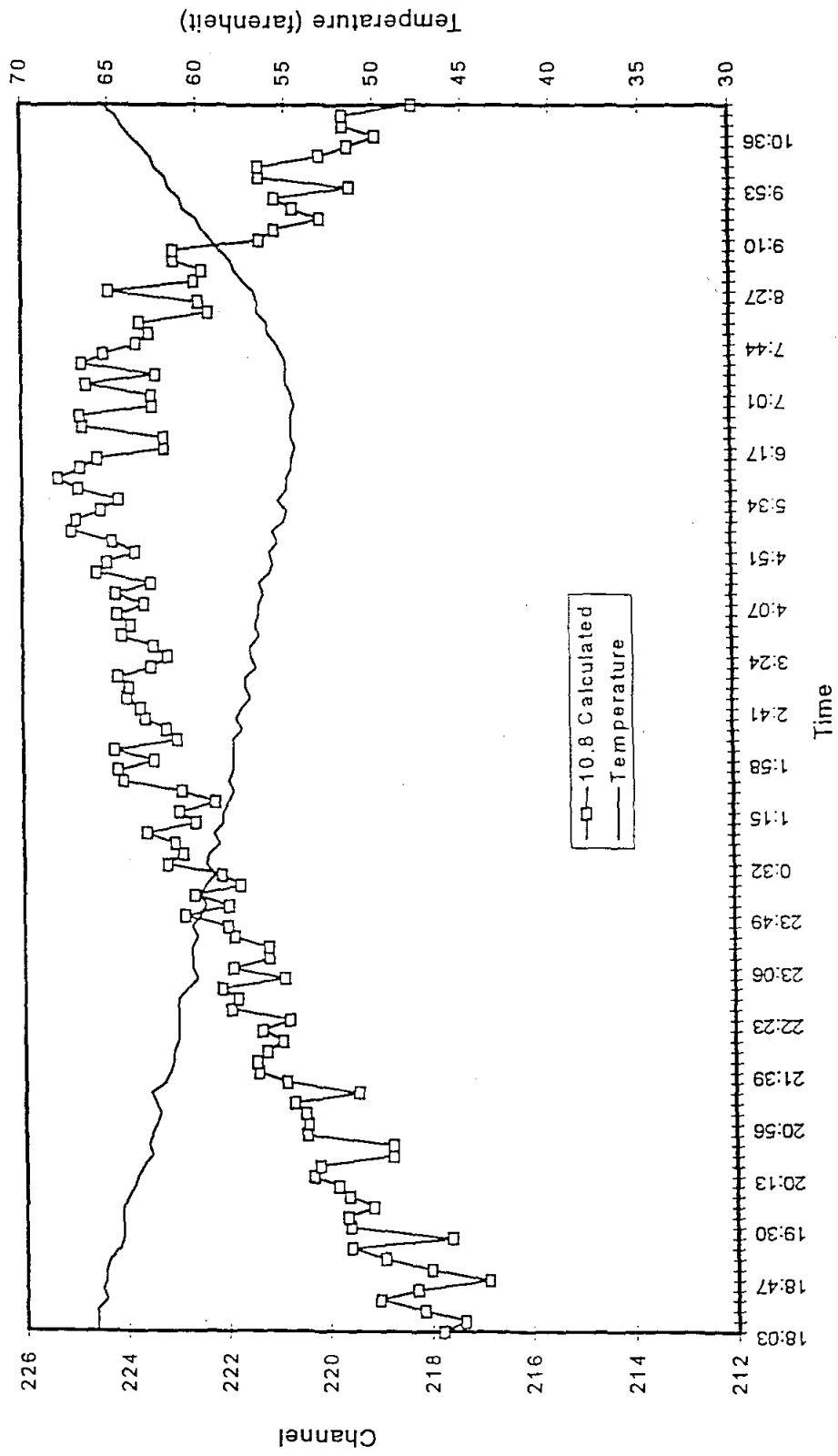


Figure 6.6 Detector gain drift followed by automated stabilization software.

The number of detectors were increase from 8 to 12 with no additional electronic components. This is equivalent to reducing the inspection time by 35%. Figure 6.7 shows the configuration of the TNA sensor with 12 detectors. Experiments were carried out to determine the reduction of the detector count rates with additional shielding. The total count rate dropped from 125,000 cps to 95,000 cps, while the source term contribution in the nitrogen region dropped from 40 cpm to 30 cpm.

The maximum source intensity that the detectors can operate without significant pileup was investigated. Preliminary results show that sources larger than the original source were producing some pileup that might introduce systematic errors in the background subtraction.

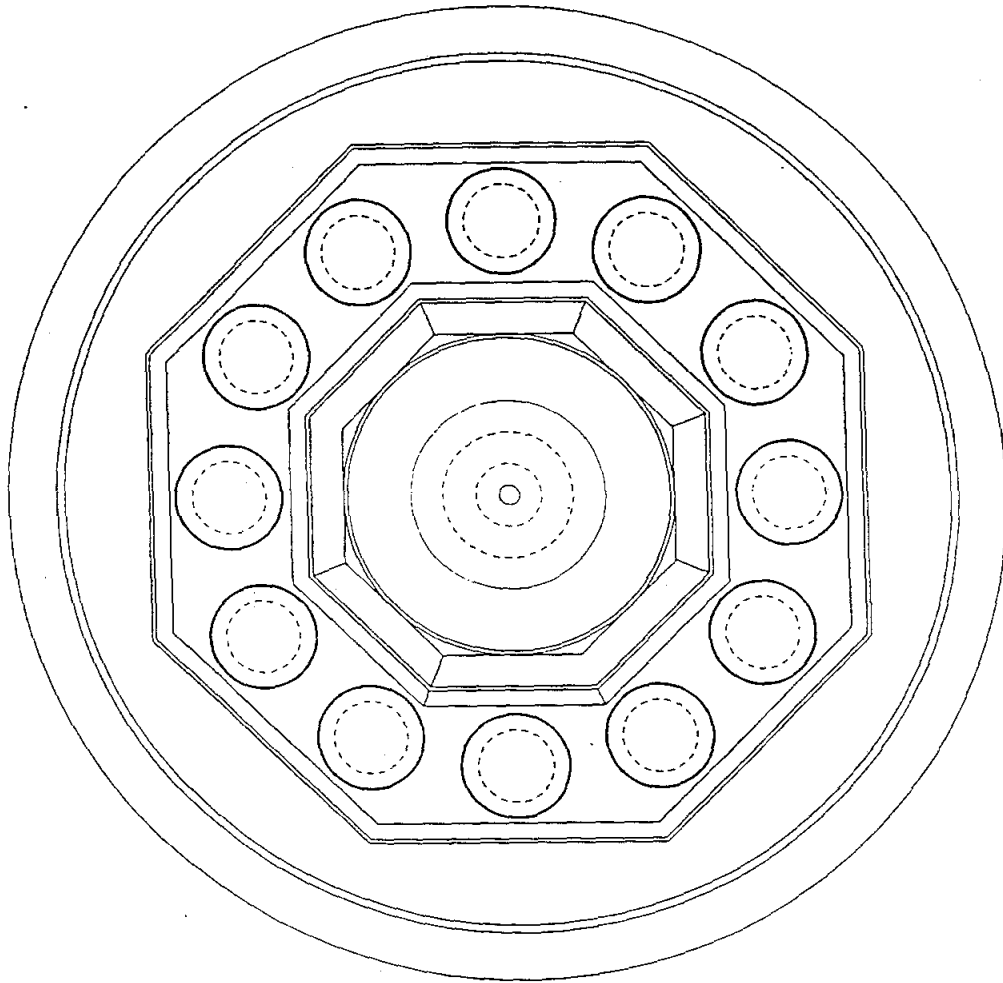
6.6 SOURCES OF ERRORS

The sources of errors in the computation of the net nitrogen region are classified as statistical and systematic. The statistical errors are based on counting statistics and propagation of the errors introduced by the SCM. The system average error for a large number of measurements is 0.92 counts/minute.

The sources of systematic errors include the error introduced by incorrect energy calibration, variation in spectral shape, variation of dead time, variation of electronic thresholds, effect of temperature to the detector response and to the electronics.

The systematic error due to the variation of the energy calibration was quantified with the set of measurements described in Section 6.4. The results were histogrammed and are shown in Figure 6.8. The solid curves correspond to gaussians with mean and standard deviation of the observed values. To determine whether the error is statistically dominated, two 10 minute, and four 10 minute measurements were combined. The standard deviations were computed to be 0.86, 0.62 and 0.38 for 10, 20 and 40 minute respectively. The nearly square root of time dependence shows that the systematic errors introduced by the energy stabilization are very small.

To determine the systematic errors introduced due to variation of spectral shape the net nitrogen counts obtained for measurements used in the determination of the SCM coefficients were histogrammed (Figure 6.9). The standard deviations were computed for each detector and for the sum of 12 detectors. The results are shown in Table 6-2 with the corresponding statistical errors.



SAIC-97GB-48

Figure 6.7. Configuration of the TNA Sensor Using 12 Detectors.

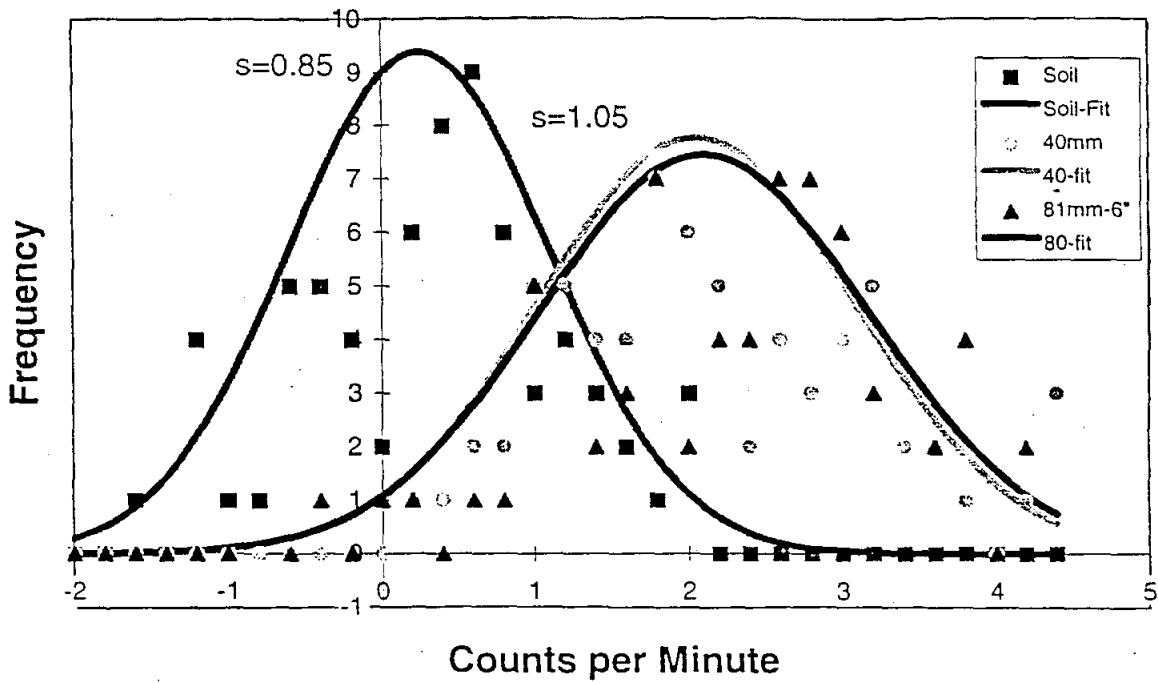
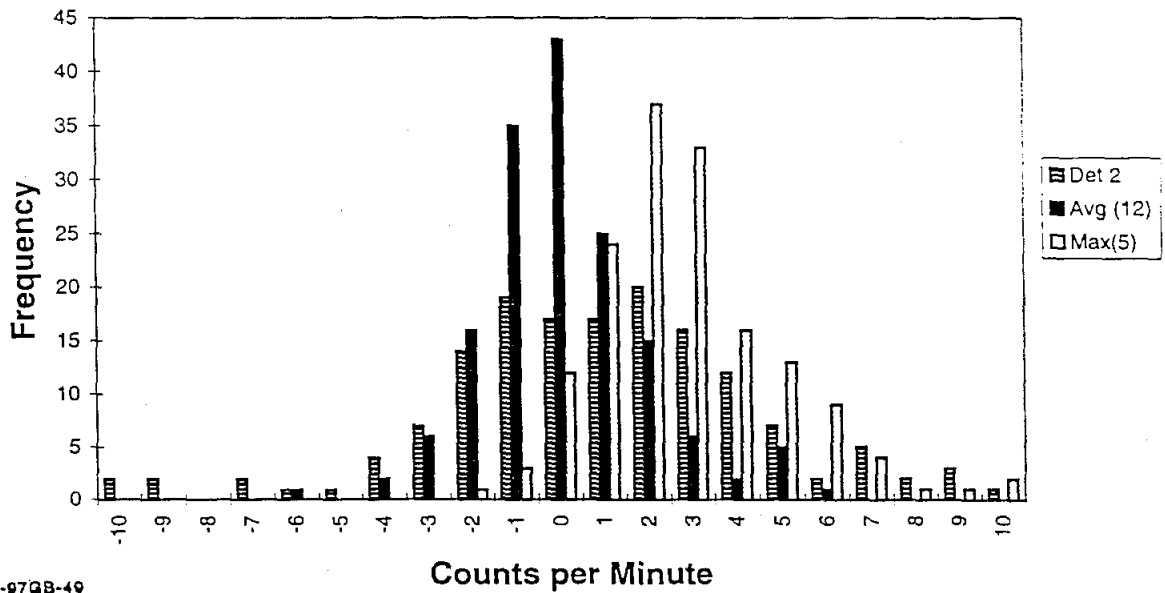


Figure 6.8. Distribution of Net Nitrogen Counts with 10 Minute Acquisitions.



SAIC-97QB-49

Figure 6.9. Distribution of Net Nitrogen Counts (SCM Data).

TABLE 6-2 Standard Deviations for 10 minute measurements normalized to 1 minute

Detector No	System	Statistics	Systematics
1	2.88	3.01	0.00
2	2.70	2.91	0.00
3	3.32	2.98	1.45
4	2.85	3.05	0.00
5	2.86	3.04	0.00
6	2.97	2.90	0.64
7	3.05	3.04	0.28
8	3.18	2.94	1.20
9	2.89	3.02	0.00
10	3.16	3.13	0.47
11	3.35	2.89	1.69
12	3.71	3.14	1.98
Prop. (12)	0.89	0.87	0.28
Avg.(12)	1.11	0.87	0.69
Max.(5)	1.30	1.35	0.00

The larger measured error of 1.11 compared with the statistical 0.92 shows that there is an additional error due to systematics (0.63). If there is no correlation between the statistical and systematic errors, for infinite time the error will go down to 0.63. Significant improvement in the UXO detection using TNA technology requires reduction of the systematic errors.

7. NAVIGATION AND MAPPING

7.1 OVERVIEW

Navigation and mapping have been identified as very important ingredients in a system intended to detect UXO. Accordingly, a good deal of emphasis has been put on these subjects all along the project. We have chosen to use differential GPS as the cornerstone of our navigation system. Although other systems exist that can provide better positional accuracy, the advantages of GPS are that it is absolute, it does not require setting up a local reference system (such as beacons), and that it can, in itself, provide all the needed navigational elements, including orientation and distance traveled.

As the vehicle travels, availability in real time of its position and orientation allows us to display a map or an image of the metal detector array signals. This can be done both in a small scale, displaying the area immediately in front of the vehicle (waterfall display in detection window), or in a large scale (showing ground coverage and the path of the vehicle in a navigation window).

In what follows, we first give details on the transformations and systems of coordinates used by the software navigation module. Secondly, we present some results on the performance of the various navigation elements.

7.2 SYSTEMS OF COORDINATES AND TRANSFORMATIONS

Four systems of coordinates are used to represent both the position of the vehicle and the metal detector signals. The systems of coordinates which are used are illustrated in Figure 7.1 and described below:

Local System (Navigation Window)

This system of coordinates is fixed with the site, and is characterized as follows:

Units: meters
X axis: Points East
Y axis: Points North
Origin: User defined, such that the current position of the GPS antenna is at ΔX , ΔY from the origin

Local Pixel System (Navigation Window)

This system of coordinates is fixed with the display screen, and is characterized as follows:

Units: pixels
IX axis: Points right
IY axis: Points down
Scale: Specified by user (number of pixels per meter)
Origin: Default value

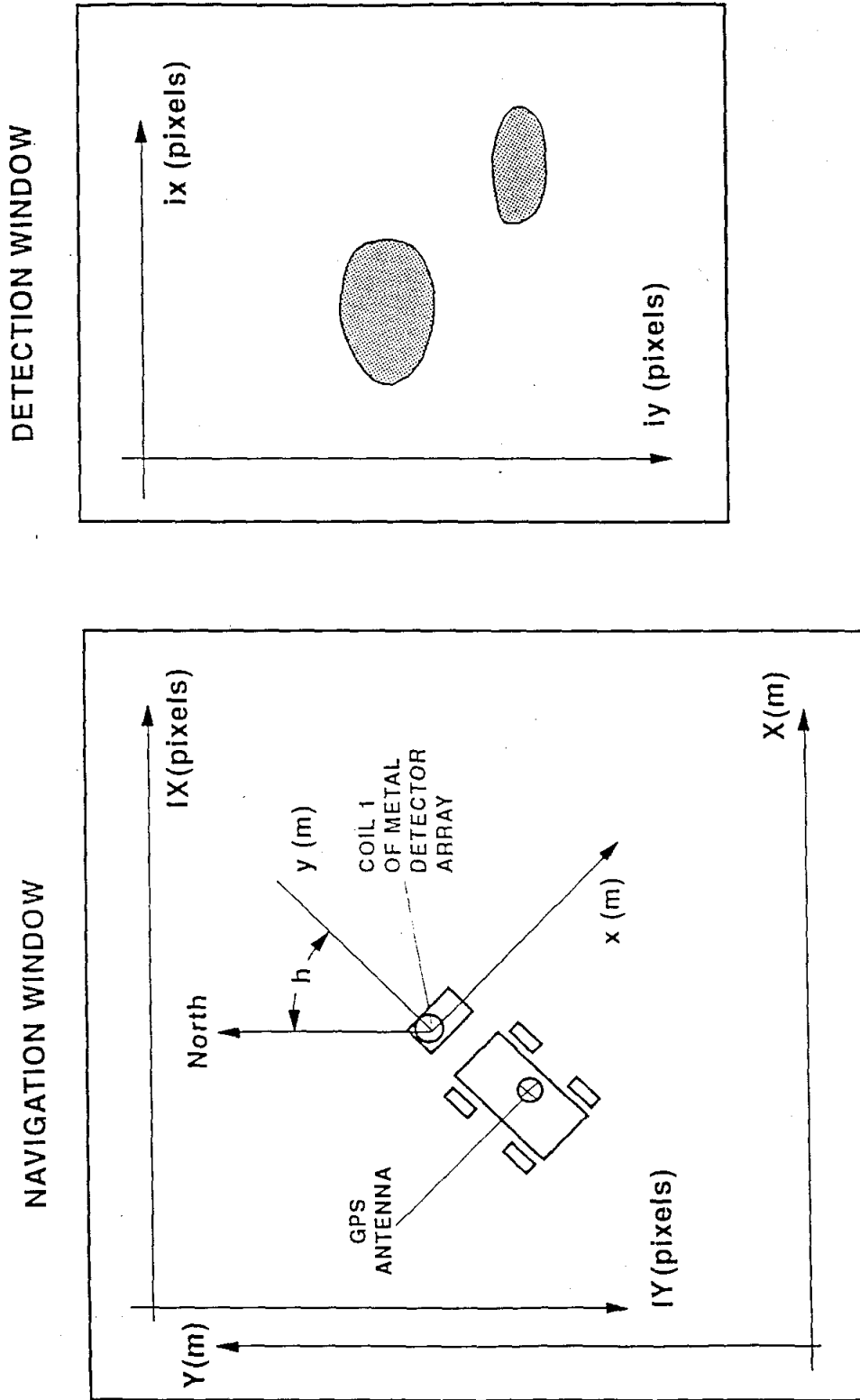


Figure 7.1 Systems of coordinates for navigation and detection windows.

Vehicle System (Detection Window)

This system of coordinates is fixed with the vehicle, and is characterized as follows:

Units: meters
x axis: Points to the right of the vehicle
y axis: Points to the front of the vehicle
Origin: Center of coil #1 in the metal detector array.

Vehicle pixel system (detection window)

This system of coordinates is fixed with the display screen, and is characterized as follows:

Units: pixels
ix axis: Points right
iy axis: Points down
Scale: Default value (number of pixels per meter)
Aspect ratio: Specified by user through a variable COMPRESS. For example, COMPRESS = 3 means that the display in the detection window is compressed three times in the iy (vertical) direction. This is done in order to display a longer stretch in front of the vehicle.
Origin: Default value

The following transformations (and their inverses) are used to convert from one system of coordinates to another:

Transformation from Pixels to Meters (Detection Window)

$$x = \frac{ix - ix_0}{VEH_PIX_PER_METER}$$

$$y = -\frac{(iy - iy_0) * COMPRESS}{VEH_PIX_PER_METER}$$

where

ix_0, iy_0 = origin of the detection window on the screen,

VEH_PIX_PER_METER = number of pixels per meter in the pixel vehicle system,

COMPRESS = compression factor in the y direction.

Transformation from Meters to Pixels (Navigation Window)

$$IX = IX_0 + X * NAV_PIX_PER_METER$$

$$IY = IY_0 - Y * NAV_PIX_PER_METER$$

where

IX_0, IY_0 = origin of the navigation window on the screen,

$NAV_PIX_PER_METER$ = number of pixels per meter in the local pixel system.

Transformation from Vehicle System to Local System

In order to use the following equations the origin of the local system must have been defined first.

$$X = X_{GPS} + (x - x_{antenna}) \cos(h) + (y - y_{antenna}) \sin(h)$$

$$Y = Y_{GPS} - (x - x_{antenna}) \sin(h) + (y - y_{antenna}) \cos(h)$$

where

$x_{antenna}, y_{antenna}$ = coordinates of the GPS antenna in the vehicle system,

$$X_{GPS} = (360 - \text{longitude}) \cos(\text{site_lat}) * NAV_CONST - X_{origin},$$

$$Y_{GPS} = \text{latitude} * NAV_CONST - Y_{origin},$$

longitude = current longitude in degrees,

latitude = current latitude in degrees,

site_lat = latitude at the origin of the navigation window,

h = heading or orientation of the vehicle measured clockwise from the North direction,

$$NAV_CONST = 111,194.93 \text{ meters/deg.}$$

X_{origin}, Y_{origin} and site_lat are computed when the user defines the origin of the local system, as follows:

$$\text{site_lat} = \text{latitude}$$

$$X_{origin} = (360 - \text{longitude}) \cos(\text{site_lat}) * NAV_CONST - \Delta X$$

$$Y_{origin} = \text{latitude} * NAV_CONST - \Delta Y$$

($\Delta X, \Delta Y$ represent the position of the GPS antenna from the origin of the local system when the origin itself is defined).

Transformation from Local System to Vehicle System

In order to use the following equations the origin of the local system must have been defined first.

$$x = x_{\text{antenna}} + (X - X_{\text{GPS}}) \cos(h) - (Y - Y_{\text{GPS}}) \sin(h)$$

$$y = y_{\text{antenna}} + (X - X_{\text{GPS}}) \sin(h) + (Y - Y_{\text{GPS}}) \cos(h)$$

7.3 IMPLEMENTATION

In order to use the navigation equations described in Section 7.2, one needs a number of parameters, or constants, and the following four variables, which are updated periodically in real time as the vehicle moves: latitude, longitude, heading, and distance traveled.

Latitude and longitude are provided by the differential GPS and are used to plot a symbol (corresponding to the instantaneous location of the GPS antenna) in the navigation window.

The heading is used to plot a symbol of the vehicle and to calculate the position of points other than the center of the antenna.

The distance traveled is used to scroll the image of the metal detector array signals in the detection window. While latitude and longitude must be obtained by differential GPS, there are two independent ways of obtaining heading and distance travelled.

7.3.1 Hardware

The navigation system is comprised of a wheel encoder, a differential GPS, and a digital compass.

The encoder is intended to provide short range accuracy (order of one inch). It allows one to display images of the metal detector signals and to control the motion of the vehicle in positioning the TNA over a detected target.

The differential GPS is intended to provide long range accuracy (order of one meter or less). It allows one to display a symbol of the vehicle in a navigation window and to record the position of detected targets. The differential GPS consists of an Ashtech Super C/A (Model SCA12) receiver, with 12 independent channels. Another Ashtech SCA12, with base station option, is used to generate the differential corrections in RTCM 104 format. The corrections are transmitted from the base station to the vehicle GPS receiver using RF modems. In areas where the service is available, such as in San Diego, we have also used the differential corrections broadcast by DCI Inc. through an FM station. The Ashtech unit is configured to make code-phase (not carrier-phase) measurements, and can provide latitude and longitude updates once every second. Communication between the Ashtech GPS and the on-board computer is by RS-232. In addition, the SCA-12 can provide other information that can be used to assess the accuracy of the measurements.

The digital compass (Model TCM2 by Precision Navigation, Inc.) provides the heading of the vehicle and is accurate to a tenth of a degree. The TCM2 combines a three-axis magnetometer and a two-axis tilt sensor. The tilt sensor allows the microprocessor in the compass to internally correct the compass indications for tilt. The digital compass is needed to plot the symbol of the vehicle in the correct orientation and is also used to calculate the coordinates of a detection (because the GPS antenna, of which latitude and longitude are determined, is not located at the same position as the detector, either Schiebel coil or TNA unit).

7.3.2 Compass and Wheel Encoder

The most direct way of obtaining heading and distance traveled is by using dedicated hardware, namely an electronic compass and an encoder attached to the wheels. In this case the heading is provided by the compass as follows:

$$h = h_{\text{mag}} - h_0$$

where h_{mag} is the output of the compass and h_0 is the magnetic declination. In order for the compass to provide correct values it must have been subjected to a multipoint calibration which corrects for hard iron field effects due to ferromagnetic masses on the vehicle.

The distance traveled is directly proportional to the wheel encoder value. The encoder is calibrated in meters. The amount to be scrolled between two successive times t_1 and t_2 is (in pixels)

$$\Delta(iy) = \frac{e(t_2) - e(t_1)}{\text{COMPRESS}} \text{VEH_PIX_PER_METER}$$

where $e(t)$ is the encoder value at time t .

The number of pixels to be scrolled is an integer, and an error can be accumulated. Therefore, one should keep track of the fraction that is lost by truncation and add it as soon as it accumulates to a full pixel.

7.3.3 Doppler Based Approach

GPS provides independent means for the determination of velocity and heading, based on the Doppler effect. From GPS one obtains the heading h (in degrees) and v , the velocity in kph. We define an encoder value for a fixed direction h_f as follows:

$$e(t_2) = e(t_1) + v(t_1) \left(\frac{\text{km}}{\text{hr}} \right) \frac{1000}{3600} (t_2 - t_1) \cos(h_f)$$

and the amount to be scrolled becomes:

$$\Delta(iy) = \frac{v(t_1) (t_2 - t_1) \text{VEH_PIX_PER_METER}}{3.6 \text{COMPRESS}} \cos(h_f)$$

When using the Doppler approach one should always drive in the forward direction. If we reverse the direction of motion of the vehicle, the software will interpret this as a 180 degree turn and provide an incorrect mapping.

Figure 7.2 shows a comparison of the Doppler encoder with the actual position. Figure 7.3 shows a comparison of the magnetic heading with the GPS heading.

7.4 PERFORMANCE

We have found the performance of the GPS itself to be quite reliable. Most of the time the number of satellites in view is well above the minimum required (4) for position determination. In the few instances in which we had problems with the GPS, the cause was due either to a drop in communication between the base station and the receiver, or to poor antenna positioning, or to interference from other sources. In general, we have confirmed the submeter positional accuracy claimed by the manufacturer. More accurate receivers, using carrier phase and dual frequency, are now available, and can provide real time positional accuracy of the order of centimeters.

The digital compass has a nominal precision of 0.1 degrees, which is true when the compass is stationary. When the vehicle is moving, however, several effects come into play, which affect both precision and accuracy. It is interesting to compare the stability of the orientation as provided by the compass, with that of the heading as provided by the GPS while the vehicle is moving in a straight line. Figure 7.4 shows the variation of the compass reading during a scan, while Figure 7.5 shows the variation of the GPS heading during another scan. The GPS heading shows a high frequency component. Since the GPS heading is derived from the velocity vector (Doppler effect) it is more subject to sudden jerks and vibrations of the platform.

It is felt that combining the data from the GPS, the compass, and the encoder through a filtering algorithm (such as the Kalman filter) would lead to a significant improvement of the navigation accuracy. Only a very limited attempt was made in this area. Figure 7.6 shows the result of combining GPS and encoder signals through a running least squares method. The figure shows that the trajectory is smoothed out, and the variations in position due to GPS errors are substantially reduced.

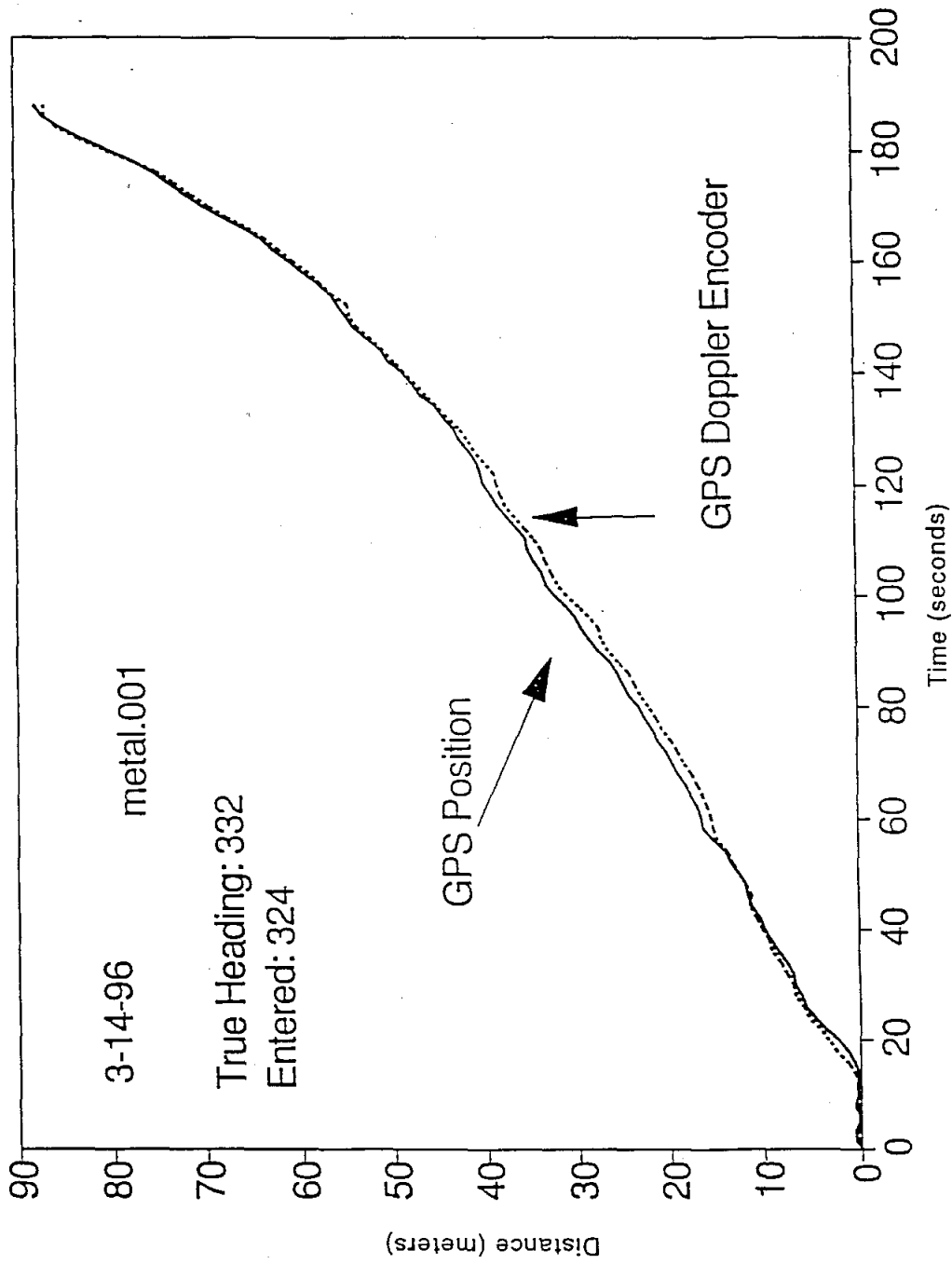


Figure 7.2 Verification of Doppler Encoder.

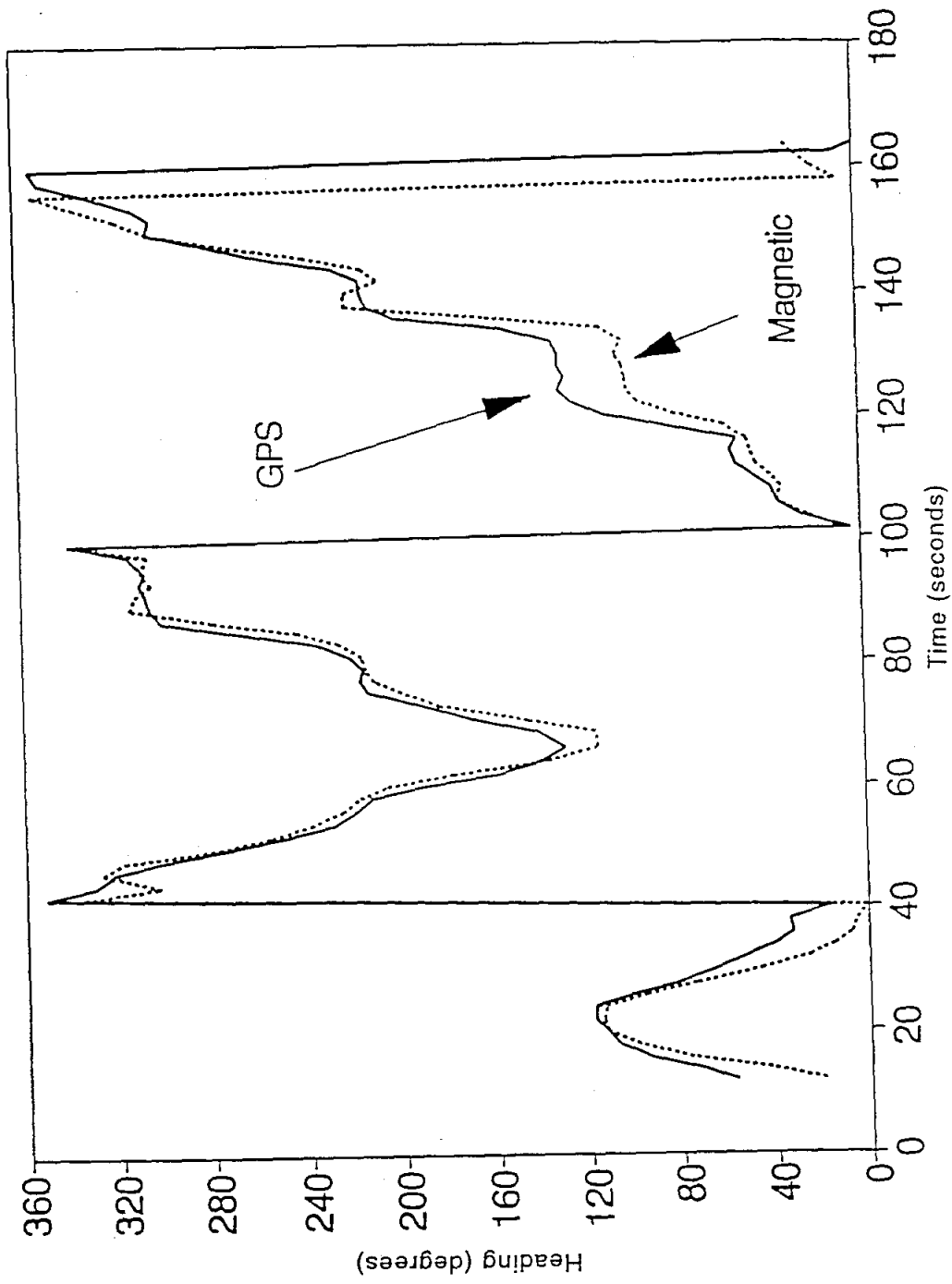


Figure 7.3 Magnetic and GPS heading.

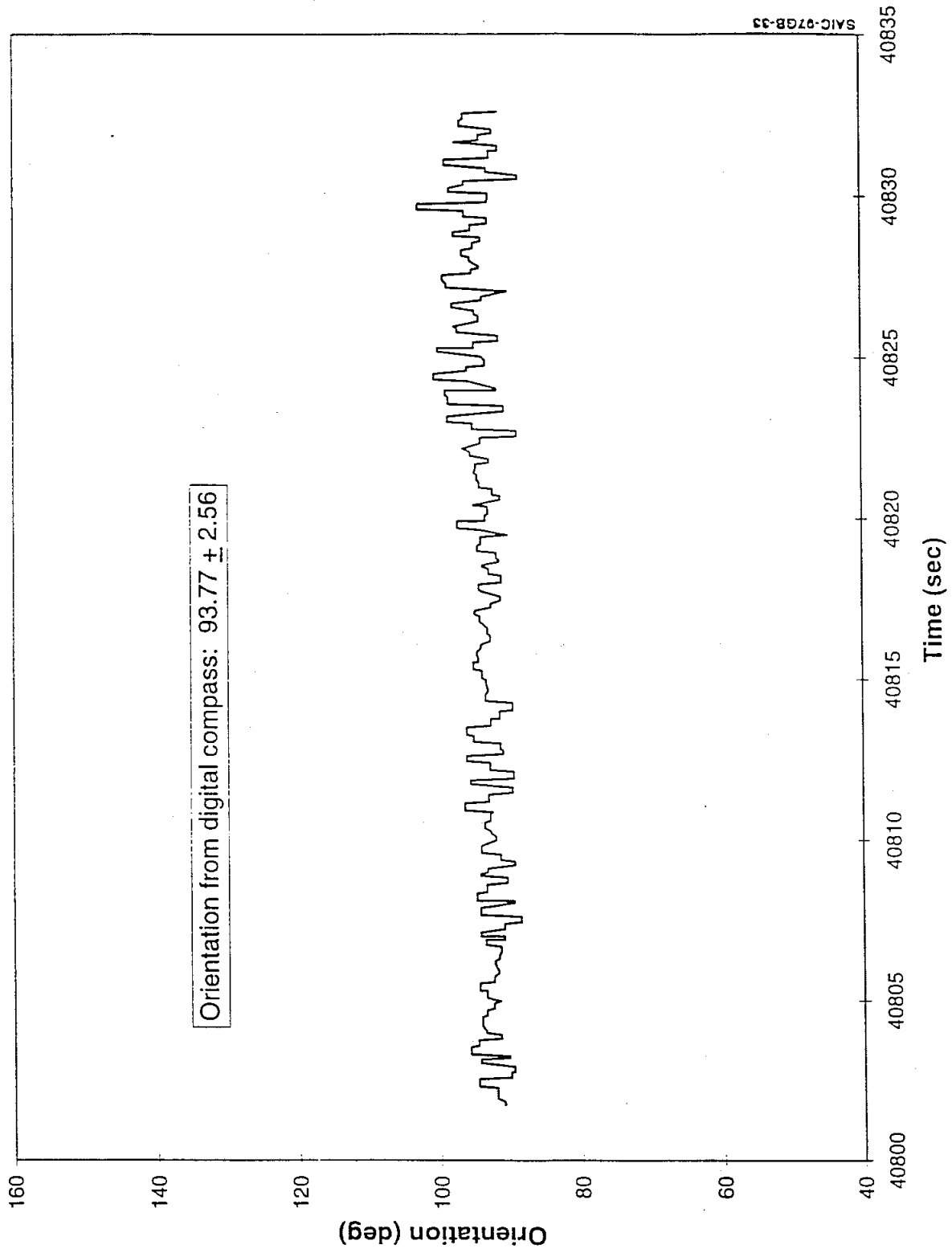


Figure 7.4. Variation of the Orientation from the Digital Compass during a Straight Line Scan.

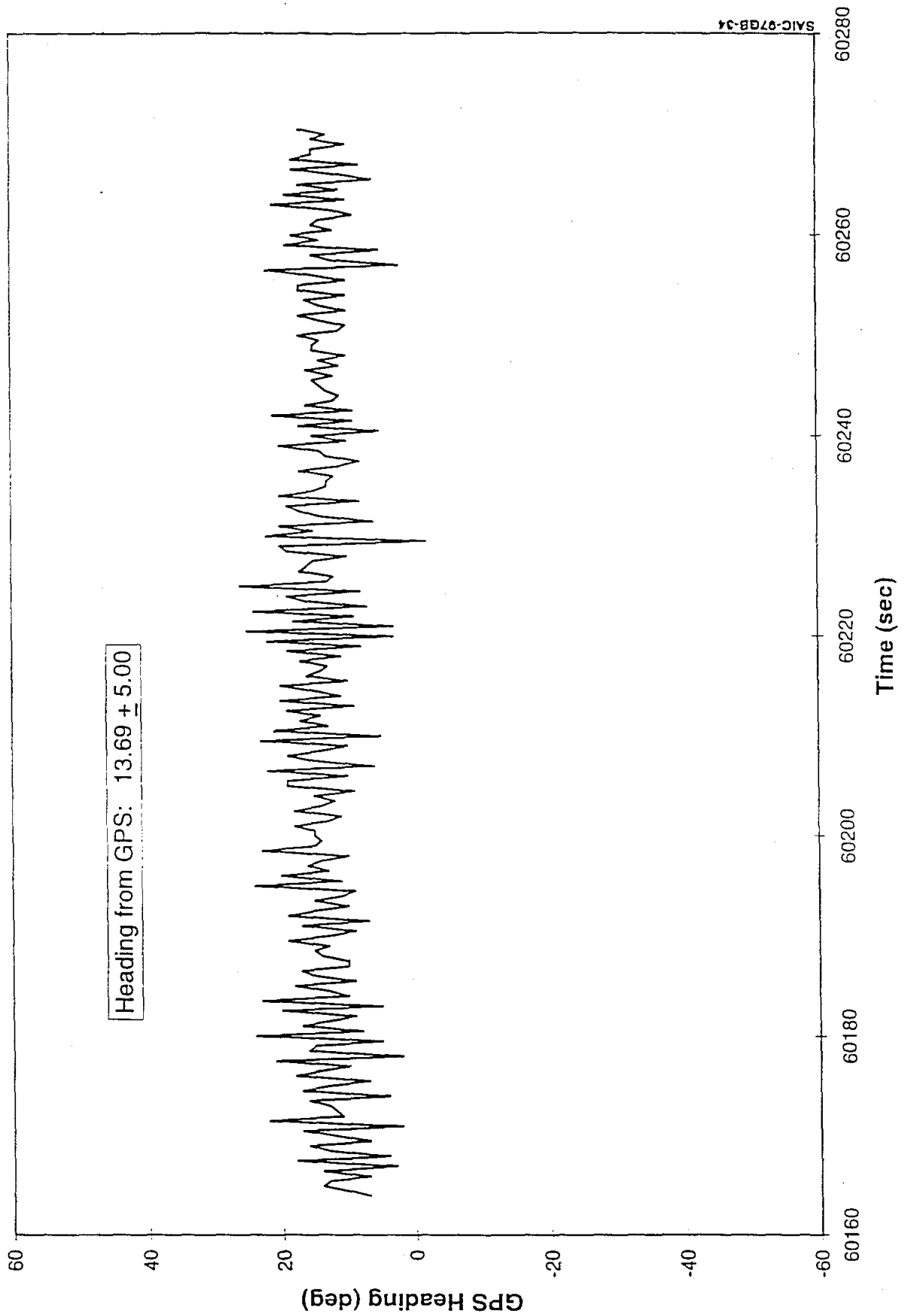


Figure 7.5. Variation of the Heading from GPS during a Straight Line Scan.

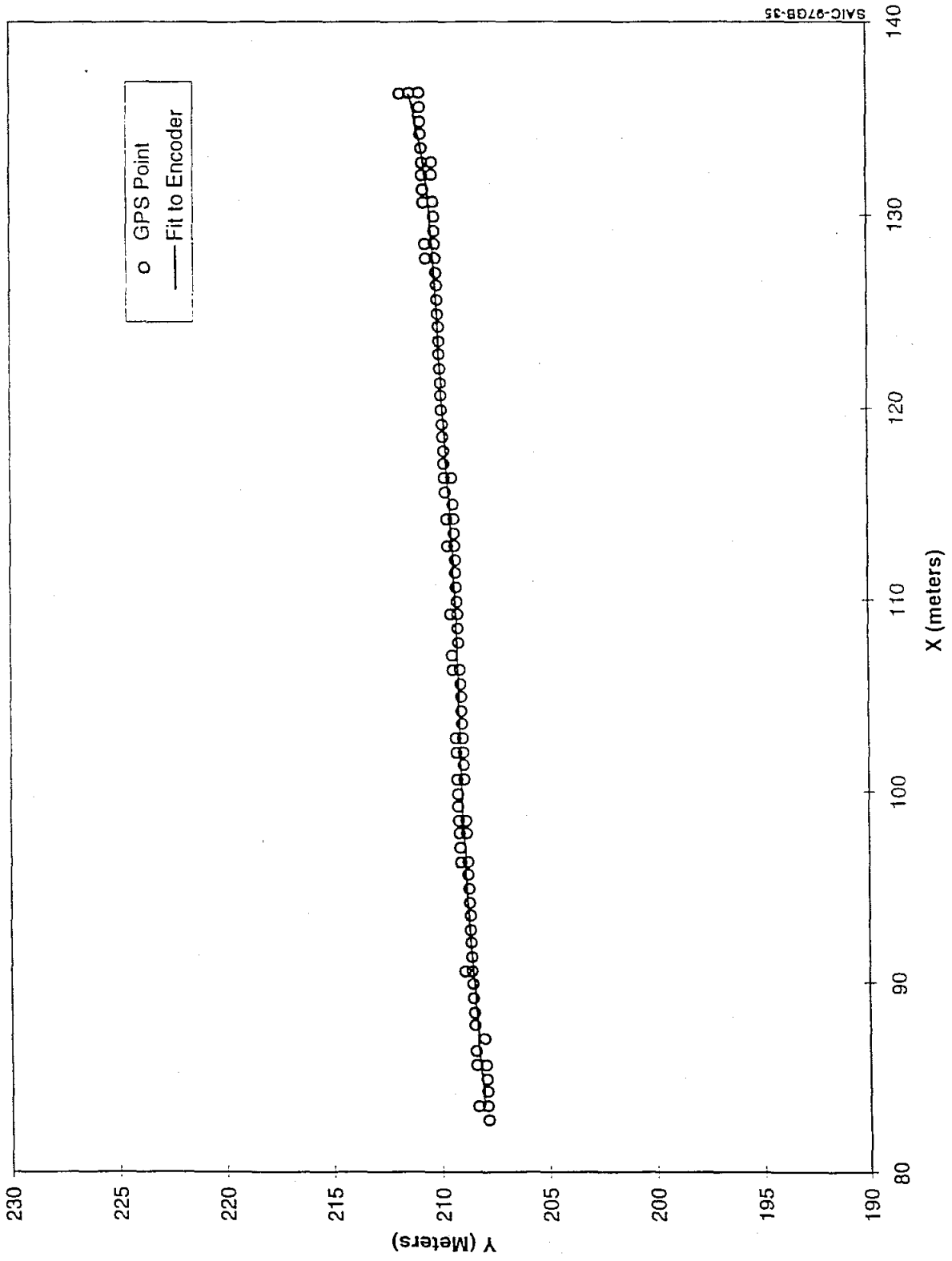


Figure 7.6. Filtering of GPS data using Running Fit to Encoder Data.

8. CONTROL STATION AND SOFTWARE

The Surface/Near Surface UXO Detector is operated remotely from a control station. The control station computer communicates via radio frequency modem with the vehicle computer. Specialized software is installed both on the control station and on the vehicle computer.

8.1 CONTROL STATION

The operator control station consists of three electronic enclosures and a remote control joystick box for vehicle control. One of these enclosures contains an RF video receiver, operating at 1720 MHz, and a standard video monitor. This monitor is used to display the zoom camera signal.

The second enclosure contains the operator console, consisting of a computer, RF data modem, color display, keyboard, and mouse, and is used for sensor control and display. The present operator display shows a detection window with a waterfall type display controlled by the encoder signal, a navigation window showing the present position and orientation of the vehicle, and a variety of commands and status parameters. Optionally, one can display a bar histogram showing the instantaneous values of the induction coil signals. All operator control commands to the vehicle computer and, hence, to the sensors, cameras, and positioning systems are input through this control console.

The third enclosure also contains a computer, RF data modem, color display, keyboard, and mouse, and is used for TNA sensor control and display.

8.2 SOFTWARE

The software has been written in Borland Turbo C under the DOS operating system. The software has undergone several stages of modification. The present version uses 256 colors and a resolution of 800 x 600 pixels. The operator interacts through the keyboard and the mouse. As far as the metal detector is concerned, the signals are displayed on a small scale in the detection window, and on a large scale in the navigation window. The instantaneous signals are displayed in the detection window, so as the vehicle moves one has a real time representation of the induction detector output over the area in front of the vehicle.

The navigation window shows the metal detector signals as they gradually build up over an area whose size is selected by the operator. The maximum value attained by the signal is displayed and stored in the buffer representing the window. Because of the fuzziness introduced by the GPS uncertainty, running the vehicle over the same area repeatedly results in "painting" of the screen and in the formation of a blob or cloud. Pointing the mouse to the centroid of such blob allows one to record the position of the detection.

The TNA software runs under Windows and displays a diagram showing the signal for each one of the twelve detectors, plus the result of the verification, and, optionally, other features such as TNA spectra.

9. SOCORRO TEST

The Socorro test was carried out with the metal detector and the TNA operated as separate sensors. Data were collected with the two sensors independently and often simultaneously. Occasionally, the two sensors shared the same vehicular platform (the Robotech vehicle).

The test was conducted at the Energetic Materials Research Test Center (EMRTC), operated by the New Mexico Institute of Mining and Technology (NMIMT) at Socorro, NM. The test was conducted during the period June 17, 1996 through June 27, 1996. Climatic conditions during the test were extremely arid with temperatures up to 105 deg F. Some high winds were encountered during the test at Socorro.

9.1 DESCRIPTION OF THE SITE

Figure 9.1 shows a general map of the area where the tests were conducted. Eight one-dimensional lanes were laid out along Track 3. Of these, one was used for calibration and the remaining ones for the blind test. The TNA data collection area was located within Track 2. The two-dimensional calibration and blind area were laid out in the field adjacent to Tracks 2 and 3. In general, the site was characterized by a very low level of metal clutter. The shielding cask containing the Californium 252 source was kept at the center of a marked exclusion area, from where the source could easily be loaded into the TNA sensor. EMRTC/NMIMT Safety Procedures were adhered to during the tests.

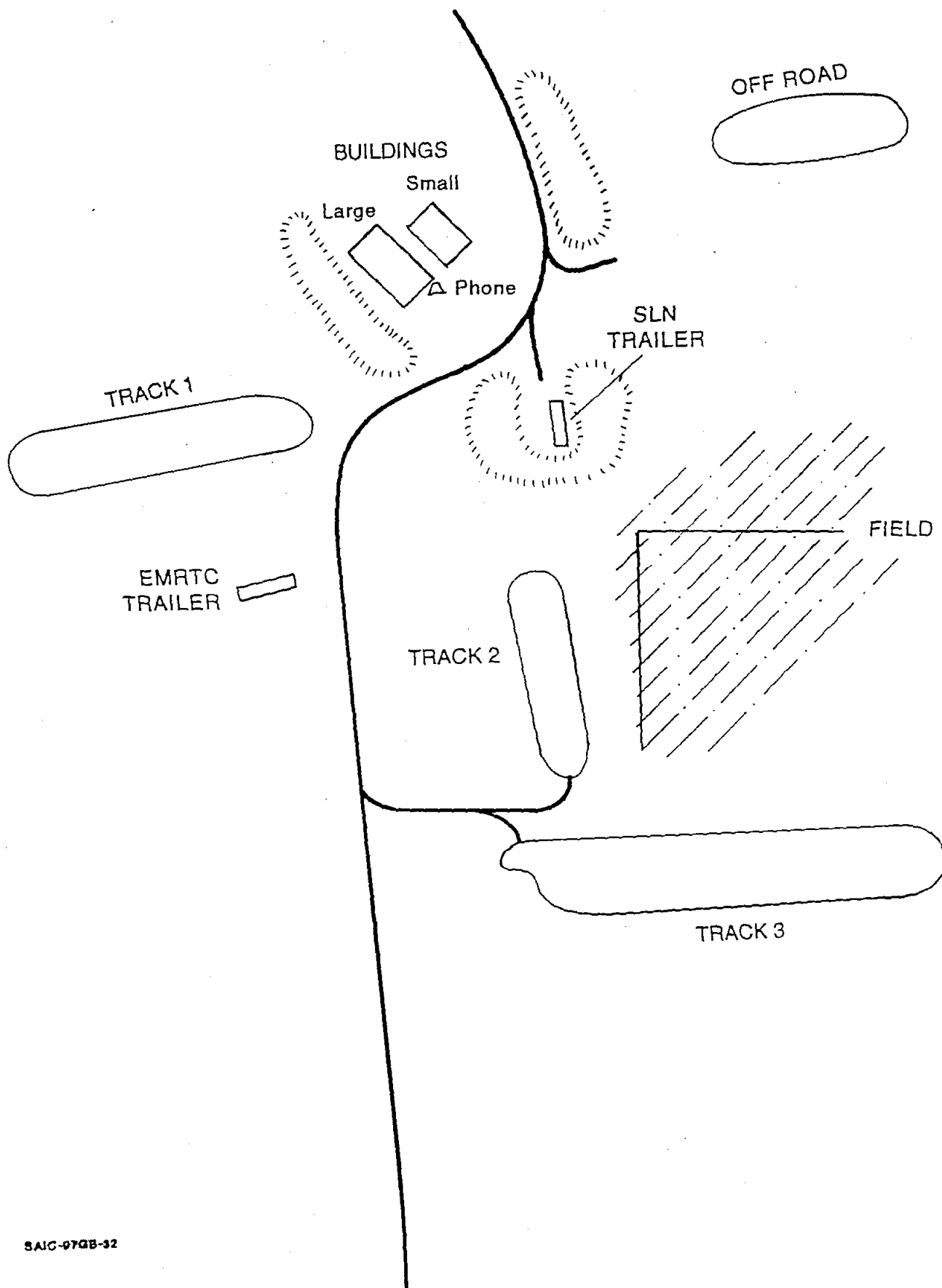
Each lane was about 100 meters long and was marked with a string tensioned along the centerline of the lane. The path to be followed was easy to see with the remote TV camera while driving the vehicle down the lane. The lanes had been graded and were quite smooth. The Government arranged for installation of a tent, under which SAIC placed the control station for the UXO detection system. The TNA sensor was controlled from its own control station located inside of a rental truck.

9.2 DESCRIPTION OF THE ORDNANCE

The targets used in the test consisted of ordnance with the fuze or devices removed for safety reasons. The type of targets, explosive contents, nitrogen content, and typical burial depth, are in Table 9.1.

Table 9-1 Ordnance Information

NAME	TYPE	EXPLOSIVE CONTENT	NITROGEN CONTENT	TYPICAL DEPTH
M56A3	20 mm HE round	10.7 g H-761 plus 38.9 g propellant	(3.53 g)+	Surface - 3 in.
M789	30 mm HEDP projectile	22 g Type PBXN-5	(7.26 g)	Surface - 3 in.
Simulant	Cylinder	100 g C4	34 g	Surface - 6 in.
Simulant	Cylinder	200 g C4	68 g	Surface - 12 in.
M49A5	60 mm mortar	.79 lb. (359 g) Comp B	111.1 g	Surface - 12 in.
M393A2	105 mm HEP-T projectile	4.4 lb. Comp B	1.34 lb. (609.3 g)	Surface - 12 in.



SAIC-97GB-32

Figure 9.1. Map of the Area used in the Socorro Test.

9.3 SUMMARY OF DATA ACQUISITION

Since data from the two sensors were collected independently at Socorro, a variety of vehicular platforms were used. Four different configurations were used, as follows:

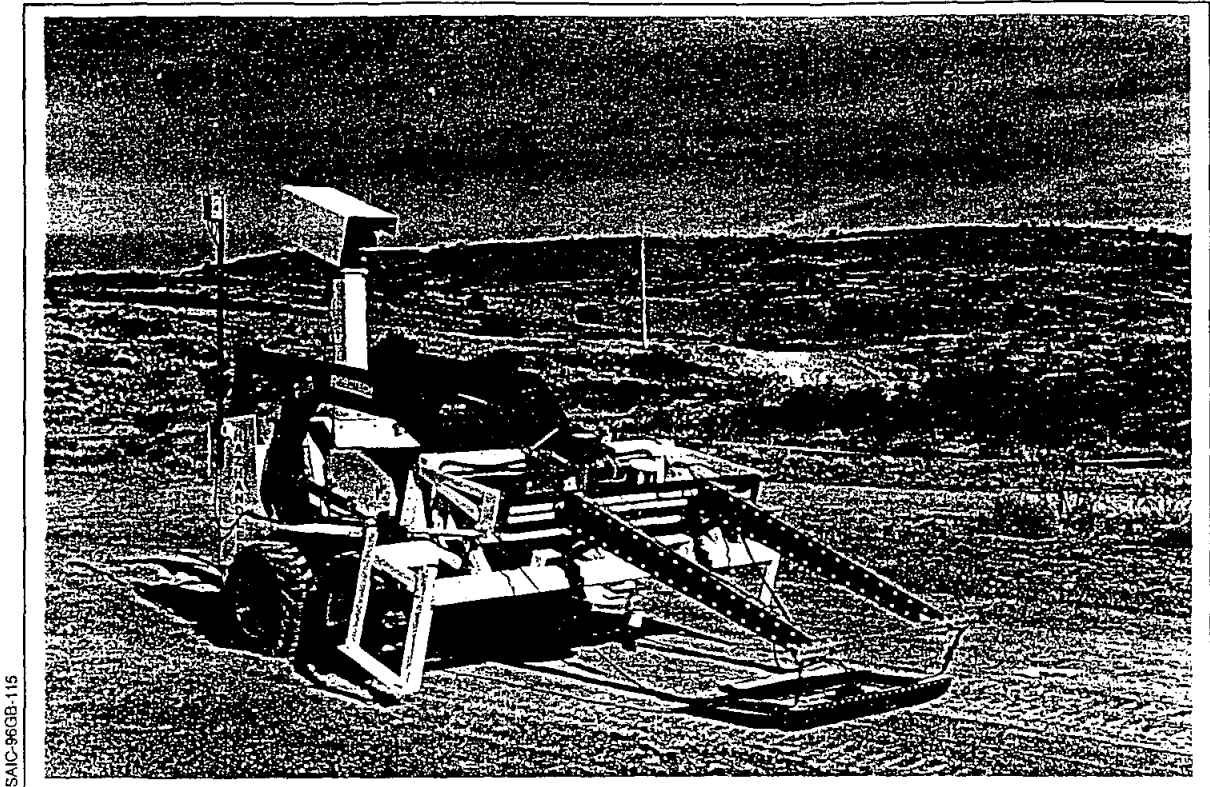
- Metal detector array mounted on the Robotech vehicle (no TNA). The metal detector was mounted with straps to the vehicle boom, as shown in Figure 9.2. This configuration was used first to search the one-dimensional lanes (stop and go) and then to scan them.
- Metal detector array mounted on the back of a Ford Explorer, as shown in Figure 9.3. This configuration was used to scan both the two dimensional areas and to rescan the one-dimensional lanes.
- TNA mounted on a hand-pushed cart, as shown in Figure 9.4. This configuration was used to carry out the TNA data collection tasks.
- TNA mounted on the Robotech vehicle (no metal detector array), as shown in Figure 9.5. This configuration was used to carry the TNA over the points previously marked by the metal detector in order to perform the verification.

Of the four configurations above, the one using the Ford Explorer had not been anticipated and was a field test improvisation. From the beginning of the test we encountered increasing problems with the remote control of the Robotech vehicle. This was due to the very high temperatures at the site, which affected the control unit (located in an enclosure not too far from the engine compartment), resulting in a vehicle that would experience more and more shutdowns as the distance from the control station increased (the control unit was later moved and remounted outside the vehicle for the Yuma test).

We managed to complete the test on the one-dimensional lanes using the Robotech, in spite of several shutdowns and restarts. However, when we got to the two-dimensional areas, the communication problems with the vehicle control unit became such that the vehicle was almost constantly shutting down. At this point it was decided to move the Schiebel detector array and the GPS receiver to the non-remotely controlled Ford Explorer, collecting the data with a portable computer and using a subset of the software that had been prepared during the development phase. Since only two ports were available on the portable computer, they were used to communicate with the Schiebel array and the GPS receiver. The compass and encoder signals were not available, however, they were replaced with the heading and velocity information provided by the GPS receiver through the Doppler effect.

The Explorer-based system, which does not require remote communication (except for the differential corrections) has proven to be robust and allowed us to collect data on both the two-dimensional areas and then back on the one-dimensional lanes. One benefit of this arrangement was that the Robotech vehicle became available (controlled by the operator from a short distance, with less frequent shutdowns) for carrying the TNA to perform verifications while data were collected in parallel with the metal detector.

Figure 9.6 illustrates the major activities that were carried out during the test period. Note the substantial overlap in the data taken with the TNA and with the metal detector.



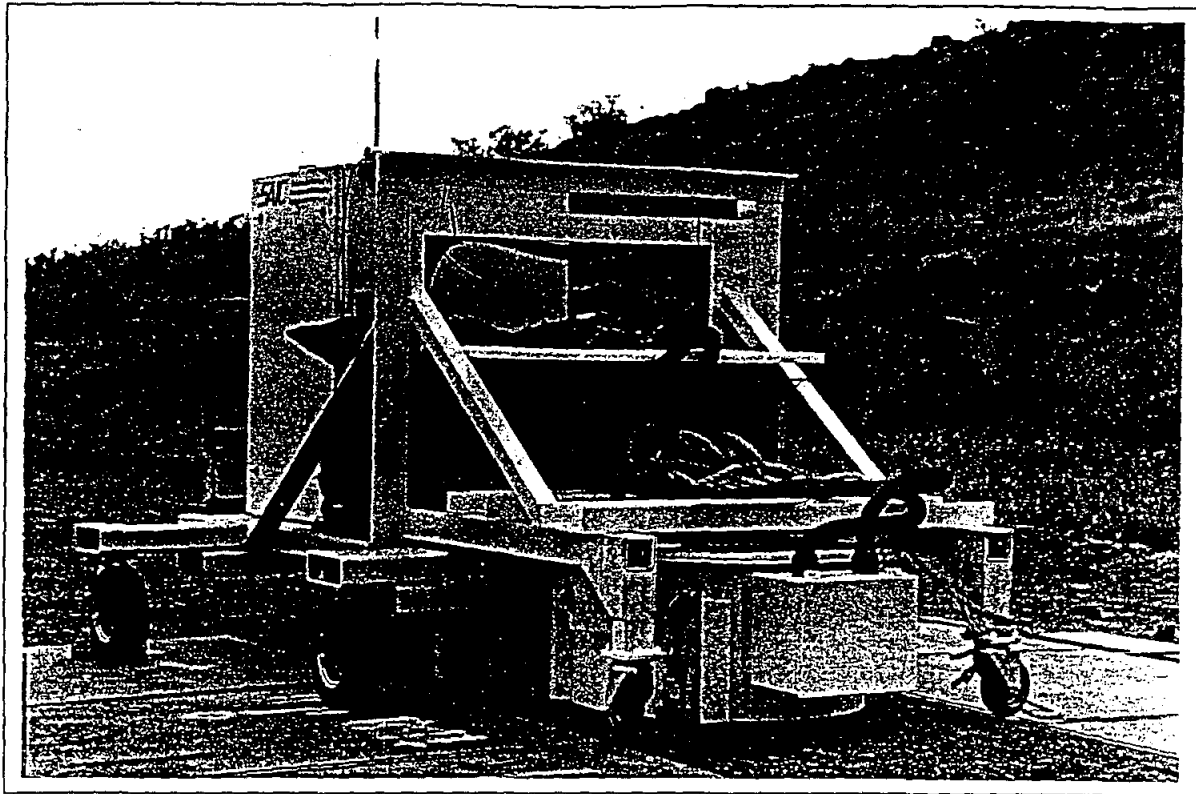
SAIC-96GB-115

Figure 9.2. Metal Detector Array Mounted on Robotech Vehicle.



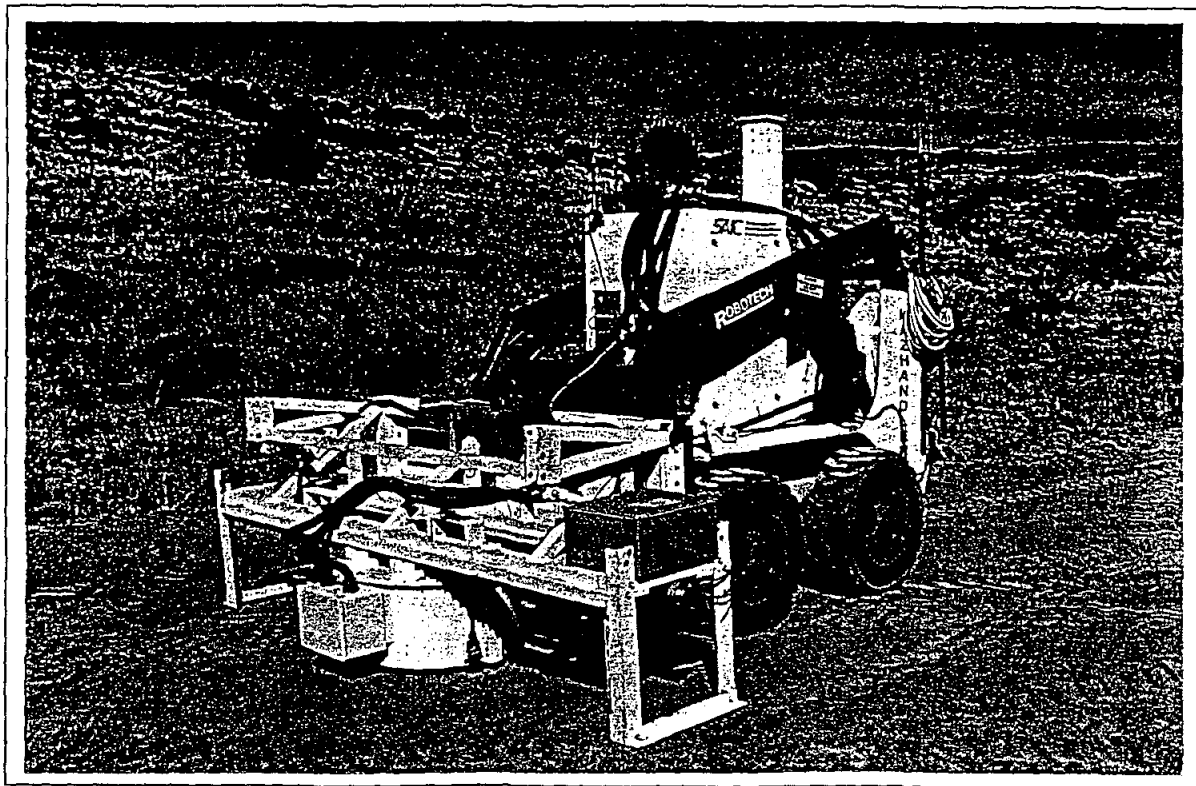
SAIC-96GB-114

Figure 9.3. Metal Detector and GPS Mounted on Non Remote Controlled Vehicle (Ford Explorer).



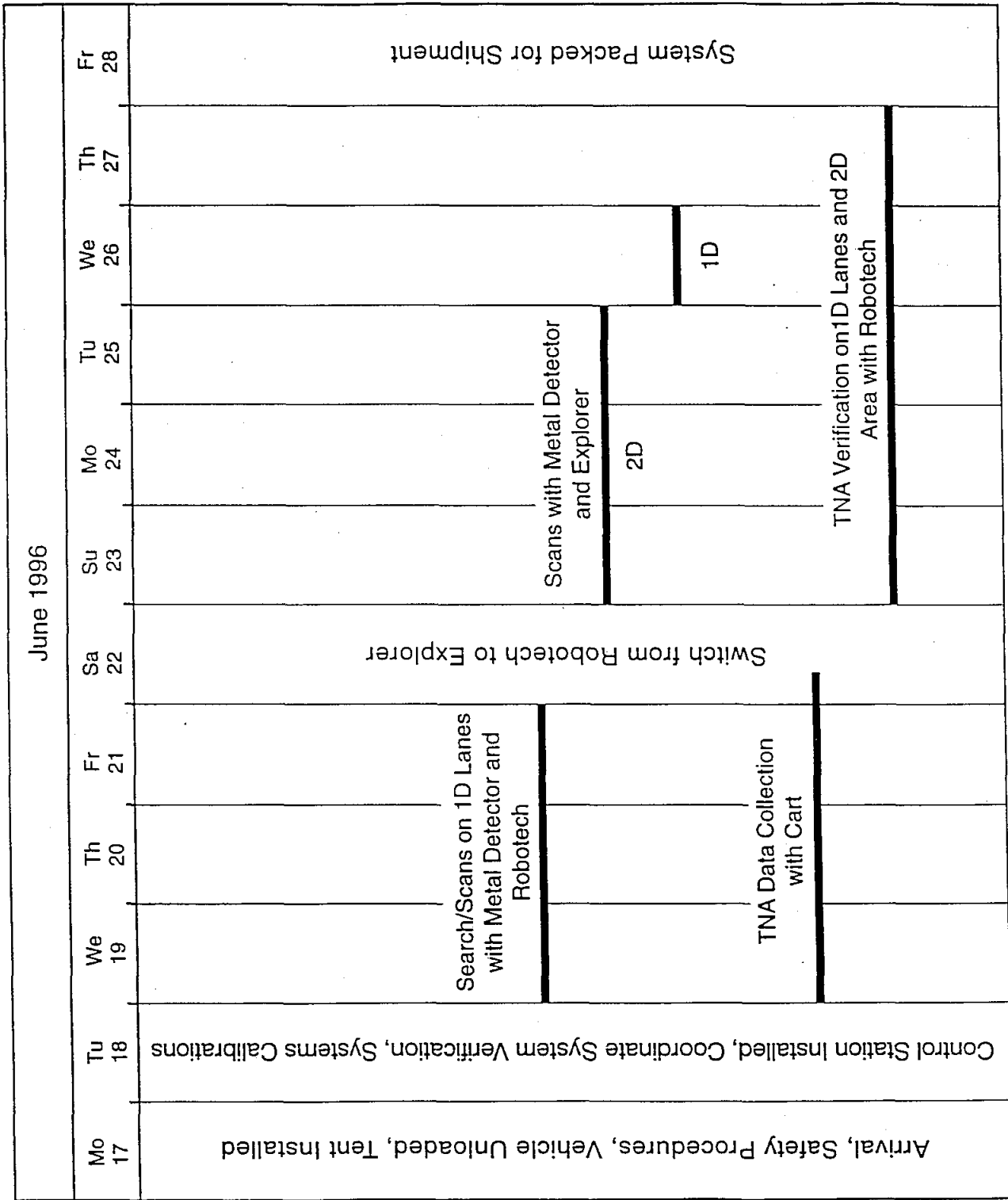
SAIC-96GB-117

Figure 9.4. TNA Standalone Cart.



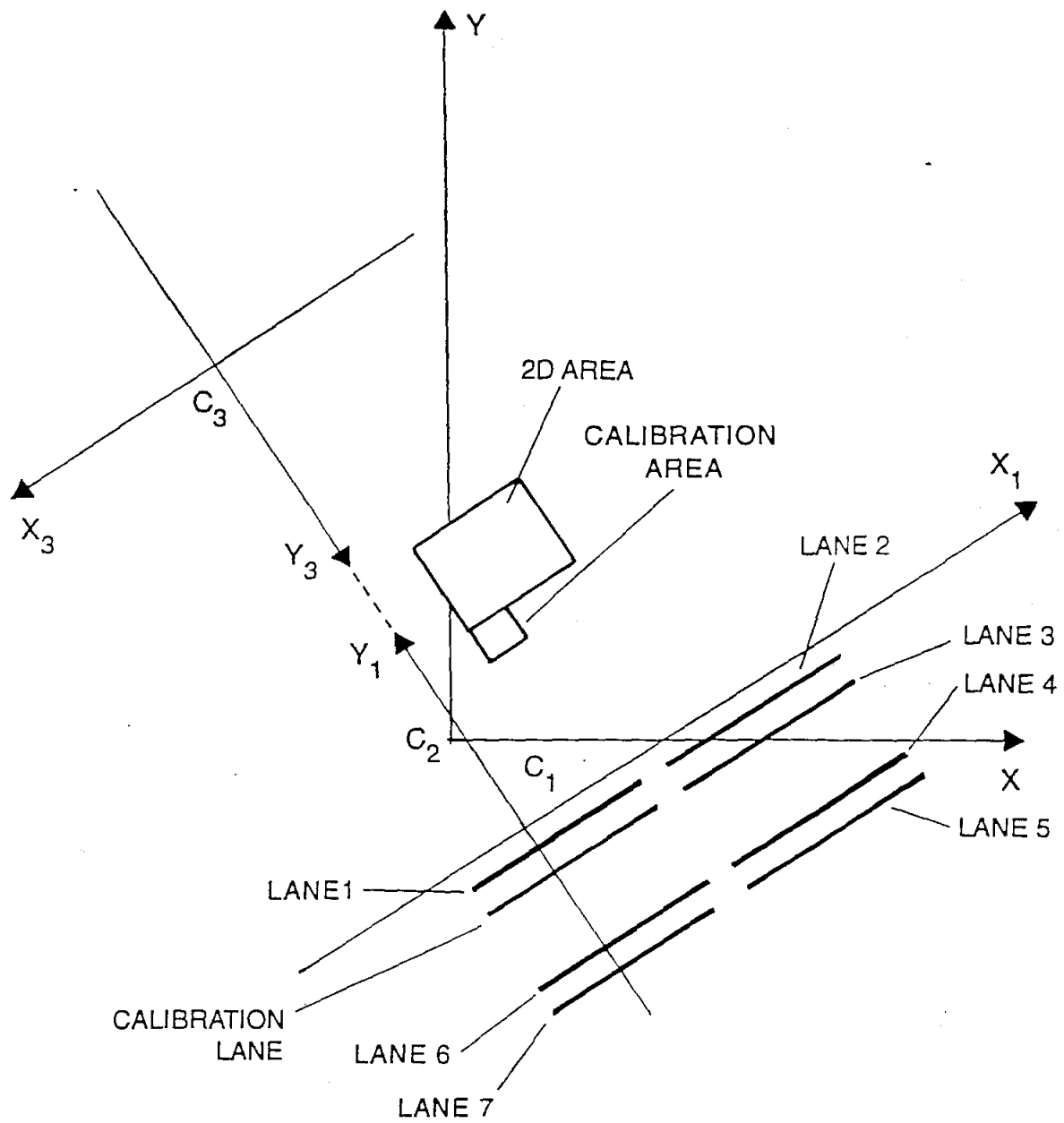
SAIC-96GB-118

Figure 9.5. TNA Mounted on Robotech Vehicle.



SAIC-97GB-5

Figure 9.6 Major Activities During Socorro Test.



SAIC-97GB-30

Figure 9.7. Coordinate Systems used in the Socorro Test.

9.4 COORDINATE SYSTEMS

The UXO targets and clutter objects emplaced by the Government in the calibration and blind areas were surveyed in using theodolites with respect to predefined coordinate systems. Also surveyed in were the points found by the metal detector and marked either automatically (by the paint sprayer, on the one-dimensional lanes) or manually (on the two dimensional area). Comparison of the two sets, ground truth and experimental estimates, is the basis for the assessment of detection probabilities. Since our system records latitude and longitude by differential GPS (with nominal submeter accuracy) we have the ability to determine a third set of observations, that is coordinates derived from latitude and longitude, as provided by GPS, to compare to the ground truth. In order to do this, we must know the relationship between latitude and longitude, and the systems of coordinates used by the Government. Accordingly, one of the first activities during the test was to determine these relationships.

At Socorro, the Government used two systems of coordinates, one for the one-dimensional lanes, and one for the two-dimensional areas. Figure 9.7 illustrates these systems of coordinates. Our base station was set at point C2, so we first transform latitude and longitude to a system centered at C2, with the X axis in the East direction, and the Y axis in the North direction, as follows:

$$X(\text{meters}) = (\text{Lon}_0 - \text{Lon}) \times N_x$$

$$Y(\text{meters}) = (\text{Lat} - \text{Lat}_0) \times N_y$$

where $\text{Lon}_0 = 106.965677$ $\text{Lat}_0 = 34.022548$ $N_x = 95,158.72$ $N_y = 111,194.93$

To convert to the Government coordinate system 1 (used for the one-dimensional lanes) we apply the following transformation:

$$X_1 = (X - X_0) \cos \alpha + (Y - Y_0) \sin \alpha$$

$$Y_1 = - (X - X_0) \sin \alpha + (Y - Y_0) \cos \alpha$$

where $\alpha = 31.7244$ deg $X_0 = 32.717$ $Y_0 = -40.252$

To convert to the Government coordinate system 3 (used for the two-dimensional areas) we apply the following transformation:

$$X_3 = (X - X_0) \cos \alpha + (Y - Y_0) \sin \alpha$$

$$Y_3 = - (X - X_0) \sin \alpha + (Y - Y_0) \cos \alpha$$

where $\alpha = 211.7244$ deg $X_0 = -105.52$ $Y_0 = 172.24$

All the plots and comparisons that follow are done using navigation data and the above sets of coordinates, as appropriate. The purpose of this is to give a graphical representation of the accuracy

U.S. ARMY YUMA PROVING GROUND
MUNITIONS, COUNTERMINE, DEMOLITIONS, & UXO
YUMA, AZ 85365

For: MR. TOM BOARCH
US ARMY BELVOIR RESEARCH AND DEVELOPMENT CENTER
NIGHT VISION ELECTRONIC SENSORS DIRECTORATE
ATTN AMSEL-RD-NV-CD-MD
FT BELVOIR, VA 22060-5876

Subject: Draft Test Report of the Surface/Near Surface UXO Detection System

Mr. Boarch,

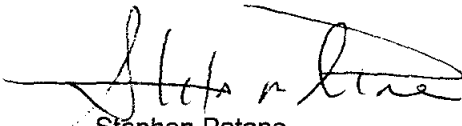
Enclosed is the test report for the test executed by Mrs. Roshni Sherbondy at YPG during the month of November 1996. The test report is ready to be published, although your office has not had a final review.

Roshni provided input and data during the initial preparation of report and reviewed the many drafts up to her departure. This is the completed draft that will require your comments and/or concurrence.

Please concentrate on the executive summary, findings, and distribution sections. These areas were mainly developed by Roshni, and to complete these sections after her departure, I had to assume some conclusions to clarify the data findings. Also, I'll need you to determine who do you want to receive the reports and how many copies.

Mr. Boarch, if I can assist in any manner or answer some questions, please don't hesitate to call me at DSN 899-7161 or email to spatane@emh1.army.mil.

Thank you,



Stephen Patane
Test Director
Munitions & Weapons Division
STEYP-MT-EW

achievable with the navigation variables. Detection probability is discussed later using the actual marks. It should be noticed that latitude and longitude (and the derived X, Y coordinates) refer to the position of the GPS antenna, which usually does not coincide with the alarming metal detector coils. Proper offsets, which depend on the orientation of the vehicle (as described by the navigation equations in Section 7) must be applied. In the plots, crosses represent the position of the targets (ground truth) while the circles are centered at the estimated position from the metal detector signals and from the navigation data. The radius of the circles is intended to give an idea of the positional uncertainty from GPS.

9.5 METAL DETECTOR RESULTS

9.5.1 One-Dimensional Lanes

There were eight one dimensional lanes, of which one was used for calibration and the remaining seven for the blind test. Each lane was 100 m long and was aligned at about 50 degrees from North. The surface of the lanes was quite smooth. All lanes were scanned once with the Robotech and repeatedly (twice for the calibration lane and four times for the blind lanes) using the Explorer. The data from the scan are used to generate an image map of the metal detector signal, which contains bright spots. The coordinates of the centers of these spots are measured on the image, converted to the proper system of coordinates, and used as the centers of the circles in the plots.

The calibration lane contained 11 targets. Figure 9.8 shows a plot of the actual position of the targets (crosses) and of the estimated positions from one of the runs with the Explorer (circles), using the GPS information and the transformations above. All the targets in the calibration lane were clearly visible. There was essentially no clutter and all the targets were detected with one false alarm only.

Lane 1 (Figure 9.9) contained 25 targets. All of them were detected with one false alarm only.

Lane 2 (Figure 9.10) contained 16 targets. One of the targets was not detected. This target was one of several 40 mm projectiles buried at 12 in. depth which could not be seen in any of the runs. In addition, two other targets were somewhat away from the corresponding circles, and there were two false alarms.

Lane 3 (Figure 9.11) contained 13 targets. There is good correspondence between targets and detections, and one false alarm.

Lane 4 (Figure 9.12) contained 8 targets. All of the targets were detected and three false alarms were registered.

Lane 5 (Figure 9.13) contained 21 targets. All but two of the targets were detected. The two undetected targets were 40 mm at 12 in. burial depth.

Lane 6 (Figure 9.14) contained 21 targets. All the target were detected.

Lane 7 (Figure 9.15) contained 17 targets. One target was not seen (40 mm at 12 in. depth), two were estimated poorly, and there was one clutter instance.

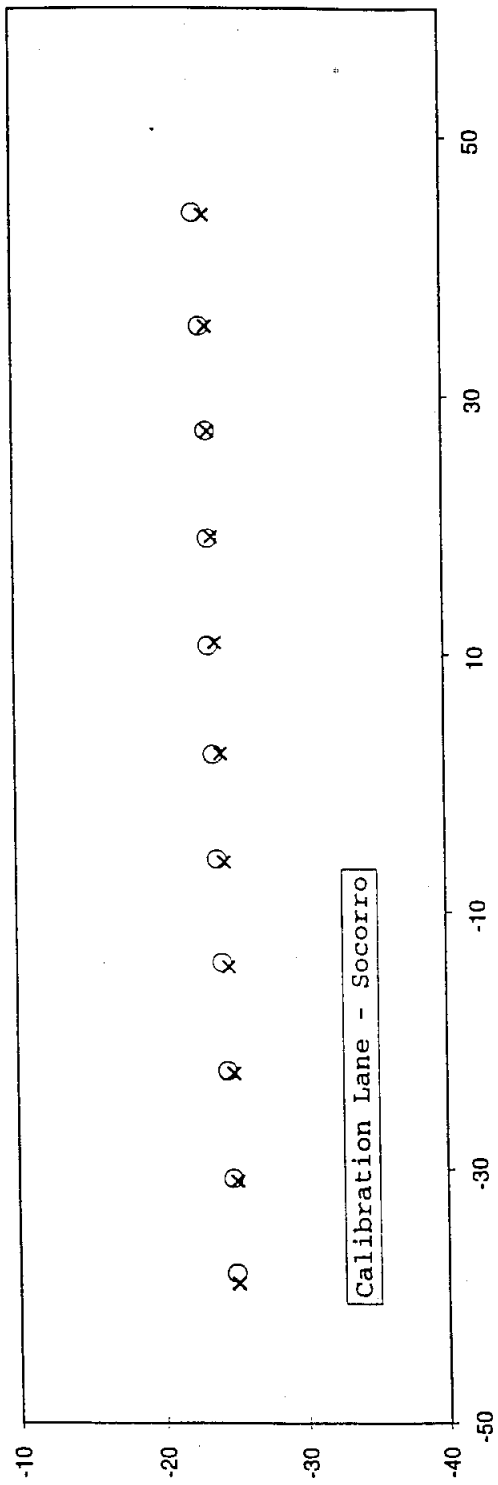


Figure 9.8. Targets and Estimated Positions in Calibration Lane.

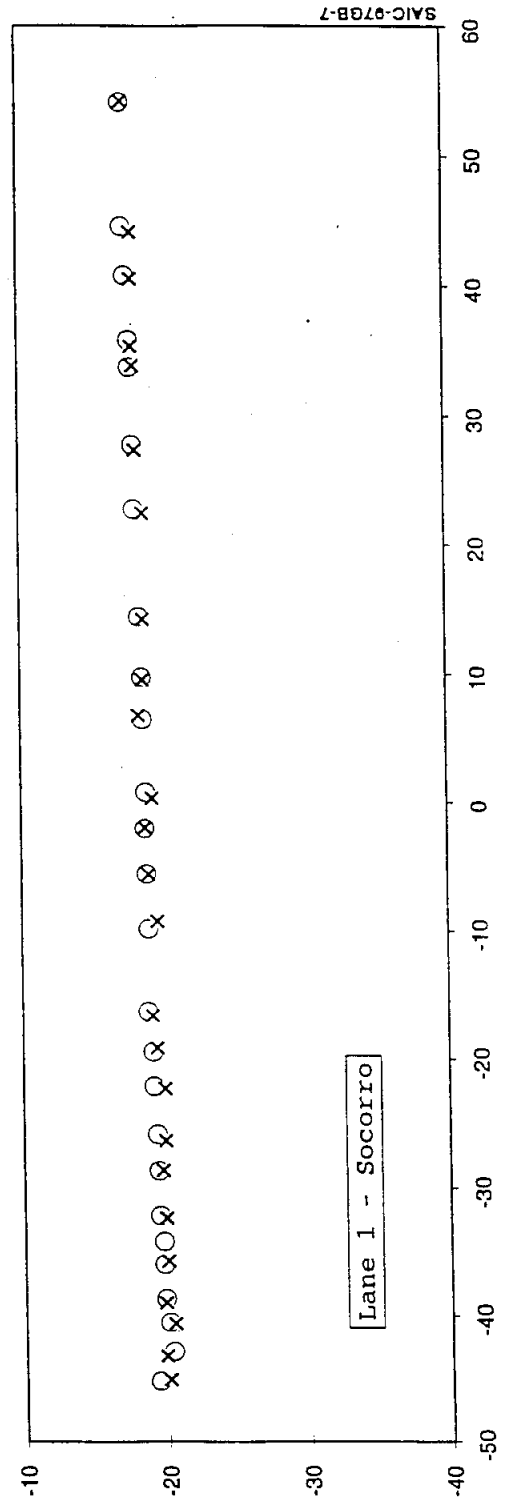


Figure 9.9. Targets and Estimated Positions in Lane 1.

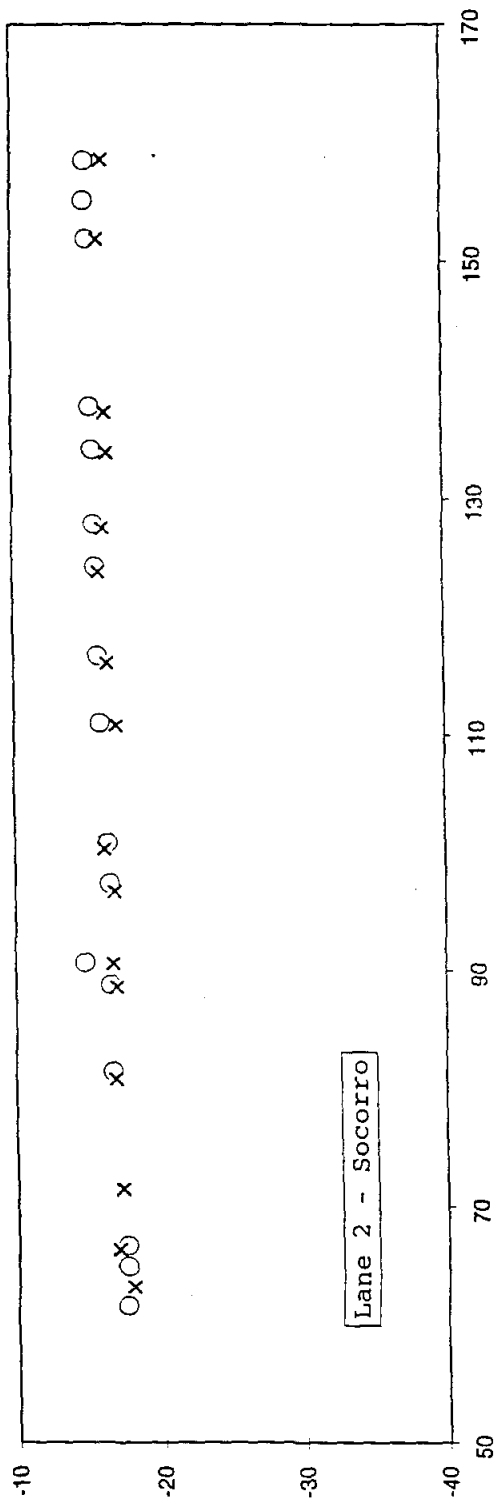


Figure 9.10. Targets and Estimated Positions in Lane 2.

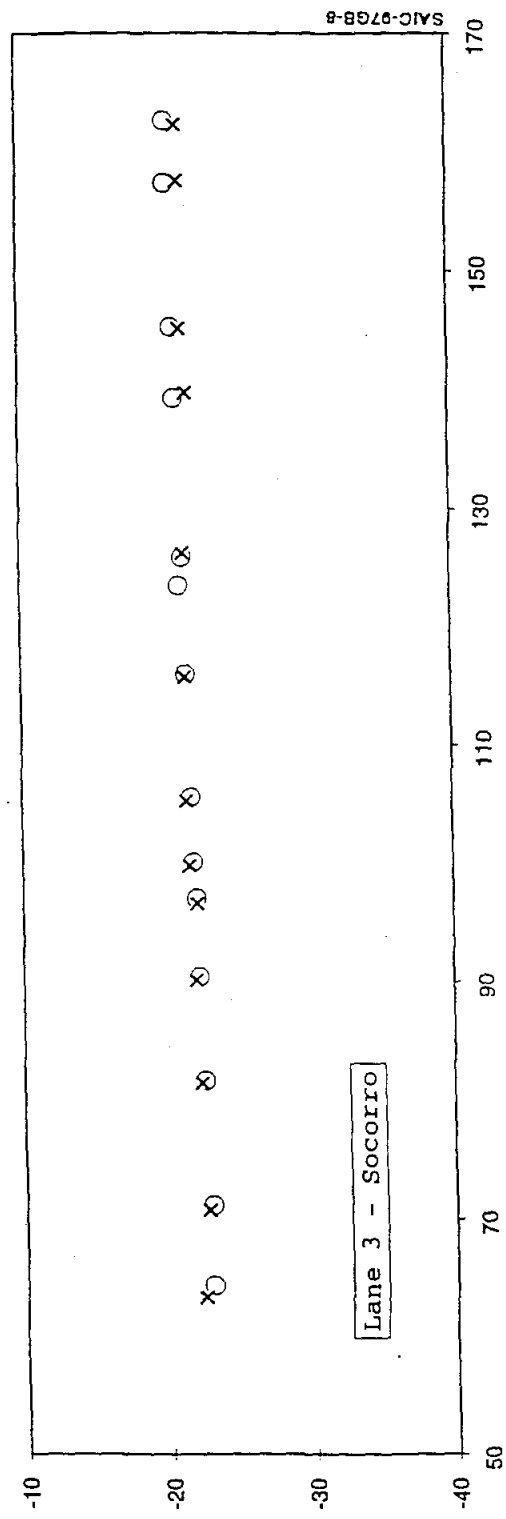


Figure 9.11. Targets and Estimated Positions in Lane 3.

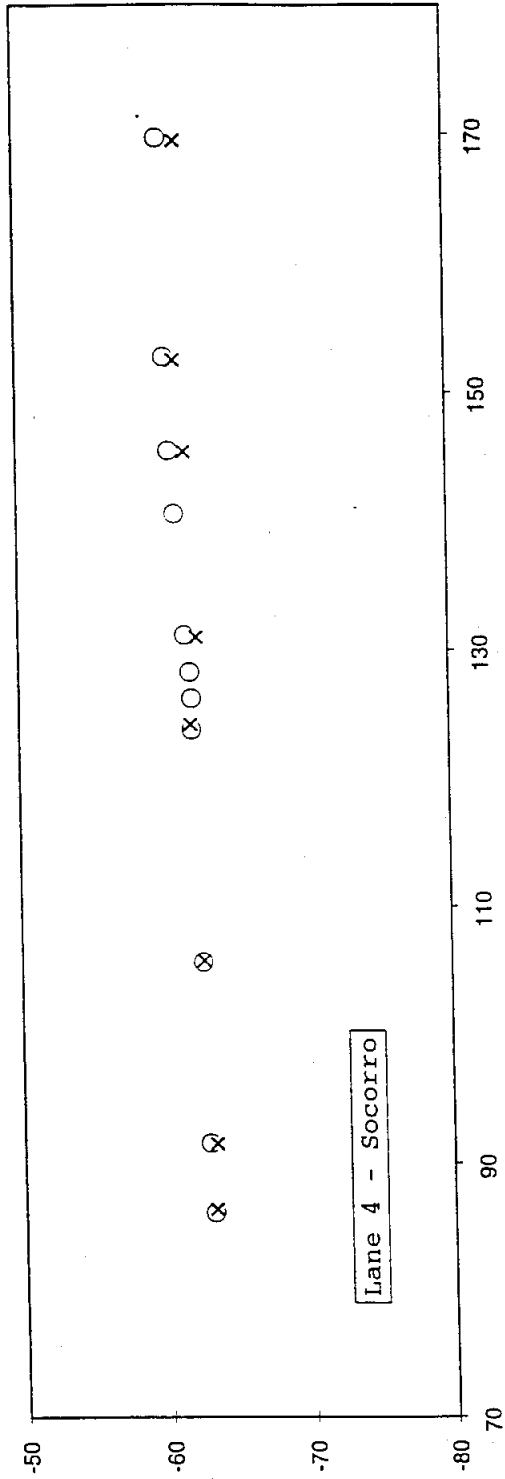


Figure 9.12. Targets and Estimated Positions in Lane 4.

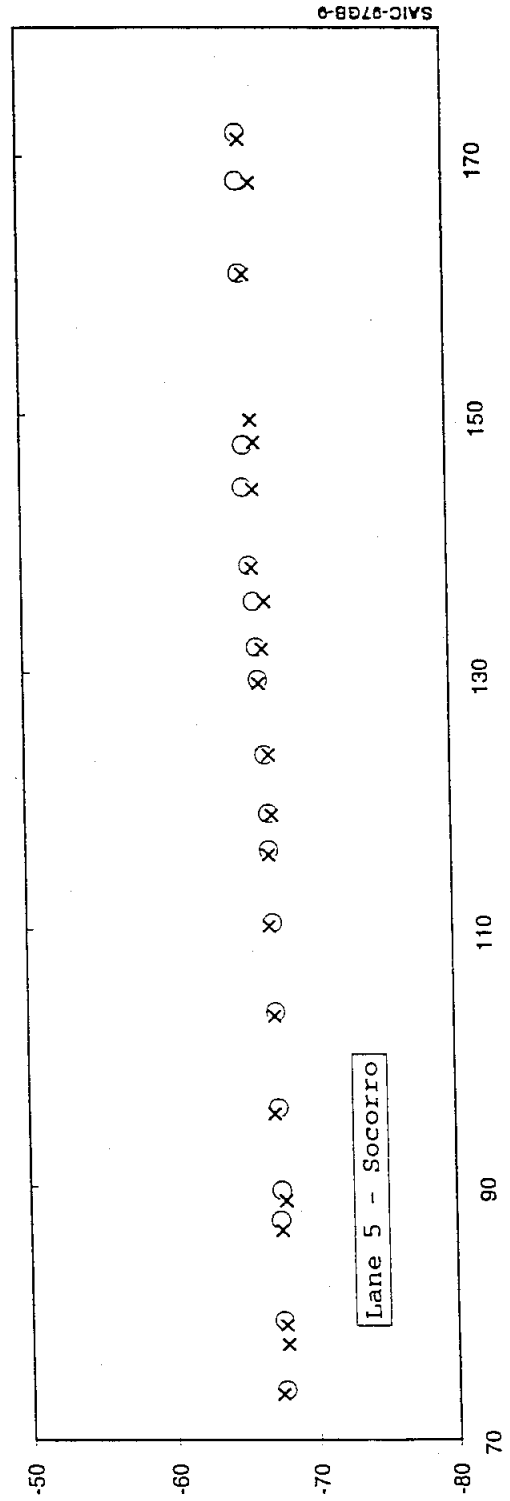


Figure 9.13. Targets and Estimated Positions in Lane 5.

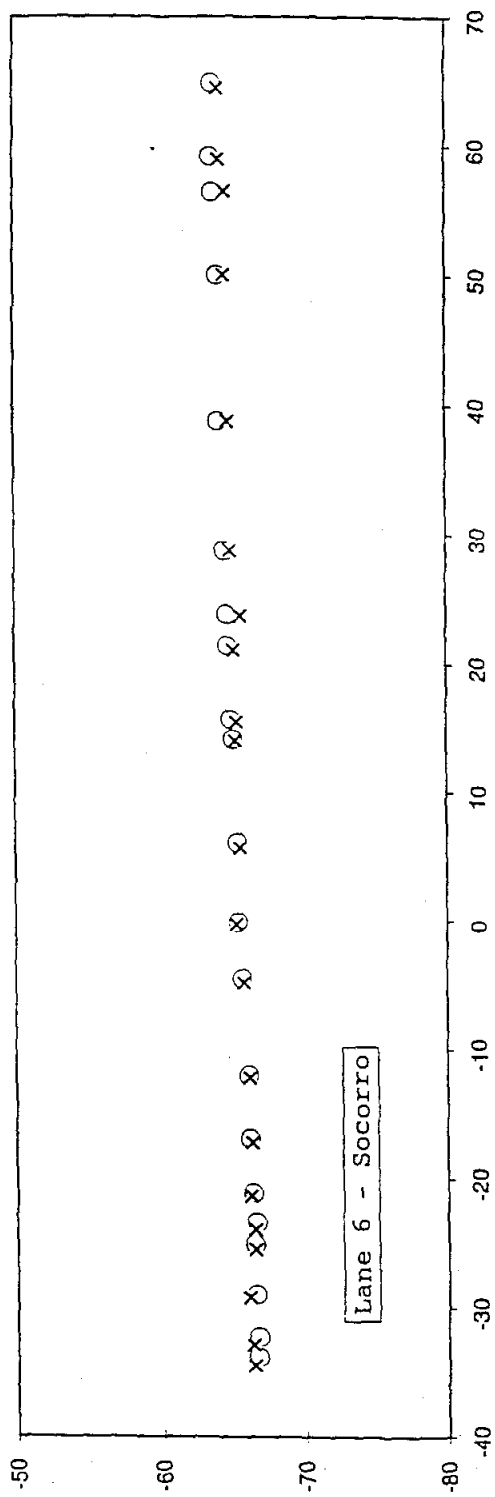


Figure 9.14. Targets and Estimated Positions in Lane 6.

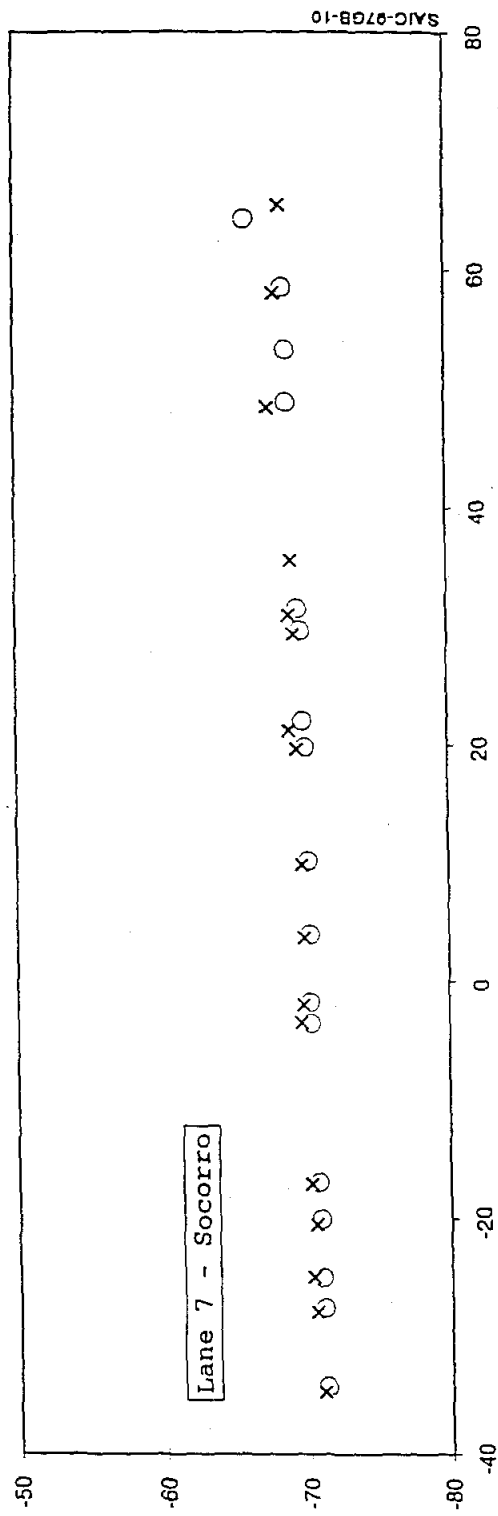


Figure 9.15. Targets and Estimated Positions in Lane 7.

The figures above provide an overall visual indication of the performance of the metal detector and of the navigation system in detecting and reporting the position of UXO targets. Note that in the scans on the one-dimensional lanes complete coverage was assured, that is we have complete confidence that the metal detector went over each target.

9.5.2 Two-Dimensional Areas

The test included two two-dimensional areas, one for calibration (20 m × 20 m), and one for the blind test (50 m × 5 m). As previously mentioned, it was impossible to scan either of these areas with the Robotech vehicle, and the scans were therefore conducted exclusively with the Explorer.

The 20 m × 20 m calibration area contained 11 targets. Figure 9.16 shows a plot of the target positions (crosses) and estimates obtained from the scan (circles). Two of the targets (a 20 mm at 3 in. depth and a 40 mm at 6 in. depth) were not seen, probably for lack of coverage. The scan of this area was conducted rather quickly, mostly for the purpose of calibrating the system of coordinates.

The 50 m × 50 m area contained 54 targets. Figure 9.17 shows a similar comparison plot. The plot shows that 37 targets were detected. In addition, 5 false alarms were registered.

In the case of the two dimensional area, we do not have assurance of complete coverage, although we tried to overlap the parallel scans. It is therefore possible that some targets were missed because the metal detector did not pass over them. In addition, the software that was used with the Explorer was oriented more towards the GPS than to the metal detector, and the readout of the metal detector was not as fast as it could have been. Thus, although we tried as much as possible to control the speed of the vehicle (the slower the speed the better the sampling), it is possible that some weaker signal targets may have been missed because of insufficient sampling of the metal detector data.

9.5.3 Detection Probabilities

The data presented above are the result of analysis of stored data. The test also included marking the ground at the points of detection and subsequent measurement by the Government of the marked points. On the one-dimensional lanes the marks were done automatically using the paint marking system on the Robotech vehicle. On the two-dimensional area the marks were done manually, using a spray paint can, after finding again the targets identified in the map generated with the Explorer. For several reasons, the manual method gave a larger error than the automated one.

Table 9-2 shows the ratios of targets found to the total number of targets and the number of false alarms per square meter for both the analysis method (navigation) and the marking method. The marking method is based on a 6 in. halo, while the navigation (or mapping) method is based on a much more relaxed (a circle with a radius of about 0.75 meter) criteria. Numbers are given separately for the one-dimensional lanes and for the two dimensional area.

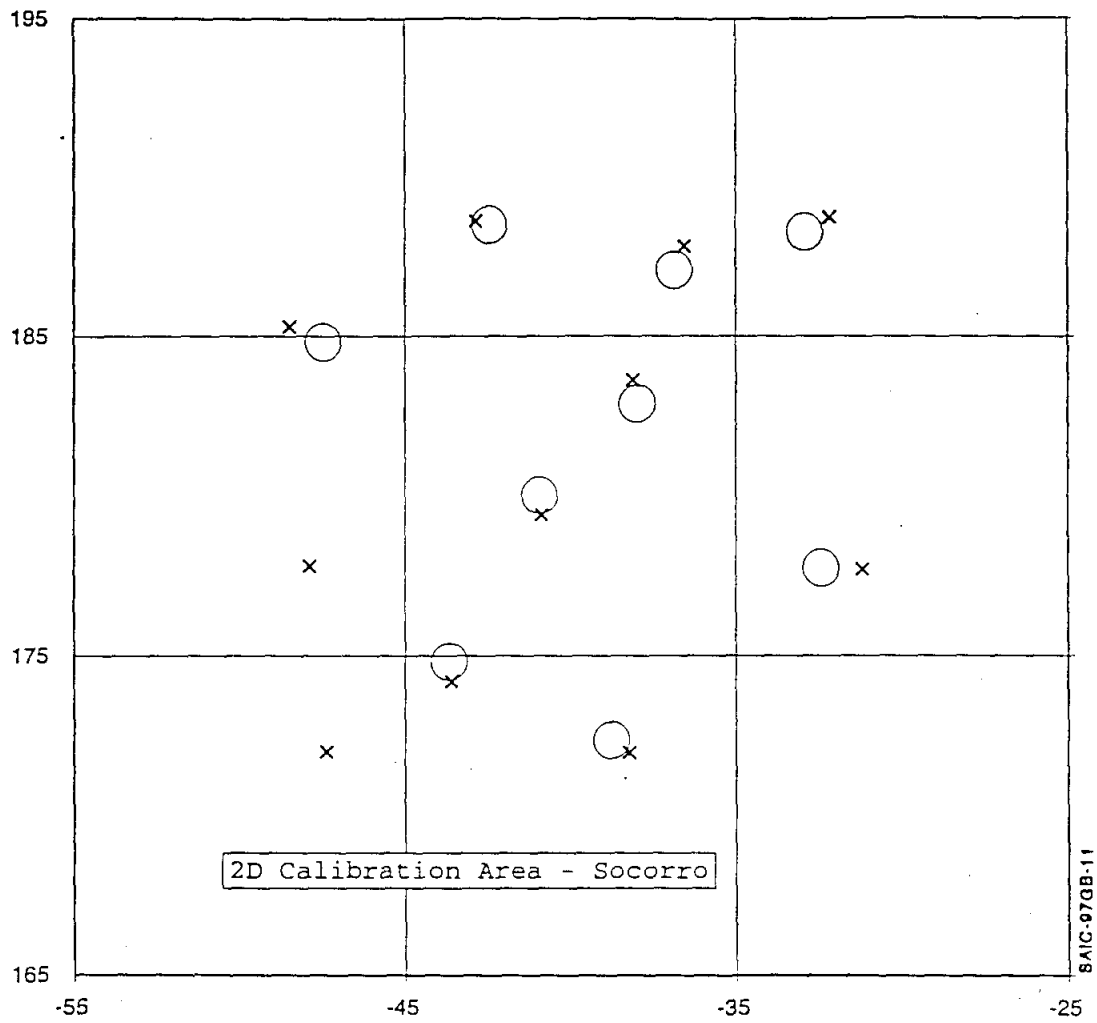


Figure 9.16. Targets and Estimated Positions in Calibration Area.

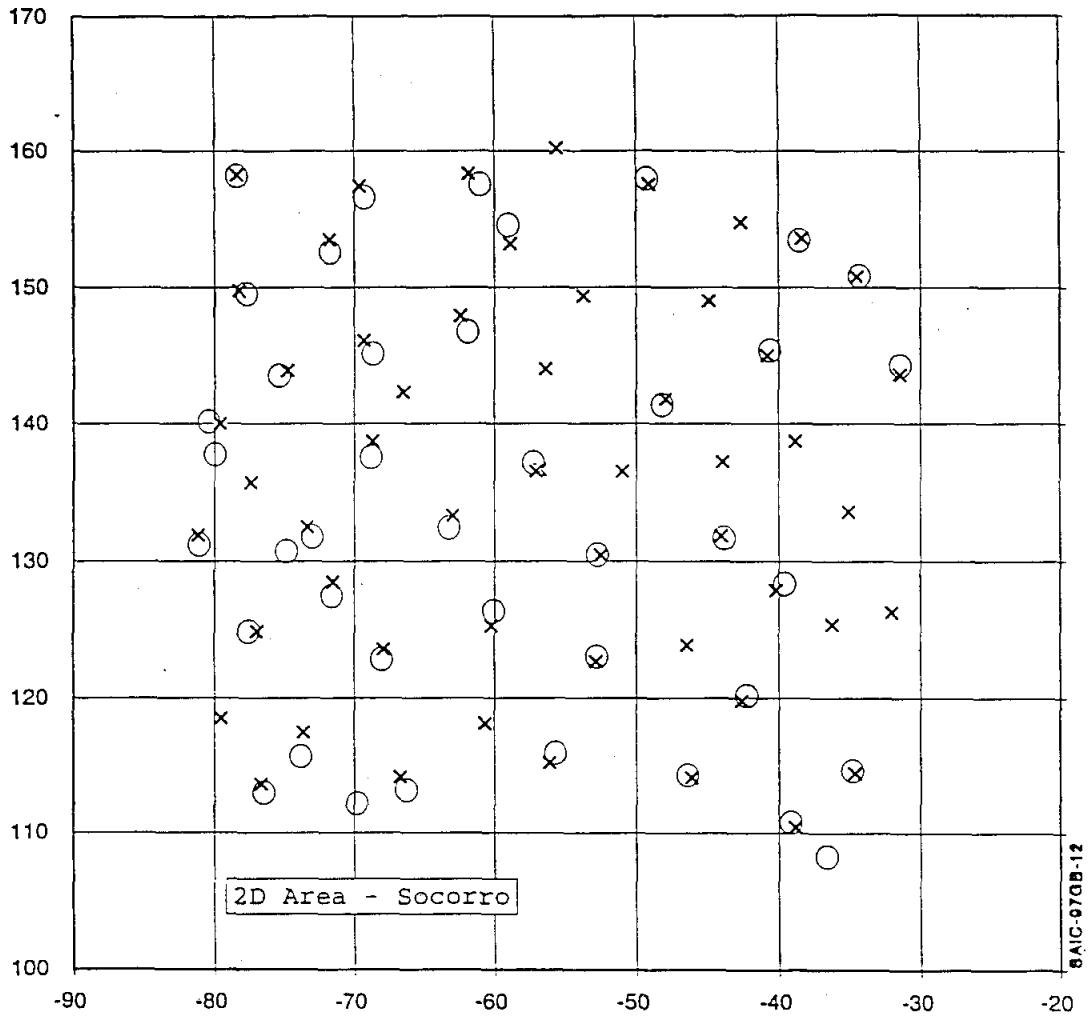


Figure 9.17. Targets and Estimated Positions in 2D Area.

Two issues are important. The first one is the sensitivity of the detection probability with respect to halo size. Figure 9.18 shows the detection probability versus halo size for the one-dimensional lanes and for the two-dimensional area. In this plot we have included only those targets that were actually found, that is were reasonably close to marks. Notice that the plot includes the effect of marking inaccuracy, which was higher for the 2D area, in which the marking was done manually rather than automatically. The second issue is the accuracy of marking, which should be closely related to the accuracy of positioning the verification detector over the detected target. Figure 9.19 shows a histogram of discrepancies between true values and marked values both along and transverse to the direction of motion. There appears to be a systematic error of about 20 cm in the direction of the scan. This systematic error was corrected before the test at Yuma.

Table 9-2 Detection and False Alarm Rates for Socorro Test

	Navigation (1m Radius)		Marking (6 in. Halo)	
	Detection Probability	False Alarm Rate	Detection Probability	False Alarm Rate
One-Dimensional	114/121	12/700m ²	72/121	46/700m ²
Two-Dimensional	37/54	5/2500m ²	14/54	17/2500m ²

9.6 TNA RESULTS

The tests of the TNA sensor carried out at Socorro were of two types. The first set of tests were to quantify the inherent performance of the TNA sensor without any of the ambiguities of overall system positioning to which the TNA was sensitive. The second set of tests were to characterize the performance of the metal detector/TNA combination by having the TNA measure positions on the test areas where alarms were found with the metal detector and the ground was marked with the system paint sprayer. As mentioned in section 9.3 to allow tests of the metal detector and TNA to proceed in parallel, for the first set of tests the TNA was mounted on a manually pushed cart, see Figure 9.4, which supported both the TNA sensor head and the signal processing electronics. For the subsequent tests on the one and two dimensional areas the TNA and signal processing electronics were mounted on the Robotech platform, see Figure 9.5.

During the tests, real time decisions were made and noted by the Government and SAIC test teams. The spectral and signal processed data were also logged and stored for post processing and further analysis.

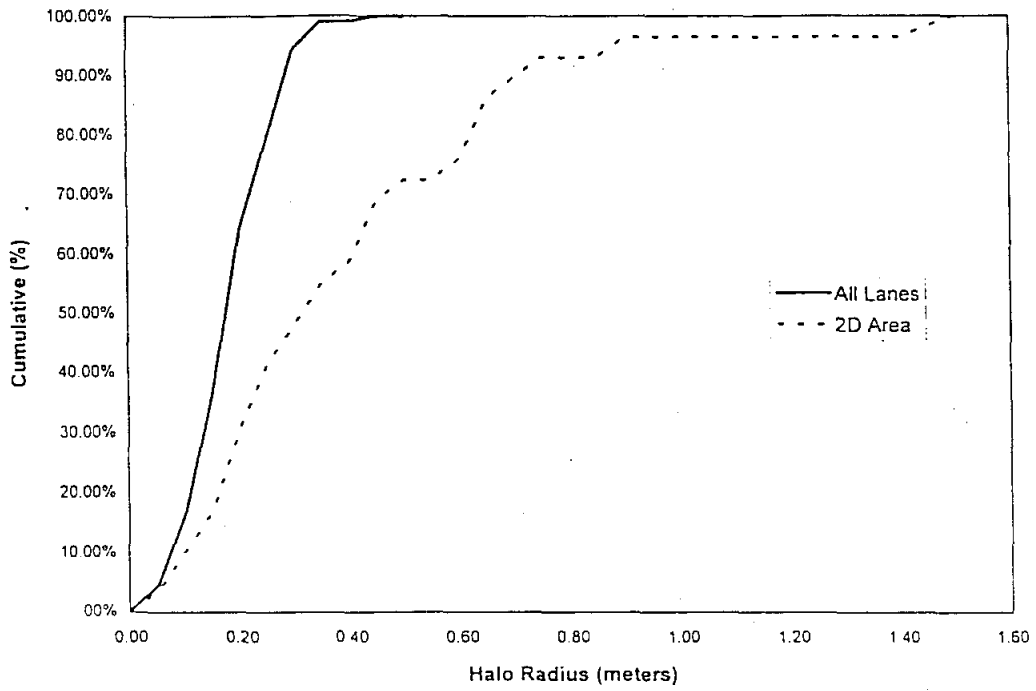


Figure 9.18. Detection Probability Versus Halo Radius.

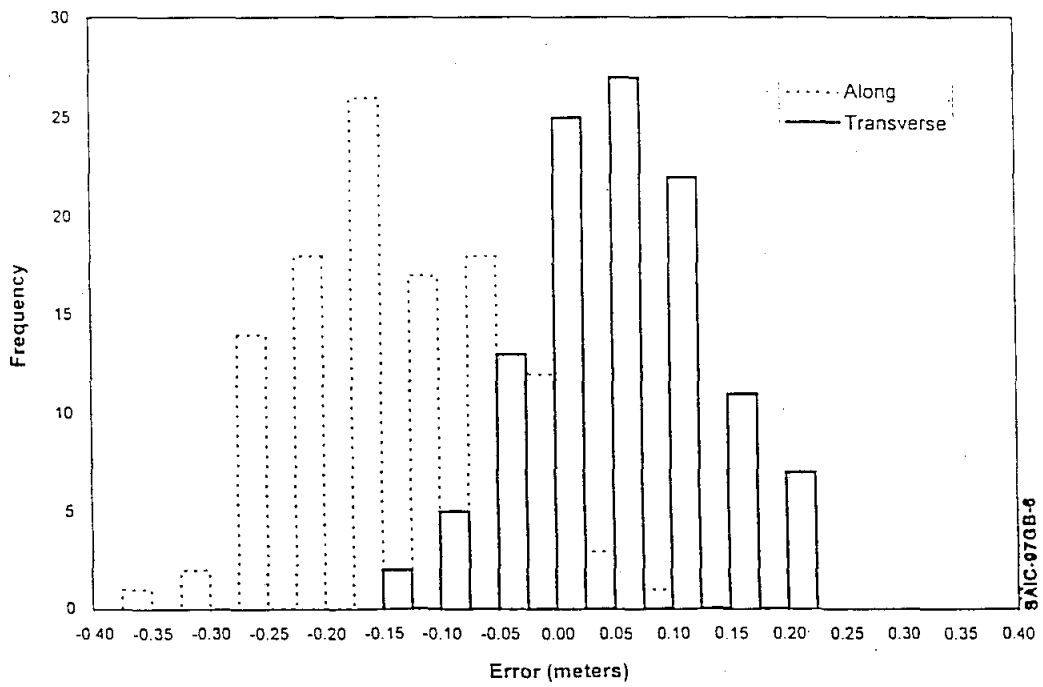


Figure 9.19. Histogram of Positioning Error Along and Transverse to Direction of Travel.

9.6.1 Data Collection Area

The data collection area was a one dimensional track in which various UXO and clutter objects were buried and the TNA sensor manually positioned over locations specified by the Government test team. These tests were designed to characterize TNA performance as a function of UXO size, burial depth and displacement from the center of the TNA sensor. In addition to measurements on the UXO items listed in Table 9.1, measurements were also made on clutter objects (inert ordnance) and on bare soil.

In these tests, the TNA showed a high detection for the larger UXO and lower for the smaller ordnance. The 20 mm UXO which contained around 10 g of explosive was beyond the detection limits of the TNA; only one out of five of the 20 mm's on the data collection area were detected during the test which was consistent with the false alarm rate of the sensor during the tests. The 30 mm which contained around 22 g explosive, was detected two out of six times during the tests and appeared to be at the statistical limit of the TNA sensor for the measurement time of around 300 seconds used. Post processing of the 20 mm and 30 mm data did not significantly improve the results.

Figure 9.20 shows the results for the 60 mm UXO and 100 g pipe simulant for burial depths up to 12 in. and displacements to 3 in.. The detections are indicated by the squares and the missed detections by the dots. The open squares are the detections that were made in post processing only (real time misses during the tests). There were two misses for the 60 mm in the post processing and one for 100 g as shown.

The results for the 200 g pipe simulant and the 105 mm UXO on the data collection area are shown in Figure 9.21. It is seen that 5 out of the 16 200 g simulants were missed. All but one of the 105 mm were detected with burial depths of up to 12 in. and displacements up to 9 in. From the data it is not clear why there was a lower detection rate for the 200 g than for the 100 g simulant. Changing the thresholds on the decision features on the data does not significantly change these results as shown in Figure 9.22 which shows a probability of detection (PD) versus a probability of false alarm (PFA) curve (Receiver Operator Characteristic or ROC curve). The detection probability rises sharply as the false alarm rate is allowed to go to 15% after which it is flat until a few additional detections are gleaned at false alarm rates in excess of 25%.

9.6.2 One and Two Dimensional Areas

The measurements made on the one and two dimensional areas by the TNA were not as well characterized as on the data collection area for a number of reasons. The TNA was mounted on the Robotech vehicular platform and was positioned over marks on the ground that represented the marked position of a previous metal detector hit. The accuracy of the positioning and marking was insufficient. As described in Section 9.5.3 and shown in Figures 9.18 and 9.19, the metal detector marks were by and large not close to the actual targets. Many indeed were outside the range of sensitivity of the TNA. For this reason, the Government test team preselected a subset of the marked targets for the TNA to measure.

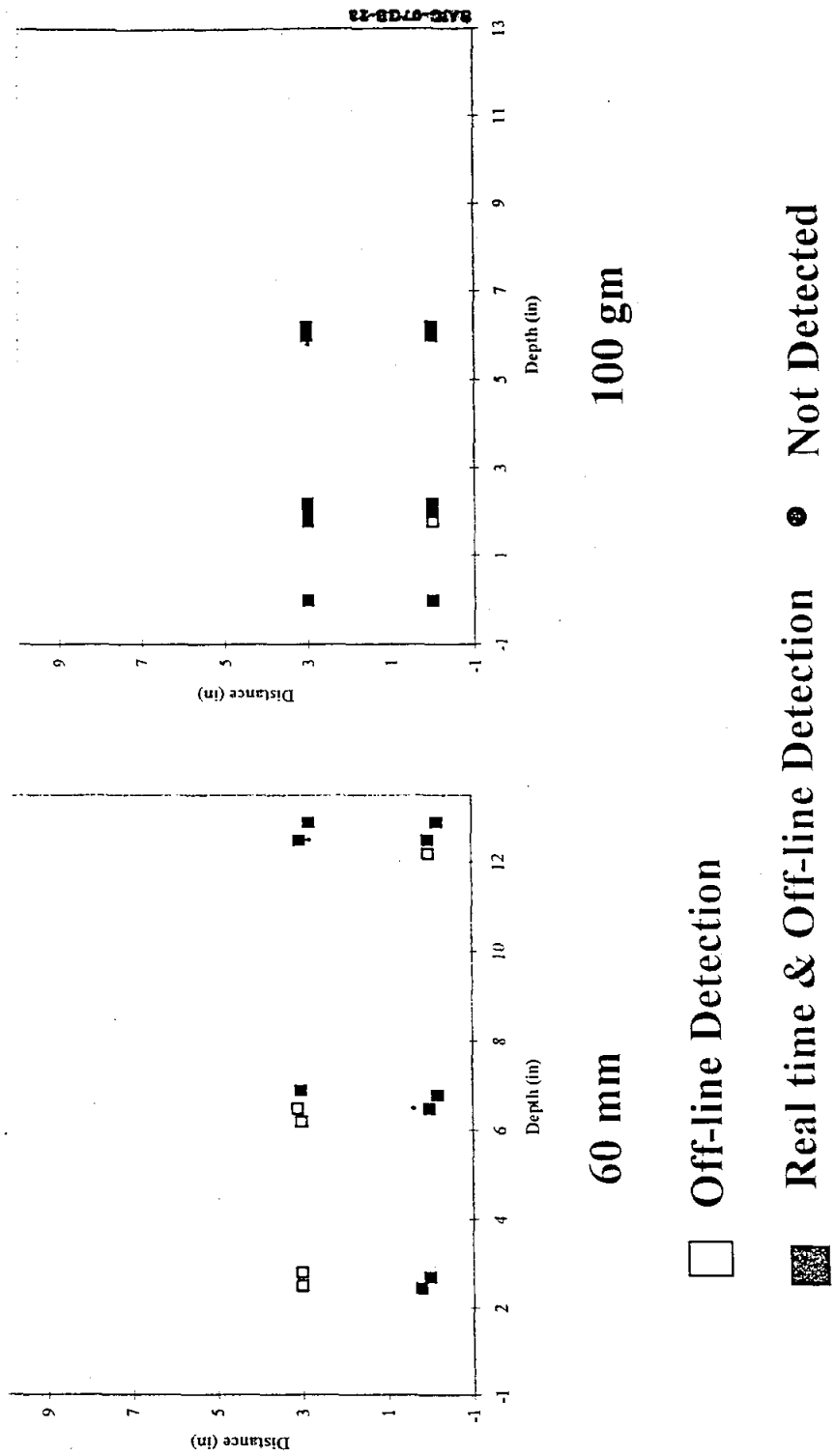


Figure 9.20. TNA Detections for 60 mm and 100 g UXO.

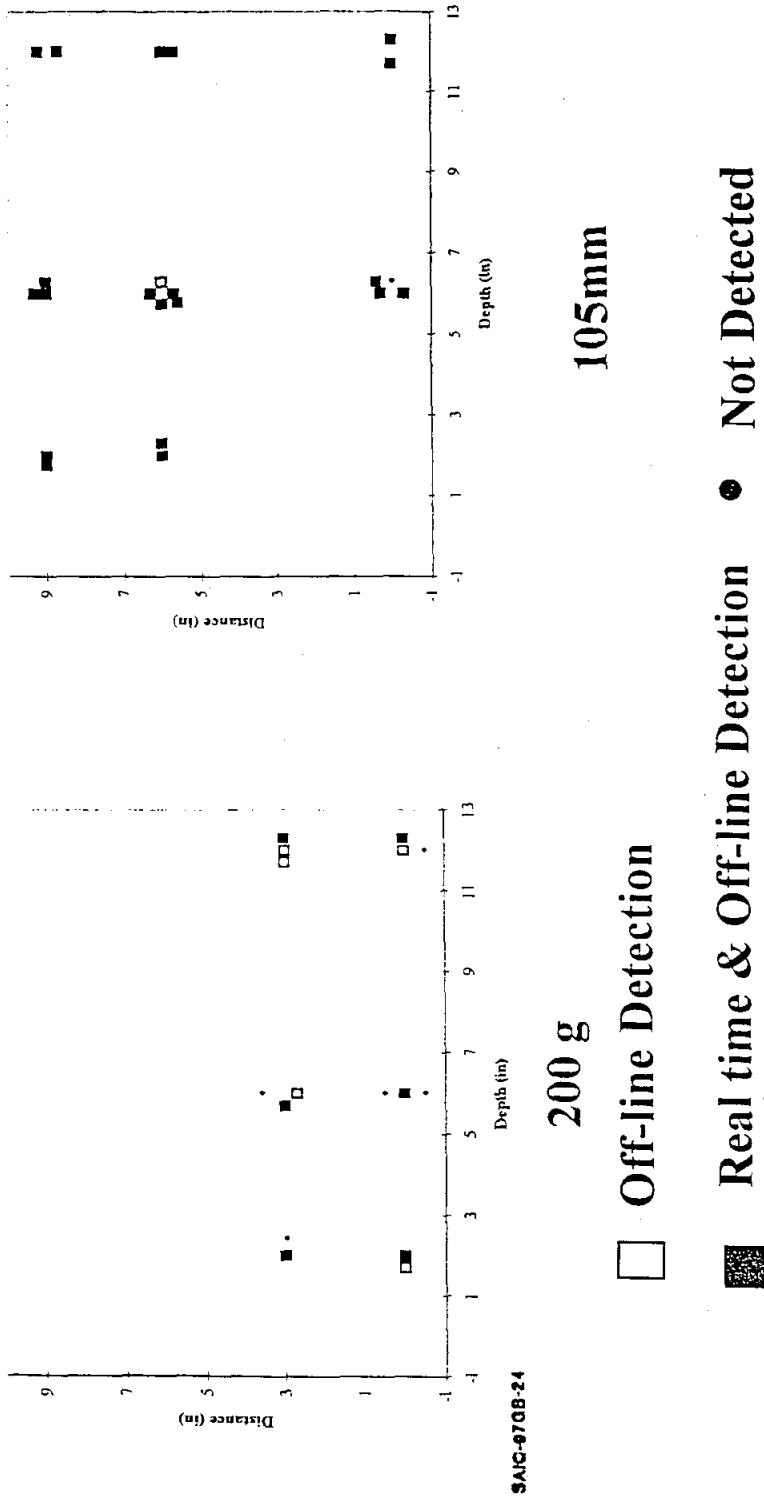


Figure 9.21. TNA Detections for 200 g and 105 mm UXO.

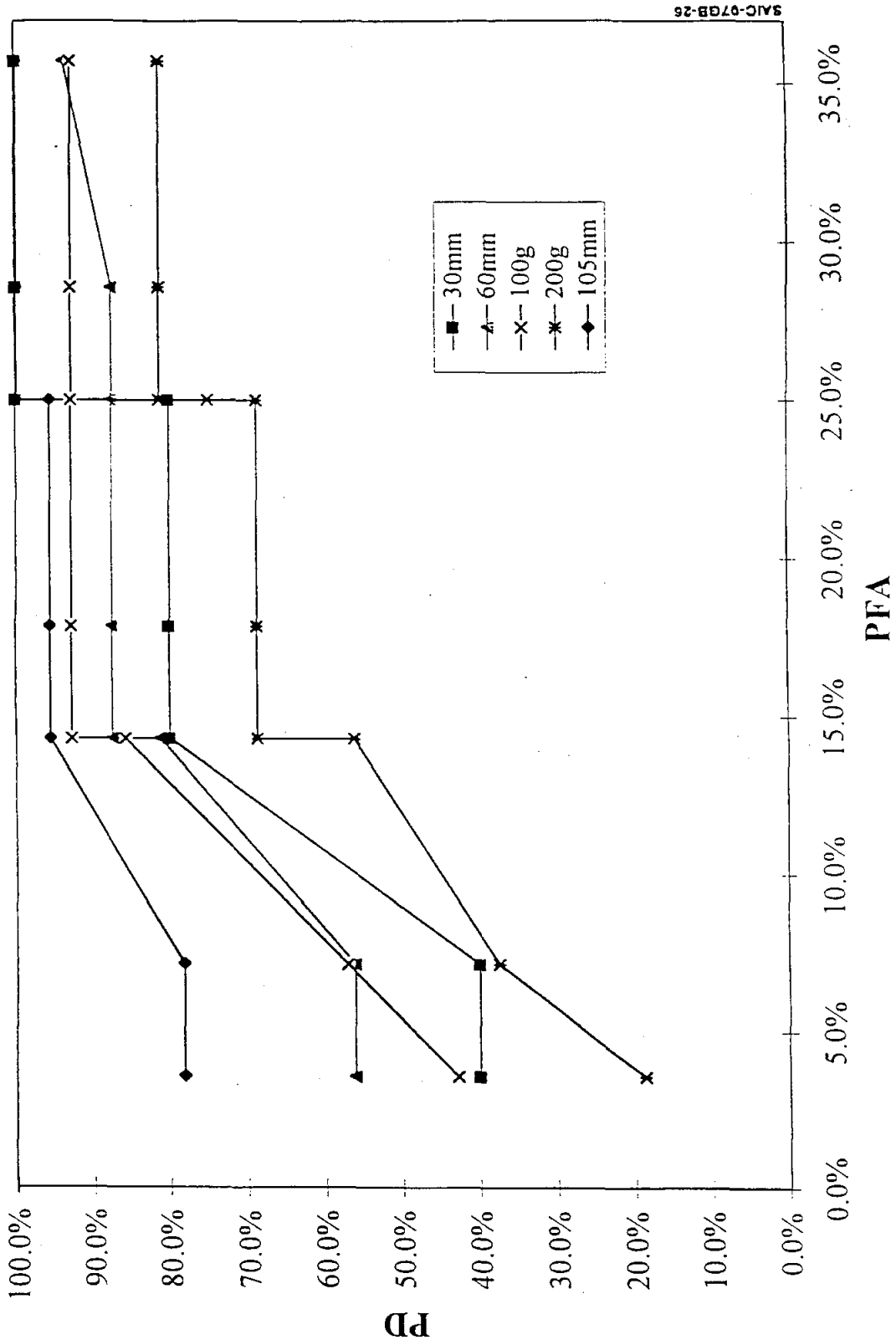


Figure 9.22. ROC Curves for Data Collection Area.

Figure 9.23 shows the PD versus PFA for the 60 mm through 105 mm UXO on the one and two dimensional areas. Except for the 105 mm, the performance was far lower than that obtained on the data collection area where the positioning error was less. Since the actual position of the TNA head relative to the target position was not measured during the tests the actual displacement is not known. The lowered performance for the one and two dimensional areas relative to the data collection area was ascribed to the positioning error.

9.7 MAIN CONCLUSIONS FROM SOCORRO TEST

A number of lessons were learned from the Socorro test and resulted in some modifications to both the equipment and the software, as follows:

- The control unit of the Robotech vehicle was affected by high temperature. It was moved outside the vehicle for the Yuma test.
- Positioning precision and accuracy in the direction of motion were not sufficient. The mounting of the metal detector array was modified from strap mounting to semi-rigid mounting. In addition, several changes were made to the software to obtain a more exact representation of the waterfall display, which is used to determine where to mark. This resulted in removal of the systematic error.
- The measurements showed that the TNA was sensitive to shallow buried UXO with sizes down to around 60 mm and relatively insensitive to 20 mm and 30 mm UXO. Based on these tests it was suggested that the number of detectors in the TNA be increased from eight to twelve which would increase the signal by 50% and that the possibility of using a stronger neutron source, which would also increase the signal, be investigated. The Government agreed to these modifications which were undertaken in the period preceding the next round of tests at Yuma Proving Ground. It was also apparent that the positioning accuracy of the system needed to be increased to allow the TNA to be positioned within a detection radius of around 13 cm (5 in.) from the UXO.
- Data collection on a two dimensional area was first demonstrated. Since the files from two-dimensional areas are much longer than the ones from the one-dimensional lanes, the need for a better file transfer capability (other than floppy disk) became obvious. Accordingly, provision was made for the use of a 100 Mbyte drive at the control station. This modification was implemented and utilized at Yuma.
- The importance and difficulty of analyzing the data from a two-dimensional area scan before performing a verification was recognized.

1D & 2D Area Performance Curves

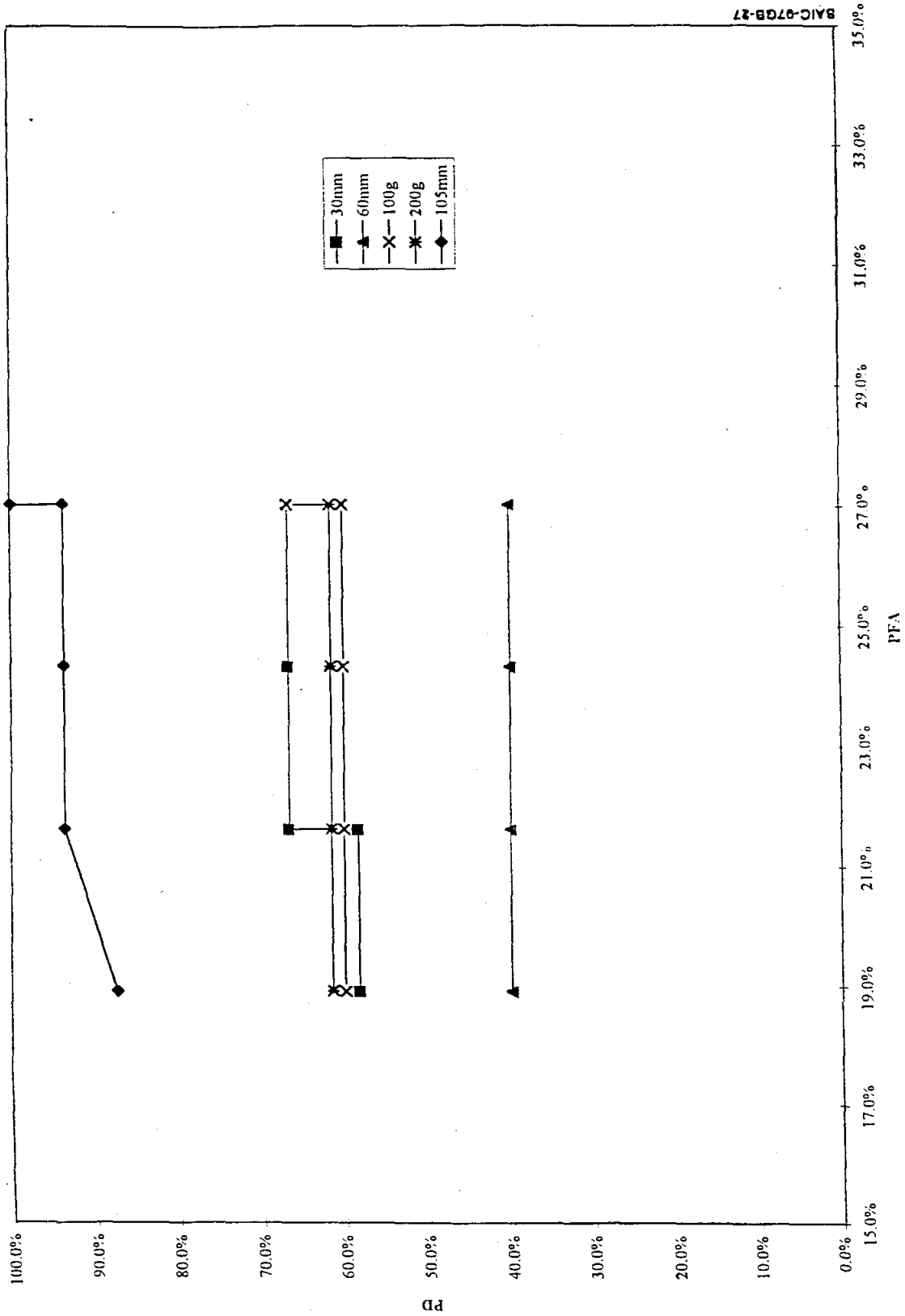


Figure 9.23. ROC Curves for 1D and 2D Areas.

of tests at Yuma Proving Ground. It was also apparent that the positioning accuracy of the system needed to be increased to allow the TNA to be positioned within a detection radius of around 13 cm (5 in.) from the UXO.

- Data collection on a two dimensional area was first demonstrated. Since the files from two-dimensional areas are much longer than the ones from the one-dimensional lanes, the need for a better file transfer capability (other than floppy disk) became obvious. Accordingly, provision was made for the use of a 100 Mbyte drive at the control station. This modification was implemented and utilized at Yuma.
- The importance and difficulty of analyzing the data from a two-dimensional area scan before performing a verification was recognized.

10. YUMA TEST

The Yuma test was carried out with the metal detector and the TNA operated together as an integrated system. While some of the data were collected with the two sensors operating independently, most of the time the two sensors operated together. Except during the TNA data collection at the beginning of the test, the two sensors were always mounted on the same vehicular platform (the Robotech vehicle).

The test was conducted at the Kofa Range within the Yuma Proving Ground, Yuma AZ. The test was conducted during the period October 29, 1996 through November 15, 1996. Climatic conditions during the tests were arid with temperatures mostly in the nineties (deg F). Moderate winds were encountered during the test at Yuma.

10.1 DESCRIPTION OF THE SITE

Figure 10.1 shows a general map of the area where the tests were conducted. Six one-dimensional lanes were laid out. Of these, one was used exclusively for TNA calibration and data collection, another one was used for calibration of the metal detector as well as the complete system, and the remaining ones for the blind test. The TNA data collection area was located across from the calibration lane. The two-dimensional calibration area and two blind 50 m x 50 m areas were laid out as shown in the map. In general, the site was characterized by a very high level of metal clutter.

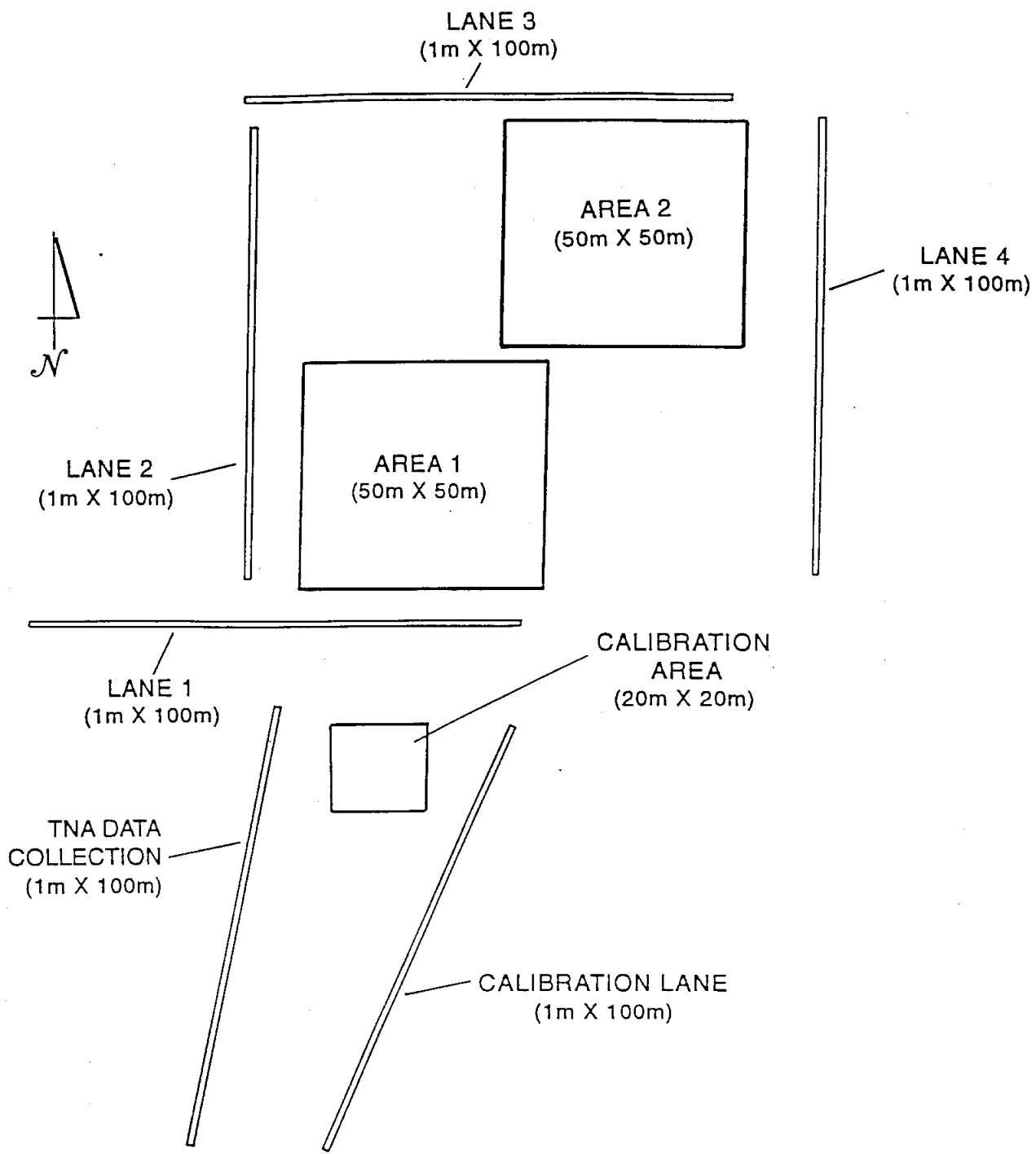
The shielding cask containing the Californium 252 source was kept at the center of a marked exclusion area, from where the source could easily be loaded into the TNA sensor. Yuma Proving Ground Safety Procedures were adhered to during the tests. During most of the tests the source remained loaded in the TNA sensor.

Each lane was about 100 m long and 1 m wide, and was marked on both sides with tensioned tapes. The path to be followed was easy to see with the remote TV camera while driving the vehicle down the lane. The surface of the lanes was quite smooth.

The Government arranged for installation of a tent, under which SAIC placed the control station for the UXO detection system. The controls for the vehicle and for all sensors were located side by side under the same tent.

10.2 DESCRIPTION OF THE ORDNANCE

The targets used in the test consisted of ordnance with the fuze or devices removed for safety reasons. The type of targets, explosive contents, nitrogen content, and typical depth, are listed in Table 10.1.



SAC-97GB-31

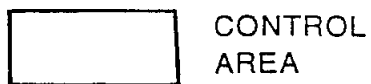


Figure 10.1. Map of Area used in the Yuma Test.

Table 10-1 Ordnance Information

Name	Type	Explosive Content	Nitrogen Content	Typical Depth
M56A3	20 mm HE round	10.7 g H-761 plus 38.9 g propellant	(3.53 g)+	Surface - 3 in.
M789	30 mm HEDP projectile	22 g Type PBXN-5	7.9 g	Surface - 3 in.
Simulant	Cylinder	100 g C4	34 g	Surface - 6 in.
M822	40 mm projectile	120 g Octol	39.6 g	Surface - 6 in.
Simulant (S)	Cylinder 9 in.× 1 in.	200 g C4	68 g	Surface - 12 in.
Simulant (L)	Cylinder 10 in.×1 in.	200 g C4	68 g	Surface - 12 in.
M49A5	60 mm mortar	.79 lb. (359 g) Comp B	111.1 g	Surface - 12 in.
M821	81 mm mortar	1.6 lb. RDX/TNT	-	Surface - 12 in.
Simulant	Cylinder 6 in.×5 in.	2.5 lb. C4	.83 lb. (378.3 g)	Surface - 12 in.
M393A2	105 mm HEP-T projectile	4.4 lb. Comp B	1.34 lb. (609.3 g)	Surface - 12 in.

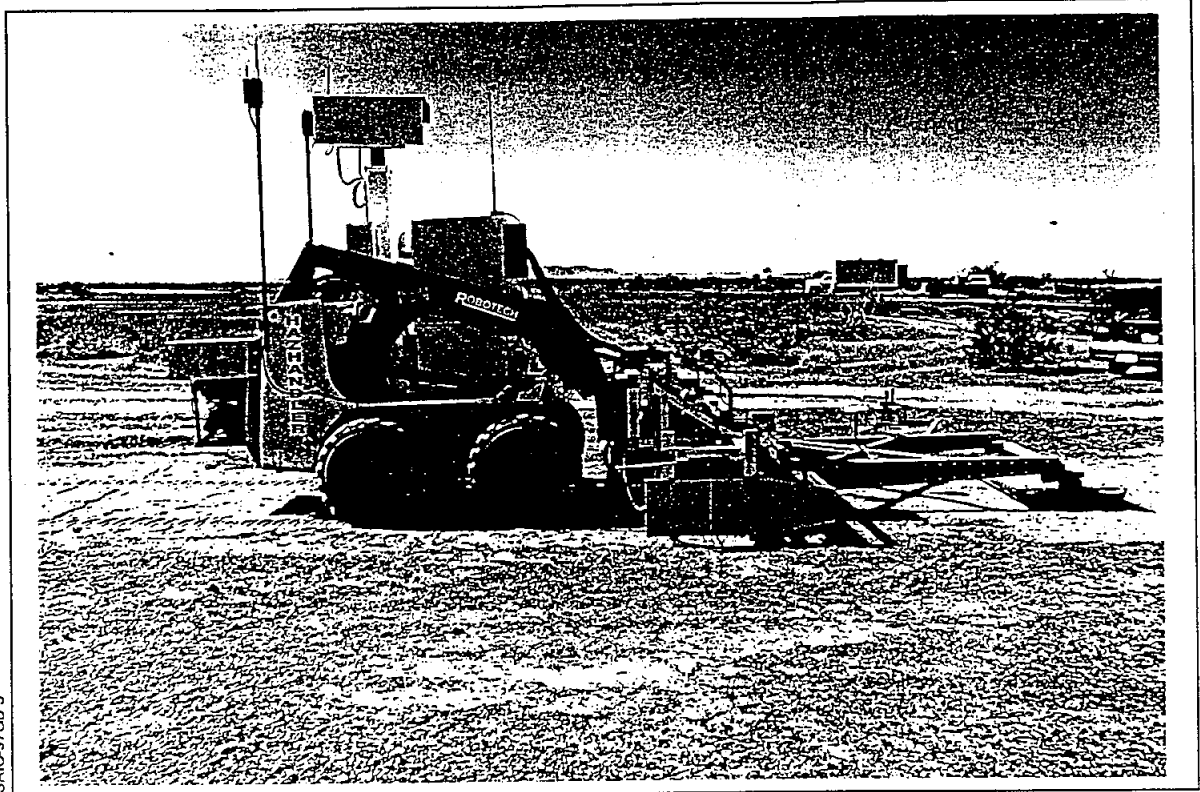
10.3 SUMMARY OF DATA ACQUISITION

Since data from the two sensors were collected mostly in an integrated way at Yuma, the only platform used was the Robotech vehicle. The metal detector was mounted with a semi-rigid attachment to the vehicle boom, as shown in Figure 10.2.

Preliminary activities during the test period included calibration and data collection carried out with the TNA only. During this phase, the TNA was positioned, using the Robotech vehicle, on top of targets placed by the Government test team. For the data collection, the operator knew the position of the targets, but not their nature or depth. The actual blind test was conducted on the one-dimensional lanes and on the two-dimensional areas.

Lane 1 was inspected according to the original test plan, that is finding anomalies with the metal detector, deciding immediately whether to use the TNA and conducting the verification inspection (stop and go). Because of the very large amount of clutter, it became evident that this method was not efficient enough, given the time limitations for the test. Accordingly, Lanes 2, 3, and 4 were scanned first, a cursory analysis of the scan was carried out, and candidate targets (usually large ones or characterized by negative peaks in the metal detector signal) were identified (scan and search). The vehicle was then driven to the approximate positions identified, the large signal targets were found again, and a verification was carried out. Originally we had intended to carry out scans on the four lanes at the end of the verification process. Because of the switch in the way of conducting the test, we missed carrying out a scan on Lane 1.

The scan and search mode of operation was the one anticipated for Area 1 in the test plan. The scan of Area 1 took about six hours using a "race track" pattern, which minimizes time spent by the vehicle outside the area of interest. On site analysis of the data resulted in 54 potential targets identified. The



SAIC-97GB-3

Figure 10.2. System Configuration used for the Yuma Test.

vehicle was then driven back to the targets identified, using the navigation features, the signals were found again with the metal detector, and the verification with the TNA detector was carried out.

There was very limited time left for measurements on Area 2, therefore no scans or searches were conducted. Instead, TNA verifications were made at a selected number of points specified by the test director.

Figure 10.3 illustrates the major activities that were carried out during the test period. Note that there is no overlap between the data taken with the TNA and with the metal detector.

10.4 COORDINATE SYSTEM

The UXO targets and clutter objects emplaced by the Government in the calibration and blind areas were surveyed in using theodolites with respect to a predefined coordinate system. Also surveyed in were the points found by the metal detector and marked automatically by the paint sprayer, and the center of the TNA sensor locations. Comparison of the two sets, ground truth and experimental estimates, is the basis for the assessment of detection probabilities. Since our system records latitude and longitude by differential GPS (with nominal submeter accuracy) we have the ability to determine a third set of observations, that is coordinates derived from latitude and longitude, as provided by GPS, to compare to the ground truth. In order to do this, we must know the relationship between latitude and longitude, and the system of coordinates used by the Government. Accordingly, one of the first activities during the test was to determine this relationship.

At Yuma, the Government used a single system of coordinates. To convert from latitude and longitude to the Government coordinate system we apply the following transformation:

$$X(\text{meters}) = (\text{Lon}_0 - \text{Lon}) \times N_x \cos \alpha + (\text{Lat} - \text{Lat}_0) \times N_y \sin \alpha$$

$$Y(\text{meters}) = -(\text{Lon}_0 - \text{Lon}) \times N_x \sin \alpha + (\text{Lat} - \text{Lat}_0) \times N_y \cos \alpha$$

where $\text{Lon}_0 = 114.3032975$ $\text{Lat}_0 = 32.8582336$ $N_x = 93,601$ $N_y = 110,902$
 $\alpha = -1.9544$ deg

All the plots and comparisons that follow are done using navigation data and the above sets of coordinates, as appropriate. The purpose of this is to give a graphical representation of the accuracy achievable with the navigation variables. Detection probability is discussed later using the actual marks. It should be noticed that latitude and longitude (and the derived X, Y coordinates) refer to the position of the GPS antenna, which usually does not coincide with the alarming metal detector coils. Proper offsets, which depend on the orientation of the vehicle (as described by the navigation equations in Section 7) must be applied. In the plots, crosses represent the position of the targets (ground truth) while the circles are centered at the estimated position from the metal detector signals and from the navigation data. The radius of the circles is intended to give an idea of the positional uncertainty from GPS.

10.5 METAL DETECTOR RESULTS

10.5.1 One-Dimensional Lanes

The metal detector inspected five one-dimensional lanes, of which one was used for calibration and the remaining four for the blind test. Each lane was 100 m long, with the four blind lanes roughly forming the sides of a square. The surface of the lanes was quite smooth. All lanes (except lane 1) were scanned once with the Robotech vehicle.

The calibration lane contained 10 targets. Figure 10.4 shows a plot of the actual position of the targets (crosses) and of the estimated positions from the scan with the Robotech vehicle (circles), using the GPS information and the transformation above. All the targets in the calibration lane were clearly visible. There was a limited amount of clutter and all the targets were detected.

Lane 1 contained 13 targets. It was not scanned, and therefore we do not show a comparison figure for it.

Lane 2 contained 4 targets only. Figure 10.5 shows a comparison of targets and estimated detections. All targets were detected and there were 8 false alarms.

Lane 3 contained 15 targets. Figure 10.6 shows a similar comparison. Four of the targets were missed and five false alarms were registered.

Lane 4 (Figure 10.7) contained 10 targets. All but one of the targets were detected. In addition, there were three false alarms.

The figures above provide an overall visual indication of the performance of the metal detector and of the navigation system in detecting and reporting the position of UXO targets. Note that in the scans on the one-dimensional lanes complete coverage was assured, that is we have complete confidence that the metal detector went over each target.

10.5.2 Two-Dimensional Areas

The test included three two-dimensional areas, one for calibration (20 m \times 20 m), and two for the blind test (50 m \times 50 m). All the measurements on these areas were conducted with the Robotech vehicle. The 20 m \times 20 m calibration area contained 10 targets. Figure 10.8 shows a plot of the target positions (crosses) and estimates obtained from the scan (circles). All of the targets were detected. There was a limited amount of clutter resulting in three false alarms.

The 50 m \times 50 m Area 1 contained 60 targets. Figure 10.9 shows a similar comparison plot. The estimates are represented by 66 circles. These estimates are not the ones (54) that were derived in Yuma during the blind test, but are a second set that was derived in San Diego with a more careful analysis of the data. This set of coordinates was provided to the Government in advance of receiving the ground truth. The plot shows that 39 targets were detected. In addition, 25 false alarms were registered. Area 1 contained a very large amount of clutter.

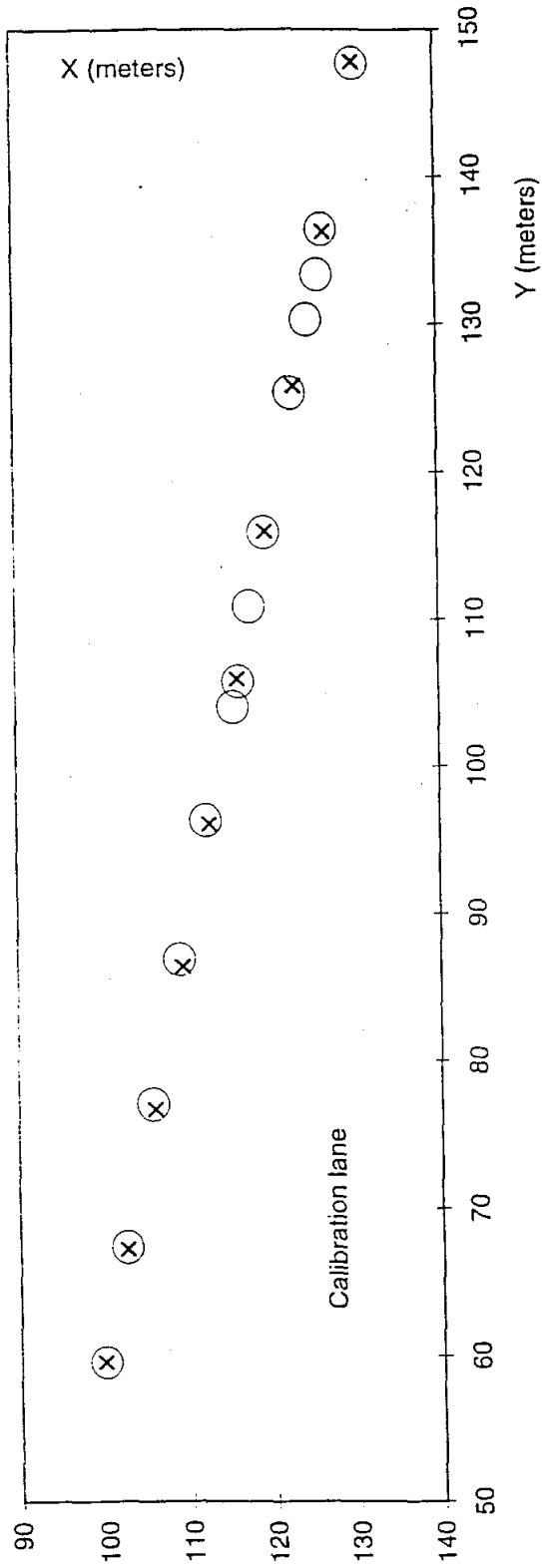


Figure 10.4. Targets and Estimated Positions in Calibration Lane.

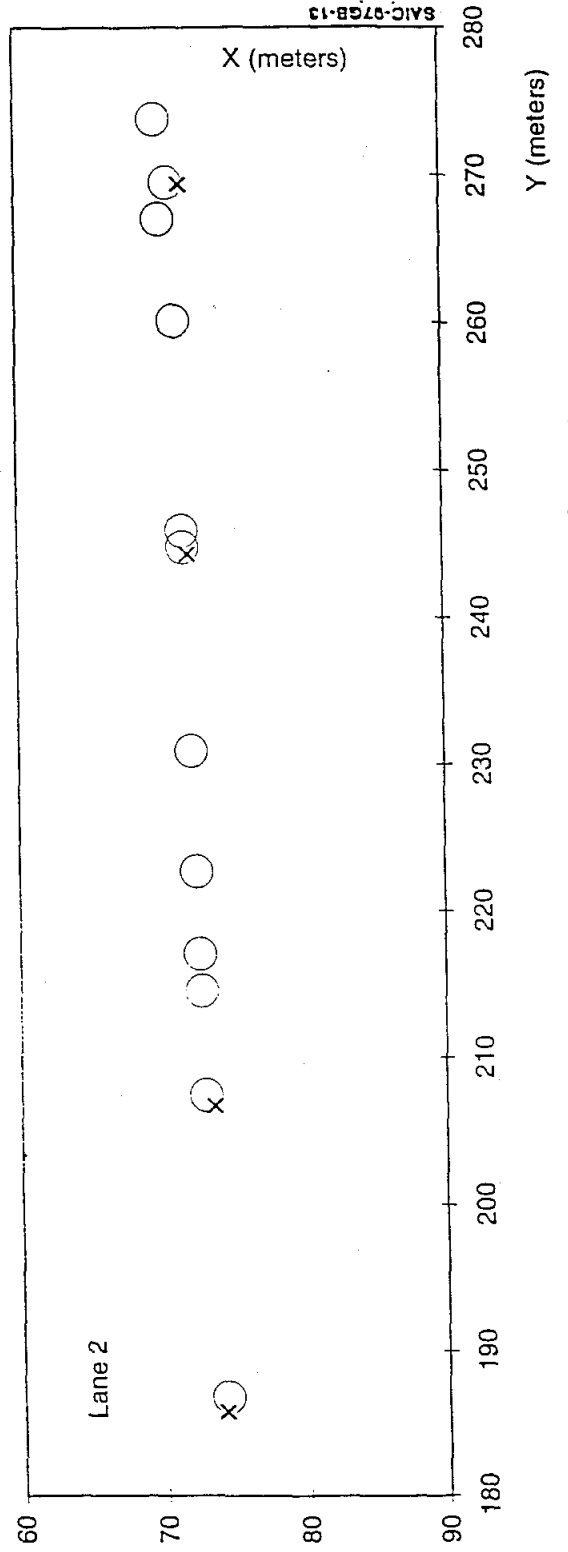


Figure 10.5. Targets and Estimated Positions in Lane 2.

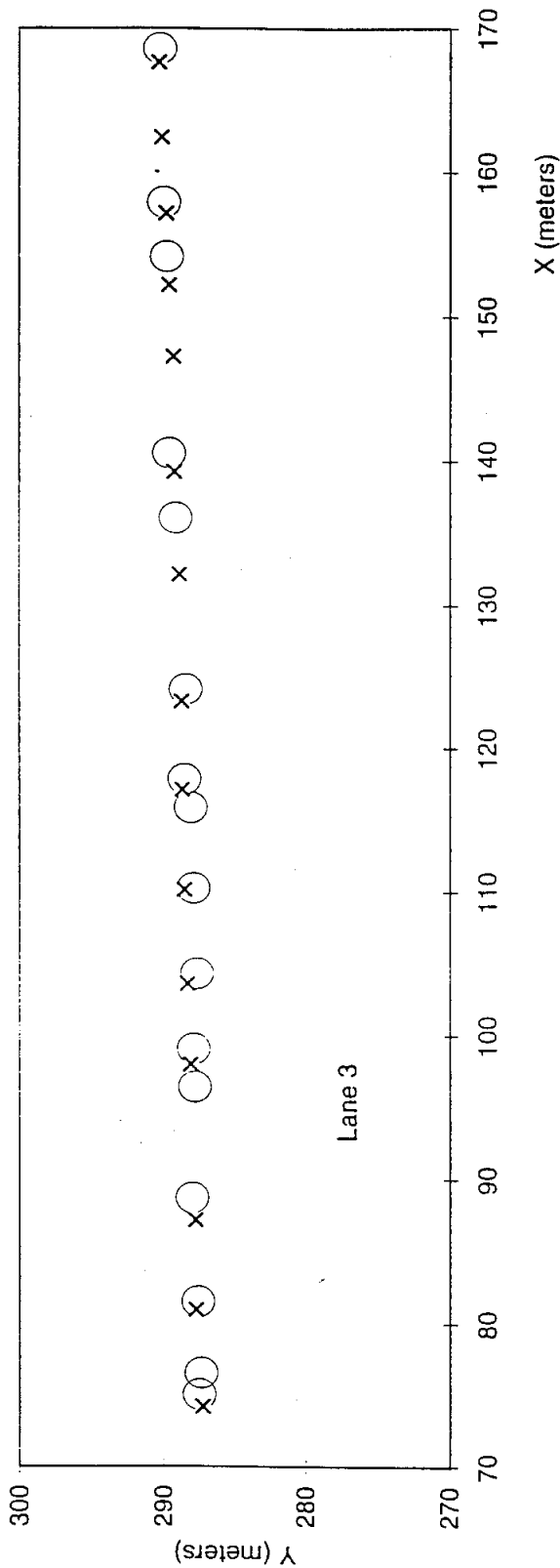


Figure 10.6. Targets and Estimated Positions in Lane 3.

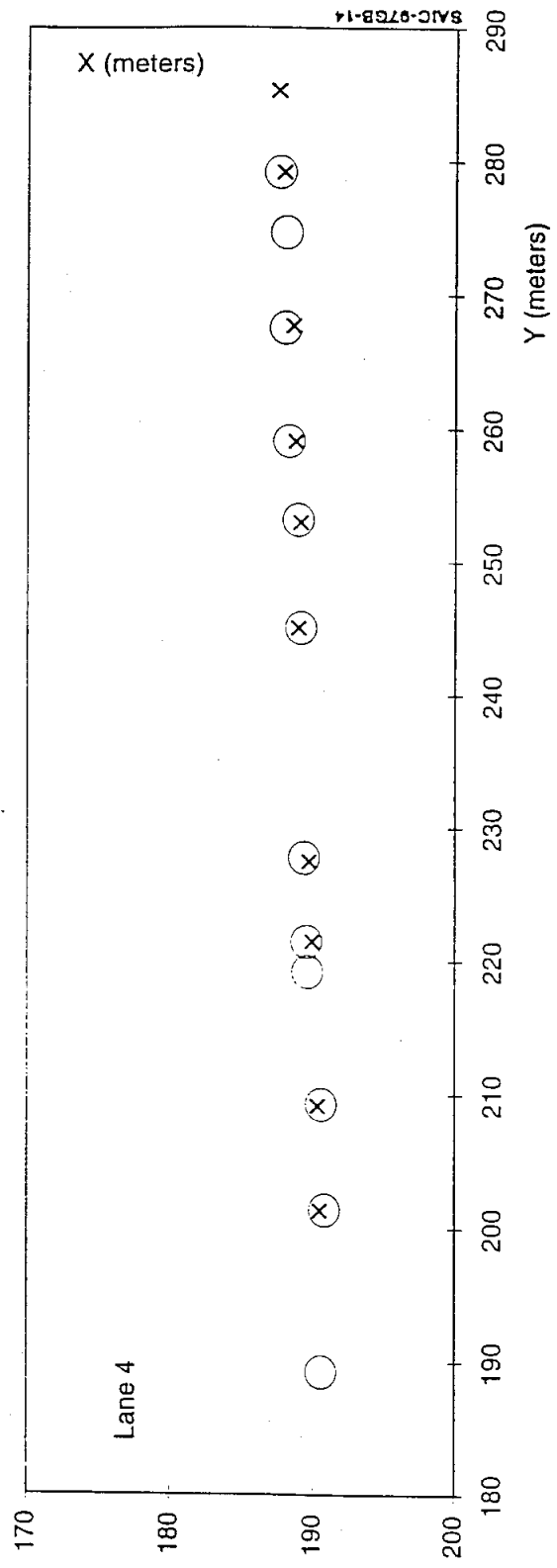


Figure 10.7. Targets and Estimated Positions in Lane 4.

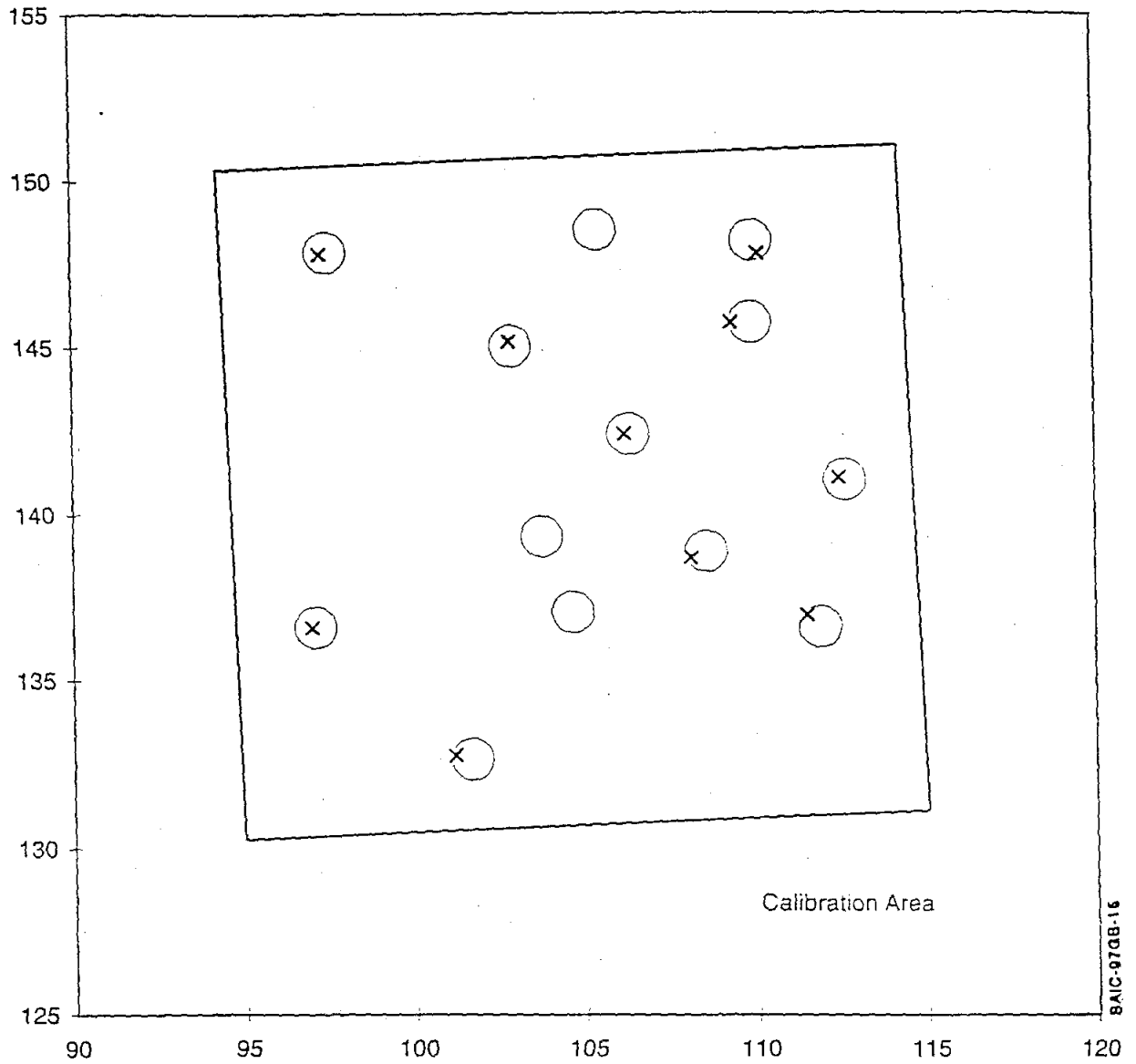
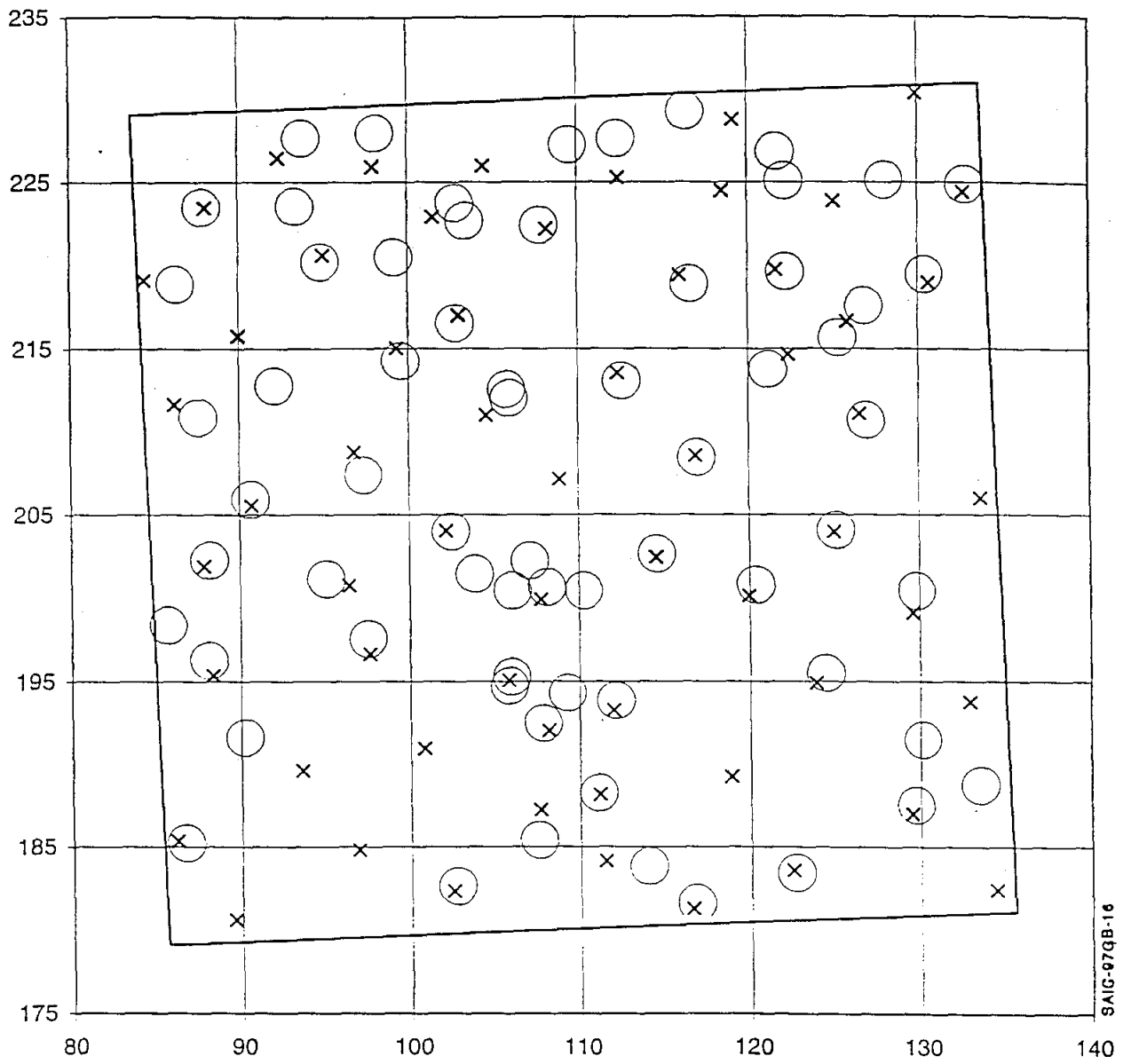


Figure 10.8. Targets and Estimated Positions in Calibration Area.



SAIG-97QB-16

Figure 10.9 Targets and Estimated Positions in Two-Dimensional Area 1.

For the two dimensional Area 1, unlike the scan at Socorro, we do have very good assurance of complete coverage of the area. Missing of the targets was due to a self imposed limit in the number of guesses made, and to competition from clutter. There was no time to scan Area 2.

10.5.3 Detection Probabilities

The data presented above are the result of analysis of stored data. The test also included marking the ground at the points of detection and subsequent measurement by the Government of the marked points. On both the one-dimensional lanes and the two dimensional areas the marks were done automatically using the paint marking system on the Robotech vehicle.

Table 10-2 shows the ratios of targets found to the total number of targets and the number of false alarms per square meter for both the analysis method (navigation) and the marking method. The marking method is based on a 6 in. halo, while the navigation (or mapping) method is based on a much more relaxed (a circle with a radius of about 1.0 meter) criteria. Numbers are given separately for the one-dimensional lanes and for the two dimensional area.

Two issues are important. The first one is the sensitivity of the detection probability with respect to halo size. Figure 10.10 shows the detection probability versus halo size for both one-dimensional lanes and two-dimensional areas. The second issue is the accuracy of marking, which should be closely related to the accuracy of positioning the verification detector over the detected target. Figure 10.11 shows a histogram of discrepancies between true values and marked values in the scan direction. The systematic positioning error that was present in the Socorro test appears to have been eliminated in the Yuma test.

Table 10-2 Detection and False Alarm Rates for Yuma Test

	Navigation (1m Radius)		Marking (6 in. Halo)	
	Detection Probability	False Alarm Rate	Detection Probability	False Alarm Rate
One-Dimensional	24/29	16/300m ²	28/35	64/360m ²
Two-Dimensional	39/60	25/2500m ²	22/60	25/2500m ²

10.6 TNA RESULTS

After initial set up and calibration, the TNA sensor was tested over a two week period on a data collection area, and on the one and two-dimensional test areas. The goals of the testing were to determine the envelope of performance of the upgraded TNA sensor and to test the overall integrated system performance. During the Socorro tests, post processing of the data showed that the TNA sensor had relatively good performance on UXO greater than 60 mm, marginal performance on 30 mm UXO and that the sensor was not sensitive to 20 mm UXO. Based on SAIC's recommendation, the number of detectors in the sensor had been increased from eight to twelve which should result in a 50% increase in signal strength. The modification was made prior to the field test at YPG.

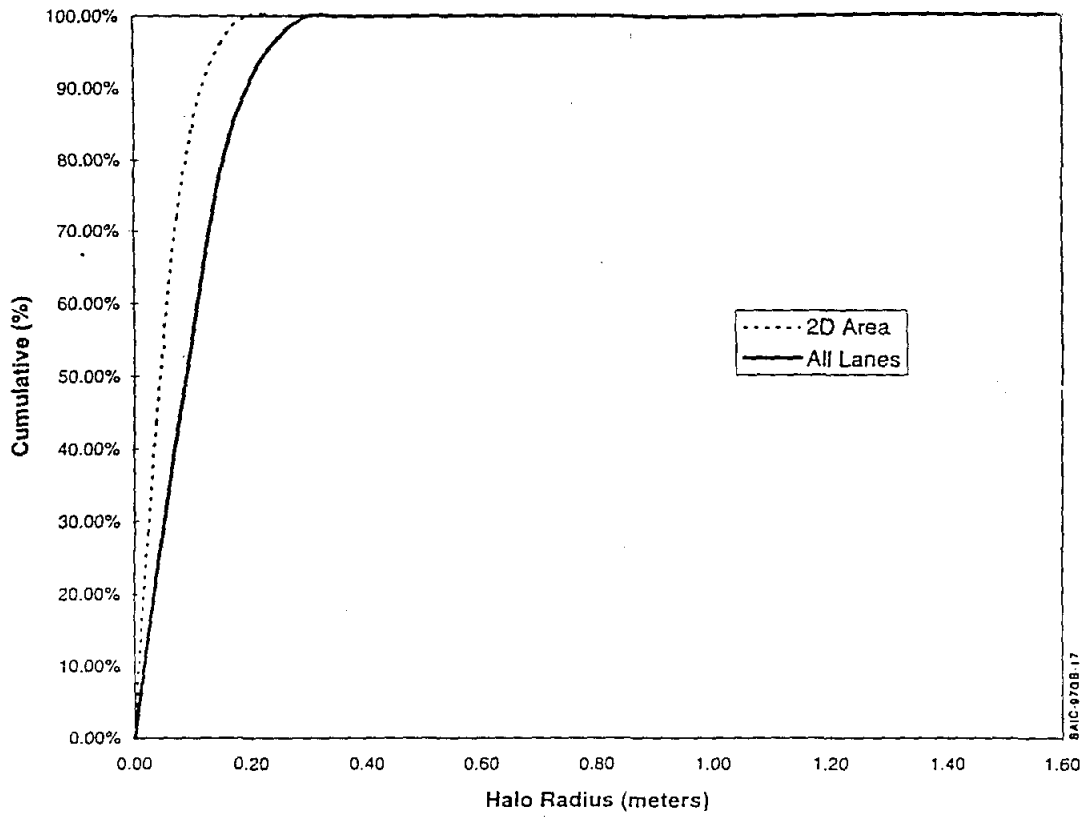


Figure 10.10. Detection Probability Versus Halo Radius.

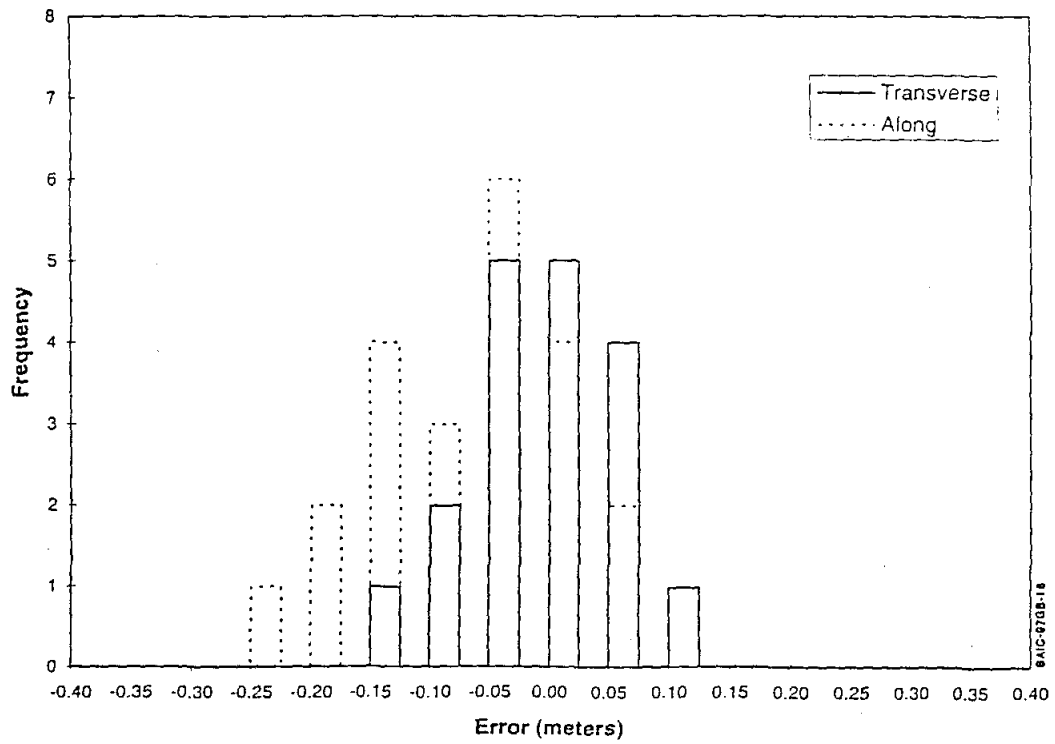


Figure 10.11. Histogram of Position Errors (absolute values).

10.6.1 Data Collection Area

The data collection area was set up to test the intrinsic performance of the TNA sensor with minimal contribution from overall positioning error. The parameters of interest were UXO size, burial depth and displacement of UXO from the center of the TNA sensor. The test was blind with a range of real UXO targets as well as inert targets. Positioning was done with the TNA mounted on the Robotech platform.

Table 10-3 summarizes the results of the measurements. In the table some of the displacements listed had large uncertainties due to the attempt to use a theodolite to remotely position the TNA sensor relative to the buried target during the first day of testing. This method was abandoned after the first day and the sensor was positioned manually. The displacement uncertainty was undocumented but estimated to be 3 in. to 6 in.

Table 10-3 Data Collection Area - TNA Decisions

Target	No. in Test	Real Time Decisions		Post Processing	
		No. Detected	Missed Targets Depth/Distance	No. Detected	Missed Targets Depth/Distance
30 mm	10	7	1 in./6 in. (*) 0 in./3 in. 0 in./3.6 in.	8	1 in./6 in. (*) 0 in./3.6 in.
100 g	11	10	1 in./3 in. (*)	10	1 in./3 in. (*)
40 mm	15	14	6 in./3.4 in.	14	6 in./3.4 in.
200 g	9	7	6 in./3 in. (*) 6 in./3.6 in.	7	6 in./3 in. (*) 6 in./3.6 in.
60 mm	27 [#]	22	6 in./6 in. 6 in./0 in. (*) 6 in./3 in. (*) 6 in./3 in. 6 in./5.5 in.	23	6 in./6 in. 6 in./0 in. (*) 6 in./3 in. (*) 6 in./3 in.
81 mm	18	17	12 in./3 in.	17	12 in./3 in.
2.5 lb.	4	4			
Total	93	81		83	
Empty Hole	3	1		3	2

(*) The distances marked with asterisks were measured on the first day of the test and may have had significant errors in the noted values.

Figures 10.12 through 10.18 show the detection results for the different size UXOs a function of burial depth and nominal displacement. These figures show the post processed decisions (filled squares), and the missed detections (open circles). Post processing on the recorded data included adding a decision feature which was a threshold sum of the maximum counting rate in three adjacent detectors.

[#] DC spot #27 was measured twice and both were alarms.

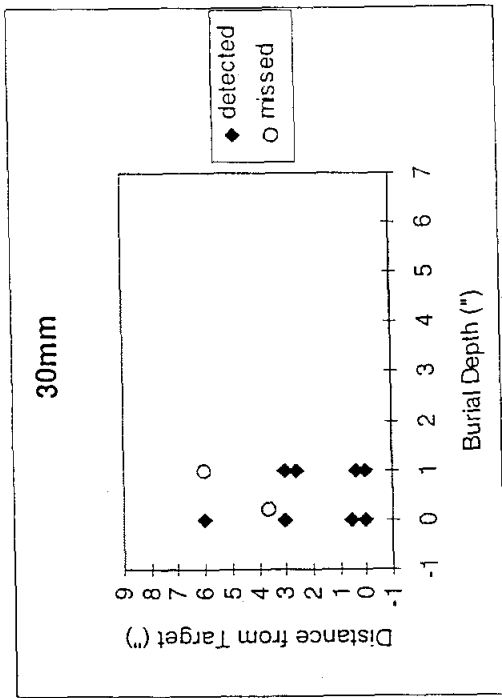


Figure 10.12. Data Collection Results for 30 mm Ordnance.

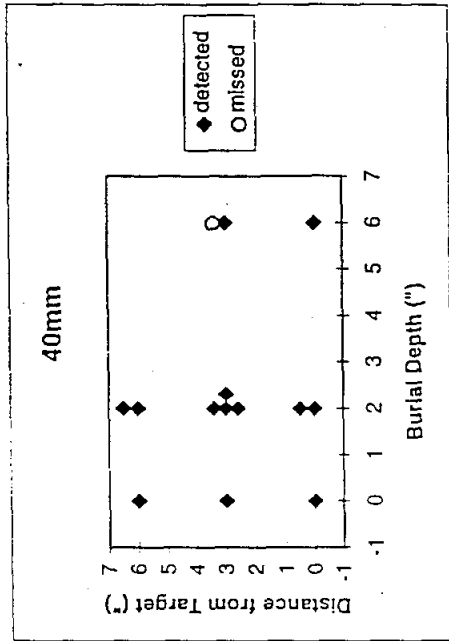


Figure 10.13. Data Collection Results for 40 mm Ordnance.

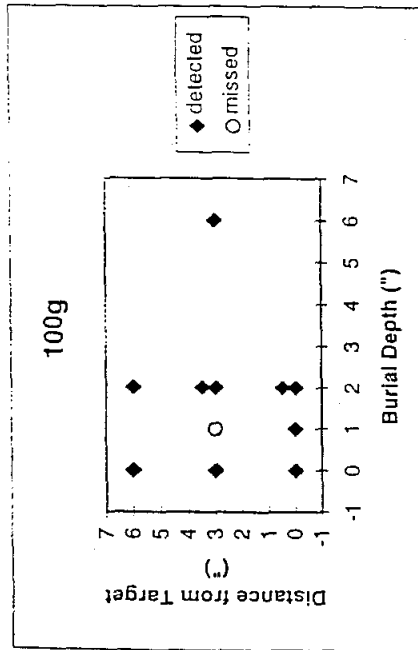


Figure 10.14. Data Collection Results for 100 g Simulant.

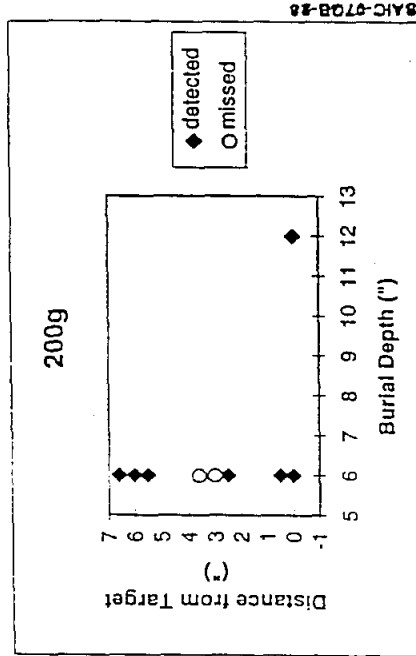


Figure 10.15. Data Collection Results for 200 g Simulant.

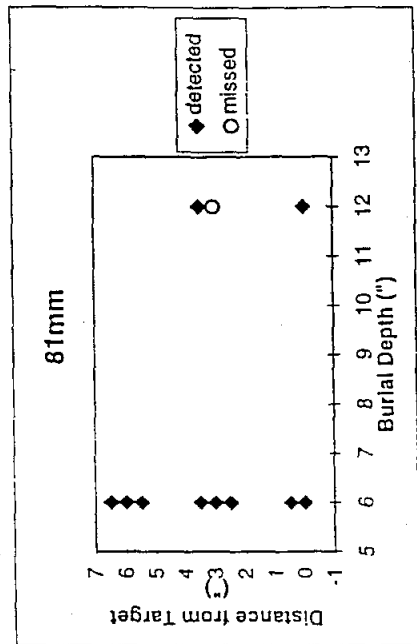


Figure 10.17. Data Collection Results for 81 mm Ordnance.

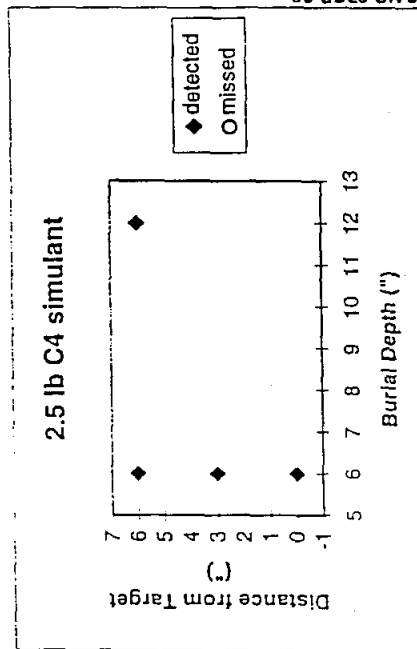


Figure 10.18. Data Collection Results for 2.5 lb. Simulant.

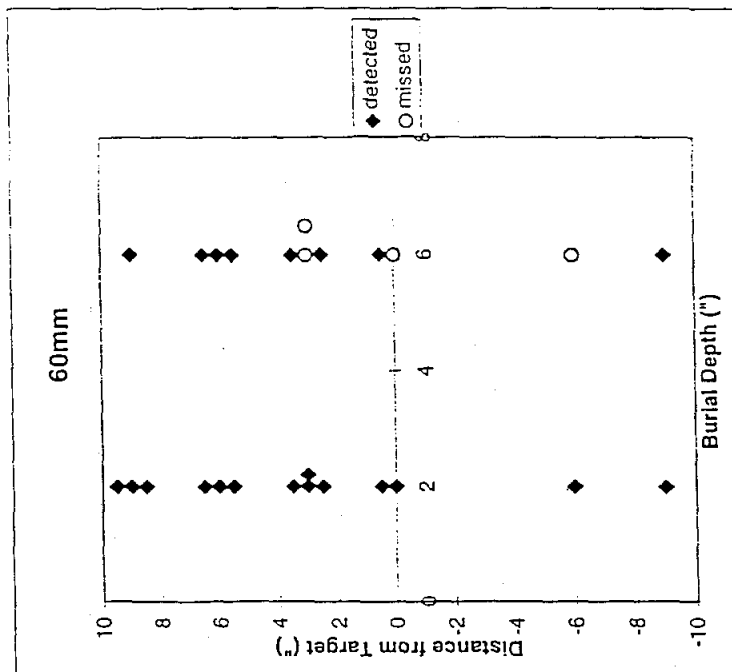


Figure 10.16. Data Collection Results for 60 mm Ordnance.

The performance on the data collection area is characterized by a high detection probability with occasional missed detections primarily for deeper targets or those further displaced from the center of the TNA.

10.6.2 One Dimensional Lanes

As described in section 10.5, the one dimensional lanes were characterized by having many metal detector hits which came from buried objects not placed by the test team. On Lane 1, the decision to interrogate the spot with the TNA was made in real time, thus all large metal detector signals were subsequently interrogated by the TNA. Subsequent lanes were first mapped by the metal detector and spots for interrogation by the TNA picked from the data maps. Because of the large amount of clutter, the TNA measured many more spurious points than test points on the lane. Figures 10.19 through 10.22 show, for each individual lane, the position of the targets (indicated by crosses) and the positions of the locations where the TNA decisions were made. The alarms are indicated by open circles and the clears by open squares. These figures give a quick visual indication of the results, however because of the scale, it is not possible to tell when the target was not in the detection range of the TNA.

Table 10-4 lists detailed results of these measurements using the post processed data. As Table 10-4 shows, there were a significant number of these targets whose signal exceeded the thresholds set for TNA detection in both the field results and the post processed data. The magnitude of signals in the data are high and appear more systematic than statistical. As will be seen below, most of the spurious metal detector hits on the two dimensional area were cleared by the TNA. It can be speculated that there were perhaps real UXOs in the lanes or that there was a systematic uncompensated-for shift in the TNA noise level.

Table 10-4 Detailed Post Processed Results on One Dimensional Lanes

UXO Type	Lane 1			Lane 2			Lane 3			Lane 4		
	Total	Alarm	Clear									
20mm	1	1	0	-	-	-	1	0	1	1	0	1
30mm	3	1	2	1	1	0	2	1	1	1	0	1
100g	2	2	0	-	-	-	3	2	1	1	1	0
40mm	1	0	1	1	0	1	-	-	-	1	1	0
200g	1	1	0	-	-	-	1	1	0	1	0	1
60mm	1	1	0	-	-	-	1	1	0	1	1	0
81mm	2	2	0	1	1	0	2	2	0	1	0	1
105mm	1	1	0	1	1	0	-	-	-	1	1	0
2.5lb	-	-	-	-	-	-	-	-	-	1	1	0
Unknown	22	15	7	14	9	5	19	9	10	9	1	8

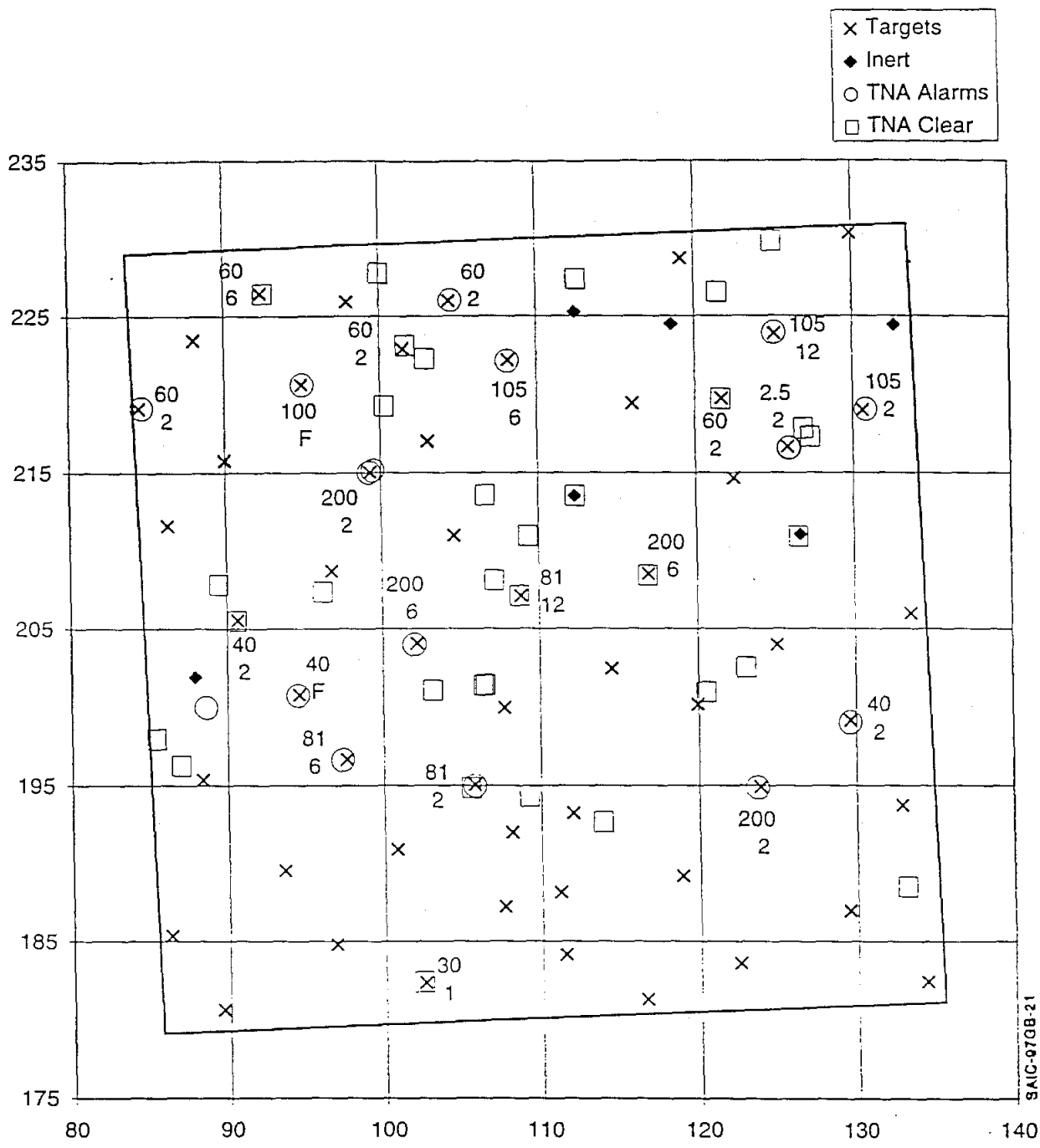
10.6.3 Two Dimensional Areas

Figures 10.23 and 10.24 show, for Area 1 and Area 2 respectively, the position of the targets (indicated by crosses) and the positions of the locations where the TNA decisions were made. The alarms are indicated by open circles and the clears by open squares. In addition, the inert targets are indicated with a different symbol. These figures give a quick visual indication of the results, however because of the scale, it is not possible to tell when the target was not in the detection range of the TNA.

As can be seen from the map, on Area 1 many of the buried targets were not selected for interrogation by the TNA. Likewise, many TNA interrogations were made of metal detector hits which had no test UXO buried by the Government test team. There were twenty four (24) UXO test objects, two (2) inert objects and twenty four (24) non-test ground locations which the TNA sensor measured, with interrogation times between five and ten minutes. Table 10-5 shows the results of the real time measurements as well as the post processed data which added the second decision feature. It is seen that 16 of the 24 targets were detected during the tests and that the post processing picked up an additional 3 targets, bringing the total number detected to 19. The table also includes the depth and displacement distance of the missed targets. It is seen that the 60 mm and 80 mm targets missed were at significant burial depth and/or displacement distance. The 200 g stimulant and the 105 mm UXO that were missed in real-time were picked up in the post processing decision. The 60 mm and 81 mm targets were missed in real time and post processing. Of the twenty four (24) non-target interrogations and the two inert objects, none was detected in the real-time measurements and two were detected in post processing. These results demonstrate a high level of performance for the TNA sensor.

Table 10-5 Two-Dimensional Area 1 - TNA Decisions

Target	No. Measured	Real Time Decisions		Post Processing	
		No. Detected	Missed Targets Depth/Distance	No. Detected	Missed Targets Depth/Distance
30 mm	1	0	1 in./9 cm	0	1 in./9 cm
100 g	1	1		1	
40 mm	3	2	2 in.	3	
200 g	5	4	6 in./4 cm	5	
60 mm	5	2	2 in./23 cm 2 in./2 cm 6 in./16 cm	3	2 in./23 cm 6 in. / 16 cm
81 mm	4	2	2 in. / 25 cm 12 in./7 cm	2	2 in. / 25 cm 12 in./7 cm
2.5 lb.	2	2		2	
105 mm	3	2	12 in./0	3	
Total	24	15		19	
60 mm inert	1	Cleared			
81 mm inert	1	Cleared			
Metal Detector "Hits"	24	all cleared			



SAIC-9708-21

Figure 10.23. Targets and Real Time TNA Decisions on Area 1.

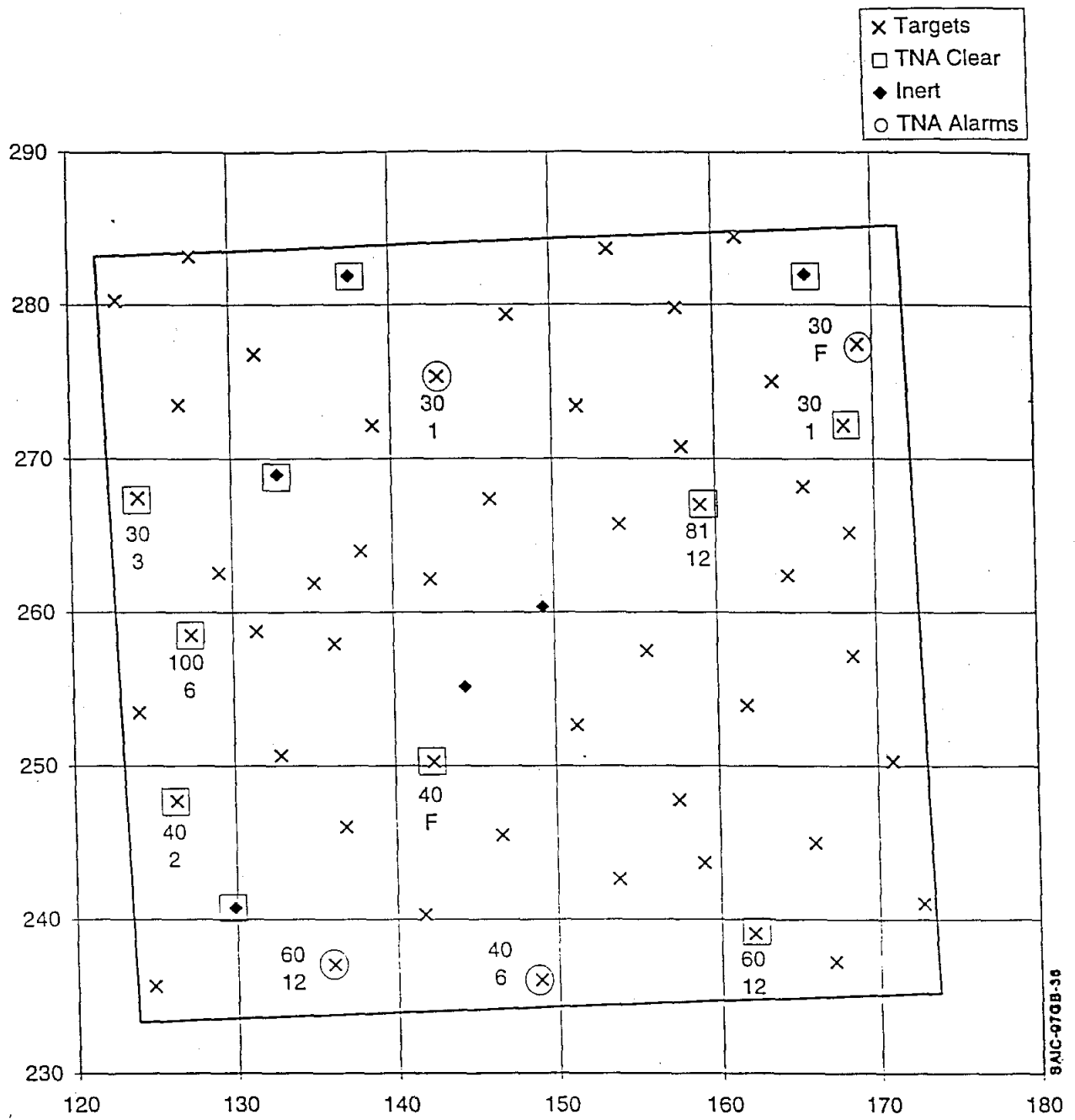


Figure 10.24. Targets and Real Time TNA Decisions on Area 2.

On two-dimensional Area 2 the government test team directed us to inspect specific targets in the area. These targets did not include the large UXO test objects and were buried at more challenging depths. The Government test team determined which targets to interrogate. This resulted in all of the interrogations to be known to the test team (i.e., no spurious metal detector hits were included). Fifteen (15) UXO targets of which four (4) were inert targets were measured. Table 10-6 shows the detection results. Only one detection was made in the real time tests and four detections were made in post processing. None of the four inerts was detected. The performance noted here, in many cases, may indicate a limit of performance of the presently configured sensor in terms of UXO size, depth and displacement. It can also be speculated that there was a systematic shift in the TNA sensor performance due to other influences. Both these hypotheses can be explored.

Table 10-6 Two-Dimensional Area 2 - TNA Decisions

Target	No. Measured	Real Time Decisions		Post Processing	
		No. Detected	Missed Targets Depth/Distance	No. Detected	Missed Targets Depth/Distance
30 mm(2) (2) (3) (3)	4	0	1 in./6.5 cm 0 in./16 cm 1 in./8.1 cm 3 in./10.5 cm	2	1 in./8.1 cm 3 in./10.5 cm
100 g	1	0	6 in./4.2 cm		6 in./4.2 cm
40 mm	3	1	2 in./3.1 cm 0 in./2.8 cm	1	2 in./3.1 cm 0 in./2.8 cm
60 mm	2	0	12 in./13.7 cm (V) 12 in./10.9 cm	1	12 in./13.7 cm (V)
81 mm	1	0	12 in./7.7 cm		12 in./7.7 cm
Total	11	1	10	4	7
30 mm Inert	1	0			
60 mm Inert	1	0			
81 mm Inert	2	0			
Total Inert	4	0		4	0

10.6.4 Summary and Extrapolations

The results from the YPG tests for the TNA showed a marked improvement over the Socorro tests, primarily in the real time decisions. The TNA performance was significantly higher on the data collection area and the 2-D Area 1 than on the 1-D lanes and the 2-D Area 2. The data collection area and 2-D Area 1 also contained the majority of the UXO targets and "non-UXO" metal detector hits (primarily 2-D Area 1).

There are several ways to summarize the overall performance of the TNA for the YPG tests. The test parameters of burial depth, displacement, and UXO orientation are too many to get a significant population in each category. In addition, the spurious low

performance on the last test area would significantly decrease the performance if included. For these reasons the data for the data collection area, the 1-D lanes, and the 2D Area 1 are presented as depth-displacement curves for the different UXO types, with no regard for orientation. Figures 10.25 through 10.32 show the detection results for the 30 mm through the 2.5 lb. UXO (first day results and 2D area 2 not included in figures). It is seen that there are a few misses with the 30 mm and that above that size there are only occasional misses which may be explained on a statistical miss basis.

Table 10.7 shows the overall results for the different targets on the different areas; targets from the first day of measurement are not listed. Also shown are the false positives measured on the spurious metal detector "hits" and the inert targets. As is seen the overall performance is much improved over the Socorro results.

Table 10-7 Overall Results TNA Decisions for Targets (only first day results not included)

Target	DC Area No. Detects		1D No. Detects		2D Area 1 No. Detects		2D Area 2 No. Detects		Total No. Detects	
30 mm	7	6	6	3	1	0	4	2	18	11
100 g	9	9	6	5	1	1	1	0	17	15
40 mm	14	14	3	1	3	3	3	1	24	19
200g	6	5	3	2	5	5			14	12
60 mm	22	20	3	3	5	3	2	1	32	27
81 mm	14	13	6	5	3	2	1	0	24	20
105mm			3	3	3	3			6	6
2.5 lb	3	3	1	1	2	2			6	6
Total Inerts and metal clutter	3	2	64	34	26	2	2	0	95	37

One of the questions not directly answered by these tests was what would the TNA performance be for a longer measurement time. Since the accuracy of the net nitrogen signal is ultimately bounded by the statistical limits of the number of nitrogen gamma rays counted, it is expected that longer counting times should lead to better separation of signal to noise. Besides the statistical limits, there is also a contribution to the signal uncertainty that comes from the signal processing algorithms and the variations in the background noise due to variables of measurement geometry, soil composition, moisture, etc. Measurements carried out during the field tests allow for a rough estimate of the performance increase that could be expected of a longer TNA measurement interval. This extrapolation is described below.

During the evenings of the second week of the tests at YPG the TNA sensor was positioned over various buried UXO and bare soil and through specially configured software logged data throughout the evening. During this period, the sensor took repeated measurements of the same target at ten minute intervals. The system

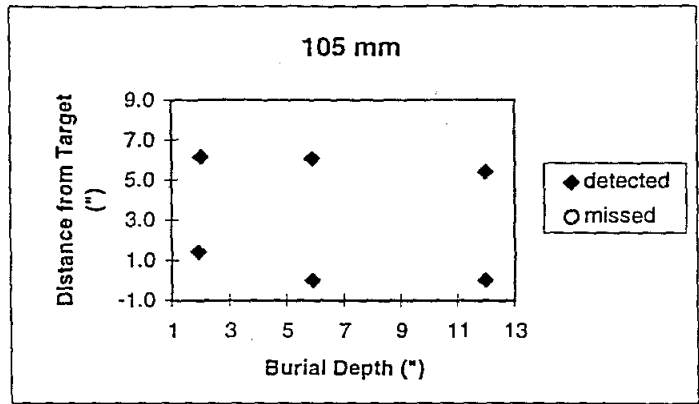


Figure 10.32. Overall Post Processed Results for 105 mm Ordnance.

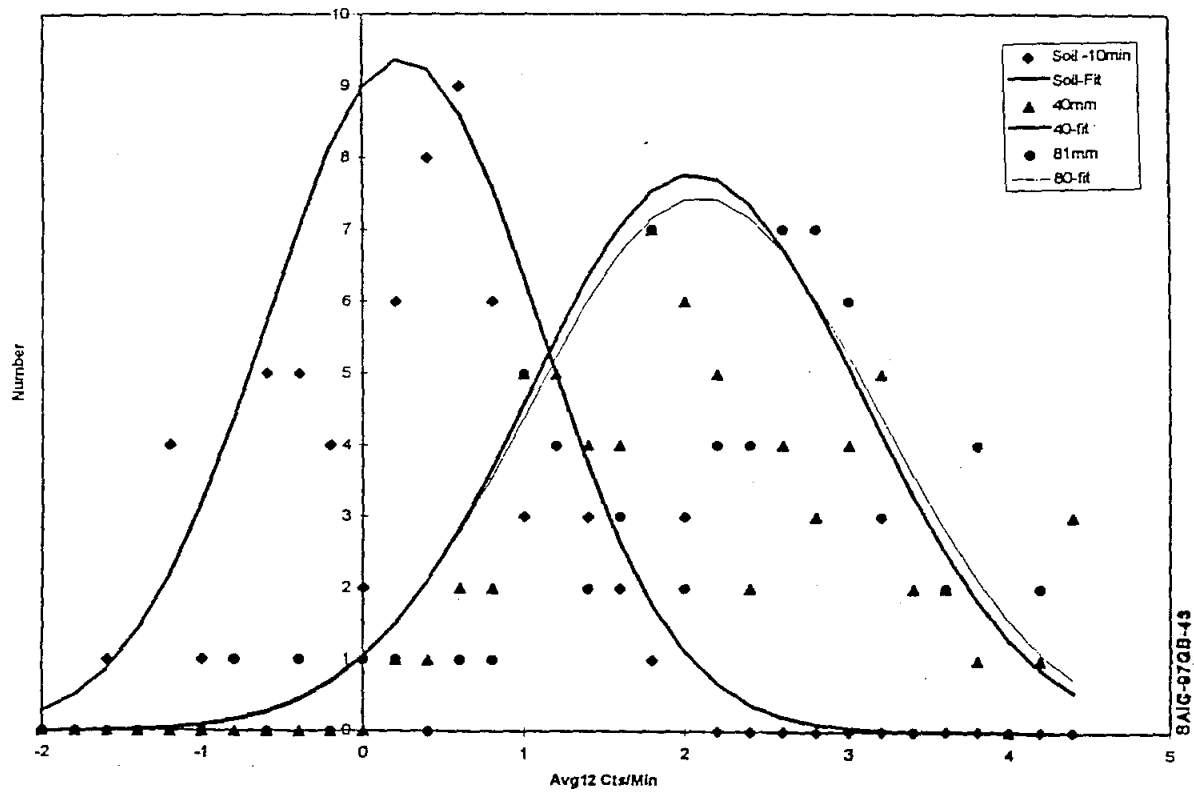


Figure 10.33. Distribution Plots for Multiple Measurements with Gaussian Fits to Distributions.

automatically stabilized the detector gains and logged both spectra from the twelve detectors along with their net nitrogen signals, and the average counting rates (in cpm) of all twelve detectors. Figure 10.33 shows the distribution of counting rates from measurements with YPG soil (diamonds), a 40 mm UXO buried at 2 in. (triangles) and an 80 mm UXO buried at 6 in. (circles). From the means and standard deviations of these net counting rates distributions, a normal (gaussian) distribution for each of the distributions has been calculated (solid lines). These calculated distributions are an estimate of the distributions if there had been many more measurements, and are easy to manipulate for the exercise at hand.

The normal distributions show the essential features of the detection trade off between probability of detection (PD) and probability of false alarm (PFA). In this case the threshold on the average counting rate in twelve detectors is raised. Fewer (false) alarms will arise from soil measurements but there is also a reduction in the number of cases from the UXO that will alarm. It is interesting to note how similar the distributions for the two different sized UXOs are; the signal from the larger 81 mm is diminished due to its deeper burial depth.

Using the same sets of data, pairs of measurements can be added to simulate results of a 20 minute measurement interval and sets of four measurements can be added to approximate the results of measurements for 40 minutes. With each addition, the means of the distributions remain the same but the standard deviations narrow. Figure 10.34 shows the normal distributions calculated from the so-combined data for the soil and the 40 mm UXO. It is seen that the distributions do indeed narrow with increased counting interval. It is also apparent that the overlap between the soil and UXO distribution is less giving a sharper decision threshold boundary. Using these distributions, PD and PFA (ROC) curves can be calculated for the three counting intervals. Figure 10.35 shows these curves. The curves give a rough estimate of the increase in performance of the present TNA sensor with counting time.

10.7 MAIN CONCLUSIONS FROM YUMA TEST

A number of lessons were learned from the Yuma test, as follows:

- In a high clutter situation preliminary mapping of the area before verification appears to be the most efficient strategy. This approach was used not only on the two-dimensional area, but also on a large portion of the one-dimensional lanes.
- It was demonstrated that it is possible to go back to a target and reacquire it as long as its signal is significantly different from the one generated by nearby clutter.
- Positioning precision, although improved over the Socorro test, could still be made better. The overall navigation accuracy, could be improved by using more advanced GPS receivers.

- While all the targets in the calibration lane and calibration area were detected, the analysis of the generated maps failed to detect all of the targets in the blind test regions. This was partially due to the fact that the targets in the calibration regions were not buried as deep as some of the ones in the blind regions. This generated a false perception, at least during the test, that we were able to recognize targets from the metal detector signals. It is apparent now that more knowledge is necessary to distinguish real targets from clutter. To some extent, this knowledge could be extracted from the data collected at YUMA.
- The overall performance of the TNA sensor as a confirming sensor was improved in YPG tests relative to the earlier Socorro Tests.
- The TNA sensor detected all 105 mm and 2.5 lb. targets down to a depth of 12 in.
- For the smaller targets there is an envelope of depth and displacement within which the detection probability is high for targets down to 40 mm.
- The 30 mm targets appear to be at the performance limit for the present TNA sensor.
- Increased interrogation time can increase the TNA sensor performance.

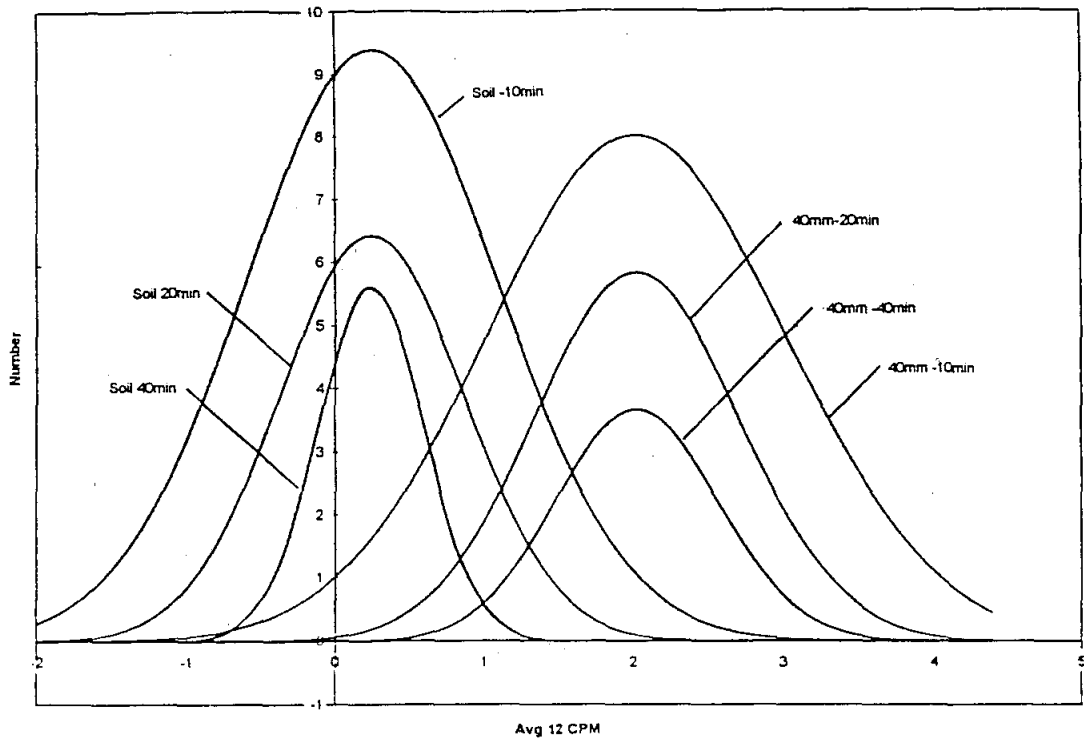


Figure 10.34. Normal Distributions for Soil and 40 mm Ordnance for Different Measurement Times.

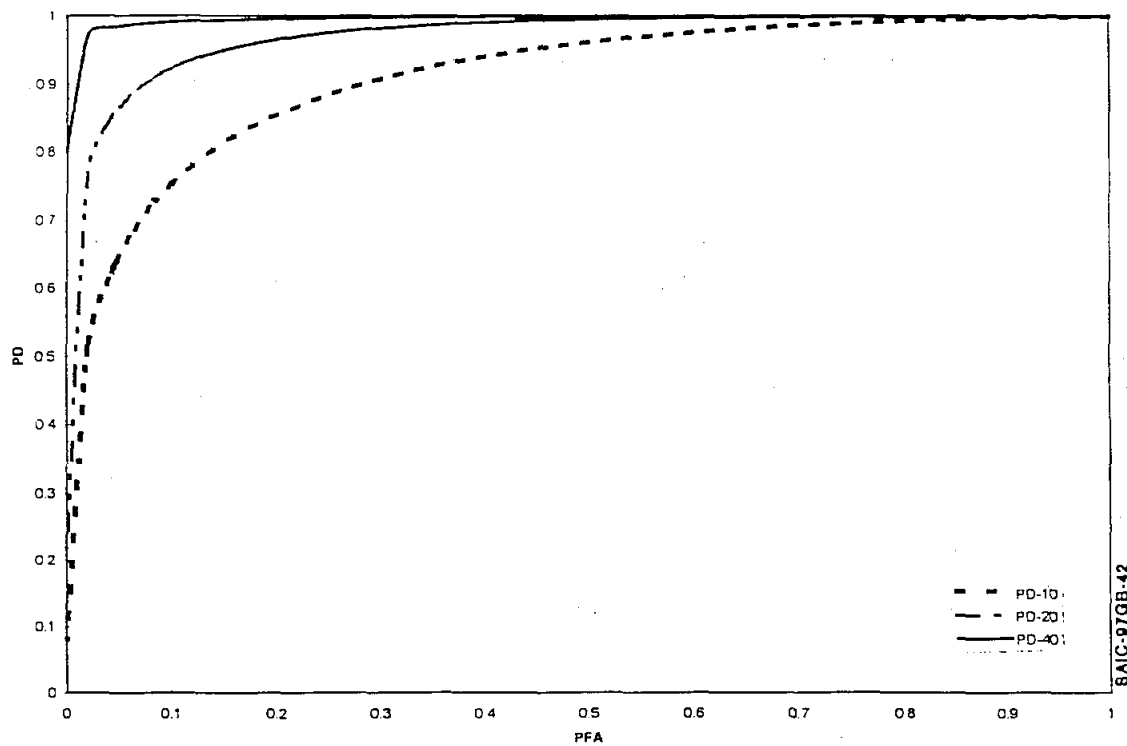


Figure 10.35. Calculated ROC Curves for 40 mm Ordnance and Different Measurement Times.

11. CONCLUSIONS

SAIC has completed both Phase 1 and Phase 2 of the Surface/Near Surface UXO Detector project. We believe that the major objectives of the project have been attained and that progress was made in several areas. We consider the following to be major positive accomplishments:

- The system has been successfully demonstrated in an integrated mode of operation, in which UXO targets were first found with the metal detector, and the presence of explosive was then confirmed with the TNA, with the entire system run remotely.
- Complete scan of a two-dimensional area was accomplished, and the ability to navigate back to an observed target was demonstrated.
- The performance of individual components, including the metal detector, TNA, and navigation equipment is now better understood.
- During the tests at YPG the TNA was in operation over the entire 18 day field test period - 24 hours per day. The sensor was self calibrating and operated under the ambient field test conditions with nearly 100% availability.

The test at Yuma Proving Ground has provided answers to some of the issues critical for the ESTCP assessment of the system. Some issues have been completely clarified and have simple answers. A second set of issues, involving detection probabilities for both the metal detector and the TNA, is more complex and does not have simple answers. The following is an assessment of the critical issues.

Mode of Operation Two modes of operation were originally considered for the system: "scan and search" (in which a map is produced, and is used to select targets that are then reacquired and verified) or "stop and go" (in which every metal detector alarm is immediately verified with the TNA). The test at Yuma proved unequivocally that in a highly cluttered area the most efficient mode of operation is "scan and search". In fact, this mode was eventually adopted on the one dimensional lanes (except for the first one), in spite of the fact that the test plan specifically called for the other mode.

Area Coverage There was some concern that the two dimensional area would not be completely covered with remote operation. The test demonstrated that it was possible to achieve complete coverage with the metal detector, by carefully following the tracks left by the vehicle. The coverage was confirmed with a laser tracking system. Utilization of a wider (2 or 3 meter) metal detector array would facilitate attaining complete coverage, which could be verified with the navigation equipment alone.

Positioning Accuracy Positioning accuracy was substantially improved over the Socorro test. The issue is not simple because it involves both the metal detector signal, its use in estimating the centroid of the UXO, and control of the vehicle. The positions of the targets and the center of the TNA during the blind test were accurately measured with a theodolite. From these measurements, the average

value of the distance from target to TNA center was 15.2 cm with a standard deviation of 9.2 cm. As one can see, there is still room for improvement of positioning.

Current Performance The probability of detection, both for the metal detector and the TNA, is a function of the ordnance size and the depth at which it is buried. Therefore, a detailed assessment is contained in the tables and figures presented in Sections 9 and 10. An overall detection probability for the entire population of targets used in the test is not an absolute quantity, since it depends on the choice of population. As long as one keeps this in mind, it is a good way of summarizing the results. There is more than one estimate of detection probability, depending on the procedure used (navigation, marking, halo size, post processing). Table 11.1 summarizes different estimates of detection probability for both the metal detector and the TNA for the part of the blind test at Yuma Proving Ground comprising the one dimensional lanes and the two dimensional Area 1 only. Also included for the TNA sensors are results from the data collection area, one dimensional lanes, and two dimensional Area 1.

Table 11.1
Different Estimates of Detection Probability

	Metal Detector	TNA
Navigation Estimate (SAIC) (*)	63/89	----
Marking Estimate (SAIC, 6 in. halo) (*)	50/95	----
Government Estimate (12 in. halo) (**)	56/91	32/51
Post Processing (SAIC) (***)	----	42/51
Including Data Collection Area (****)	----	126/142

(*) From Table 10.2

(**) As presented in Meeting at Santa Clara on February 11, 1997.

(***) From Table 10.7

(****) All data within range, excluding 2D Area 2

TNA Parameterization The behavior of the TNA response as a function of ordnance size, burial depth and displacement (position error) have been fairly well characterized in the tests at YPG (see Figures 10.25-10.32). The data show the general envelope of sensitivity. The response dependence on ordnance orientation is not clear from the measurements, largely because the populations were not great enough to draw meaningful conclusions.

TNA Acquisition Time The TNA measurement times at Yuma ranged between 5 and 10 minutes, with most of the measurements being carried out at 10 minutes. An analysis of the effect of increasing the measurement time to 20 and 40 minutes has been carried out, and shows a strong increase in detection probability and a lowering of the false alarm rate, as long as the errors are dominated by random counting statistics. The trade off between performance and acquisition time can realistically only be made in the overall context of a UXO clearance scenario which would involve the performance characteristics of all the sensors involved and the cost of false positives and missed detections. These important considerations are beyond the scope of the present program.

Although the performance has been substantially improved over the Socorro test, we are aware of limitations in the current system. The following is a list of such limitations, together with some ideas and recommendations for overcoming them:

- Not all the targets were found with the metal detector, especially in the two-dimensional areas. At Yuma, this was due to the large amount of clutter present and also to insufficient knowledge of the response of the metal detector from deep buried targets. We believe that the metal detector signals contain more information that has been utilized up to now. A more complete understanding of the metal detector signatures from the Yuma targets would allow one to make more correct calls. In this regard, the data collected at Yuma are a valuable resource.
- Not all the targets found by the metal detector were verified correctly with the TNA. The performance of the TNA can be further improved (higher PD, lower FAR).
- It is difficult to quantify the accuracy of the current navigation system. Most of the times the positions are accurate to half a meter, but under some circumstances errors of about one meter are possible. The navigation accuracy of the system could be increased to the centimeter level, by utilizing more advanced, commercially available, GPS receivers which use phase observables and dual frequency, and by introducing accuracy monitoring techniques.

The system developed and demonstrated was based on the two sensors, primary and verification, carried by the same vehicle. If the most efficient operational strategy is, as was demonstrated at Yuma, to scan first and verify later, and if the navigation ability can be improved to the point that the verification detector can be taken directly (that is without additional searches) to the suspect point, it may be advantageous to place the sensors on separate vehicles, which would result in simpler, less interfering, and easier to maintain systems.

**U.S. ARMY
YUMA PROVING GROUND**

TECOM Project No. 8-CO-160-UXO-003
YPG No. 97-TF-0075-L5

**TEST RECORD OF THE
ENVIRONMENTAL SECURITY TECHNOLOGY
CERTIFICATION PROGRAM DEMONSTRATION
OF THE
SAIC REMOTE CONTROLLED SURFACE/
NEAR SURFACE UXO DETECTOR**



BY

STEPHEN M. PATANE, MATERIEL TEST CENTER, YPG, AZ
AND

ROSHNI SHERBONDY, NIGHT VISION ELECTRONIC SENSOR DIRECTORATE, FT BELVOIR, VA

Prepared for:

Commander, U.S. Army Fort Belvoir
Night Vision Electronic Sensor Directorate
ATTN: NVESD
Ft. Belvoir, VA 22060

Commander, U.S. Army Test and Evaluation Command
ATTN: AMSTE-TA-S
Aberdeen Proving Ground, MD 21005-5055

Distribution limited.

Other requests for this document must be referred to:

Commander, U.S. Army Fort Belvoir
Night Vision Electronic Sensor Directorate
ATTN: NVESD
Ft. Belvoir, VA 22060

Disposition Instructions

Destroy this test report when no longer needed. Do not return to originator.

TABLE OF CONTENTS

<u>SECTION</u>	<u>PAGE</u>
1. <u>EXECUTIVE DIGEST</u>	
1.1 SUMMARY.....	1
1.2 TEST OBJECTIVES.....	2
1.3 TESTING AUTHORITY.....	2
1.4 TEST CONCEPT.....	2
1.5 SYSTEM DESCRIPTION.....	2
2. <u>DETECTOR TESTING</u>	
2.1 OBJECTIVES.....	6
2.2 TEST PROCEDURES.....	6
2.2.1 TARGETS.....	6
2.2.2 TEST SITES.....	7
2.2.3 TARGET PLACEMENT.....	8
2.2.3.1 CALIBRATION TARGETS.....	9
2.2.3.2 DATA COLLECTION TARGETS.....	10
2.2.3.3 TEST TARGETS.....	12
2.2.4 OPERATIONAL PROCEDURES.....	12
2.2.4.1 METHOD A: STOP AND ANALYZE.....	13
2.2.4.2 METHOD B: SCAN AND SEARCH.....	14
2.3 DEMONSTRATION FINDINGS.....	15
<u>APPENDICES</u>	
A. UXO TEST SITES.....	A-2
TARGET DETECTIONS.....	A-3
SOIL SAMPLE DATA.....	A-13
METEOROLOGICAL DATA.....	A-22
B. TARGET PICTURES.....	B-2
TARGET DESCRIPTIONS.....	B-4
C. RADIO FREQUENCY USAGE.....	C-1
D. ABBREVIATIONS.....	D-1
E. DISTRIBUTION LIST.....	E-1

SECTION 1. EXECUTIVE DIGEST

1.1 SUMMARY

a. A technical demonstration was coordinated and analyzed by U.S. Army Night Vision Lab, Fort Belvoir, and performed at Yuma Proving Ground (YPG) to determine and demonstrate the capabilities of the Remote Controlled Surface/Near Surface Unexploded Ordnance (UXO) Detector. The technical demonstration was funded by the Environmental Security Technology Certification Program (ESTCP). This detector incorporated three sensors into a remote-controlled ground-based platform for the detection, location, and verification of surface and near-surface UXO. The contractor for this project was Science Applications International Corporation (SAIC) of San Diego, CA.

b. The SAIC UXO detection array included a Schiebel metal detector array and a thermal neutron activation (TNA) sensor. The metal detector located metal on or near the surface (within a 12-inch depth), and the TNA confirmed the detection of UXO by sensing the nitrogen content of the explosive in the UXO. The detector system also included a navigational system that incorporated differential Global Positioning System GPS, a digital compass, and an on-board video camera.

c. Testing consisted of running the detector system over five rectangular lanes and three square areas. Buried in the lanes and areas were various targets: high explosive (HE) ordnance (without fuzes), HE simulators (100 grams (g), 200 g, and 2.5 pounds (lb) of C-4 explosive in metal and plastic pipes), and inert ordnance. The ordnance items were of various types and sizes, from 20 millimeter (mm) to 105mm, and a variety of explosive materials. For system calibration and verification, and to assist in target identification, some target type and location data were made known to the system operators.

d. The demonstration at YPG for the SAIC Remote Controlled Surface/Near Surface UXO Detector system yielded two categories of assessments: detections and false alarms.

(1) Out of 91 targets buried for this demonstration, the complete system, the TNA in conjunction with the metal detector, detected and identified 32 UXO HE targets successfully (35%). The metal detector located 62% of the emplaced UXO targets, and the TNA confirmed that 63% of those detected positions were HE UXO targets. Detection success varied according to target size, as shown in Table 1.

TABLE 1. Detection Results as Point Estimates for SAIC UXO Detector System Testing

TARGET CATEGORY	DETECTIONS	TARGET QTY	POINT ESTIMATES
Overall System Performance	32	91	35%
20mm-40mm targets (including simulator with 100 g C-4)	10	39	26%
60mm-81mm targets (including simulator with 200 g C-4)	15	44	34%
105mm targets (including simulator with 2.5 lb C-4)	7	8	88%

(2) During operation of the system over a total scanned area of 2,860 square meters, 87 false alarms occurred when only the metal detector was used. When those 87 false alarms were later reinspected using the metal detector and the TNA as a complete system, 68 were correctly identified as non-targets; 19 remained as false alarms, resulting in a TNA false alarm rate of 22%.

1.2 TEST OBJECTIVES

- a. To demonstrate the capability of the integrated unexploded ordnance (UXO) detection system to detect UXO typically found in the first foot of soil.
- b. To determine the technical detection parameters of the system in terms of the probability of UXO detection and false alarm rates (FAR).
- c. To determine if the system can assure complete coverage of a designated site by remote operation.

1.3 YPG TESTING AUTHORITY

TECOM No. 8-CO-160-UXO-003

1.4 TEST CONCEPT

The detection demonstration matrix at YPG was performed in three phases:

- a. Calibration Phase: where information about the emplaced ordnance type, location, and depth was released to the contractor.
- b. Data Collection Phase: where the contractor was given information about the location of the emplaced ordnance/clutter, but not the depth, orientation, and type of target.
- c. Performance (Blind) Phase: where the contractor was not given any information about the ordnance/clutter present.

1.5 SYSTEM DESCRIPTION

The Surface-Near Surface UXO Detector is a remotely controlled system for unexploded ordnance detection and verification. The system contained six subsystems as described below. All subsystems were integrated together for this technical demonstration. All remote control and data signals were transmitted and received via radio frequency (RF) links. Detailed RF signal information is included in Appendix C.

1.5.1 Tele-Operated Vehicle

- a. The vehicle chassis is a Melroe Bobcat 773, which was diesel powered and used skid steering. There were two degrees of freedom, lifting and tilting, on the boom that supported the sensors. Correctly positioning the neutron sensor required coordinating both motions.
- b. All vehicle functions are controlled from a single remote operator using twin, dual axis, self-centering joysticks. The joysticks effected proportional control of vehicle speed/direction and boom lift/tilt operations.
- c. The vehicle chassis is equipped with a remote control system manufactured by Robotech of Calgary, Alberta, Canada.

1.5.2 Schiebel Metal Detector Array

The metal detector array sensor used at YPG was a one-meter-wide Schiebel coil induction array. The array had eight transmitting and receiving coils powered from an electronics unit housed in a 19-inch enclosure. The array was rigidly encased in fiberglass and was operated flush to the ground, as shown in Figure 1. The resolution of the sensor was ten inches in diameter due to the coil spacing. The operator determined if the signal indication was a target by inspecting the intensity and shape of the image on the operator's display monitor.



Figure 1. Schiebel metal detector array.

1.5.3 Thermal Neutron Activation Sensor

a. The system incorporated a thermal neutron activation (TNA) sensor, shown in Figure 2. The sensor detected the nitrogen composition specific to high explosives. The TNA was a secondary or confirmatory sensor to analyze the buried object detected by the Schiebel metal detector. The TNA sensor employed a single low intensity isotopic neutron source. The TNA was configured with a 20 microgram isotopic Cf-252 radioactive source and twelve NaI(Tl) gamma-ray detectors, and weighed about 350 pounds. The source was in the center of the TNA container, and was symmetrically surrounded by the detectors.

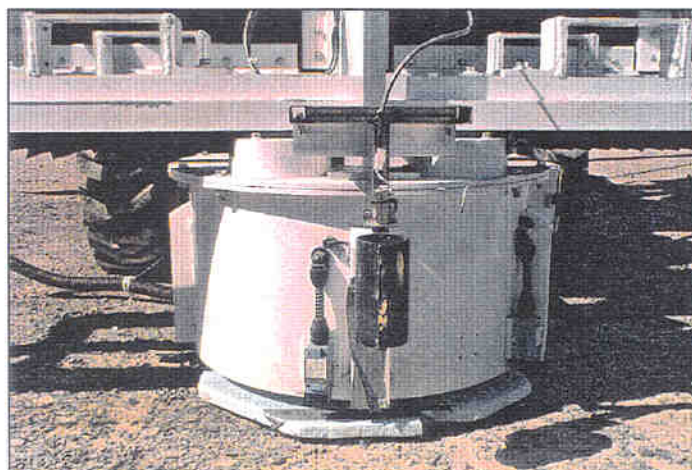


Figure 2. Thermal neutron activation (TNA) sensor.

SECTION 2: DETECTOR TESTING

2.1 OBJECTIVES

- a. To determine the target detection parameters of the system with respect to: target size and shape, orientation, explosive content, and burial depth.
- b. To determine the sensitivity of the TNA sensor array in detecting HE targets.
- c. To determine the accuracy of the metal detector system, and locating targets to within four inches of the center of the TNA sensor.
- d. To determine the capability of the system to cover a defined area.

2.2 TEST PROCEDURES

2.2.1 Targets

Three types of targets were used: HE ordnance, HE simulators, and inert ordnance.

a. The HE ordnance had the fuzing mechanisms removed for safety reasons. All components removed for safety purposes were documented. The targets are listed in Table 2; detailed target information is attached in Appendix B.

b. The HE simulators were fabricated by placing a specific amount of C4 explosive in metal pipes. (See Figure 4.) The ends of the pipes were secured with steel or plastic caps. Four configurations of simulators were used. The simulators are described in Table 2.



Figure 4. HE simulator targets.

c. Inert ordnance was also buried to determine the TNA's ability to distinguish between actual UXO and metallic clutter. The clutter was buried in the test areas only. (Existing metal fragments, from past YPG activity in the test site area, were also present in significant quantities in the test areas, providing a high cluttered background.)

1.5.7 Operator Control Station

The operator control station for the system, as shown in Figure 3, consisted of two computer processors and monitors, a remote control joystick box, and a Closed Circuit Display (CCD) monitor for vehicle control. Separate RF modems were used for each sensor, the metal detector, GPS position, and TNA measurements. Separate RF modems were also used for controlling the vehicle and for CCD transmission and control.



Figure 3. Operator control station.

TABLE 2. HE and HE Simulator Specifications

QTY.	TARGET NAME	TARGET TYPE	EXPLOSIVE WEIGHT	EXPLOSIVE TYPE
10	M56A3	20mm projectile	10.7 g	H-761
40	M789	30mm HEDP projectile	22 g	PBXN-5
20	Simulator	Cylinder - 6"X1"	100 g	C4
2	M822	40mm projectile	120 g	Octol
17	M811	40mm projectile	165 g	Octol
20	Simulator	Cylinder - 8"X1"	200 g	C4
20	Simulator	Cylinder - 6"X1-1/2"	200 g	C4
40	M49A5	60mm mortar	358.3 g	Comp B
50	M821	81mm mortar	725.8 g	RDX/TNT
20	Simulator	Cylinder - 6"X5"	1134 g (2.5 lb)	C4
10	M393A2	105mm HEP-T projectile	1995.8 g	Comp B

2.2.2 Test Sites

2.2.2.1 Lanes and Areas

The targets were buried in six lanes and three test areas. All lanes were 1 meter (m) wide and 100m long. The calibration area was 20m square, and the two test areas were 50m square. Figure 5 shows a typical lane and area.



Figure 5. Targets were buried in lanes (left) and areas (right).

a. Calibration sites

For the calibration sites, target location, type, and orientation information was provided. Two sites were used: a lane 1 m wide by 100 m long, and an area 20 m square.

These sites allowed operators to become familiar with targets and ground-truth characteristics, as well as to calibrate and verify the operational functioning of the detection system. The operators used the target characteristic data to form baseline descriptions of the various types of targets. This allowed the operators to distinguish between various targets by the strength and position of the metallic intensity and the TNA quantitative analysis.

b. Data collection lane

The data collection lane provided data on the system operational limitations. This information provided scoring parameters for system performance during lane and area assessments. Targets were buried in the data collection lane with only locations known to the system operators.

The TNA sensor was positioned at various distances away from the center of the target (or the point on the surface vertically above the target center). This assessed the sensitivity of the sensor.

c. Performance test areas and lanes

Four test lanes, 1m wide by 100m long, and two test areas, each 50m square, were used for the performance (Blind) phase. The lanes and areas were marked to provide boundary references for the system operator.

2.2.2.2 Soil Characteristics

a. Samples of soil were taken from each test area. Samples were taken at the surface, one to six inches, and six to twelve inches below the surface for measurements of moisture and chemical content. The samples were marked with the date and depth.

b. The soil data obtained is shown in Appendix A.

2.2.3 Target Placement

a. Targets were buried in the lanes and areas as follows:

(1) The calibration lane and area each had ten buried targets, with target type, burial depth, and target location known to the system operators.

(2) The data collection area targets were buried in positions known to the operators, and were rearranged after each pass to provide multiple data points. Target type and depth information was not provided to the system operator.

(3) The test lanes and areas had various amounts of targets buried. No target information was provided to the system operators.

b. Targets were buried one week prior to the test.

c. All proposed target positions were located by the Belvoir Test Director. Surveys were taken at the top center of each target for grid coordinates, and at each end of each target for target orientation. (See Figure 6.)



Figure 6. Surveying a target for position and orientation.

2.2.3.1 Calibration targets

- a. Ten targets at varying depths were buried in the calibration lane as shown in Table 3.

TABLE 3. Calibration Lane Target Positions

TARGET DESIGNATOR	TARGET TYPE	DEPTH (INCHES)
1000	60mm	1
1002	105mm	6
1004	2.5 lb. simulator	2
1006	30mm	1
1008	6-in 200 g simulator	1
1010	100 g simulator	2
1014	20mm	FLUSH
1016	40mm	FLUSH
1039	81mm	6
1073	8-in 200 g simulator	1

b. Ten targets were buried in the calibration area, as shown in Table 4. The target designators correspond to the calibration area diagram in Appendix A. The depth below the ground surface is in inches, measured to the top surface of the target.

TABLE 4. Calibration Area Target Positions

TARGET DESIGNATOR	TARGET TYPE	DEPTH (INCHES)
1018	20mm	FLUSH
1020	100 g simulator	2
1022	30mm	1
1026	40mm	2
1030	2.5 lb. simulator	6
1032	60mm	1
1036	105mm	12
1041	6-in 200 g simulator	1
1043	81mm	2
1045	8-in 200 g simulator	1

2.2.3.2 Data collection targets

A total of 18 different target emplacement configurations were used. By rearranging the location, depth, and orientation of the targets after each pass of the system, a matrix of 108 data points was developed. The matrix is described in Table 5.

TABLE 5. Data Collection Lane Target Position Matrix

TARGET TYPE	DEPTH/DISTANCE (INCHES)	NO. OF TESTS
30mm	F/C, F/3, F/6, 1/C, 1/3, 1/6	6
30mm	F/C, F/3, 1/C, 1/3	4
40mm	F/C, F/3, F/6, 2/C, 2/3, 2/6, 6/C, 6/3	8
40mm	F/3, F/6, 2/3, 2/6, 6/3	5
40mm	F/C, F/3, F/6, 2/C, 2/3	5
60mm	2/C, 2/Nose, 2/9, 6/C, 6/Nose, 6/9, 12/C	7
60mm	2/Tail, 2/9, 6/Tail, 6/9	4
60mm	2/3, 2/6, 2/9, 6/C, 6/3, 6/6	5
60mm	2/C, 2/3, 2/6, 6/C, 6/3, 6/6	6
105mm	2/C, 2/End, 2/9, 6/C, 6/End, 6/9, 12/C, 12/End	8
105mm	2/3, 2/6, 2/9, 6/3, 6/6, 12/3	6
105mm	2/C, 2/3, 2/6, 2/9, 6/C, 6/3, 6/6, 12/C	8
100g	F/C, F/3, F/6, 2/C, 2/3, 2/6, 6/C, 6/3	8
100g	F/3, F/6, 2/3, 2/6, 6/3	5
100g	F/C, F/3, F/6, 2/C, 2/3	5
200g (short)	2/C, 2/3, 2/6, 2/9, 6/C, 6/3, 6/6, 12/C	8
200g (short)	2/3, 2/6, 6/3, 6/6	4
200g (short)	2/C, 2/3, 2/6, 6/C, 6/3, 6/6	6
TOTAL DATA POINTS		108

NOTES:

The first character is burial depth in inches ("F" = flush with surface).
 The second character is horizontal distance of TNA sensor from center of target ("C" = centered; "3" = 3 inches off-center).

2.2.3.3 Test sites

a. Each target type was buried at depths according to Table 6. Burial depths were measured from the ground surface to the top of the ordnance item (as shown in Figure 6).

TABLE 6. Typical Test Target Depths

TYPE	BURIAL DEPTH
20mm round	Flush, 1"
30mm HEDP projectile	Flush, 1", 3"
100g Cylinder- 6"X1"	Flush, 2", 6"
40mm projectile	Flush, 2", 6"
200g Cylinder - 8"X1"	2", 6", 12"
200g Cylinder - 6"X1-1/2"	2", 6", 12"
60mm mortar	2", 6", 12"
81mm mortar	2", 6", 12"
2.5 lb C-4 Cylinder - 6"X5"	2", 6", 12"
105mm HEP-T projectile	2", 6", 12"

b. Target matrix and site layouts for test lanes and areas are illustrated in Appendix A.



Figure 6. Typical ordnance (left) and simulator (right) burial.

2.2.4 Operational Procedures

a. During the test runs, the operator of the remote-controlled vehicle remained in an enclosed shelter where the test lanes and areas were not visible. A spotter communicated with the vehicle operator, providing information in addition to the remote cameras on the vehicle.

b. Throughout the demonstration, the operators returned to the calibration lane periodically to reinspect known target signatures.

c. The approach in the test target areas was conducted using two methods:

(1) Method A: The system stopped after each metal detection to verify the presence of a target using the TNA, then continued on to the next target.

(2) Method B: The area was first scanned with the metal detector only for target locations. After determining the potential target locations in a test area, the operator sent the system back for TNA assessment to predetermined selections only.

d. Method A was used only for the first test lane. A high number of non-test background clutter targets (see Paragraph 2.2.1 c) slowed testing significantly using Method A. The determination was made that Method B would be more time efficient for data collection and would facilitate test purposes. The two methods are diagrammed in Figure 7.

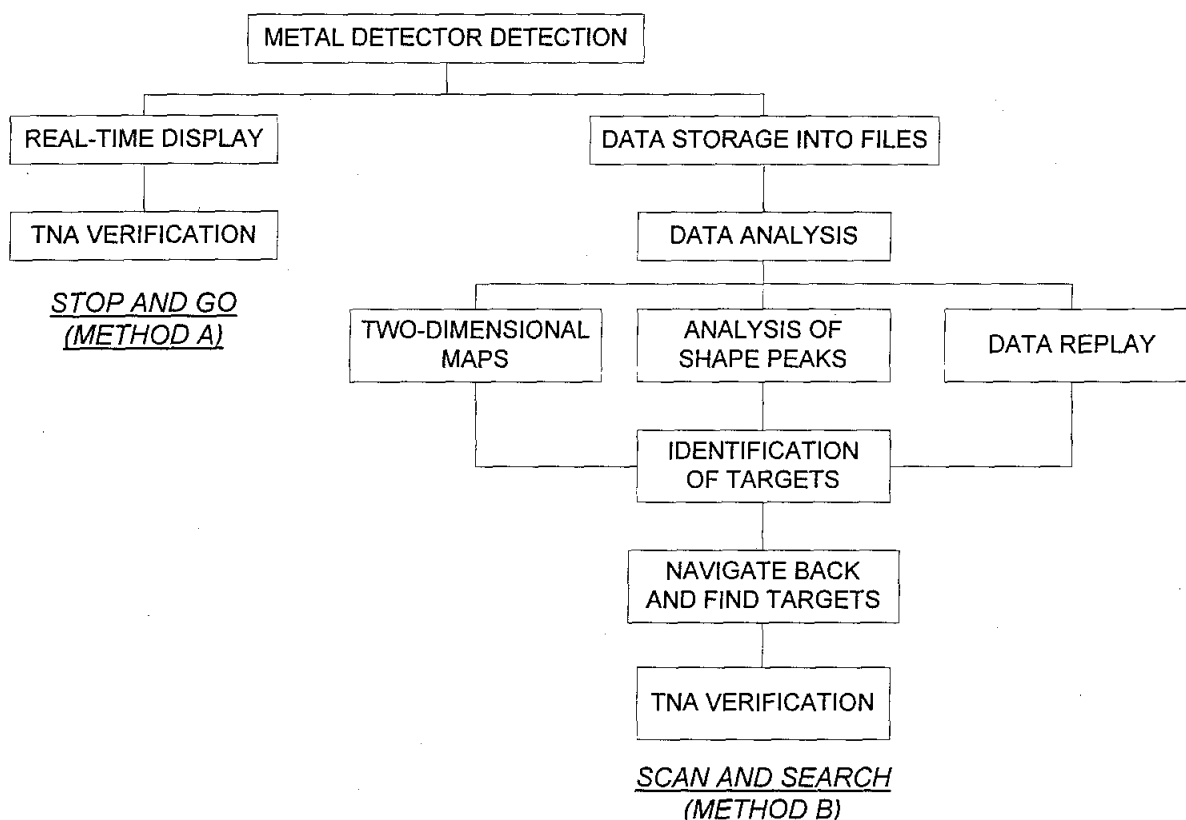


Figure 7. Operational mode flowchart diagram

2.2.4.1 Method A: Stop and Analyze

2.2.4.1.1 Metal Detecting and Marking

The vehicle was driven along the centerline of the lane using the camera to navigate the system. When a suspected target was detected, the vehicle stopped and the signal was verified. At each potential target position, the ground was marked with a fluorescent orange paint dot. The coordinates of the paint mark were measured using both the GPS (within positional error) and the survey equipment. This phase of the test resulted in a set of marks on the ground and in a list of coordinates for each of the suspected target indications.

2.2.4.1.2 TNA Verification

a. Target explosive analysis was carried out with the TNA unit. After positioning the TNA over the suspected target location, the TNA measurement was performed and the results were recorded. A maximum of fifteen minutes was allowed per investigation.

b. After TNA verification, the location of the TNA head was surveyed using a theodolite reflector head mounted above the center of the TNA heads. This measurement gave the ground plane distance of the TNA head center from the target center.

2.2.4.2 Method B: Scan and Search

2.2.4.2.1 Metal Detection Localization and Marking

a. Initial test runs were carried out without TNA assessment. Passes over the lanes and parallel scans over the areas with the metal detector were carried out using the camera, the differential GPS, and the electronic compass.

b. The differential GPS helped to insure complete coverage of a test area. This phase resulted in a mapping of potential target positions. During this part of the demonstration, the vehicle did not stop on the suspected targets.

c. After reviewing the metallic signatures of a mapped area, positions registering the greatest intensity were selected for TNA assessment. The navigation equipment was used to retrieve the coordinate positions and to return the vehicle into close proximity of each target. When a target was relocated with the metal detector, the signal was optimized, and the coordinates of the target were recorded using both the GPS (within positional error) and the survey equipment. At each potential target position, the ground was marked remotely with a dot of paint. At this time, positioning for TNA assessment was performed.

2.2.4.2.2 TNA Verification

After the mapping of the field was completed, selected positions were verified using the TNA module. After positioning the TNA over the mark, the TNA measurement was recorded. A maximum of fifteen minutes was allowed per analysis.

2.3 DEMONSTRATION FINDINGS

2.3.1 Detection and Identification Scoring

a. Data Collection:

Table 7 is the TNA detection assessment for the Data Collection test matrix. The TNA was able to quantitatively measure detectable levels of nitrates from explosive material from 69 of the 74 emplaced targets (93%). The findings are for the TNA only; the metal detector was not assessed during this testing phase.

TABLE 7. TNA Detection Ratio for Data Collection Area

TARGET TYPE	TNA DETECTION RATIO
30mm	5/7
100g	9/9
40mm	13/14
200g Short	5/6
60mm	21/21
81mm	13/14
2.5 lb C-4	3/3
TOTAL	69/74

b. UXO Targets:

During the demonstration in Test Lanes 1-4 and Area 1, a total of 143 positions were identified by the metal detector as potential UXO targets. (Area 2 was unable to be fully utilized for the assessment.) Ground truth data identified 56 positions as actual target detections, and 87 as false alarms. The system was returned to the potential target positions for TNA assessment, which identified 32 of the 51 positions assessed as UXO targets, and eliminated 68 of the 87 false alarms. Figure 8 is a system summary of target detection assessment.

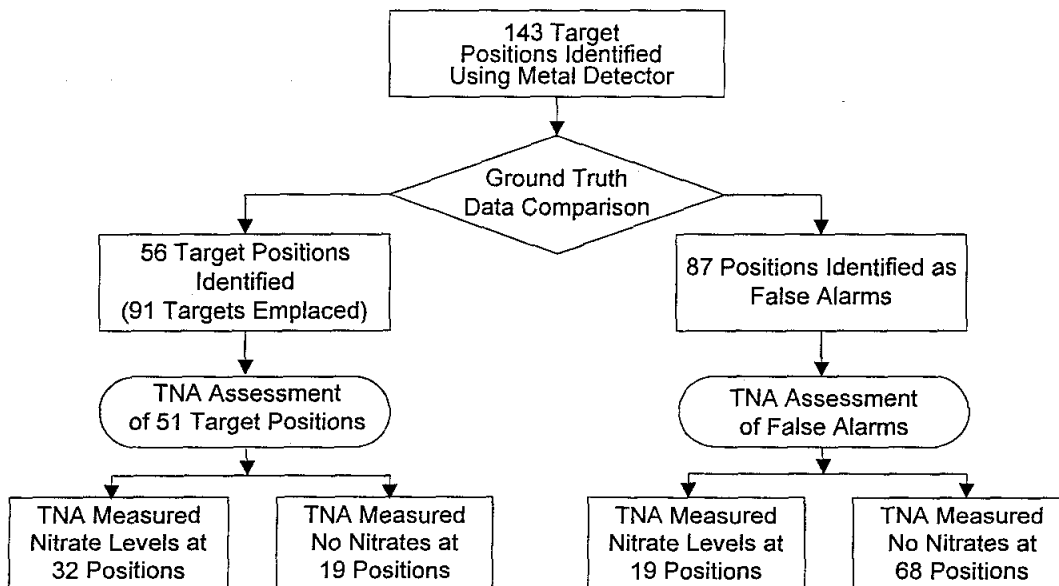


Figure 8. System Summary of Target Detection Assessment

Table 8 is a consolidation summary of target detection for UXO targets. The table identifies the ratios of targets detected versus the actual number targets in place in Test Lanes 1-4 and Area 1.

(1) MD ONLY: Using the metal detector only, 56 positions were identified out of 91 actual buried target positions (62%) as potential UXO targets, and an additional 87 positions were identified as possible targets (false alarms).

(2) TNA ONLY: The system was returned to 51 of the 56 ground truth target positions for evaluation by the TNA. The TNA assessment showed detectable levels of nitrates from explosive materials in 32 of the 51 positions assessed (63%).

(3) SYSTEM: Overall, the complete system (metal detector used in conjunction with TNA) correctly identified 32 positions out of 91 targets buried (35%) as potential UXO targets.

TABLE 8. Detection Summary For UXO Targets

TARGET TYPE	TARGET DETECTION RATIOS		
	MD ONLY	TNA ONLY	SYSTEM
20mm	3/5	1/3	1/5
30mm	8/11	3/7	3/11
(30mm)	0/3	-	0/3
((30mm))	0/1	-	0/1
40mm	6/9	2/6	2/9
60mm	8/16	6/6	6/16
81mm	9/14	6/9	6/14
105mm	6/6	5/6	5/6
100g	7/10	4/6	4/10
200g Short	3/8	2/3	2/8
200g Long	4/6	1/3	1/6
2.5 lb C-4	2/2	2/2	2/2
OVERALL	56/91	32/51	32/91

NOTES:

30mm — A single 30mm target
 (30mm) — Two 30mm targets parallel and next to each other
 ((30mm)) — Three 30mm targets parallel and next to each other

c. False Alarms:

The positions identified were compared to ground truth target grid coordinates to yield a false alarm assessment. The complete system incorrectly identified 19 positions as potential UXO targets in a total area of 2860 square meters, as shown in Figure 8. The false alarm assessment for the system is summarized as follows:

$$\frac{19}{2860} = 0.0066 \text{ False alarm / m}^2 \text{ or } 6.6 \text{ per } 1000 \text{ m}^2$$

(1) Using the metal detector only, 143 positions were identified as potential UXO targets in a total of 2860 square meters. Of those positions, 56 were actual UXO targets, and 87 were identified as false alarm positions.

(2) The system was returned to 86 of the false alarm target positions for TNA assessment, which eliminated 67 of those positions (78%). The TNA still indicated the presence of nitrates in 19 positions, resulting in a TNA false alarm rate of 22%.

2.3.2 Demonstration Accomplishments

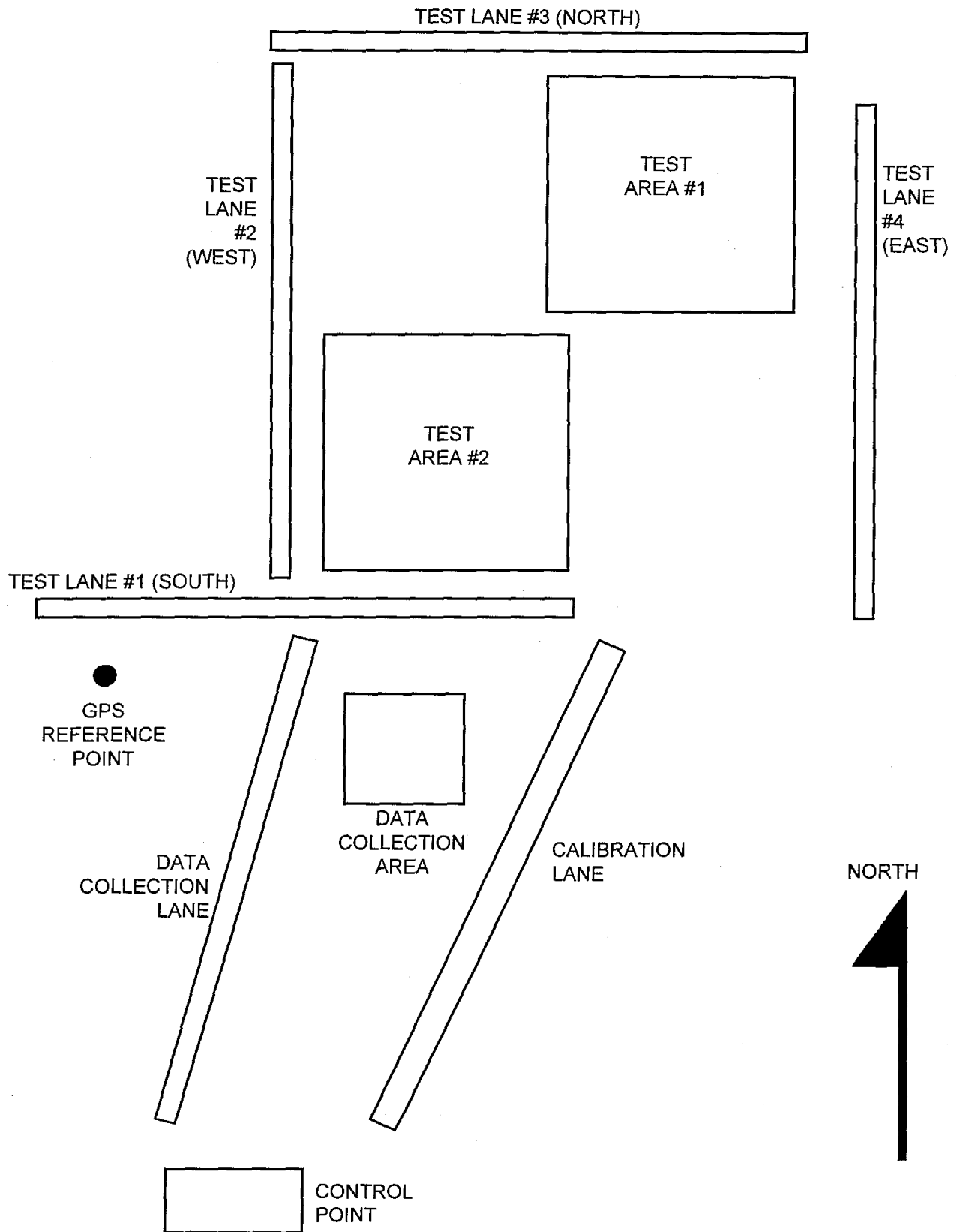
The following major objectives were accomplished:

- a. The system was successfully operated as an integrated whole system.
- b. The system successfully demonstrated the capability to remotely scan a designated area.
- c. The system successfully demonstrated the capability to initially locate and identify a target, then navigate back to the target location.
- d. The system successfully demonstrated the capability to identify large targets in a highly cluttered environment.

APPENDIX A. INDEX

<u>SECTION</u>	<u>PAGE</u>
UXO TEST SITE LAYOUT	A-2
TARGET DETECTIONS	A-3
SOIL SAMPLE DATA.....	A-13
METEOROLOGICAL DATA	A-22

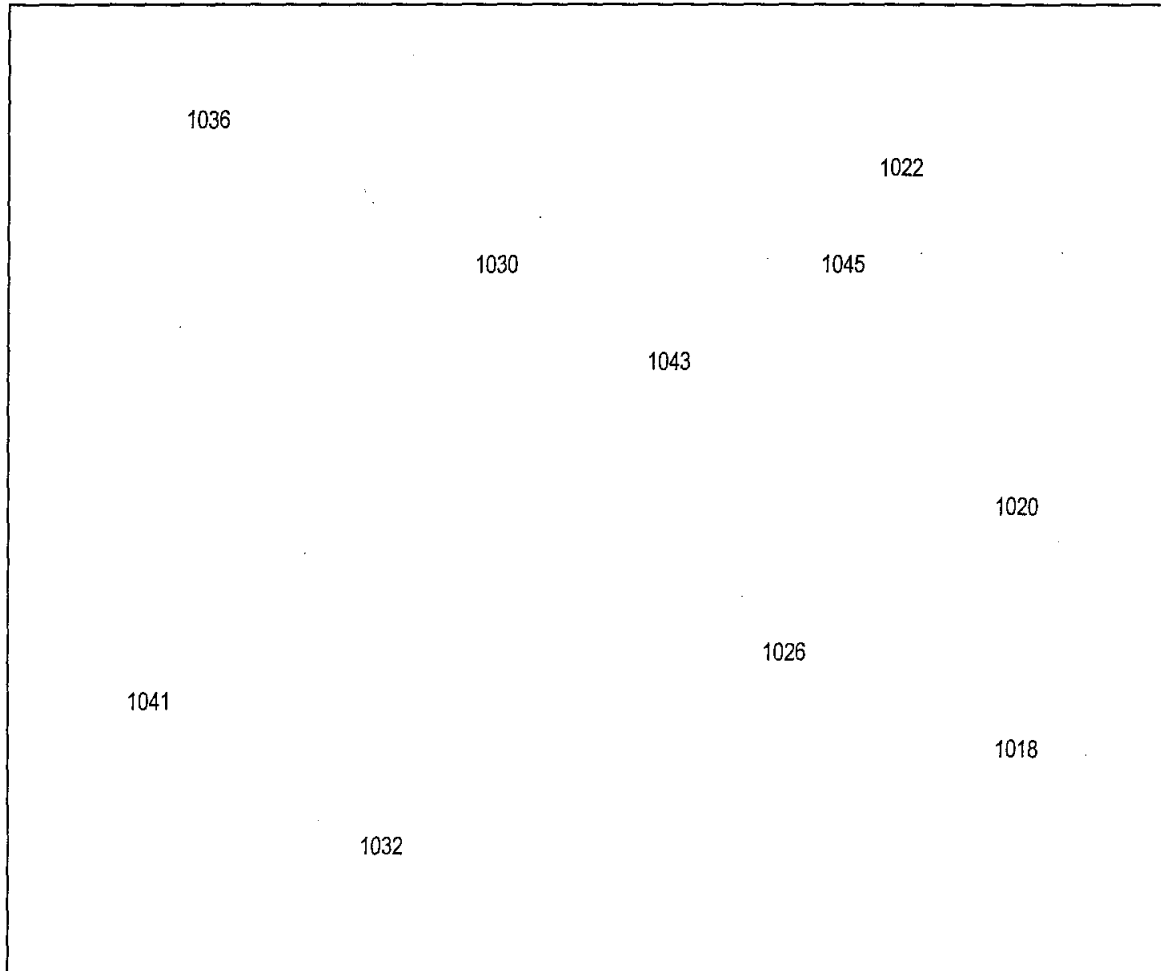
APPENDIX A. UXO TEST SITE LAYOUT



APPENDIX A. TARGET DETECTIONS

a. Calibration Area

The following diagram is a graphical representation (not to scale) of target locations in the calibration area. The entire area was 20 meters square.



TARGET NUMBER	TARGET TYPE	DEPTH (INCHES)	TARGET ORIENTATION
1018	20mm	Flush	Transverse (N)
1020	100 gram	2"	Transverse
1022	30mm	1"	Transverse (T)
1026	40mm	2"	Transverse (N)
1030	2.5 lb C-4	6"	Transverse
1032	60mm	1"	Diagonal
1036	105mm	12"	Transverse (N)
1041	200 gram-Short	1"	Transverse
1043	81mm	2"	Transverse
1045	200 gram-Long	1"	Transverse

ORIENTATION:

Longitudinal
Parallel to North/South axis
Transverse
Parallel to East/West axis
Diagonal
Not parallel to either major axis

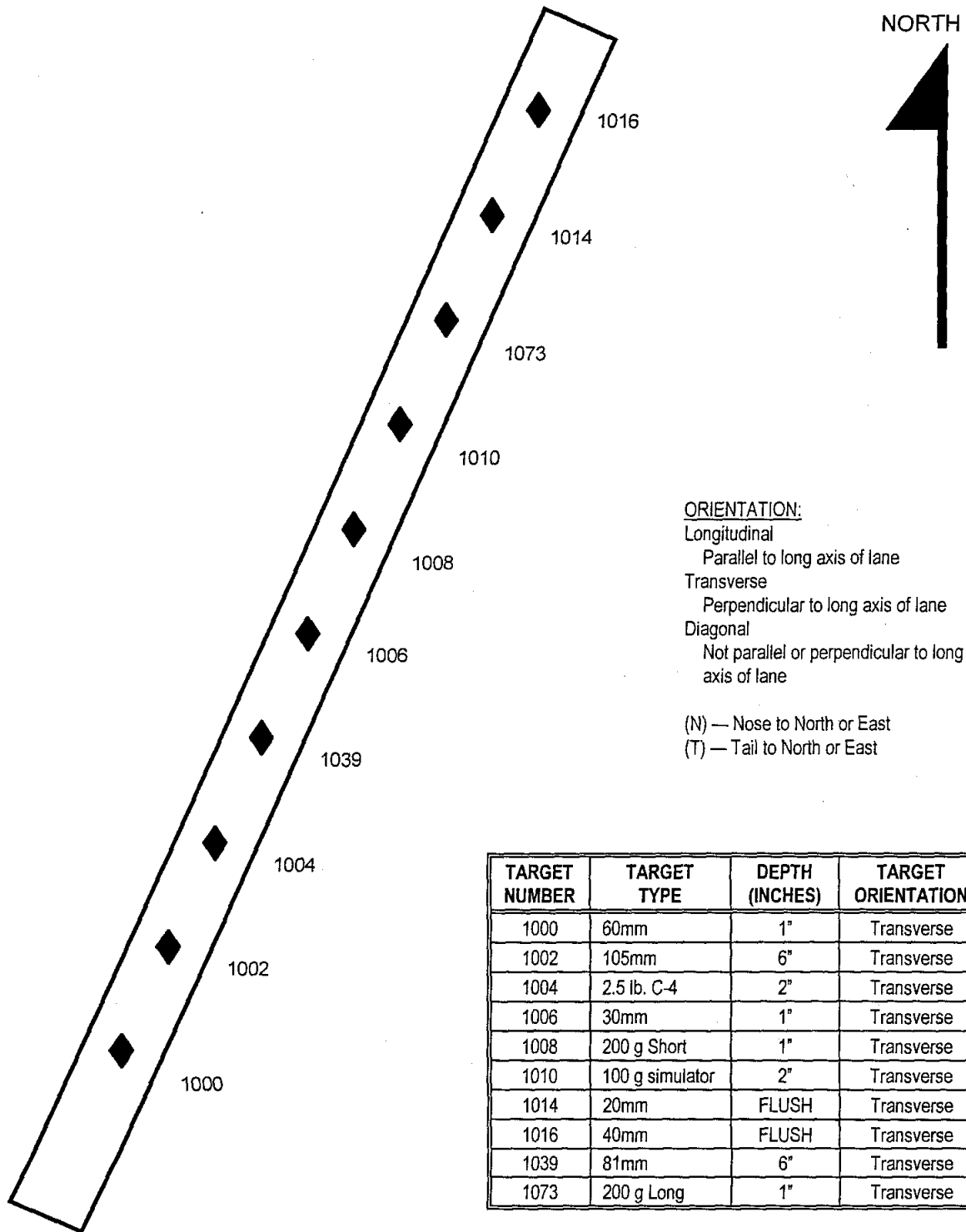
(N) — Nose to North or East
(T) — Tail to North or East

NORTH



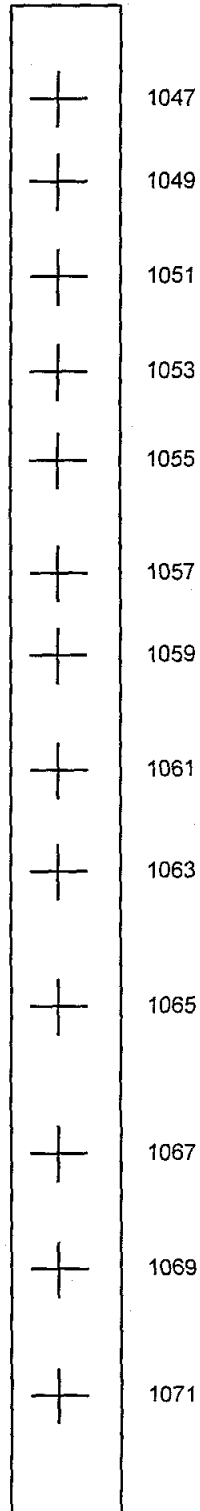
b. Calibration Lane

The following diagram is a graphical representation (not to scale) of target locations in the calibration lane. The lane was 1m wide by 100m long.



c. Test Lane 1

The following diagram is a graphical representation (not to scale) of target locations in Test Lane 1. The lane was 1m wide by 100m long.



EAST



ORIENTATION:

Longitudinal

Parallel to long axis of lane

Transverse

Perpendicular to long axis of lane

Diagonal

Not parallel or perpendicular to long axis of lane

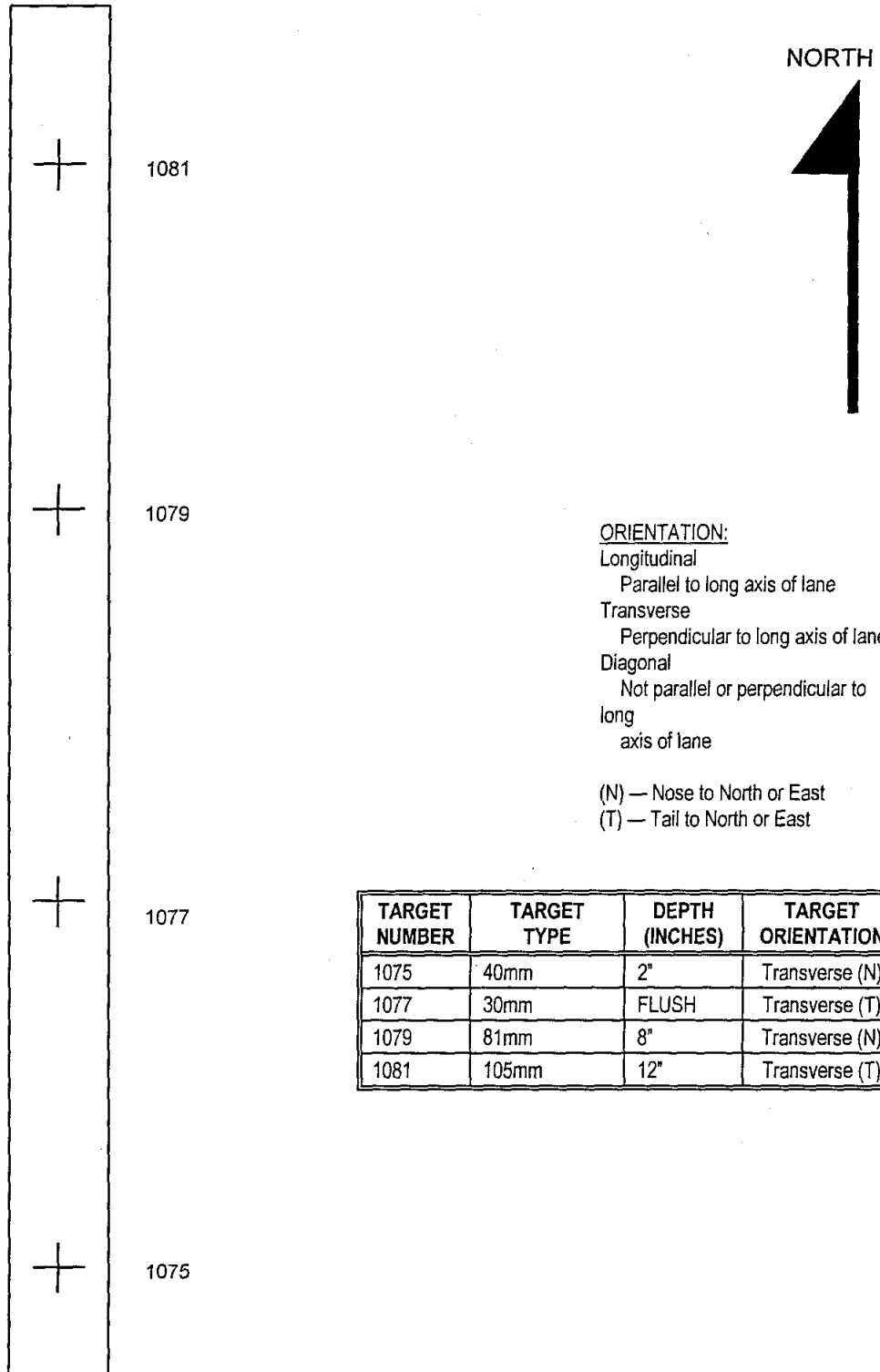
(N) — Nose to North or East

(T) — Tail to North or East

TARGET NUMBER	TARGET TYPE	DEPTH (INCHES)	TARGET ORIENTATION
1047	30mm	FLUSH	Transverse (T)
1049	100 gram	FLUSH	Transverse
1051	40mm	6"	Transverse (N)
1053	20mm	FLUSH	Transverse (T)
1055	60mm	2"	Transverse (T)
1057	105mm	2"	Transverse (T)
1059	200 gram	12"	Transverse
1061	30mm	1"	Transverse (N)
1063	81mm	6"	Transverse (T)
1065	100 gram	6"	Transverse
1067	200 L	6"	Transverse
1069	30mm	3"	Transverse (N)
1071	81mm	2"	Transverse (T)

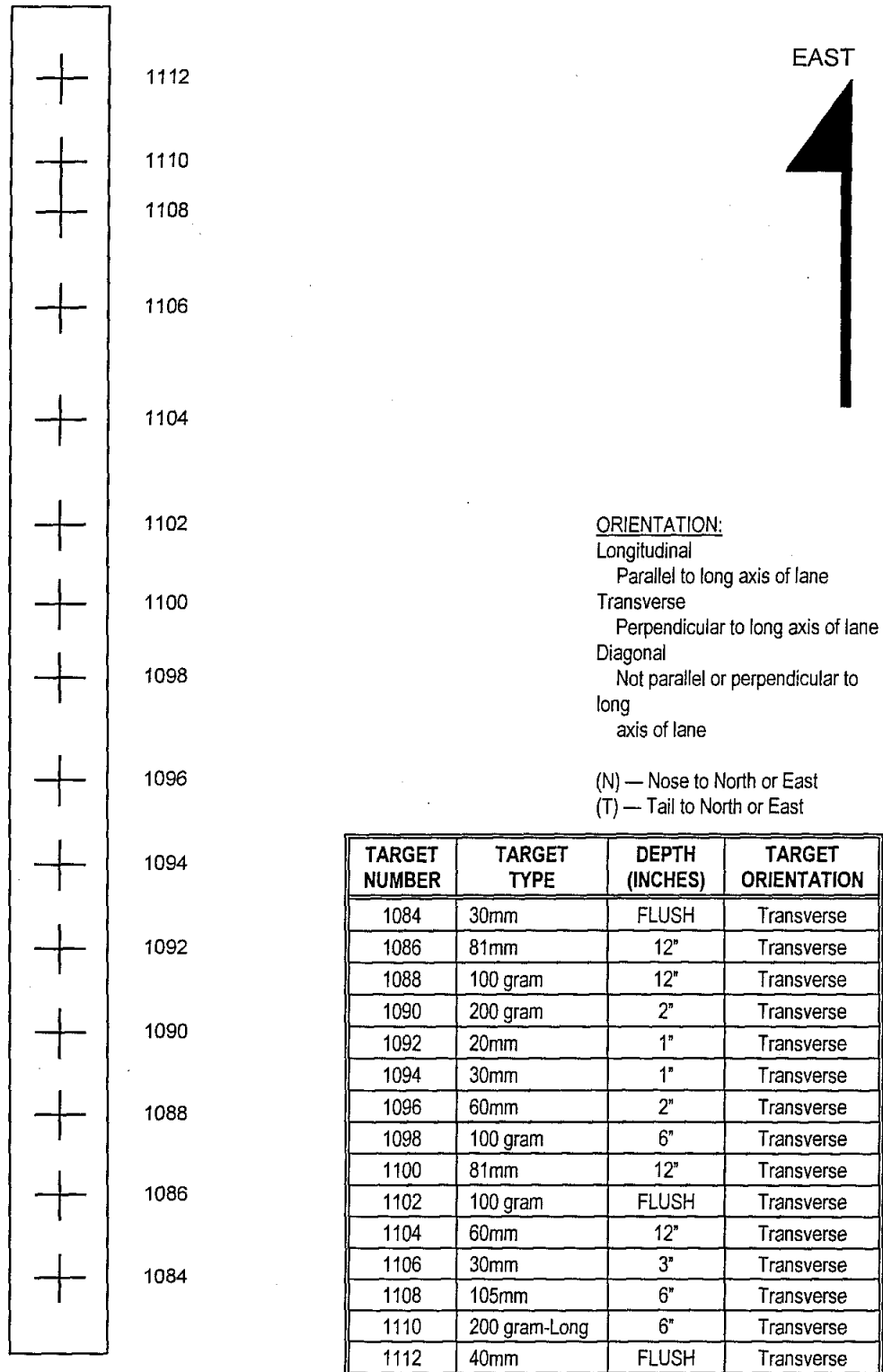
d. Test Lane 2

The following diagram is a graphical representation (not to scale) of target locations in Test Lane 2. The lane was 1m wide by 100m long.



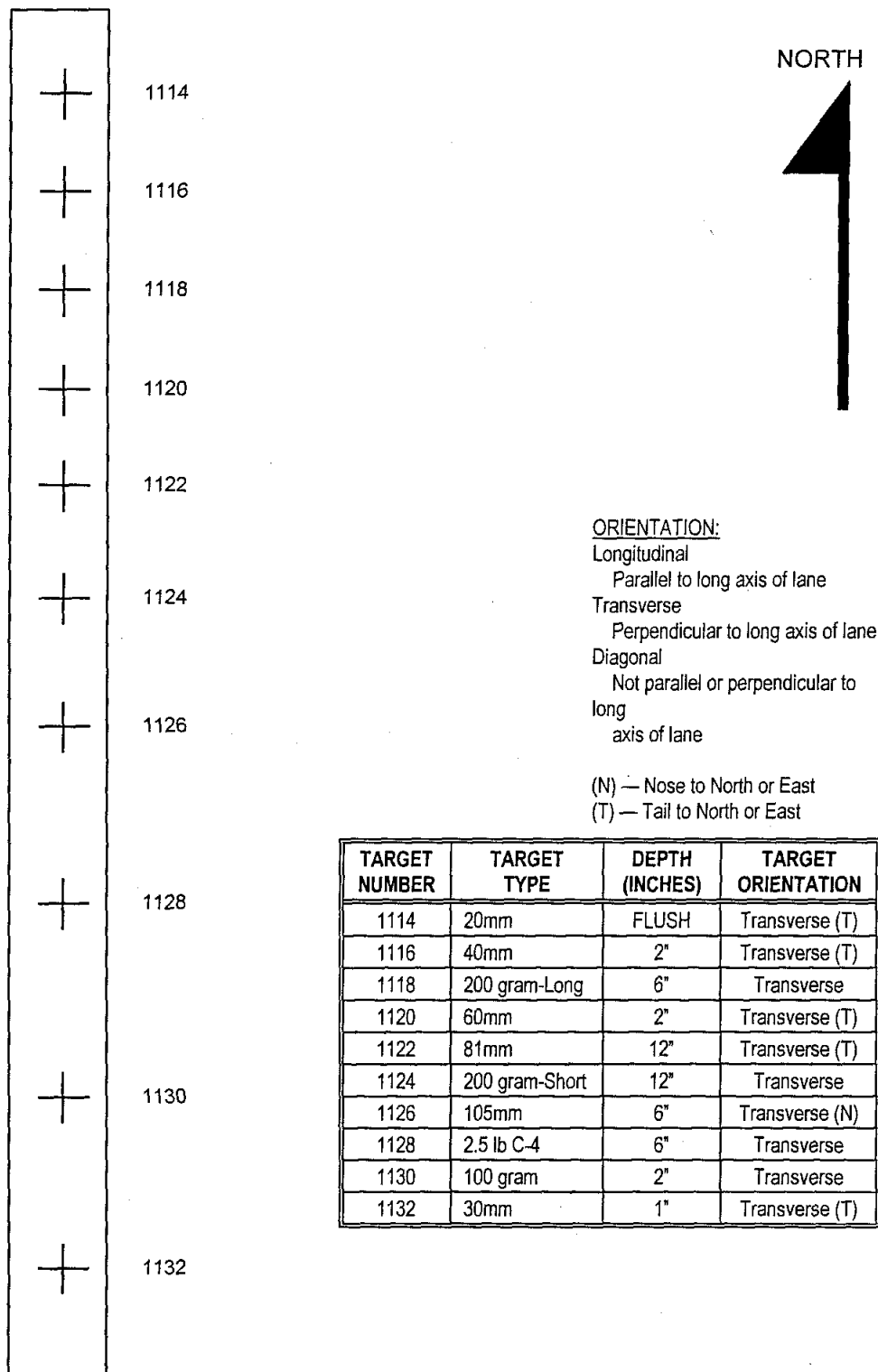
e. Test Lane 3

The following diagram is a graphical representation (not to scale) of target locations in Test Lane 3. The lane was 1m wide by 100m long.



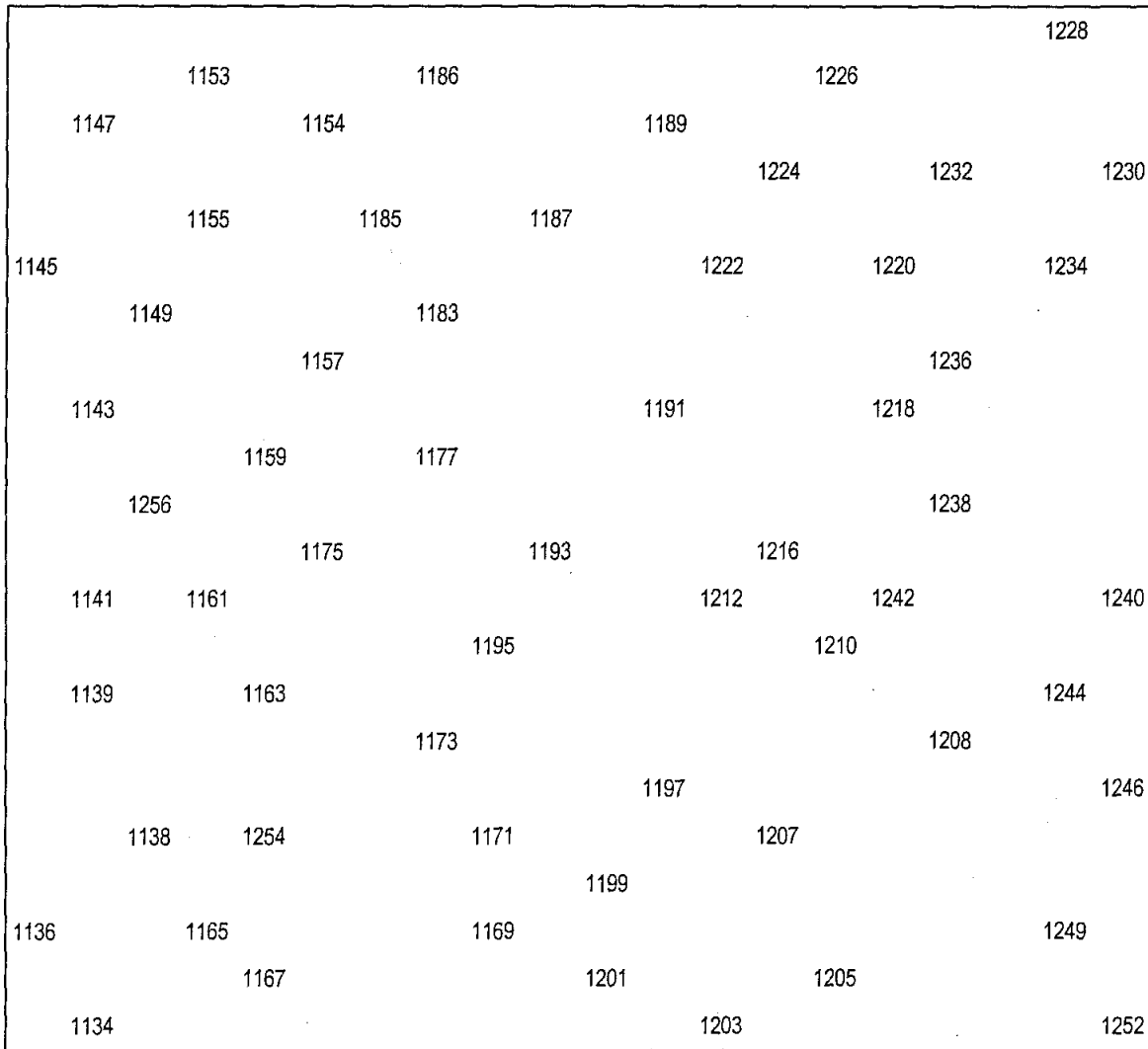
f. Test Lane 4

The following diagram is a graphical representation (not to scale) of target locations in Test Lane 4. The lane was 1m wide by 100m long.



g. Test Area 1

(1) The following diagram is a graphical representation (not to scale) of target locations in Test Area 1. The area was 50m square.



(2) Following is a table of target detections in Test Area 1.

POSITION IN LANE	TYPE OF ORDNANCE	DEPTH (INCHES)	POSITION IN LANE	TYPE OF ORDNANCE	DEPTH (INCHES)
1134	30mm	FLUSH	1195	40mm	2"
1136	81mm	2"	1197	81mm	2"
1138	60mm	12"	1199	60mm	2"
1139	40mm	6"	1201	30mm	3"
1141	30mm	FLUSH	1203	20mm	FLUSH
1143	200 gram-Short	2"	1205	30mm	3"
1145	60mm	2"	1207	60mm	12"
1147	100 gram	2"	1208	200 gram-Long	2"
1149	(30mm)	3"	1210	81mm	6"
1153	60mm	6"	1212	(30mm)	1"
1154	60mm	6"	1216	200 gram-Short	6"
1155	100 gram	FLUSH	1218	200 gram-Short	6"
1157	200 gram-Short	2"	1220	60mm	2"
1159	200 gram-Long	12"	1222	100 gram	FLUSH
1161	40mm	FLUSH	1224	81mm	12"
1163	81mm	6"	1226	100 gram	6"
1165	60mm	12"	1228	60mm	6"
1167	30mm	1"	1230	60mm	6"
1169	60mm	12"	1232	105mm	12"
1171	81mm	2"	1234	105mm	2"
1173	81mm	2"	1236	2.5 lb C-4	2"
1175	200 gram-Long	6"	1238	81mm	6"
1177	200 gram-Short	12"	1240	200 gram-Long	12"
1183	((30mm))	FLUSH	1242	81mm	6"
1185	60mm	2"	1244	40mm	2"
1186	60mm	2"	1246	40mm	6"
1187	105mm	6"	1249	(30mm)	FLUSH
1189	30mm	1"	1252	20mm	1"
1191	60mm	2"	1254	60mm	6"
1193	81mm	12"	1256	40mm	FLUSH

NOTES: TARGETS

30mm targets were designated three ways:

30mm — one 30mm target

(30mm) — two adjacent 30mm targets

((30mm)) — three adjacent 30mm targets

ORIENTATION

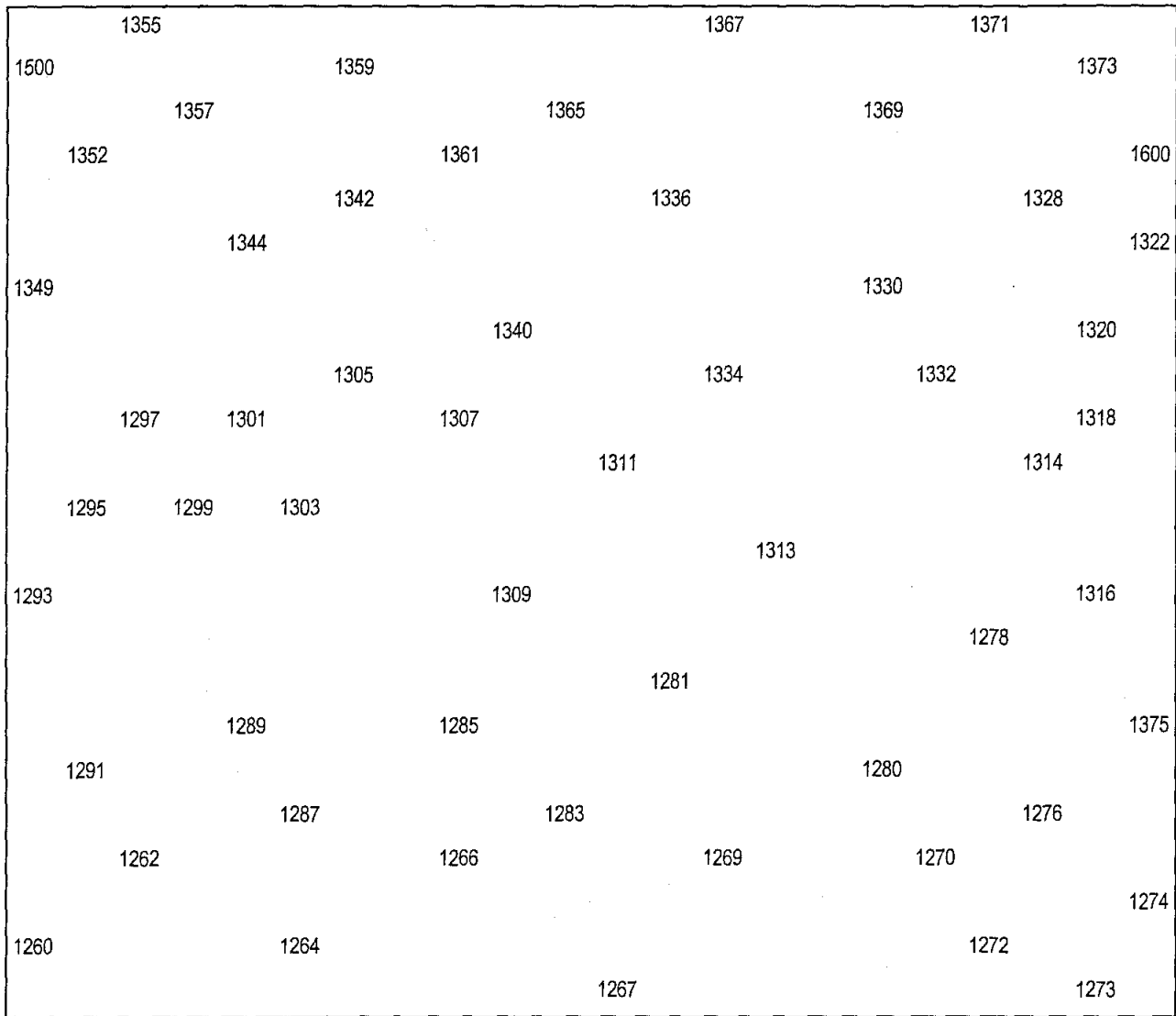
Longitudinal — Oriented East/West

Transverse — Oriented North/South

Vertical — Nose up (N) or Tail up (T)

h. Test Area 2

(1) The following diagram is a graphical representation (not to scale) of target locations in Test Area 2. The area was 50m square.



(2) Following is a table of target detections in Test Area 2.

POSITION IN LANE	TYPE OF ORDNANCE	DEPTH (INCHES)	POSITION IN LANE	TYPE OF ORDNANCE	DEPTH (INCHES)
1260	20mm	1"	1313	60mm	3"
1262	60mm	12"	1314	200 gram-Long	6"
1264	60mm	12"	1316	100 gram	2"
1266	60mm	6"	1316	105mm	6"
1267	40mm	6"	1320	100 gram	FLUSH
1269	60mm	6"	1322	((30mm))	1"
1270	60mm	12"	1328	200 gram-Short	6"
1272	60mm	12"	1330	200 gram-Short	12"
1273	60mm	12"	1332	81mm	12"
1274	60mm	6"	1334	81mm	12"
1276	60mm	6"	1336	(30mm)	3"
1278	20mm	FLUSH	1340	200 gram-Short	12"
1280	60mm	6"	1342	81mm	6"
1281	60mm	2"	1344	81mm	6"
1283	60mm	6"	1349	((30mm))	3"
1285	40mm	FLUSH	1352	81mm	6"
1287	40mm	6"	1355	30mm	1"
1289	105mm	12"	1357	81mm	2"
1291	40mm	2"	1359	81mm	2"
1293	200 gram-Long	12"	1361	(30mm)	1"
1295	100 gram	6"	1365	200 gram-Short	6"
1297	2.5 lb C-4	12"	1367	200 gram-Short	2"
1299	105mm	2"	1369	30mm	3"
1301	200 gram-Long	2"	1371	200 gram-Short	2"
1303	200 gram-Long	12"	1373	30mm	1"
1305	200 gram-Long	2"	1375	40mm	FLUSH
1307	100 gram	2"	1500	30mm	FLUSH
1309	60mm	2"	1600	(30mm)	FLUSH
1311	30mm	3"			

NOTE: 30mm targets were designated three ways:
 30mm — one 30mm target
 (30mm) — two adjacent 30mm targets
 ((30mm)) — three adjacent 30mm targets

APPENDIX A. SOIL SAMPLE DATA

a. Analysis

Soil data was obtained from the test area. Samples were taken at the surface and six to twelve inches below the surface for measurements of moisture and chemical content.

The soil samples were analyzed by Southwest Research Institute (SwRI). Following is an assessment sent by SwRI to explain the soil analysis:

"XRD and EDS analysis of three dirt specimens from Yuma, AZ.

# 110.62	Surface to 1" depth
# 114.73	6" to 12" depth
# 114.14	Composite of 110.62 and 114.73

Each specimen was first analyzed for chemical composition by Energy Dispersive Spectroscopy (EDS). In this analysis, the specimen is bombarded with a high energy electron beam and the resultant x-rays are counted to determine the elements present. The analyzed samples were practically identical in composition except for a small amount of Cl in the deeper specimen. Refer to the printouts for comparison.

X-ray diffraction (XRD) analysis was then performed on the samples to determine the compounds present. Each XRD spectrum was nearly identical with the largest component in each case being Quartz (SiO₂). The other constituents (not listed in any particular order) are several types of feldspar (Albite, Anorthite) and a mica mineral (Muscovite). These components were determined by using a search-match program which compares the peaks present on the spectrum with a spectrum library on CD ROM. Each possible match is then individually compared to the spectrum and then accepted or rejected by the operator. The three samples run in this case came up with the same constituent components. Refer to the XRD printouts for comparison."

b. Reports

Following are soil analysis data reports as provided by SwRI.

(1) Analysis report for Surface to one-inch depth soil sample.

GENERAL CONDITIONS

Result File : JFS292
File Version : 1
Background Method : Fit
Decon Method : Gaussian
Decon Chi Squared : 5.68
Analysis Date : 28 JAN 97
Microscope : SEM
Comments : Surface to 1" depth

ANALYSIS CONDITIONS

Quant. Method : ZAF/ASAP
Acquire Time : 200 seconds
Normalization Factor : 100.00

SAMPLE CONDITIONS

kV : 20.0
Beam Current : 60.0 picoAmps
Working Distance : 29.5 mm
Tilt Angle : 0.0 Degrees
TakeOff Angle : 31.1 Degrees
Solid Angle* Beam Current : 0.3

<u>ELEMENT</u>	<u>LINE</u>	<u>WEIGHT (%)</u>	<u>K-RATIO</u>	<u>COUNTS/SEC</u>	<u>ATOMIC %</u>
Na	Ka	3.13	0.0161	37.71	4.05
Mg	Ka	2.43	0.0157	40.64	2.97
Al	Ka	13.41	0.0970	266.63	14.78
Si	Ka	61.54	0.4230	1148.71	65.18
K	Ka	5.29	0.0394	80.75	4.03
Ca	Ka	6.47	0.0515	97.56	4.80
Ti	Ka	0.81	0.0064	10.24	0.50
Fe	Ka	6.93	0.0608	60.40	3.69

(2) Analysis report for 6- to 12-inch depth soil sample.

GENERAL CONDITIONS

Result File : JFS293
File Version : 1
Background Method : Fit
Decon Method : Gaussian
Decon Chi Squared : 8.33
Analysis Date : 28 JAN 97
Microscope : SEM
Comments : 6" to 12" depth

ANALYSIS CONDITIONS

Quant. Method : ZAF/ASAP
Acquire Time : 200 seconds
Normalization Factor : 100.00

SAMPLE CONDITIONS

kV : 20.0
Beam Current : 60.0 picoAmps
Working Distance : 29.5 mm
Tilt Angle : 0.0 Degrees
TakeOff Angle : 31.1 Degrees
Solid Angle* Beam Current : 0.3

<u>ELEMENT</u>	<u>LINE</u>	<u>WEIGHT (%)</u>	<u>K-RATIO</u>	<u>COUNTS/SEC</u>	<u>ATOMIC %</u>
Na	Ka	2.88	0.0144	46.96	3.77
Mg	Ka	2.34	0.0148	53.47	2.89
Al	Ka	13.11	0.0936	358.53	14.60
Si	Ka	58.89	0.4035	1526.30	63.03
Cl	Ka	0.74	0.0044	14.44	0.633
K	Ka	5.35	0.0401	114.58	4.11
Ca	Ka	9.03	0.0722	190.48	6.77
Ti	Ka	0.75	0.0059	13.16	0.47
Fe	Ka	6.90	0.0604	83.51	3.71

(3) Analysis report for composite of both soil samples.

GENERAL CONDITIONS

Result File : JFS294
File Version : 1
Background Method : Fit
Decon Method : Gaussian
Decon Chi Squared : 3.76
Analysis Date : 28 JAN 97
Microscope : SEM
Comments : Composite

ANALYSIS CONDITIONS

Quant. Method : ZAF/ASAP
Acquire Time : 200 seconds
Normalization Factor : 100.00

SAMPLE CONDITIONS

kV : 20.0
Beam Current : 60.0 picoAmps
Working Distance : 29.5 mm
Tilt Angle : 0.0 Degrees
TakeOff Angle : 31.1 Degrees
Solid Angle* Beam Current : 0.3

<u>ELEMENT</u>	<u>LINE</u>	<u>WEIGHT (%)</u>	<u>K-RATIO</u>	<u>COUNTS/SEC</u>	<u>ATOMIC %</u>
Na	Ka	3.14	0.0142	19.69	4.17
Mg	Ka	2.35	0.0138	20.97	2.95
Al	Ka	12.75	0.0859	138.99	14.46
Si	Ka	56.78	0.3764	601.52	61.83
Cl	Ka	0.50	0.0030	4.13	0.43
K	Ka	5.02	0.0378	45.57	3.93
Ca	Ka	6.94	0.0559	62.27	5.29
Ti	Ka	0.83	0.0066	6.24	0.53
Fe	Ka	11.70	0.1031	60.32	6.41

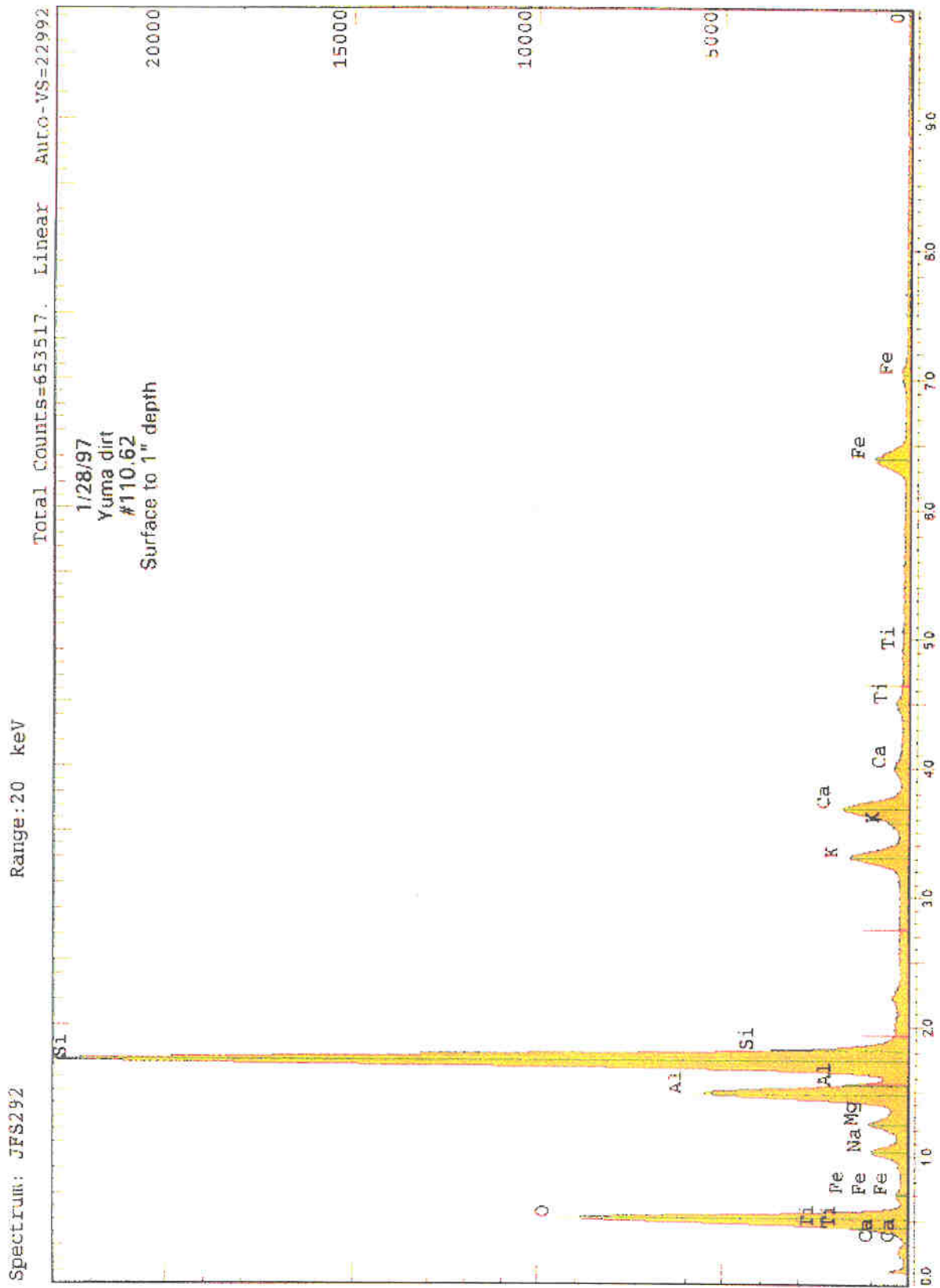


Figure A-1. Soil data at 1-inch depth.

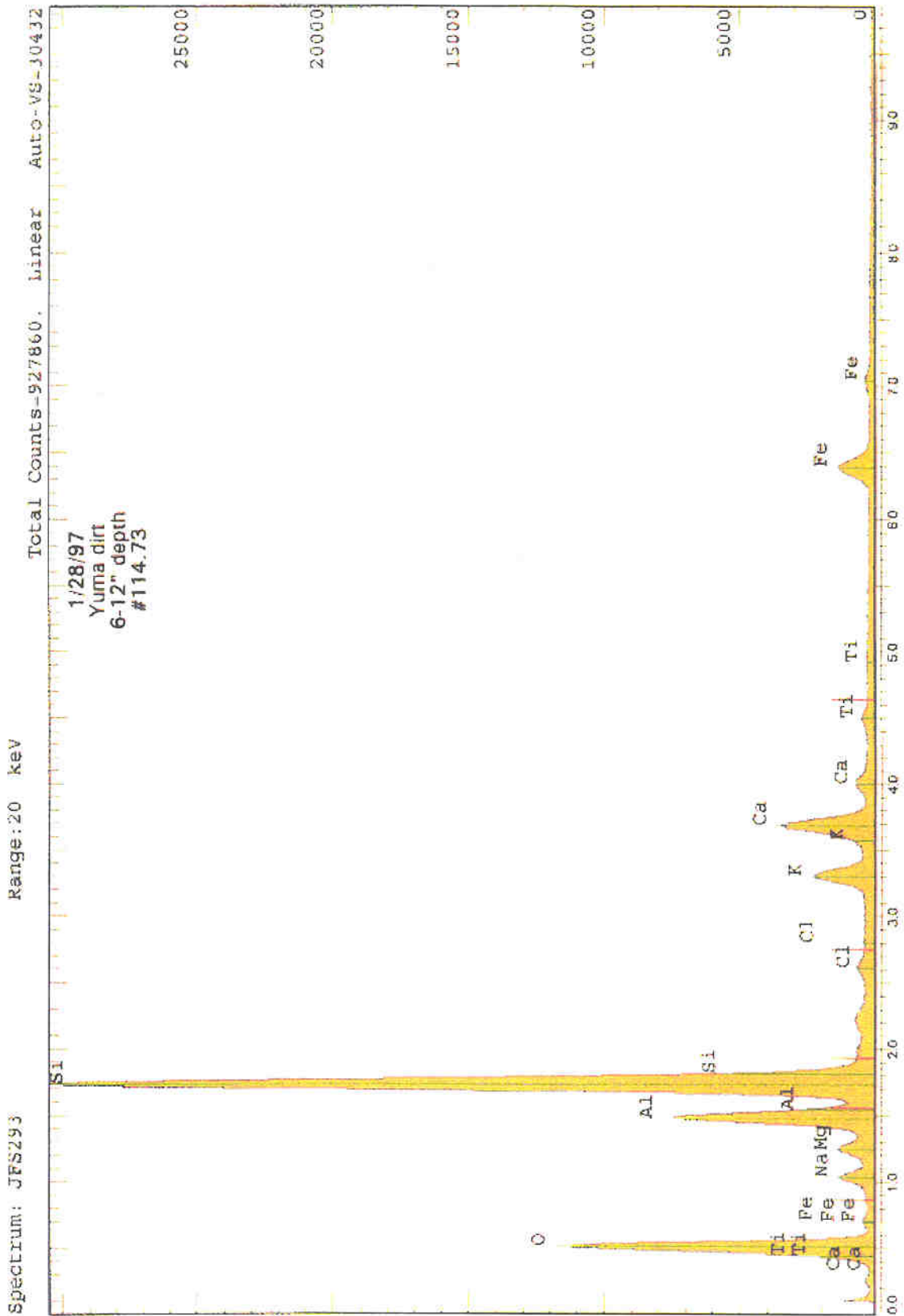


Figure A-2. Soil data at 12-inch depth

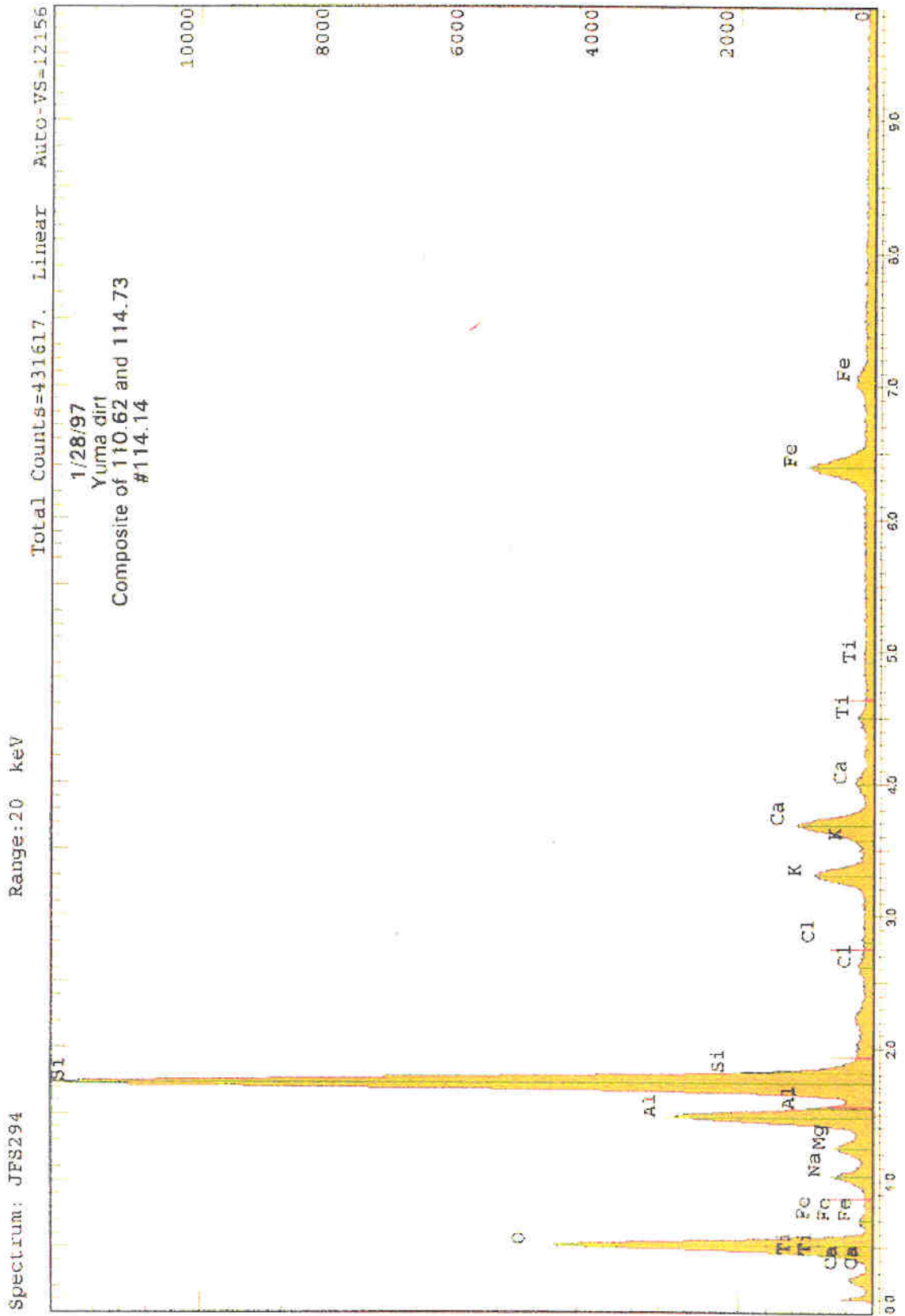


Figure A-3. Composite soil data.

d. XRD Graphs

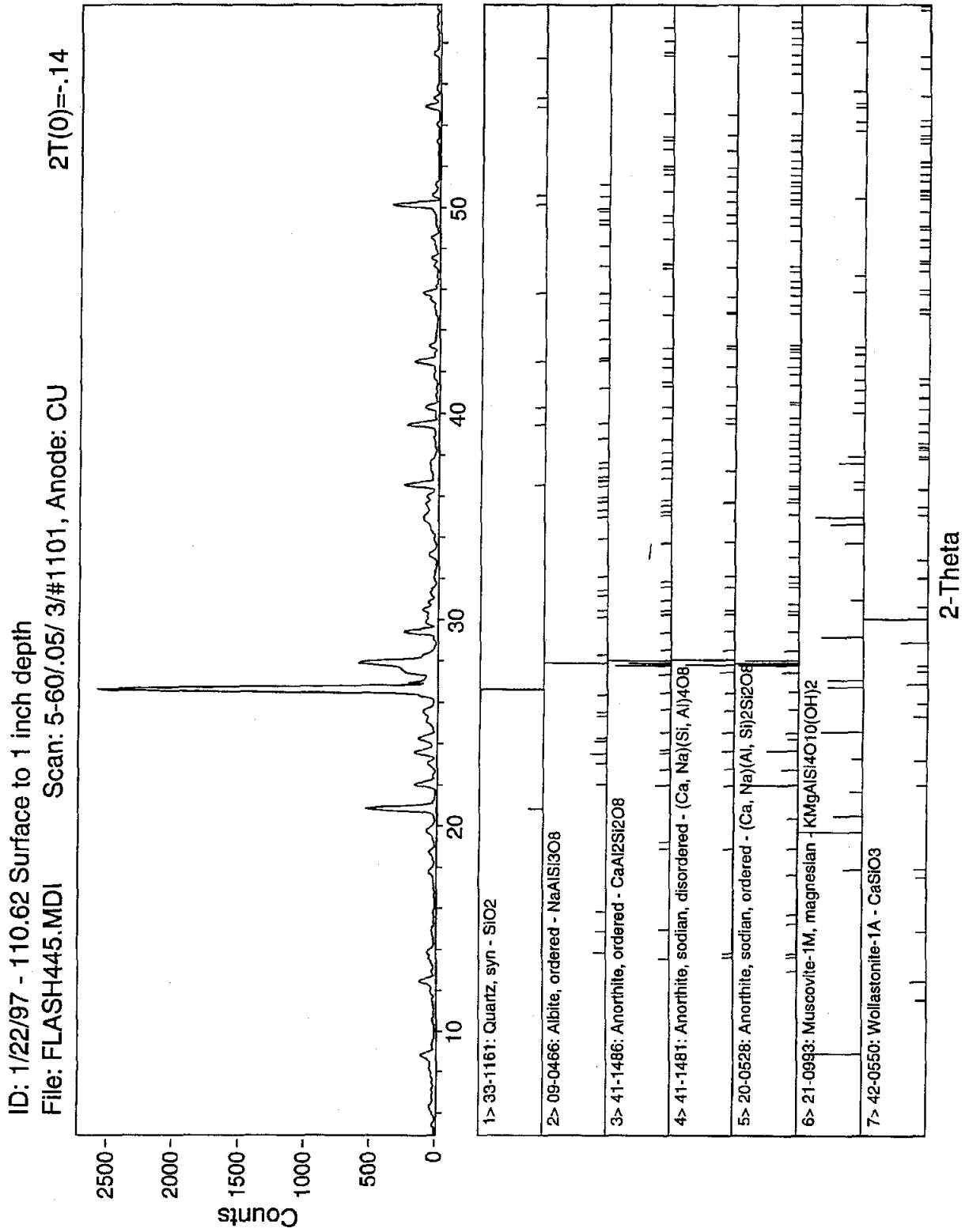


Figure A-4. XRD Soil data at 1-inch depth.

ID: 114.73 - 6 to 12 inches depth
 File: FLASH446.MDI Scan: 5-60/.05/ 3/#1101, Anode: CU 2 θ (0)=-.16

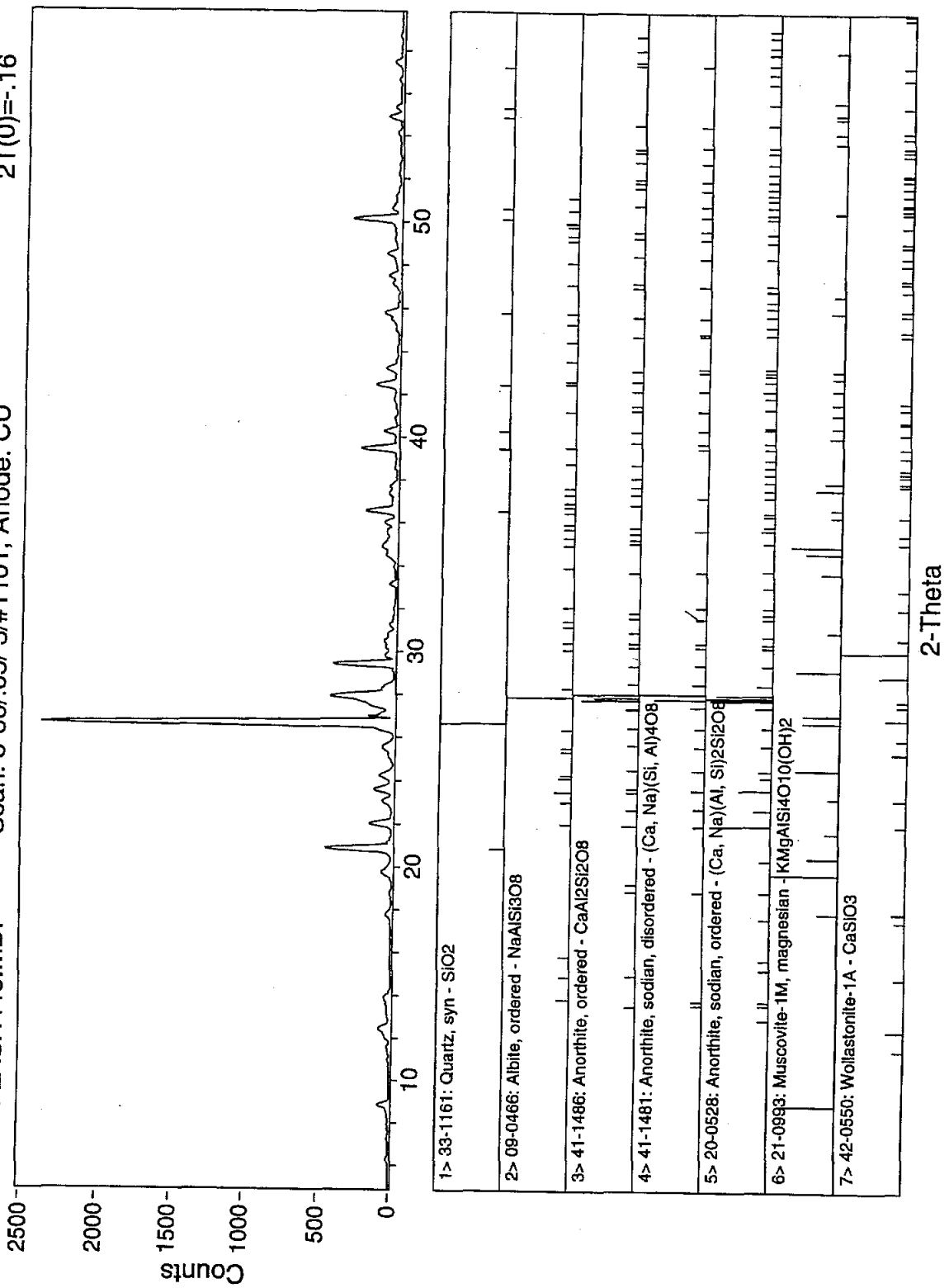


Figure A-5. XRD Soil data at 12-inch depth.

ID: 114.14 Composite
 File: FLASH449.MDI Scan: 5-60/05/3/#1101, Anode: CU 2 θ (0)=-.08

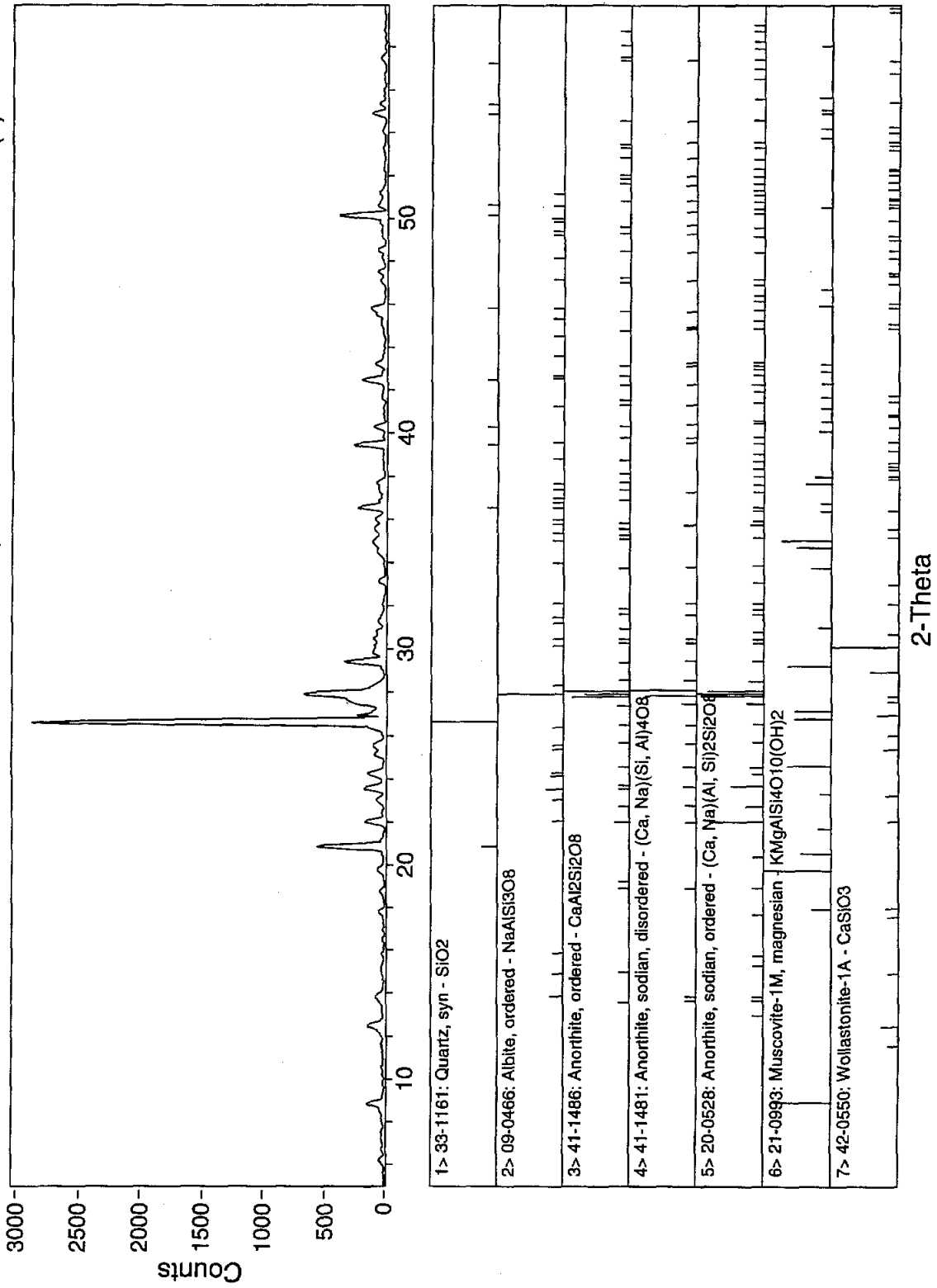


Figure A-6. Composite XRD soil data.

APPENDIX A. METEOROLOGICAL DATA

HHMM	PRESS	TEMP	RH	SURFACE WINDS			15 FOOT WINDS			SOIL	SOLAR	PRECIP
	Mbs	F	%	DIR	SPD	PK SP	DIR	SPD	PK SPD	TEMP	RAD	INCHES
600	997.1	49.3	38	3	0	0.4	17	7.2	7	46.4	0	0
615	997.0	49.8	39	5	0	0.4	38	5.3	7	46.4	0	0
630	997.0	49.7	38	310	0	0	10	4.8	5.9	46.3	0	0
645	997.0	48.8	39	1	0	0.2	28	4.4	5.9	45.9	0	0
700	997.0	49.3	40	18	0	0.2	52	4.6	6.3	45.8	2	0
715	997.0	49.7	40	45	0	0	54	5	5.9	45.7	11	0
730	997.1	51.2	38	29	0	0.4	36	2.8	6.5	46.1	42	0
745	997.2	51.8	36	8	0	0	20	4.2	4.6	47.6	87	0
800	997.3	53.9	35	307	0	0	9	2.8	4.8	49.5	137	0
815	997.5	57.8	32	85	0.2	0.4	112	7	8	52.6	189	0
830	997.7	60.9	30	72	7.7	9	99	12.1	13	56.1	239	0
845	997.7	62.0	29	84	9.4	10	97	13.4	14	59.3	289	0
900	997.7	63.0	28	84	8.1	10	104	11.6	16	62.3	338	0
915	997.8	63.9	28	93	7.9	13	114	11.4	16	65.1	384	0
930	997.7	65.1	27	70	7.7	10	98	14	17	68	429	0
945	997.8	66.5	25	128	5.9	10	159	5.9	14	71.2	472	0
1000	997.7	67.0	25	172	0.2	6.7	204	5.9	7	74.8	512	0
1015	997.5	67.3	25	185	0	0.6	213	4.4	7	78.3	550	0
1030	997.4	67.9	24	207	0	0.4	245	3.3	6.7	81.2	586	0
1045	997.2	68.7	24	255	2.6	6.7	270	3.7	7	83.9	615	0
1100	997.1	69.3	24	183	0	5.4	231	3.7	7	86.6	643	0
1115	996.8	70.1	24	193	3.7	6.3	253	4.4	7	88.6	669	0
1130	996.6	71.4	23	248	0	5.2	289	3.3	5.9	91.4	689	0
1145	996.4	72.8	21	269	4.4	7	304	7.9	8	93.9	702	0
1200	996.1	73.5	19	180	5.3	10	214	5	14	95.1	714	0
1215	995.9	74.0	18	131	3.9	9	199	4.2	9	96.3	723	0
1230	995.6	74.6	18	128	6.6	8	143	7	9	98.2	725	0
1245	995.3	74.6	19	180	8.3	8	202	8.8	10	99.3	720	0
1300	994.8	75.2	19	185	6.6	9	201	7.4	10	99.8	716	0
1315	994.5	75.7	18	165	3.5	10	195	4.4	13	10.1	711	0
1330	994.1	75.9	18	183	7.9	10	195	8.8	13	10.3	700	0
1345	993.8	76.4	18	133	5.7	10	153	6.8	13	99.7	685	0
1400	993.6	76.7	18	219	7.4	10	246	10.3	13	99.8	664	0
1415	993.3	76.8	18	272	6.8	10	285	7.2	13	98.8	640	0
1430	993.1	77.5	19	201	0.2	10	241	6.6	14	98.1	612	0
1445	992.9	77.7	22	186	5.7	10	217	7.9	14	98.3	581	0
1500	992.8	78.1	25	105	3.3	10	166	2.6	13	97.4	546	0
1515	992.7	78.2	26	160	6.6	10	210	8.6	14	96.3	507	0
1530	992.6	78.2	28	207	5.3	10	227	5.9	14	94.6	468	0
1545	992.5	78.3	28	201	7.2	11	225	11	16	92.9	422	0
1600	992.2	78.4	30	190	6.8	16	216	8.3	19	91	379	0
1615	992.0	78.3	31	170	5	17	206	7.7	20	88.5	334	0
1630	991.8	78.1	32	186	12.3	17	213	16.9	20	86.4	287	0
1645	991.6	78.0	33	176	7	16	193	9.6	18	84.3	235	0
1700	991.5	77.9	33	141	11	13	173	14.9	16	82.1	183	0
1715	991.4	77.7	34	179	7.4	10	207	9.9	15	79.4	130	0
1730	991.2	77.0	36	149	6.4	13	182	9.2	15	77.5	81	0
1745	991.0	76.4	37	157	7.2	10	174	9.4	14	76	37	0
1800	991.1	75.8	37	135	7	11	166	9.9	15	74.4	7	0
MAX TEMP		MIN TEMP		MAX RH			MIN RH			MAX PRESS		MIN PRESS
1512		63		2130			2359			1		173
79		49		77			17			999.5		992
MAXIMUM WINDS:				2 FOOT LEVEL			23.0 AT 211:11			24 HR PRECIP: 0		
				15 FOOT LEVEL			35.0 AT 211:10			24 HR TOTAL PRECIP: 0		

Figure A-7. Met Data for 29 Oct 96

HHMM	PRESS	TEMP	RH	SURFACE WINDS			15 FOOT WINDS			SOIL	SOLAR	PRECIP	
	Mbs	F	%	DIR	SPD	PK SPD	DIR	SPD	PK SPD	TEMP	RAD	INCHES	
600	998.2	51.3	52	4	0.0	0.0	70	2.0	5.9	47.4	0	0.00	
615	998.4	50.2	54	7	0.0	0.0	20	4.6	5.0	47.0	0	0.00	
630	998.4	48.7	56	291	0.0	0.4	1	2.4	6.7	46.7	0	0.00	
645	998.7	48.3	57	28	0.2	0.4	44	7.0	7.0	46.3	0	0.00	
700	999.0	48.3	57	285	0.0	0.4	31	0.4	7.0	46.1	1	0.00	
715	999.1	48.6	57	32	0.0	0.2	49	7.4	7.0	46.0	11	0.00	
730	999.4	50.1	55	293	0.0	0.4	8	2.4	7.0	46.3	42	0.00	
745	999.6	50.9	53	12	0.0	0.4	16	2.0	7.0	47.6	85	0.00	
800	999.9	53.4	50	32	0.0	0.4	52	3.7	6.3	49.7	134	0.00	
815	1000.1	55.2	48	304	0.0	0.0	0	3.3	5.4	52.4	183	0.00	
830	1000.3	57.9	44	55	0.0	0.0	7	0.0	4.3	55.5	235	0.00	
845	1000.6	63.1	37	114	0.0	0.0	126	0.7	0.8	59.0	286	0.00	
900	1000.6	62.4	38	186	0.0	0.0	212	0.0	3.7	62.4	331	0.00	
915	1000.7	62.9	37	168	0.0	0.0	217	3.3	3.9	65.8	376	0.00	
930	1000.9	62.7	37	201	0.0	0.2	244	1.3	5.4	69.0	423	0.00	
945	1001.1	63.3	37	249	5.3	7.0	295	5.9	10.0	71.7	468	0.00	
1000	1001.0	64.3	35	241	5.3	8.0	300	5.9	11.0	74.0	508	0.00	
1015	1000.8	64.3	35	322	5.5	8.0	333	6.8	10.0	76.2	550	0.00	
1030	1000.8	64.7	35	294	8.3	10.0	318	10.1	14.0	78.3	587	0.00	
1045	1000.9	65.2	34	305	5.3	8.0	324	6.4	11.0	80.3	616	0.00	
1100	1000.8	66.1	32	261	4.2	8.0	264	5.3	10.0	82.8	645	0.00	
1115	1000.9	66.9	31	276	7.2	8.0	303	8.8	12.0	85.5	671	0.00	
1130	1000.8	67.3	29	264	6.1	9.0	296	6.6	13.0	86.9	692	0.00	
1145	1000.8	67.6	28	253	3.7	8.0	278	6.1	9.0	89.3	708	0.00	
1200	1000.7	68.4	28	224	2.6	8.0	227	5.0	9.0	91.5	716	0.00	
1215	1000.4	69.2	27	301	4.6	8.0	319	6.1	11.0	92.9	725	0.00	
1230	1000.3	69.2	27	293	3.7	7.0	328	4.4	11.0	94.7	729	0.00	
1245	1000.1	69.5	26	198	4.6	8.0	250	6.1	10.0	95.8	729	0.00	
1300	1000.0	69.9	25	277	7.4	7.0	299	9.4	9.0	96.6	724	0.00	
1315	999.7	70.5	25	238	2.4	8.0	262	2.6	11.0	96.3	720	0.00	
1330	999.6	70.6	25	274	5.3	10.0	291	7.7	13.0	96.3	708	0.00	
1345	999.5	71.0	25	306	5.7	10.0	340	11.2	14.0	96.4	692	0.00	
1400	999.4	71.8	24	170	0.0	10.0	186	3.1	13.0	95.8	673	0.00	
1415	999.3	72.3	24	277	8.3	10.0	299	9.9	15.0	96.1	647	0.00	
1430	999.3	71.7	24	215	2.2	9.0	260	2.4	12.0	93.8	622	0.00	
1445	999.3	72.0	24	290	6.4	8.0	322	9.0	11.0	93.9	592	0.00	
1500	999.3	72.1	24	296	2.2	8.0	335	3.1	11.0	92.9	557	0.00	
1515	999.4	72.4	23	279	5.9	8.0	313	6.8	11.0	92.0	520	0.00	
1530	999.4	72.3	22	273	6.4	8.0	317	7.2	10.0	91.0	481	0.00	
1545	999.4	72.6	22	24	5.5	10.0	17	6.8	15.0	89.5	436	0.00	
1600	999.4	72.6	22	286	5.7	10.0	309	7.7	13.0	87.3	390	0.00	
1615	999.4	72.3	22	254	5.5	9.0	281	7.4	12.0	85.4	343	0.00	
1630	999.6	72.9	22	293	6.4	8.0	310	9.9	10.0	83.2	293	0.00	
1645	999.6	72.6	22	294	6.6	10.0	321	8.3	13.0	80.9	241	0.00	
1700	999.7	72.1	22	267	6.4	10.0	303	8.1	13.0	77.8	188	0.00	
1715	999.7	71.7	22	280	6.1	9.0	320	8.6	12.0	74.6	136	0.00	
1730	999.7	71.2	22	255	7.2	10.0	280	10.5	14.0	72.5	86	0.00	
1745	999.7	70.7	23	294	6.1	8.0	301	9.2	12.0	70.9	40	0.00	
1800	999.8	69.9	23	283	4.6	8.0	297	7.0	12.0	69.2	10	0.00	
MAX TEMP		MIN TEMP		MAX RH			MIN RH			MAX PRESS		MIN PRESS	
1543		71		714			2359			235		0	
73		48		60			21			1002		997.1	
MAXIMUM WINDS:				2 FOOT LEVEL			11.0 AT 1:18			24 HR PRECIP: 0			
				15 FOOT LEVEL			15.0 AT 1:22			24 HR TOTAL PRECIP: 0			

Figure A-8. Met Data for 30 Oct 96

HHMM	PRESS	TEMP	RH	SURFACE WINDS			15 FOOT WINDS			SOIL	SOLAR	PRECIP
	Mbs	F	%	DIR	SPD	PK SPD	DIR	SPD	PK SPD	TEMP	RAD	INCHES
600	1002.7	51.4	49	102	0.0	0.0	127	3.3	3.5	45.4	0	0.00
615	1002.9	50.8	50	106	0.0	0.0	107	0.4	4.6	45.1	0	0.00
630	1003.0	54.6	47	7	0.0	0.0	11	1.5	3.5	45.4	0	0.00
645	1003.1	53.3	47	67	0.0	0.0	95	1.8	3.5	45.2	0	0.00
700	1003.3	53.3	48	98	0.0	0.0	143	0.7	3.7	45.0	1	0.00
715	1003.4	53.3	48	54	0.0	0.0	58	2.2	2.8	44.8	6	0.00
730	1003.5	54.3	47	5	0.0	0.0	42	2.2	3.0	45.1	38	0.00
745	1003.5	53.4	47	82	0.0	0.0	43	1.3	2.6	45.8	59	0.00
800	1003.7	52.6	47	51	0.0	0.0	73	2.0	3.7	47.5	106	0.00
815	1003.9	54.4	46	137	0.0	0.0	128	1.5	4.3	50.4	175	0.00
830	1004.2	56.3	44	100	0.0	0.4	127	2.2	5.9	53.7	231	0.00
845	1004.4	58.0	41	132	0.0	0.2	161	4.4	5.2	57.1	283	0.00
900	1004.6	59.5	40	258	0.0	0.4	288	2.8	4.8	60.4	328	0.00
915	1004.7	60.5	38	247	0.0	0.4	282	2.4	5.0	63.8	374	0.00
930	1004.8	62.9	36	187	0.0	0.0	196	2.2	3.0	67.5	421	0.00
945	1004.8	64.4	34	272	1.5	6.1	309	2.0	7.0	71.0	466	0.00
1000	1004.7	65.6	32	1	5.7	7.0	357	6.6	8.0	74.2	506	0.00
1015	1004.6	67.6	30	35	3.9	6.7	33	6.1	9.0	76.9	546	0.00
1030	1004.5	68.4	28	31	4.4	8.0	27	4.4	10.0	79.4	584	0.00
1045	1004.3	69.3	27	303	3.1	6.7	345	4.2	8.0	82.5	613	0.00
1100	1004.2	69.7	26	51	0.0	3.2	62	5.5	7.0	85.4	642	0.00
1115	1004.0	70.2	26	18	5.7	7.0	35	5.7	9.0	87.9	670	0.00
1130	1003.9	71.0	25	59	0.0	6.3	37	1.3	7.0	90.4	691	0.00
1145	1003.8	71.7	24	56	0.0	7.0	72	3.7	9.0	92.5	706	0.00
1200	1003.6	72.2	24	152	0.0	8.0	255	1.3	8.0	94.2	716	0.00
1215	1003.3	72.9	23	41	0.0	0.4	58	5.3	7.0	96.5	724	0.00
1230	1003.2	73.6	22	329	0.0	7.0	7	2.4	8.0	96.7	728	0.00
1245	1002.9	73.7	21	268	0.7	7.0	309	3.7	8.0	98.5	727	0.00
1300	1002.7	74.0	21	113	0.0	0.6	130	3.3	5.9	99.6	722	0.00
1315	1002.6	74.7	20	29	3.1	7.0	59	2.6	10.0	100.5	715	0.00
1330	1002.4	75.5	19	311	0.0	3.5	3	2.8	4.6	101.3	703	0.00
1345	1002.3	76.3	18	29	5.0	10.0	36	7.0	12.0	101.6	685	0.00
1400	1002.1	75.6	19	95	2.6	8.0	125	2.6	9.0	99.7	667	0.00
1415	1001.9	75.7	19	95	0.0	5.0	95	3.1	7.0	99.8	643	0.00
1430	1001.7	76.4	18	270	5.3	9.0	317	6.8	12.0	99.0	618	0.00
1445	1001.4	76.0	18	215	0.0	6.1	255	3.5	6.7	97.9	589	0.00
1500	1001.2	77.4	17	174	0.0	0.4	200	3.1	6.5	98.0	554	0.00
1515	1001.0	77.8	17	287	3.5	9.0	6	6.6	12.0	96.7	516	0.00
1530	1001.0	77.3	17	179	0.0	6.1	247	0.4	7.0	94.7	476	0.00
1545	1000.9	78.0	17	311	2.2	7.0	315	3.3	9.0	93.8	433	0.00
1600	1000.8	77.5	17	290	4.6	7.0	347	7.0	10.0	91.2	387	0.00
1615	1000.8	77.6	17	227	0.2	5.4	272	5.5	7.0	89.8	342	0.00
1630	1000.7	77.6	17	189	0.0	6.1	228	2.6	6.7	87.7	297	0.00
1645	1000.5	77.8	17	277	0.0	0.4	312	3.5	6.1	85.9	244	0.00
1700	1000.4	77.4	16	322	2.6	8.0	357	6.1	12.0	82.7	192	0.00
1715	1000.1	77.3	16	40	5.3	6.3	3	5.5	9.0	79.0	130	0.00
1730	1000.0	77.3	16	315	3.5	7.0	347	5.5	11.0	76.8	95	0.00
1745	1000.1	76.9	17	293	3.9	5.6	333	5.3	7.0	74.9	41	0.00
1800	1000.1	75.5	18	275	5.0	6.7	300	5.9	9.0	73.1	10	0.00
MAX TEMP		MIN TEMP		MAX RH			MIN RH			MAX PRESS		MIN PRESS
1534		60		549			2359			93		234
79		50		52			16			1005		1000
MAXIMUM WINDS:		2 FOOT LEVEL			10.0 AT 133:21			24 HR PRECIP: 0				
		15 FOOT LEVEL			12.0 AT 142:11			24 HR TOTAL PRECIP: 0				

Figure A-9. Met Data for 31 Oct 96

HHMM	PRESS	TEMP	RH	SURFACE WINDS			15 FOOT WINDS			SOIL	SOLAR	PRECIP
	Mbs	F	%	DIR	SPD	PK SPD	DIR	SPD	PK SPD	TEMP	RAD	INCHES
600	997.5	51.5	40	68	0.0	0.0	101	2.2	3.0	47.1	0	0.00
615	997.5	51.3	41	46	0.0	0.0	84	4.4	5.6	46.9	0	0.00
630	997.5	51.5	42	26	0.0	0.0	45	5.0	5.2	46.8	0	0.00
645	997.5	50.8	43	29	0.0	0.0	69	3.1	6.1	46.7	0	0.00
700	997.5	51.0	43	65	0.0	0.0	80	5.5	5.9	46.5	0	0.00
715	997.5	51.1	43	7	0.0	0.0	37	2.6	5.6	46.5	4	0.00
730	997.6	51.3	42	25	0.0	0.0	60	2.6	3.5	46.6	22	0.00
745	997.7	53.0	38	234	0.0	0.0	8	0.0	3.0	47.8	66	0.00
800	997.8	52.6	38	126	0.0	0.0	160	3.9	3.9	49.3	106	0.00
815	997.9	55.6	36	88	0.0	0.0	114	2.8	4.6	52.4	173	0.00
830	998.0	58.8	33	68	0.0	0.2	91	2.4	4.6	55.7	223	0.00
845	998.1	62.0	30	162	0.0	0.0	200	1.5	2.4	59.1	273	0.00
900	998.3	63.2	29	188	0.0	0.0	239	0.4	2.4	62.5	318	0.00
915	998.2	65.4	26	310	0.0	0.4	342	4.8	7.0	66.0	362	0.00
930	998.0	67.3	23	16	4.8	6.7	12	6.6	10.0	69.2	409	0.00
945	997.9	69.1	21	309	5.7	7.0	345	8.3	9.0	72.2	454	0.00
1000	997.7	70.2	20	285	3.5	7.0	328	5.3	9.0	75.4	495	0.00
1015	997.6	71.2	19	297	3.7	7.0	298	4.6	9.0	78.7	533	0.00
1030	997.6	72.4	18	327	0.0	6.7	357	4.6	7.0	82.1	570	0.00
1045	997.6	73.8	17	28	0.0	6.1	35	2.0	7.0	85.8	598	0.00
1100	997.5	75.5	16	19	0.0	0.4	18	3.7	5.2	89.2	628	0.00
1115	997.3	76.0	16	130	0.0	0.2	145	0.0	4.6	92.0	654	0.00
1130	997.2	77.1	15	71	0.0	0.4	70	5.0	7.0	94.8	676	0.00
1145	997.0	77.0	16	77	0.0	7.0	101	2.8	8.0	96.2	693	0.00
1200	996.6	77.6	16	100	6.6	14.0	114	8.8	14.0	97.6	702	0.00
1215	996.4	78.3	15	121	7.4	10.0	128	8.1	14.0	97.8	710	0.00
1230	996.2	78.7	15	121	2.6	11.0	85	3.7	14.0	98.5	714	0.00
1245	995.9	79.0	15	49	0.0	9.0	68	3.3	11.0	100.5	715	0.00
1300	995.6	79.7	15	188	9.2	13.0	214	11.8	13.0	101.7	711	0.00
1315	995.4	79.6	16	165	6.1	14.0	188	7.2	16.0	100.3	705	0.00
1330	995.2	79.7	15	185	9.4	11.0	214	12.3	12.0	100.5	693	0.00
1345	995.1	79.6	15	178	5.0	12.0	219	5.9	15.0	100.4	676	0.00
1400	994.9	79.9	15	234	5.5	21.0	235	5.5	23.0	100.1	656	0.00
1415	994.7	79.8	15	229	3.5	9.0	265	3.9	10.0	100.1	633	0.00
1430	994.6	80.3	15	243	2.6	8.0	278	4.4	11.0	99.9	607	0.00
1445	994.5	80.3	15	176	6.8	8.0	203	7.7	11.0	99.4	581	0.00
1500	994.3	80.5	15	185	7.2	9.0	216	8.3	10.0	98.6	547	0.00
1515	994.2	80.5	15	175	6.8	10.0	220	9.4	13.0	97.4	507	0.00
1530	994.2	79.8	16	193	7.4	12.0	227	11.2	15.0	95.2	466	0.00
1545	994.2	80.1	15	166	7.4	10.0	201	9.4	15.0	93.3	424	0.00
1600	994.1	79.7	16	193	9.2	13.0	229	11.0	16.0	91.3	376	0.00
1615	994.0	79.7	16	217	8.3	16.0	233	12.5	18.0	88.9	330	0.00
1630	994.0	79.4	16	187	9.2	14.0	213	10.5	17.0	86.6	282	0.00
1645	994.0	79.0	17	198	6.4	12.0	238	9.2	14.0	84.6	230	0.00
1700	994.0	78.7	18	187	9.2	10.0	208	10.1	14.0	81.9	178	0.00
1715	993.9	78.6	18	174	8.6	10.0	204	10.5	16.0	79.2	128	0.00
1730	993.9	78.1	19	164	5.0	10.0	194	7.2	14.0	77.3	79	0.00
1745	993.8	77.4	19	196	6.8	8.0	236	7.9	12.0	75.6	32	0.00
1800	993.8	76.2	19	185	6.1	8.0	218	6.8	10.0	73.8	6	0.00
MAX TEMP		MIN TEMP		MAX RH		MIN RH		MAX PRESS		MIN PRESS		
1507		60		657		2359		235		173		
81		50		44		14		1000		994.7		
MAXIMUM WINDS: 2 FOOT LEVEL				21.0 AT 134:33				24 HR PRECIP: 0				
15 FOOT LEVEL				23.0 AT 134:33				24 HR TOTAL PRECIP: 0				

Figure A-10. Met Data for 1 Nov 96

HHMM	PRESS	TEMP	RH	SURFACE WINDS			15 FOOT WINDS			SOIL	SOLAR	PRECIP
	Mbs	F	%	DIR	SPD	PK SPD	DIR	SPD	PK SPD	TEMP	RAD	INCHES
600	996.8	56.8	53	330	0.0	5.6	277	0.4	8.0	51.2	0	0.00
615	997.0	56.3	53	27	0.0	0.0	30	2.4	3.5	50.5	0	0.00
630	997.2	55.0	56	5	0.0	0.0	32	0.0	2.8	50.0	0	0.00
645	997.4	55.9	55	52	0.0	0.0	53	1.1	1.5	49.6	0	0.00
700	997.6	55.8	53	50	0.0	0.0	96	2.4	2.6	49.3	0	0.00
715	997.8	54.7	56	58	0.0	0.0	99	3.3	3.5	49.1	6	0.00
730	997.9	54.8	54	65	0.0	0.0	94	3.7	5.9	49.4	28	0.00
745	998.2	54.4	54	59	0.0	0.0	82	3.5	4.8	50.2	68	0.00
800	998.5	55.2	52	67	0.0	0.0	90	3.3	4.3	52.1	115	0.00
815	998.7	57.4	50	3	0.0	0.0	3	2.6	4.6	54.5	161	0.00
830	999.0	60.7	44	78	0.0	0.0	121	0.0	3.5	57.4	210	0.00
845	999.4	64.0	40	148	0.0	0.0	139	0.0	0.8	60.5	257	0.00
900	999.5	64.4	40	247	0.0	0.0	269	3.3	3.7	63.6	302	0.00
915	999.7	64.3	41	282	0.0	0.2	252	0.7	3.9	66.8	346	0.00
930	999.9	65.3	40	264	0.0	0.4	258	1.3	5.6	70.0	391	0.00
945	1000.0	66.1	39	254	0.0	0.4	265	2.6	7.0	73.0	438	0.00
1000	999.9	67.2	38	241	2.8	7.0	255	4.2	8.0	76.0	479	0.00
1015	999.9	67.7	37	165	5.3	8.0	189	5.0	9.0	78.6	517	0.00
1030	1000.0	68.9	37	219	6.4	10.0	242	9.4	13.0	80.9	554	0.00
1045	1000.2	69.3	36	230	4.8	10.0	245	6.6	14.0	82.3	581	0.00
1100	1000.2	69.7	36	203	5.9	8.0	235	6.8	12.0	84.5	612	0.00
1115	1000.2	70.1	35	243	7.7	9.0	247	9.6	11.0	86.6	636	0.00
1130	1000.4	70.6	34	222	6.8	10.0	259	9.0	14.0	87.6	658	0.00
1145	1000.3	71.4	33	210	7.2	12.0	237	10.7	15.0	88.7	674	0.00
1200	1000.3	72.0	32	196	6.4	16.0	234	11.8	21.0	89.8	683	0.00
1215	1000.2	72.4	31	187	5.9	12.0	228	7.2	15.0	91.5	691	0.00
1230	1000.1	73.9	29	244	7.7	10.0	270	10.3	14.0	92.9	695	0.00
1245	1000.1	73.8	29	179	7.9	14.0	214	10.1	17.0	93.1	694	0.00
1300	999.9	74.2	29	190	5.9	12.0	226	9.4	16.0	93.8	692	0.00
1315	999.7	74.8	28	196	6.6	11.0	218	7.0	15.0	94.5	685	0.00
1330	999.5	75.6	26	185	8.3	11.0	207	10.3	15.0	95.4	676	0.00
1345	999.4	75.9	27	209	8.6	10.0	234	11.2	15.0	95.7	660	0.00
1400	999.2	76.7	26	218	11.0	12.0	216	14.7	16.0	95.4	638	0.00
1415	999.1	76.7	26	220	7.7	14.0	249	12.3	16.0	95.3	618	0.00
1430	999.0	77.4	25	216	8.8	14.0	248	13.1	17.0	95.3	593	0.00
1445	998.9	78.0	24	233	5.7	13.0	236	5.7	16.0	94.8	565	0.00
1500	999.1	78.2	24	196	7.4	10.0	223	9.6	14.0	93.6	527	0.00
1515	999.2	78.4	24	261	6.4	10.0	295	6.8	14.0	92.9	489	0.00
1530	999.2	78.3	23	176	6.8	10.0	203	11.8	15.0	91.6	448	0.00
1545	999.2	77.9	24	196	5.0	10.0	234	3.3	14.0	90.0	407	0.00
1600	999.2	78.5	23	213	5.7	10.0	206	9.4	14.0	89.0	362	0.00
1615	999.1	78.0	24	210	5.3	10.0	247	6.4	14.0	87.1	314	0.00
1630	999.2	78.1	24	211	7.0	10.0	215	8.8	14.0	85.2	266	0.00
1645	999.1	77.7	24	168	7.7	10.0	206	10.5	15.0	82.9	215	0.00
1700	999.1	77.3	24	178	9.4	11.0	200	11.2	16.0	80.4	166	0.00
1715	999.0	77.2	24	193	7.0	10.0	215	11.8	14.0	77.7	118	0.00
1730	999.1	76.8	25	178	6.1	10.0	216	7.0	13.0	76.0	72	0.00
1745	999.2	76.4	25	175	5.9	7.0	208	8.8	10.0	74.4	32	0.00
1800	999.3	75.5	25	196	4.8	7.0	219	6.8	10.0	72.8	7	0.00
MAX TEMP		MIN TEMP		MAX RH			MIN RH			MAX PRESS		MIN PRESS
1548		61		456			2359			235		0
79		54		59			21			1003		996.7
MAXIMUM WINDS: 2 FOOT LEVEL				16.0 AT 114.25				24 HR PRECIP: 0				
15 FOOT LEVEL				21.0 AT 114.25				24 HR TOTAL PRECIP: 0				

Figure A-11. Met Data for 2 Nov 96

HHMM	PRESS	TEMP	RH	SURFACE WINDS			15 FOOT WINDS			SOIL	SOLAR	PRECIP
	Mbs	F	%	DIR	SPD	PK SPD	DIR	SPD	PK SPD	TEMP	RAD	INCHES
600	1001.5	52.6	53	48	0.0	0.0	79	3.9	4.6	48.5	0	0.00
615	1001.6	53.1	51	36	0.0	0.0	63	3.7	4.6	48.4	0	0.00
630	1001.6	52.3	52	19	0.0	0.0	56	2.8	4.1	48.3	0	0.00
645	1001.6	51.7	52	203	0.0	0.0	69	0.7	3.2	48.0	0	0.00
700	1001.7	50.8	52	204	0.0	0.0	165	0.7	2.1	47.6	1	0.00
715	1001.8	50.0	54	20	0.0	0.0	116	0.0	0.6	47.3	6	0.00
730	1001.9	51.8	51	8	0.0	0.4	44	3.7	6.1	47.5	29	0.00
745	1002.1	54.1	46	55	0.0	0.0	67	2.8	5.0	48.6	68	0.00
800	1002.2	55.8	44	36	0.0	0.0	88	0.9	3.7	50.8	114	0.00
815	1002.3	58.6	40	98	0.0	0.0	133	3.5	4.1	53.5	162	0.00
830	1002.4	58.1	42	139	0.0	0.0	156	0.9	4.1	56.2	212	0.00
845	1002.4	60.0	42	203	0.2	0.2	238	3.7	3.7	59.2	264	0.00
900	1002.5	60.4	39	236	0.0	0.0	285	1.8	4.1	62.2	307	0.00
915	1002.5	62.7	36	160	0.0	0.0	221	0.7	3.2	65.6	352	0.00
930	1002.5	65.6	33	132	0.0	0.0	192	1.8	3.5	69.2	399	0.00
945	1002.5	67.5	32	157	0.0	0.2	185	1.8	3.9	72.9	444	0.00
1000	1002.3	69.7	29	77	8.6	9.0	99	11.6	12.0	76.2	484	0.00
1015	1002.1	70.5	28	107	6.4	13.0	120	11.4	16.0	78.3	522	0.00
1030	1002.0	71.9	27	89	6.4	10.0	95	9.4	13.0	80.8	559	0.00
1045	1002.0	73.1	26	110	7.2	9.0	119	9.2	11.0	83.8	589	0.00
1100	1001.9	73.7	26	136	3.1	7.0	166	3.5	9.0	87.0	618	0.00
1115	1001.7	74.3	26	71	0.0	7.0	77	1.1	6.7	90.3	644	0.00
1130	1001.5	76.0	24	99	0.0	0.6	86	2.4	7.0	93.0	665	0.00
1145	1001.2	76.3	24	165	0.0	0.4	212	3.9	7.0	95.4	680	0.00
1200	1000.9	77.1	23	62	7.4	10.0	79	10.1	12.0	97.0	691	0.00
1215	1000.6	77.2	22	59	5.5	9.0	83	6.1	12.0	97.2	700	0.00
1230	1000.4	77.6	22	50	0.0	8.0	50	2.6	12.0	98.2	704	0.00
1245	1000.1	78.1	21	120	4.6	8.0	114	4.4	10.0	99.4	704	0.00
1300	999.7	78.4	21	88	2.6	7.0	87	4.8	9.0	100.7	700	0.00
1315	999.5	79.0	20	54	0.0	8.0	55	3.3	9.0	101.0	694	0.00
1330	999.3	79.3	20	272	0.0	7.0	295	1.8	8.0	102.1	682	0.00
1345	999.0	80.0	19	77	5.7	7.0	99	6.8	8.0	103.1	667	0.00
1400	998.7	80.5	19	82	0.0	6.5	93	5.7	8.0	103.3	648	0.00
1415	998.5	80.9	18	129	0.0	8.0	158	2.8	10.0	103.3	625	0.00
1430	998.2	80.7	18	124	5.7	10.0	146	7.2	12.0	102.2	600	0.00
1445	998.0	81.0	18	216	0.4	7.0	105	0.4	8.0	101.2	572	0.00
1500	998.0	81.3	18	191	5.9	7.0	225	7.9	9.0	100.7	537	0.00
1515	997.7	81.6	17	159	5.7	7.0	181	6.6	9.0	99.4	499	0.00
1530	997.6	81.2	17	204	3.1	8.0	215	5.3	10.0	97.3	455	0.00
1545	997.5	81.6	17	41	0.0	8.0	81	1.1	10.0	95.7	411	0.00
1600	997.3	81.8	17	175	0.0	0.4	235	3.5	7.0	94.7	368	0.00
1615	997.0	81.6	17	149	3.1	7.0	173	4.2	8.0	92.7	323	0.00
1630	996.9	81.2	18	114	3.9	8.0	135	5.7	9.0	90.5	274	0.00
1645	996.9	81.2	17	195	0.0	6.1	188	1.5	7.0	88.2	222	0.00
1700	996.9	81.8	17	128	0.0	0.4	173	2.8	6.5	85.5	171	0.00
1715	996.8	80.7	18	192	6.6	8.0	221	7.4	10.0	82.0	120	0.00
1730	996.8	79.9	19	200	4.6	7.0	225	7.0	10.0	79.6	72	0.00
1745	996.8	79.2	20	184	3.1	6.1	200	3.9	7.0	77.6	29	0.00
1800	996.8	78.0	21	184	0.0	3.2	205	4.4	5.9	75.7	6	0.00
MAX TEMP		MIN TEMP		MAX RH		MIN RH		MAX PRESS		MIN PRESS		
1550		70		549		2359		92		170		
82		50		56		16		1003		997.7		
MAXIMUM WINDS: 2 FOOT LEVEL				13.0 AT 100.43				24 HR PRECIP: 0				
15 FOOT LEVEL				16.0 AT 100.35				24 HR TOTAL PRECIP: 0				

Figure A-12. Met Data for 3 Nov 96

HHMM	PRES	TEMP	RH	SURFACE WINDS			15 FOOT WINDS			SOIL	SOLAR	PRECIP
	Mbs	F	%	DIR	SPD	PK SPD	DIR	SPD	PK SPD	TEMP	RAD	INCHES
600	996.1	54.2	43	58	0.0	0.2	79	4.2	6.7	49.0	0	0.00
615	996.1	52.7	45	86	0.0	0.0	105	0.9	5.0	48.7	1	0.00
630	996.2	51.9	46	60	0.0	0.0	76	3.5	3.7	48.2	0	0.00
645	996.2	51.5	46	335	0.0	0.0	15	3.3	4.1	47.9	0	0.00
700	996.5	49.8	46	292	0.0	0.0	347	0.4	4.3	47.6	0	0.00
715	996.6	49.7	48	50	0.0	0.0	44	4.2	4.1	47.3	5	0.00
730	996.7	50.2	45	68	0.0	0.0	68	2.6	4.3	47.4	28	0.00
745	996.6	51.6	43	108	0.0	0.0	93	0.9	3.9	48.0	67	0.00
800	996.9	54.4	39	10	0.0	0.0	19	2.6	2.8	50.2	115	0.00
815	997.2	56.8	38	49	0.0	0.0	64	1.8	3.9	52.9	162	0.00
830	997.3	58.1	37	111	0.0	0.4	123	3.3	4.8	55.8	212	0.00
845	997.3	59.3	36	101	0.0	0.0	121	2.8	3.9	58.8	264	0.00
900	997.5	62.8	34	173	0.0	0.0	115	0.0	3.2	62.3	308	0.00
915	997.8	64.2	32	182	0.0	0.0	227	0.9	3.2	65.8	351	0.00
930	997.5	66.1	30	129	0.0	0.0	153	3.3	4.3	69.4	398	0.00
945	997.4	67.0	29	183	0.0	0.2	181	3.3	4.6	72.8	445	0.00
1000	997.3	68.9	28	125	0.0	0.4	145	2.4	3.7	76.4	486	0.00
1015	997.2	69.7	27	205	0.0	0.0	233	2.2	3.7	79.8	523	0.00
1030	997.2	70.6	26	246	0.0	0.2	262	3.7	5.0	82.8	559	0.00
1045	997.3	70.4	27	242	0.0	0.4	269	4.4	5.4	85.4	589	0.00
1100	997.3	71.5	26	201	0.2	0.4	252	5.9	5.9	87.7	619	0.00
1115	997.1	72.4	25	190	0.0	0.4	190	2.4	6.3	90.1	644	0.00
1130	997.0	73.8	25	174	0.0	0.4	184	4.6	7.0	92.8	665	0.00
1145	997.1	74.6	24	235	3.3	7.0	279	3.3	8.0	94.2	678	0.00
1200	996.9	75.6	23	209	3.9	6.7	265	4.2	7.0	95.9	689	0.00
1215	996.8	76.5	21	184	3.5	7.0	225	4.8	7.0	97.6	696	0.00
1230	996.6	76.7	19	193	2.6	8.0	231	2.4	10.0	98.8	702	0.00
1245	996.5	77.4	17	204	6.4	7.0	243	7.4	9.0	99.9	705	0.00
1300	996.1	77.8	17	95	4.4	8.0	128	3.9	9.0	100.7	701	0.00
1315	995.8	78.1	16	45	0.0	6.7	49	1.8	8.0	101.9	695	0.00
1330	995.4	79.0	15	121	3.5	6.7	133	3.9	7.0	102.6	683	0.00
1345	995.1	78.9	16	194	5.3	9.0	207	7.7	10.0	102.2	667	0.00
1400	994.8	79.0	16	242	2.6	8.0	270	5.3	9.0	101.8	647	0.00
1415	994.6	79.5	16	205	7.2	8.0	232	8.6	10.0	101.2	625	0.00
1430	994.4	79.6	17	213	3.3	8.0	233	5.7	11.0	100.4	600	0.00
1445	994.3	79.6	17	228	8.6	9.0	262	11.0	13.0	99.6	569	0.00
1500	994.3	80.1	17	209	9.9	10.0	235	12.3	14.0	97.8	536	0.00
1515	994.2	80.1	17	261	6.1	10.0	276	8.8	14.0	96.2	499	0.00
1530	994.1	80.3	16	188	4.6	9.0	220	9.2	12.0	94.9	457	0.00
1545	994.1	80.2	16	208	6.4	10.0	246	9.6	14.0	93.1	410	0.00
1600	994.0	80.2	17	191	5.3	9.0	225	7.2	13.0	91.3	362	0.00
1615	993.8	80.3	17	177	2.4	7.0	224	2.6	9.0	89.7	318	0.00
1630	993.7	80.3	16	188	4.6	8.0	256	6.4	10.0	87.8	273	0.00
1645	993.8	80.0	16	246	3.7	9.0	271	4.4	14.0	85.4	222	0.00
1700	993.7	79.7	15	255	5.3	8.0	278	6.6	10.0	82.5	169	0.00
1715	993.6	79.3	16	215	5.5	8.0	247	8.1	10.0	79.3	117	0.00
1730	993.6	78.7	16	216	3.9	7.0	245	9.0	10.0	77.2	69	0.00
1745	993.6	77.8	16	229	3.3	7.0	253	6.1	10.0	75.4	28	0.00
1800	993.5	76.4	17	195	2.2	5.4	224	3.9	7.0	73.5	5	0.00
MAX TEMP		MIN TEMP		MAX RH		MIN RH		MAX PRESS		MIN PRESS		
1530		65		2321		2359		90		182		
81		49		61		14		999		994.4		
MAXIMUM WINDS:2 FOOT LEVEL				10.0 AT 154:13				24 HR PRECIP: 0				
15 FOOT LEVEL				14.0 AT 151:20				24 HR TOTAL PRECIP: 0				

Figure A-13. Met Data for 4 Nov 96

HHMM	PRESS	TEMP	RH	SURFACE WINDS			15 FOOT WINDS			SOIL	SOLA	PRECIP
	Mbs	F	%	DIR	SPD	PK SPD	DIR	SPD	PK SPD	TEMP	RAD	INCHES
600	997.1	63.5	27	316	6.8	16.0	343	14.0	21.0	56.4	0	0.00
615	997.2	63.1	27	313	8.1	17.0	356	11.6	22.0	56.2	0	0.00
630	997.4	63.1	26	321	10.5	16.0	345	16.9	21.0	56.3	0	0.00
645	997.7	63.2	26	313	15.1	18.0	347	21.5	25.0	56.6	0	0.00
700	998.0	63.1	26	1	12.1	18.0	340	16.9	26.0	56.7	0	0.00
715	998.2	63.1	26	308	8.6	17.0	329	18.9	23.0	56.8	5	0.00
730	998.4	63.1	26	310	9.9	19.0	334	15.1	24.0	57.0	22	0.00
745	998.8	63.2	26	319	13.1	19.0	334	22.1	25.0	57.5	57	0.00
800	999.1	63.5	25	323	10.5	19.0	341	15.1	25.0	58.8	103	0.00
815	999.7	63.5	25	335	10.3	17.0	336	17.1	22.0	60.0	150	0.00
830	999.9	63.7	25	332	15.1	18.0	345	22.8	26.0	61.3	200	0.00
845	1000.0	65.1	23	298	17.3	23.0	343	14.7	32.0	63.2	253	0.00
900	1000.3	66.0	22	308	17.8	22.0	349	23.5	33.0	65.0	298	0.00
915	1000.4	66.5	21	318	11.6	23.0	338	20.2	34.0	66.7	342	0.00
930	1000.4	67.4	20	342	15.8	21.0	344	22.4	30.0	68.6	390	0.00
945	1000.5	67.9	19	344	13.8	22.0	352	16.9	30.0	70.3	436	0.00
1000	1000.7	68.4	19	323	16.4	22.0	330	22.1	31.0	72.2	479	0.00
1015	1001.0	69.2	18	329	17.3	21.0	344	26.3	31.0	74.2	517	0.00
1030	1000.8	69.8	18	2	16.9	21.0	357	23.9	30.0	76.0	555	0.00
1045	1000.8	70.2	18	318	9.4	20.0	337	17.8	29.0	77.5	585	0.00
1100	1001.0	70.8	17	344	16.4	22.0	353	24.8	29.0	79.0	616	0.00
1115	1001.0	71.5	17	339	12.1	22.0	353	21.9	30.0	80.4	643	0.00
1130	1001.3	71.8	16	317	10.1	21.0	339	20.0	30.0	81.9	663	0.00
1145	1001.4	72.3	16	337	12.5	19.0	349	20.2	26.0	83.4	681	0.00
1200	1001.4	73.4	15	56	10.7	19.0	3	17.1	25.0	84.9	689	0.00
1215	1001.4	73.9	15	33	9.4	20.0	342	16.2	27.0	86.1	697	0.00
1230	1001.2	74.2	14	11	14.7	20.0	341	22.4	28.0	86.3	703	0.00
1245	1001.2	74.4	14	3	12.1	23.0	345	21.7	30.0	86.6	703	0.00
1300	1001.0	74.6	14	344	10.5	20.0	332	16.4	26.0	86.8	700	0.00
1315	1001.0	75.3	13	320	16.0	20.0	349	23.7	29.0	87.5	692	0.00
1330	1001.0	75.6	13	321	15.3	21.0	349	22.4	28.0	87.4	681	0.00
1345	1000.9	75.6	13	310	14.5	23.0	335	25.0	32.0	87.0	664	0.00
1400	1000.8	75.7	13	320	7.9	20.0	331	14.5	28.0	87.2	643	0.00
1415	1000.8	75.9	13	327	8.1	20.0	336	16.2	26.0	87.3	621	0.00
1430	1000.8	75.8	13	343	8.6	19.0	340	12.9	26.0	86.8	596	0.00
1445	1000.8	76.0	12	333	10.1	17.0	334	14.7	23.0	86.8	569	0.00
1500	1000.9	75.8	12	332	16.2	19.0	354	20.6	26.0	85.9	535	0.00
1515	1001.0	75.6	12	314	7.0	16.0	310	8.1	22.0	84.8	499	0.00
1530	1001.0	75.6	12	301	9.2	17.0	313	15.6	24.0	84.0	460	0.00
1545	1001.0	75.5	12	340	7.9	18.0	346	14.0	23.0	82.7	417	0.00
1600	1001.2	75.5	12	327	7.7	16.0	319	9.6	22.0	81.7	371	0.00
1615	1001.4	75.3	12	330	9.6	14.0	348	13.6	19.0	80.4	326	0.00
1630	1001.4	74.8	12	287	6.1	16.0	325	11.4	19.0	78.8	277	0.00
1645	1001.7	74.5	12	289	7.7	14.0	316	11.0	18.0	77.2	223	0.00
1700	1001.8	74.1	11	317	8.3	14.0	307	12.9	19.0	74.8	170	0.00
1715	1001.9	73.8	11	315	9.6	14.0	321	12.7	18.0	72.3	119	0.00
1730	1001.9	73.3	10	313	7.4	11.0	332	12.1	16.0	70.6	70	0.00
1745	1002.2	72.4	11	315	7.7	10.0	325	11.8	16.0	69.2	29	0.00
1800	1002.3	71.3	11	311	5.7	10.0	307	11.0	15.0	67.7	5	0.00
MAX TEMP		MIN TEMP		MAX RH		MIN RH		MAX PRESS		MIN PRESS		
1403		233		410		2359		2311		2		
76		55		54		10		1006		995.2		
MAXIMUM WINDS: 2 FOOT LEVEL				23.0 AT 90:54				24 HR PRECIP: 0				
15 FOOT LEVEL				34.0 AT 90:33				24 HR TOTAL PRECIP: 0				

Figure A-14. Met Data for 5 Nov 96

HHMM	PRESS	TEMP	RH	SURFACE WINDS			15 FOOT WINDS			SOIL	SOLA	PRECIP	
	Mbs	F	%	DIR	SPD	PK SPD	DIR	SPD	PK SPD	TEMP	RAD	INCHES	
600	997.1	63.5	27	316	6.8	16.0	343	14.0	21.0	56.4	0	0.00	
615	997.2	63.1	27	313	8.1	17.0	356	11.6	22.0	56.2	0	0.00	
630	997.4	63.1	26	321	10.5	16.0	345	16.9	21.0	56.3	0	0.00	
645	997.7	63.2	26	313	15.1	18.0	347	21.5	25.0	56.6	0	0.00	
700	998.0	63.1	26	1	12.1	18.0	340	16.9	26.0	56.7	0	0.00	
715	998.2	63.1	26	308	8.6	17.0	329	18.9	23.0	56.8	5	0.00	
730	998.4	63.1	26	310	9.9	19.0	334	15.1	24.0	57.0	22	0.00	
745	998.8	63.2	26	319	13.1	19.0	334	22.1	25.0	57.5	57	0.00	
800	999.1	63.5	25	323	10.5	19.0	341	15.1	25.0	58.8	103	0.00	
815	999.7	63.5	25	335	10.3	17.0	336	17.1	22.0	60.0	150	0.00	
830	999.9	63.7	25	332	15.1	18.0	345	22.8	26.0	61.3	200	0.00	
845	1000.0	65.1	23	298	17.3	23.0	343	14.7	32.0	63.2	253	0.00	
900	1000.3	66.0	22	308	17.8	22.0	349	23.5	33.0	65.0	298	0.00	
915	1000.4	66.5	21	318	11.6	23.0	338	20.2	34.0	66.7	342	0.00	
930	1000.4	67.4	20	342	15.8	21.0	344	22.4	30.0	68.6	390	0.00	
945	1000.5	67.9	19	344	13.8	22.0	352	16.9	30.0	70.3	436	0.00	
1000	1000.7	68.4	19	323	16.4	22.0	330	22.1	31.0	72.2	479	0.00	
1015	1001.0	69.2	18	329	17.3	21.0	344	26.3	31.0	74.2	517	0.00	
1030	1000.8	69.8	18	2	16.9	21.0	357	23.9	30.0	76.0	555	0.00	
1045	1000.8	70.2	18	318	9.4	20.0	337	17.8	29.0	77.5	585	0.00	
1100	1001.0	70.8	17	344	16.4	22.0	353	24.8	29.0	79.0	616	0.00	
1115	1001.0	71.5	17	339	12.1	22.0	353	21.9	30.0	80.4	643	0.00	
1130	1001.3	71.8	16	317	10.1	21.0	339	20.0	30.0	81.9	663	0.00	
1145	1001.4	72.3	16	337	12.5	19.0	349	20.2	26.0	83.4	681	0.00	
1200	1001.4	73.4	15	56	10.7	19.0	3	17.1	25.0	84.9	689	0.00	
1215	1001.4	73.9	15	33	9.4	20.0	342	16.2	27.0	86.1	697	0.00	
1230	1001.2	74.2	14	11	14.7	20.0	341	22.4	28.0	86.3	703	0.00	
1245	1001.2	74.4	14	3	12.1	23.0	345	21.7	30.0	86.6	703	0.00	
1300	1001.0	74.6	14	344	10.5	20.0	332	16.4	26.0	86.8	700	0.00	
1315	1001.0	75.3	13	320	16.0	20.0	349	23.7	29.0	87.5	692	0.00	
1330	1001.0	75.6	13	321	15.3	21.0	349	22.4	28.0	87.4	681	0.00	
1345	1000.9	75.6	13	310	14.5	23.0	335	25.0	32.0	87.0	664	0.00	
1400	1000.8	75.7	13	320	7.9	20.0	331	14.5	28.0	87.2	643	0.00	
1415	1000.8	75.9	13	327	8.1	20.0	336	16.2	26.0	87.3	621	0.00	
1430	1000.8	75.8	13	343	8.6	19.0	340	12.9	26.0	86.8	596	0.00	
1445	1000.8	76.0	12	333	10.1	17.0	334	14.7	23.0	86.8	569	0.00	
1500	1000.9	75.8	12	332	16.2	19.0	354	20.6	26.0	85.9	535	0.00	
1515	1001.0	75.6	12	314	7.0	16.0	310	8.1	22.0	84.8	499	0.00	
1530	1001.0	75.6	12	301	9.2	17.0	313	15.6	24.0	84.0	460	0.00	
1545	1001.0	75.5	12	340	7.9	18.0	346	14.0	23.0	82.7	417	0.00	
1600	1001.2	75.5	12	327	7.7	16.0	319	9.6	22.0	81.7	371	0.00	
1615	1001.4	75.3	12	330	9.6	14.0	348	13.6	19.0	80.4	326	0.00	
1630	1001.4	74.8	12	287	6.1	16.0	325	11.4	19.0	78.8	277	0.00	
1645	1001.7	74.5	12	289	7.7	14.0	316	11.0	18.0	77.2	223	0.00	
1700	1001.8	74.1	11	317	8.3	14.0	307	12.9	19.0	74.8	170	0.00	
1715	1001.9	73.8	11	315	9.6	14.0	321	12.7	18.0	72.3	119	0.00	
1730	1001.9	73.3	10	313	7.4	11.0	332	12.1	16.0	70.6	70	0.00	
1745	1002.2	72.4	11	315	7.7	10.0	325	11.8	16.0	69.2	29	0.00	
1800	1002.3	71.3	11	311	5.7	10.0	307	11.0	15.0	67.7	5	0.00	
MAX TEMP		MIN TEMP		MAX RH			MIN RH			MAX PRESS		MIN PRESS	
1403		233		410			2359			2311		2	
76		55		54			10			1006		995.2	
MAXIMUM WINDS: 2 FOOT LEVEL				23.0 AT 90:54				24 HR PRECIP: 0					
15 FOOT LEVEL				34.0 AT 90:33				24 HR TOTAL PRECIP: 0					

Figure A-14. Met Data for 5 Nov 96

HHMM	PRESS	TEMP	RH	SURFACE WINDS			15 FOOT WINDS			SOIL	SOLA	PRECIPI
	Mbs	F	%	DIR	SPD	PK SPD	DIR	SPD	PK SPD	TEMP	RAD	INCHES
600	1006.3	54.9	15	322	0.0	0.2	351	6.6	7.0	45.6	0	0.00
615	1006.5	53.6	16	320	0.2	0.4	352	7.4	9.0	45.4	0	0.00
630	1006.6	54.7	16	299	4.8	9.0	17	9.9	13.0	46.2	0	0.00
645	1006.7	56.4	15	322	6.8	10.0	340	12.3	14.0	47.4	0	0.00
700	1006.9	57.3	15	289	5.7	9.0	355	9.4	14.0	48.1	1	0.00
715	1007.3	56.8	15	105	0.0	7.0	137	3.9	10.0	47.8	4	0.00
730	1007.6	54.2	16	248	0.0	0.0	330	0.0	5.0	46.6	24	0.00
745	1007.8	58.0	15	56	0.0	0.4	57	2.2	5.4	47.2	64	0.00
800	1008.0	57.7	14	62	0.0	0.0	64	1.3	4.8	49.0	111	0.00
815	1008.1	59.3	14	1	0.0	0.0	0	2.6	3.5	51.3	161	0.00
830	1008.2	60.7	13	41	0.0	0.0	53	2.4	3.9	54.0	212	0.00
845	1008.4	61.7	13	87	0.0	0.0	97	0.4	2.8	57.0	264	0.00
900	1008.8	63.4	13	203	0.0	0.0	230	3.1	3.7	60.2	311	0.00
915	1008.9	63.9	13	242	0.0	0.0	273	0.4	3.0	63.5	355	0.00
930	1009.0	64.5	12	223	0.0	0.4	232	2.0	4.1	66.8	403	0.00
945	1009.0	66.4	12	300	5.3	7.0	335	6.8	10.0	70.2	450	0.00
1000	1009.1	68.0	11	309	4.4	8.0	334	7.4	11.0	72.8	491	0.00
1015	1009.1	69.1	11	297	5.5	10.0	332	9.6	13.0	75.1	530	0.00
1030	1009.2	70.4	10	318	6.8	10.0	344	9.6	16.0	77.4	566	0.00
1045	1009.2	71.8	10	306	6.6	10.0	350	11.2	14.0	80.1	596	0.00
1100	1009.2	72.5	10	308	7.9	10.0	335	11.6	16.0	82.2	626	0.00
1130	1009.1	74.2	9	306	7.4	10.0	345	11.0	13.0	86.9	672	0.00
1145	1009.1	75.0	9	302	5.7	10.0	332	7.7	14.0	88.8	689	0.00
1200	1008.8	76.0	8	331	7.0	9.0	0	10.1	13.0	90.7	698	0.00
1215	1008.6	76.2	8	320	3.7	10.0	338	5.3	12.0	92.0	706	0.00
1230	1008.2	76.6	8	297	2.2	9.0	337	3.1	12.0	93.6	710	0.00
1245	1007.9	77.1	8	309	3.5	7.0	325	5.5	11.0	95.8	709	0.00
1300	1007.6	77.9	8	264	0.0	9.0	278	1.3	12.0	97.1	705	0.00
1315	1007.4	78.1	8	315	5.9	8.0	342	6.8	10.0	98.3	698	0.00
1330	1007.2	78.6	8	308	3.9	7.0	338	4.2	7.0	98.6	688	0.00
1345	1007.1	79.4	7	1	5.5	7.0	357	8.1	9.0	99.4	671	0.00
1400	1006.9	79.1	8	293	0.0	6.7	355	0.2	8.0	99.2	651	0.00
1415	1006.7	79.6	8	287	3.3	7.0	315	3.7	10.0	99.8	629	0.00
1430	1006.6	79.3	8	36	5.7	8.0	29	6.4	12.0	98.2	603	0.00
1445	1006.6	80.0	8	233	0.0	9.0	284	2.2	12.0	96.8	573	0.00
1500	1006.5	80.3	8	283	6.8	9.0	340	10.3	12.0	96.3	536	0.00
1515	1006.4	80.5	7	331	6.1	8.0	353	10.7	12.0	94.9	501	0.00
1530	1006.3	80.5	7	1	2.8	10.0	3	3.7	15.0	93.3	459	0.00
1545	1006.2	80.4	7	330	7.4	8.0	356	9.6	12.0	91.3	415	0.00
1600	1006.2	80.5	7	274	6.1	9.0	294	7.2	12.0	89.3	370	0.00
1615	1006.1	80.6	7	0	5.0	9.0	6	8.1	14.0	87.3	323	0.00
1630	1006.1	80.7	7	318	4.6	10.0	341	5.0	17.0	85.0	274	0.00
1645	1006.0	80.3	7	338	4.6	10.0	0	8.6	15.0	82.8	222	0.00
1700	1005.9	79.8	7	318	6.4	10.0	345	14.0	15.0	80.0	169	0.00
1715	1005.9	79.0	8	318	8.1	11.0	334	13.6	16.0	77.1	117	0.00
1730	1005.9	78.2	8	308	8.6	10.0	337	12.1	17.0	75.1	68	0.00
1745	1005.9	77.3	8	305	6.6	10.0	345	11.6	15.0	73.4	27	0.00
1800	1005.9	76.1	8	331	4.6	10.0	346	8.6	16.0	71.8	5	0.00
MAX TEMP		MIN TEMP		MAX RH		MIN RH		MAX PRESS		MIN PRESS		
1615		34		311		2359		103		3		
81		49		18		7		1010		1006		
MAXIMUM WINDS:		2 FOOT LEVEL		11.0 AT 110:38		24 HR PRECIP: 0						
		15 FOOT LEVEL		17.0 AT 172:28		24 HR TOTAL PRECIP: 0						

Figure A-15. Met Data for 6 Nov 96

HHMM	PRESS	TEMP	RH	SURFACE WINDS			15 FOOT WINDS			SOIL	SOLAR	PRECIP			
	Mbs	F	%	DIR	SPD	PK SPD	DIR	SPD	PK SPD	TEMP	RAD	INCHES			
600	1006.9	56.4	16	126	0.0	0.0	141	2.0	4.1	46.7	0	0.00			
615	1007.0	56.7	16	19	0.0	0.0	94	0.2	2.1	46.4	0	0.00			
630	1007.0	55.7	16	47	0.0	0.0	50	5.3	5.6	46.0	0	0.00			
645	1007.3	50.0	18	83	0.0	0.0	184	0.0	6.5	45.7	1	0.00			
700	1007.4	50.6	18	72	0.0	0.0	79	3.5	4.3	45.3	0	0.00			
715	1007.4	49.8	18	75	0.0	0.0	71	3.7	5.6	45.2	4	0.00			
730	1007.6	50.2	18	33	0.0	0.0	82	3.3	4.8	45.2	23	0.00			
745	1007.6	52.5	17	140	0.0	0.0	143	3.1	3.9	45.6	62	0.00			
800	1007.7	54.8	16	58	0.0	0.0	80	4.4	4.8	47.9	110	0.00			
815	1007.7	58.2	16	204	0.0	0.4	193	1.3	5.4	50.9	159	0.00			
830	1007.9	58.7	14	208	0.0	0.0	225	1.5	2.4	53.8	209	0.00			
845	1008.0	60.8	14	66	0.0	0.0	158	0.2	4.1	57.0	263	0.00			
900	1008.2	63.7	13	170	0.0	0.0	204	2.6	3.9	60.5	309	0.00			
915	1008.2	65.5	13	169	0.0	0.0	213	2.0	3.5	64.1	351	0.00			
930	1008.2	67.0	12	149	0.0	0.0	172	1.8	3.2	67.6	392	0.00			
945	1008.1	69.5	11	194	0.0	0.0	237	3.5	3.9	71.4	443	0.00			
1000	1008.1	71.5	11	232	0.2	0.4	234	5.0	5.2	75.2	488	0.00			
1015	1007.9	74.0	10	280	6.8	8.0	325	8.8	10.0	78.5	525	0.00			
1030	1007.8	75.8	9	319	7.2	9.0	347	8.3	12.0	81.2	559	0.00			
1045	1007.7	76.7	9	329	9.4	12.0	342	11.8	15.0	83.4	590	0.00			
1100	1007.6	77.7	8	309	8.1	10.0	335	15.3	15.0	85.4	620	0.00			
1115	1007.4	78.9	8	322	6.6	13.0	336	10.5	17.0	87.1	645	0.00			
1130	1007.1	79.8	8	307	11.8	17.0	316	18.0	20.0	88.6	665	0.00			
1145	1006.9	80.5	7	324	8.1	16.0	343	14.5	20.0	89.8	680	0.00			
1200	1006.6	81.2	7	310	9.2	16.0	332	12.3	20.0	91.1	687	0.00			
1215	1006.2	81.8	7	289	12.3	16.0	321	16.4	20.0	92.2	698	0.00			
1230	1005.8	82.7	7	314	8.3	15.0	322	13.6	18.0	93.6	703	0.00			
1245	1005.5	83.7	7	321	8.1	14.0	353	17.5	17.0	95.0	703	0.00			
1300	1005.2	84.0	7	311	9.4	16.0	316	14.5	20.0	96.0	700	0.00			
1315	1004.7	84.5	6	291	7.7	16.0	325	12.7	21.0	96.4	694	0.00			
1330	1004.5	84.9	6	307	8.6	18.0	314	15.1	22.0	96.7	682	0.00			
1345	1004.2	85.3	6	295	8.1	19.0	312	11.2	22.0	96.9	665	0.00			
1400	1003.9	85.6	6	296	10.3	16.0	317	14.3	20.0	96.9	646	0.00			
1415	1003.6	85.8	6	289	9.0	17.0	312	15.6	21.0	96.3	623	0.00			
1430	1003.2	86.3	6	310	9.6	19.0	322	16.0	23.0	95.8	597	0.00			
1445	1003.0	86.8	6	291	9.6	18.0	316	12.7	23.0	95.4	567	0.00			
1500	1002.9	87.7	6	316	8.6	15.0	341	14.0	22.0	94.8	534	0.00			
1515	1002.8	88.1	5	13	9.0	14.0	354	15.1	21.0	94.3	496	0.00			
1530	1002.7	88.3	5	328	7.2	16.0	22	14.0	18.0	93.4	455	0.00			
1545	1002.6	88.3	5	6	12.3	16.0	357	16.4	20.0	92.0	411	0.00			
1600	1002.6	88.1	5	320	9.4	14.0	14	14.5	20.0	90.8	366	0.00			
1615	1002.5	87.5	5	340	10.5	15.0	357	14.7	18.0	89.2	320	0.00			
1630	1002.4	86.9	6	327	5.0	14.0	344	10.3	19.0	87.5	270	0.00			
1645	1002.4	86.6	6	320	7.2	11.0	334	14.7	16.0	85.7	219	0.00			
1700	1002.3	85.9	6	327	9.2	15.0	345	12.9	17.0	83.4	166	0.00			
1715	1002.3	85.0	6	337	5.3	11.0	349	9.9	17.0	80.7	115	0.00			
1730	1002.2	84.1	6	334	7.9	10.0	344	11.6	16.0	78.8	67	0.00			
1745	1002.2	82.8	7	321	6.1	9.0	336	10.1	14.0	77.1	26	0.00			
1800	1002.2	81.1	7	321	5.3	8.0	339	10.3	12.0	75.3	4	0.00			
MAX TEMP		MIN TEMP		MAX RH			MIN RH			MAX PRESS		MIN PRESS			
1549		63		641			2359			91		171			
89		49		19			5			1009		1003			
MAXIMUM WINDS:				2 FOOT LEVEL				19.0 AT 133:20				24 HR PRECIP: 0			
				15 FOOT LEVEL				23.0 AT 142:55				24 HR TOTAL PRECIP: 0			

Figure A-16. Met Data for 7 Nov 96

HHMM	PRESS	TEMP	RH	SURFACE WINDS			SOIL	SOLAR	PRECIP
	Mbs	F	%	DIR	SPD	PK SPD	TEMP	RAD	INCHES
600	1001.8	58	15	175	2	3	48	-0.0	0.00
615	1001.9	58	15	161	2	7	48	-0.0	0.00
630	1002.1	58	15	151	2	4	47	-0.0	0.00
645	1002.2	59	15	161	2	4	47	-0.0	0.00
700	1002.2	59	15	141	1	3	47	-0.0	0.00
715	1002.3	57	16	68	1	5	47	0.1	0.00
730	1002.3	58	15	81	2	5	48	0.7	0.00
745	1002.5	57	16	94	2	5	48	1.8	0.00
800	1002.7	61	14	90	2	3	50	2.8	0.00
815	1002.8	63	13	103	2	4	53	3.9	0.00
830	1002.8	64	14	79	3	4	57	5.0	0.00
845	1003.1	66	13	72	2	5	62	6.0	0.00
900	1003.1	69	12	79	1	4	66	7.0	0.00
915	1003.2	71	11	349	1	2	71	8.0	0.00
930	1003.2	71	11	341	1	3	75	9.0	0.00
945	1003.2	73	11	318	1	3	79	9.8	0.00
1000	1003.1	76	10	47	0	2	83	10.6	0.00
1015	1003.0	77	10	315	1	2	87	11.3	0.00
1030	1002.9	77	10	290	1	3	91	12.0	0.00
1045	1002.8	79	9	129	1	4	94	12.6	0.00
1100	1002.6	80	9	323	1	5	97	13.2	0.00
1115	1002.4	80	9	354	2	5	100	13.7	0.00
1130	1002.2	82	9	307	2	7	102	14.1	0.00
1145	1002.0	83	8	340	1	5	105	14.4	0.00
1200	1001.6	86	8	323	2	8	107	14.7	0.00
1215	1001.3	85	8	6	4	8	108	14.8	0.00
1230	1001.0	85	8	55	5	9	109	14.9	0.00
1245	1000.6	86	8	38	4	9	109	14.6	0.00
1300	1000.1	86	8	102	4	11	109	13.1	0.00
1315	999.7	87	7	96	5	11	109	13.0	0.00
1330	999.4	87	7	56	4	11	109	13.3	0.00
1345	999.1	88	7	342	2	6	110	13.2	0.00
1400	998.8	89	7	338	4	11	110	12.6	0.00
1415	998.7	89	7	43	3	9	109	12.1	0.00
1430	998.4	89	7	342	6	12	107	11.1	0.00
1445	998.3	89	7	315	4	10	106	10.3	0.00
1500	998.1	89	7	320	4	9	103	8.1	0.00
1515	997.9	89	7	333	5	10	102	9.5	0.00
1530	997.7	89	7	339	5	10	102	8.6	0.00
1545	997.5	89	7	333	5	11	99	7.9	0.00
1600	997.4	89	7	342	7	12	98	6.9	0.00
1615	997.3	88	7	331	9	15	94	4.8	0.00
1630	997.2	87	7	321	9	16	91	5.0	0.00
1645	997.0	87	7	323	10	16	89	4.2	0.00
1700	997.0	87	7	329	9	15	87	2.8	0.00
1715	997.1	86	8	344	7	12	84	1.2	0.00
1730	997.1	85	8	352	6	11	82	0.4	0.00
1745	997.0	84	8	352	6	11	80	0.1	0.00
1800	997.1	82	8	353	5	10	78	-0.0	0.00

Figure A-17. Met Data for 8 Nov 96

HHMM	PRESS	TEMP	RH	SURFACE WINDS			SOIL	SOLAR	PRECIP
	Mbs	F	%	DIR	SPD	PK SPD	TEMP	RAD	INCHES
600	997.7	52	21	48	2	4	49	-0.0	0.00
615	997.7	51	21	75	3	4	49	-0.0	0.00
630	997.6	51	22	80	3	5	49	-0.0	0.00
645	997.7	52	22	73	1	3	49	-0.0	0.00
700	997.8	51	23	16	2	3	49	0.0	0.00
715	997.9	52	23	42	2	3	48	0.2	0.00
730	998.0	52	22	45	2	3	49	0.7	0.00
745	998.2	53	21	83	3	5	50	1.7	0.00
800	998.4	54	20	82	4	5	52	2.7	0.00
815	998.5	57	19	72	3	4	54	3.2	0.00
830	998.5	60	18	73	3	4	58	4.9	0.00
845	998.7	64	17	60	3	4	63	6.1	0.00
900	998.7	68	17	32	2	4	67	6.6	0.00
915	998.8	71	15	343	0	1	72	7.4	0.00
930	998.8	74	14	304	0	2	76	8.1	0.00
945	998.7	75	14	259	1	4	80	9.5	0.00
1000	998.7	75	14	284	2	5	84	9.7	0.00
1015	998.6	74	14	302	2	4	85	9.1	0.00
1030	998.6	75	14	288	1	3	85	8.6	0.00
1045	998.5	77	13	61	1	4	91	12.6	0.00
1100	998.4	79	12	353	1	4	95	12.3	0.00
1115	998.2	79	12	306	2	6	97	11.6	0.00
1130	998.1	82	11	307	2	5	103	16.1	0.00
1145	997.8	82	10	225	1	4	103	10.1	0.00
1200	997.5	83	10	283	2	5	101	9.0	0.00
1215	997.4	83	10	292	3	6	103	14.8	0.00
1230	997.0	85	9	358	3	6	108	13.4	0.00
1245	996.9	85	10	223	7	12	104	11.7	0.00
1300	996.6	86	9	237	5	11	108	13.9	0.00
1315	996.3	87	9	234	6	10	105	8.9	0.00
1330	996.1	85	10	227	7	11	97	4.7	0.00
1345	996.0	85	10	234	6	9	94	5.0	0.00
1400	995.9	85	11	224	7	12	94	6.2	0.00
1415	995.7	85	11	251	7	12	95	7.1	0.00
1430	995.7	84	11	264	6	10	94	5.5	0.00
1445	995.6	84	11	262	6	11	92	4.7	0.00
1500	995.5	84	11	242	5	9	91	4.2	0.00
1515	995.4	85	11	242	5	10	90	5.0	0.00
1530	995.4	86	11	226	5	8	94	9.8	0.00
1545	995.3	87	11	263	5	9	96	6.1	0.00
1600	995.2	85	12	263	5	9	92	3.2	0.00
1615	995.3	85	12	272	6	10	88	2.5	0.00
1630	995.3	84	12	272	5	9	86	3.0	0.00
1645	995.2	84	12	273	4	7	86	5.0	0.00
1700	995.1	84	13	252	5	7	85	3.7	0.00
1715	995.1	83	13	254	5	8	83	1.3	0.00
1730	995.1	82	14	248	4	7	80	1.1	0.00
1745	995.2	81	14	225	3	4	78	0.3	0.00
1800	995.2	79	14	214	3	4	76	0.0	0.00

Figure A-18. Met Data for 9 Nov 96

HHMM	PRESS	TEMP	RH	SURFACE WINDS			SOIL	SOLAR	PRECIP
	Mbs	F	%	DIR	SPD	PK SPD	TEMP	RAD	INCHES
600	997.6	51	27	81	2	3	48	-0.0	0.00
615	997.7	50	27	72	3	4	47	-0.0	0.00
630	997.8	50	28	40	2	4	47	-0.0	0.00
645	997.8	51	28	29	1	2	47	-0.0	0.00
700	998.1	51	27	107	1	3	47	-0.0	0.00
715	998.2	49	28	89	3	4	47	0.1	0.00
730	998.3	51	27	74	4	6	47	0.6	0.00
745	998.5	52	26	67	5	6	49	1.6	0.00
800	998.6	54	25	65	4	5	50	2.3	0.00
815	998.9	56	23	40	1	3	53	3.6	0.00
830	999.2	60	20	0	0	0	57	4.3	0.00
845	999.4	62	19	86	0	2	60	5.4	0.00
900	999.4	64	19	137	0	2	65	7.8	0.00
915	999.5	66	18	238	2	4	70	7.5	0.00
930	999.6	66	18	235	3	5	74	8.8	0.00
945	999.7	67	18	257	3	5	77	8.3	0.00
1000	999.7	67	17	261	2	4	77	6.4	0.00
1015	999.8	68	17	292	2	4	77	5.8	0.00
1030	999.8	69	16	276	1	3	77	5.8	0.00
1045	999.9	70	16	278	2	4	79	6.7	0.00
1100	999.9	70	16	274	1	4	81	6.8	0.00
1115	999.9	72	15	235	1	2	81	5.5	0.00
1130	999.8	72	15	244	2	4	80	8.2	0.00
1145	999.7	75	14	329	1	3	93	16.4	0.00
1200	999.6	77	13	27	1	2	98	11.5	0.00
1215	999.4	77	13	4	1	3	94	8.7	0.00
1230	999.2	77	13	11	1	3	93	8.2	0.00
1245	999.0	78	12	8	2	5	96	12.2	0.00
1300	998.8	80	12	298	2	5	102	15.2	0.00
1315	998.7	81	11	30	2	5	105	14.9	0.00
1330	998.6	83	11	11	1	3	108	14.9	0.00
1345	998.4	85	10	333	2	5	108	13.9	0.00
1400	998.3	84	10	7	2	7	108	13.4	0.00
1415	998.2	84	10	46	2	6	108	12.8	0.00
1430	998.1	85	10	298	3	7	107	12.1	0.00
1445	998.0	85	10	16	2	6	106	11.5	0.00
1500	997.9	86	9	31	2	7	106	11.5	0.00
1515	997.7	89	9	276	1	4	106	10.5	0.00
1530	997.7	88	9	124	1	4	104	9.1	0.00
1545	997.6	87	9	90	2	5	102	8.1	0.00
1600	997.5	87	9	102	2	5	99	7.2	0.00
1615	997.5	86	9	82	3	5	97	6.2	0.00
1630	997.5	86	9	41	2	4	94	5.1	0.00
1645	997.5	86	9	88	2	5	91	3.9	0.00
1700	997.5	86	9	27	1	3	87	2.8	0.00
1715	997.6	85	11	242	3	5	84	1.8	0.00
1730	997.6	84	12	228	3	5	82	0.8	0.00
1745	997.8	82	13	245	3	4	79	0.1	0.00
1800	998.0	80	13	256	2	3	76	-0.0	0.00

Figure A-19. Met Data for 10 Nov 96

HHMM	PRESS	TEMP	RH	SURFACE WINDS			15 FOOT WINDS			SOIL	SOLAR	PRECIP
	Mbs	F	%	DIR	SPD	PK SPD	DIR	SPD	PK SPD	TEMP	RAD	INCHES
600	1002.2	53.8	28	25	0.0	0.0	59	3.3	4.3	50.0	0	0.00
615	1002.3	54.1	27	31	0.0	0.0	56	4.4	5.6	49.7	0	0.00
630	1002.4	54.0	27	235	0.0	0.0	45	0.0	4.6	49.5	0	0.00
645	1002.5	52.8	27	24	0.0	0.0	46	0.9	1.3	49.1	0	0.00
700	1002.7	53.2	28	32	0.0	0.0	56	2.4	3.0	48.8	0	0.00
715	1002.9	52.6	28	41	0.0	0.0	41	2.0	3.0	48.6	2	0.00
730	1003.0	52.0	28	43	0.0	0.0	73	2.4	3.5	48.4	14	0.00
745	1003.2	52.7	27	8	0.0	0.0	40	3.5	3.9	48.8	48	0.00
800	1003.3	54.3	26	1	0.0	0.0	13	3.3	4.8	50.4	93	0.00
815	1003.5	56.4	25	5	0.0	0.0	12	3.9	4.6	52.9	141	0.00
830	1003.6	59.3	23	22	0.0	0.0	21	2.0	4.1	55.7	189	0.00
845	1003.8	63.0	21	14	0.0	0.0	15	1.5	2.1	58.9	239	0.00
900	1004.0	65.6	20	49	0.0	0.0	42	0.4	2.4	62.2	287	0.00
915	1004.1	68.3	18	59	0.0	0.0	333	0.4	1.7	65.7	328	0.00
930	1004.3	67.7	19	289	0.0	0.4	347	2.4	4.1	69.1	371	0.00
945	1004.4	67.9	19	255	0.0	0.4	303	1.8	4.6	72.3	417	0.00
1000	1004.5	69.4	18	268	0.0	0.0	309	2.8	4.6	75.6	459	0.00
1015	1004.6	70.5	18	268	0.0	0.0	310	3.1	5.2	78.8	499	0.00
1030	1004.7	71.7	17	284	0.0	0.4	325	2.0	5.0	81.9	536	0.00
1045	1004.7	74.0	16	265	0.0	0.0	320	4.2	4.1	85.3	563	0.00
1100	1004.6	76.1	15	283	0.0	0.4	118	0.7	4.6	88.6	592	0.00
1115	1004.5	78.3	14	172	0.0	0.0	223	1.3	4.6	91.9	625	0.00
1130	1004.4	79.8	13	80	0.0	0.0	304	0.4	4.1	94.8	640	0.00
1145	1004.3	81.4	13	119	0.0	0.0	120	2.8	3.7	97.1	638	0.00
1200	1004.1	81.9	12	117	0.0	0.4	152	4.4	5.0	99.2	661	0.00
1215	1003.9	83.7	12	151	0.0	0.2	199	3.3	6.3	101.4	669	0.00
1230	1003.7	84.0	12	204	0.0	0.4	207	3.9	5.9	102.7	673	0.00
1245	1003.4	84.5	11	236	0.0	0.6	284	3.5	7.0	103.8	674	0.00
1300	1003.1	85.4	11	231	4.8	7.0	248	5.0	8.0	104.8	672	0.00
1315	1003.0	85.3	11	169	3.3	6.7	191	4.4	8.0	105.0	662	0.00
1330	1002.8	86.0	11	222	6.8	7.0	227	7.4	9.0	105.2	656	0.00
1345	1002.6	86.5	11	182	6.6	7.0	203	6.4	9.0	105.2	640	0.00
1400	1002.4	87.2	11	213	5.0	7.0	244	5.5	9.0	105.3	620	0.00
1415	1002.3	87.1	11	209	2.6	7.0	240	2.2	8.0	105.0	597	0.00
1430	1002.1	87.6	11	227	0.2	6.1	275	4.4	7.0	104.0	536	0.00
1445	1002.0	88.7	10	136	0.0	0.4	155	2.8	5.4	104.0	533	0.00
1500	1001.9	88.7	10	303	3.1	8.0	325	3.5	8.0	103.7	498	0.00
1515	1001.9	89.7	10	93	0.0	4.8	92	1.8	5.0	101.9	425	0.00
1530	1001.9	89.3	10	55	0.0	9.0	27	0.9	9.0	100.4	415	0.00
1545	1001.9	89.9	10	108	0.0	0.6	133	1.8	4.3	99.6	384	0.00
1600	1001.9	90.1	10	243	0.0	0.0	273	4.6	5.4	98.2	346	0.00
1615	1001.8	90.5	9	306	0.0	0.4	292	1.8	5.4	96.4	301	0.00
1630	1001.8	91.3	9	285	0.0	0.0	314	2.4	3.2	94.6	253	0.00
1645	1001.7	91.1	9	43	0.0	0.0	10	0.7	3.9	92.3	204	0.00
1700	1001.7	91.3	9	316	0.0	0.0	339	2.6	3.5	89.3	151	0.00
1715	1001.7	90.3	9	303	0.0	0.0	317	2.0	2.8	85.8	101	0.00
1730	1001.7	89.7	10	193	0.0	0.0	282	0.7	2.4	83.2	56	0.00
1745	1001.7	88.6	10	242	0.0	0.0	267	1.8	1.7	80.8	16	0.00
1800	1001.7	85.9	11	283	0.0	0.0	272	3.5	4.1	78.5	2	0.00
MAX TEMP		MIN TEMP		MAX RH		MIN RH		MAX PRESS		MIN PRESS		
1648		72		639		2359		102		2		
92		52		28		9		1005		1001		
MAXIMUM WINDS: 2 FOOT LEVEL				9.0 AT 151:19				24 HR PRECIP: 0				
15 FOOT LEVEL				9.0 AT 151:29				24 HR TOTAL PRECIP: 0				

Figure A-20. Met Data for 11 Nov 96

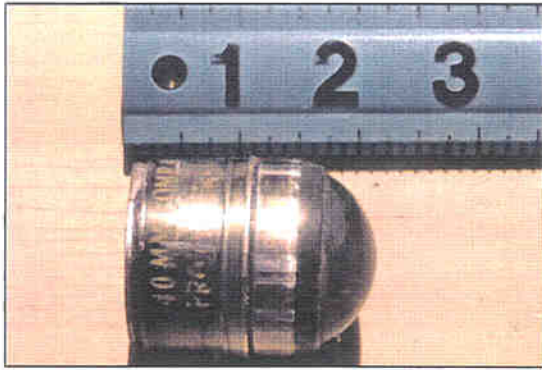
HHMM	PRESS	TEMP	RH	SURFACE WINDS			15 FOOT WINDS			SOIL	SOLAR	PRECIP	
	Mbs	F	%	DIR	SPD	PK SPD	DIR	SPD	PK SPD	TEMP	RAD	INCHES	
600	1003.0	55.7	24	8	0.0	0.0	45	3.3	4.3	52.3	0	0.00	
615	1003.1	55.3	25	29	0.0	0.0	49	4.4	4.8	52.0	0	0.00	
630	1003.2	55.7	25	41	0.0	0.0	67	3.5	5.2	51.9	0	0.00	
645	1003.3	55.7	25	30	0.0	0.0	67	3.1	3.5	51.7	0	0.00	
700	1003.2	56.0	26	35	0.0	0.0	69	3.7	4.1	51.4	0	0.00	
715	1003.2	55.7	25	18	0.0	0.0	32	3.5	4.1	51.4	4	0.00	
730	1003.3	54.9	25	39	0.0	0.0	33	3.3	4.3	51.3	14	0.00	
745	1003.5	56.3	25	172	0.0	0.0	42	0.0	3.2	51.6	40	0.00	
800	1003.7	57.1	24	206	0.0	0.0	23	0.7	1.0	52.7	74	0.00	
815	1004.0	58.5	23	278	0.0	0.0	318	2.2	2.1	55.0	147	0.00	
830	1004.2	60.1	22	307	0.0	0.0	348	3.7	4.8	58.1	180	0.00	
845	1004.3	62.8	21	322	0.0	0.0	344	3.3	4.6	60.2	183	0.00	
900	1004.4	65.2	20	303	0.0	0.0	313	0.9	3.7	63.0	272	0.00	
915	1004.3	67.5	19	173	0.0	0.0	212	0.7	1.9	66.3	265	0.00	
930	1004.4	69.0	18	205	0.0	0.0	238	2.2	2.8	69.1	351	0.00	
945	1004.4	70.0	18	285	0.0	0.0	299	4.4	5.0	73.1	402	0.00	
1000	1004.4	70.9	18	245	0.0	0.4	281	3.1	4.8	75.3	400	0.00	
1015	1004.4	72.6	17	286	0.0	0.0	325	2.2	4.1	78.9	467	0.00	
1030	1004.4	74.1	16	0	0.0	0.2	344	2.2	4.8	82.5	517	0.00	
1045	1004.3	75.7	15	185	0.0	0.2	207	1.8	5.2	85.1	497	0.00	
1100	1004.3	77.4	15	171	0.0	0.0	209	2.8	2.8	87.0	490	0.00	
1115	1004.3	77.7	14	0	0.0	0.0	320	2.2	4.1	88.7	523	0.00	
1130	1004.3	78.5	14	167	0.0	0.0	168	0.7	4.3	91.5	567	0.00	
1145	1004.1	79.7	14	159	0.0	0.4	186	2.6	4.6	94.7	631	0.00	
1200	1003.8	80.5	13	212	0.0	0.2	250	3.5	5.4	96.7	606	0.00	
1215	1003.5	81.3	13	141	0.0	0.6	177	1.3	6.3	98.4	660	0.00	
1230	1003.1	82.7	12	202	0.0	0.4	232	1.5	5.6	101.2	661	0.00	
1245	1002.8	83.6	12	223	0.0	0.2	263	3.1	4.8	101.8	633	0.00	
1300	1002.5	84.8	11	246	0.0	7.0	248	2.8	7.0	103.1	626	0.00	
1315	1002.2	84.8	11	273	0.0	7.0	284	5.0	7.0	102.0	534	0.00	
1330	1001.9	85.9	11	223	0.0	0.4	224	2.2	5.6	103.2	640	0.00	
1345	1001.6	87.6	11	201	0.0	0.6	218	5.7	6.7	106.2	669	0.00	
1400	1001.4	87.8	11	206	0.0	6.1	219	2.0	7.0	106.1	609	0.00	
1415	1001.2	88.4	11	194	0.0	0.4	238	3.9	6.1	106.0	582	0.00	
1430	1001.0	88.4	12	246	0.0	0.4	264	5.9	6.7	105.2	529	0.00	
1445	1000.9	89.2	12	205	0.0	0.6	225	4.6	6.5	104.5	536	0.00	
1500	1000.7	89.4	12	235	0.0	0.4	234	3.1	5.2	104.1	500	0.00	
1515	1000.6	89.9	12	328	0.0	0.4	324	1.8	5.6	103.2	459	0.00	
1530	1000.3	90.2	12	260	0.0	0.4	308	2.4	4.8	101.9	419	0.00	
1545	1000.2	90.4	11	258	0.0	0.4	261	3.3	6.1	100.5	378	0.00	
1600	1000.1	91.4	11	241	0.0	0.2	276	2.2	4.3	98.8	321	0.00	
1615	999.9	91.1	11	253	0.0	0.4	284	5.3	6.7	96.9	286	0.00	
1630	999.8	91.1	10	235	0.0	0.6	266	3.9	5.6	94.9	247	0.00	
1645	999.7	91.6	10	225	0.0	0.0	252	3.7	4.3	92.8	198	0.00	
1700	999.5	90.4	9	225	0.0	0.4	255	3.5	5.4	89.8	128	0.00	
1715	999.4	89.7	10	252	0.0	0.4	263	3.9	5.0	86.5	83	0.00	
1730	999.4	87.7	10	228	0.0	0.0	250	4.2	5.0	83.8	24	0.00	
1745	999.4	86.0	11	235	0.0	0.0	244	2.6	4.8	81.3	8	0.00	
1800	999.3	84.7	11	224	0.0	0.0	239	2.6	3.5	79.0	1	0.00	
MAX TEMP		MIN TEMP		MAX RH			MIN RH			MAX PRESS		MIN PRESS	
1639		71		702			2359			93		235	
92		55		26			9			1005		999.3	
MAXIMUM WINDS: 2 FOOT LEVEL				7.0 AT 125:3				24 HR PRECIP: 0					
15 FOOT LEVEL				7.0 AT 130:7				24 HR TOTAL PRECIP: 0					

Figure A-21. Met Data for 12 Nov 96

APPENDIX B. INDEX

<u>SECTION</u>	<u>PAGE</u>
TARGET PICTURES	B-2
ORDNANCE TARGET DESCRIPTIONS.....	B-4

APPENDIX B. TARGET PICTURES



a. 40mm M822 projectile (without fuze)



b. 20mm M56A3 projectile (without fuze)



c. 30mm M789 HEDP projectile (without fuze)



d. 40mm M811 projectile (without fuze)



f. 60mm M49A5 mortar (without fuze or tailfin)



g. 105mm M393A1 HEP-T projectile (without fuze)

Figure B-1. Ordnance used for UXO detection targets.



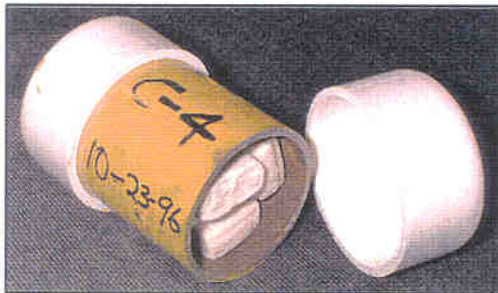
a. Simulator targets.

TOP — 6x5-inch cylinder with 1134 g (2.5 lb.) C-4.

CENTER — 8x1-inch cylinder with 200 g C-4 (200 g Long).

BOTTOM — 6x1½-inch cylinder with 200 g C-4 (200 g Short).

(NOT SHOWN — Cylinder with 100 g C-4.)

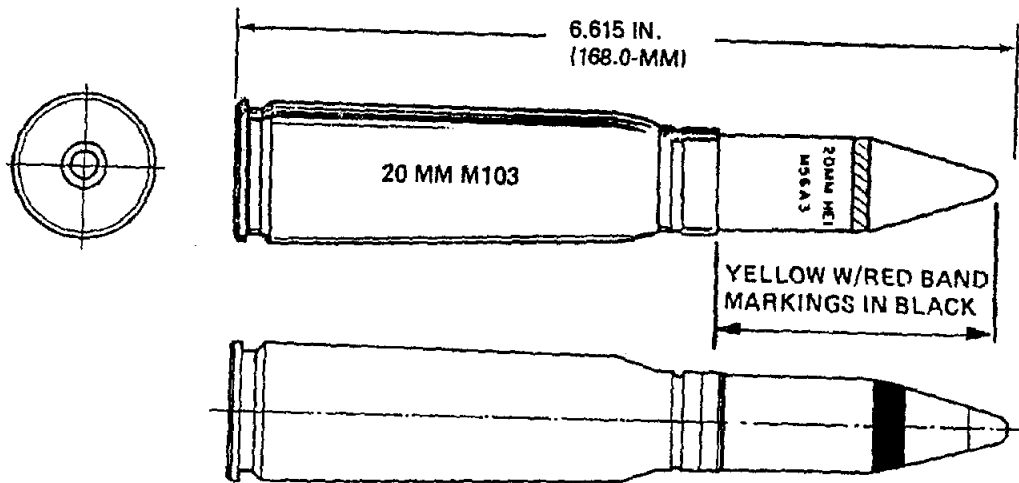


b. Simulators opened to show C-4 packing configurations.

Figure B-2. Simulators filled with C4 used for UXO detection targets.

APPENDIX B. ORDNANCE TARGET DESCRIPTIONS

CARTRIDGE, 20MM, HIGH EXPLOSIVE INCENDIARY, M56A3/M56A4



U
AR 5981

Type Classification:

M56A3: STD - LCC-B, MSR 03816015.
M56A4: STD - LCC-A, MSR 03816015.

Use:

Guns, 20mm, M39, M61, M168 and M195. The cartridge is for use against ground targets, including lightly armored vehicles, functioning with both explosive and incendiary effect. The projectile consists of a high explosive incendiary (HEI) charge and is assembled with the M505A3 fuze.

Description:

HIGH EXPLOSIVE INCENDIARY Cartridge. The projectile is thin-walled steel. A base plate is attached to the projectile to prevent ignition of the incendiary mixture by the propellant gases. A point-detonating (PD) fuze is screwed into the nose of the projectile.

Function:

The M505A3 fuze is a point-detonating, single-action fuze intended to function upon impact with the target.

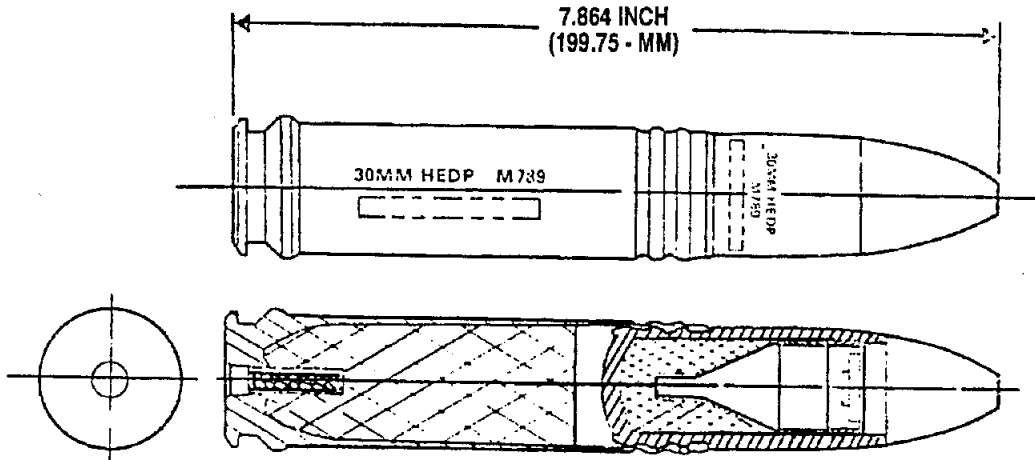
Difference Between Models:

The models differ in the method of loading the projectiles. The M56A3 has the HE mix and the incendiary mix combined in one pellet. The M56A4 has the incendiary pellet inserted into the projectile, then the HE mix pellet is added. This improves fire start capability.

Tabulated Data:

DODAC-----	1305-A890
UNO serial number -----	0321
UNO proper shipping name -----	Cartridges for weapons, with bursting charge
Weight -----	3965 gr
Length -----	6.615 in. (168 mm)
Tracer -----	NA
Primer -----	Electric, M52A3B1
Fuze -----	PD, M505A3
Explosive:	
Type -----	H761
Weight -----	165 gr
Incendiary:	
Type -----	I136
Weight -----	20 gr
Propellant:	
Type -----	WC 870 or WC 872
Weight -----	MBR (585 or 605 gr)

CARTRIDGE, 30MM, HIGH EXPLOSIVE DUAL PURPOSE, M789



U
AR 6003

Type Classification:

STD.

Use:

Automatic cannon, 30mm, M230 (U.S.).

Description:

HIGH EXPLOSIVE DUAL PURPOSE Cartridge. The cartridge consists of a steel projectile body loaded with HMX explosive and spin compensated shaped charge liner, point detonating (PD) bore safe fuze and aluminum cartridge case.

Purpose:

The projectile fuze arms in flight. Upon impact, the fuze initiates the projectile explosive filler. Detonation of the filler charge collapses the shaped charge liner resulting in the formation of an armor-piercing jet. In addition, main charge detonation produces fragmentation of the projectile body resulting in antipersonnel effects in target vicinity.

Tabulated Data:

DODAC----- 1305-B129
UNO serial number ----- 0321

UNO proper shipping

name-----	Cartridges for weapons, with bursting charge
Weight-----	5371 gr
Length-----	7.864 in. (199.75 mm)
Tracer-----	NA
Primer-----	Electric, PA520
Fuze-----	PD, M759
Explosive:	
Type-----	PBXN-5
Weight-----	340 gr
Incendiary:	
Type-----	NA
Weight-----	NA
Propellant:	
Type-----	WC 855
Weight-----	MBR, 50 gr

Performance:

Chamber pressure (avg)-----	40,000 to 44,950 psi (280-310 MPa)
Velocity-----	2640 fps (805 mps)

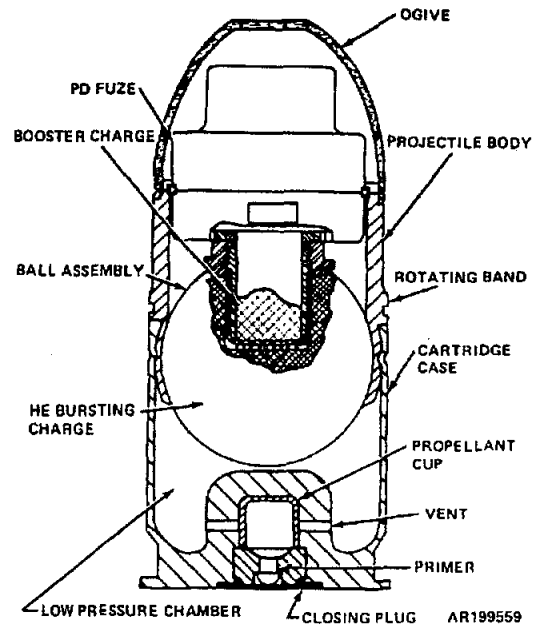
Shipping and Storage Data:

Quantity-distance class/ SCG-----	1.2E (0.4)
Storage code-----	Class V
DOT shipping class-----	A

CARTRIDGE, 40-MILLIMETER: HE, M406



AR199560



Type Classification:

Std AMCTC 9392 dtd 1972

Use:

This cartridge is a high explosive round designed to inflict personnel casualties using ground burst effect, and is fired from 40mm Grenade Launchers M79 or M203 (attached to the M16 series rifle).

Description:

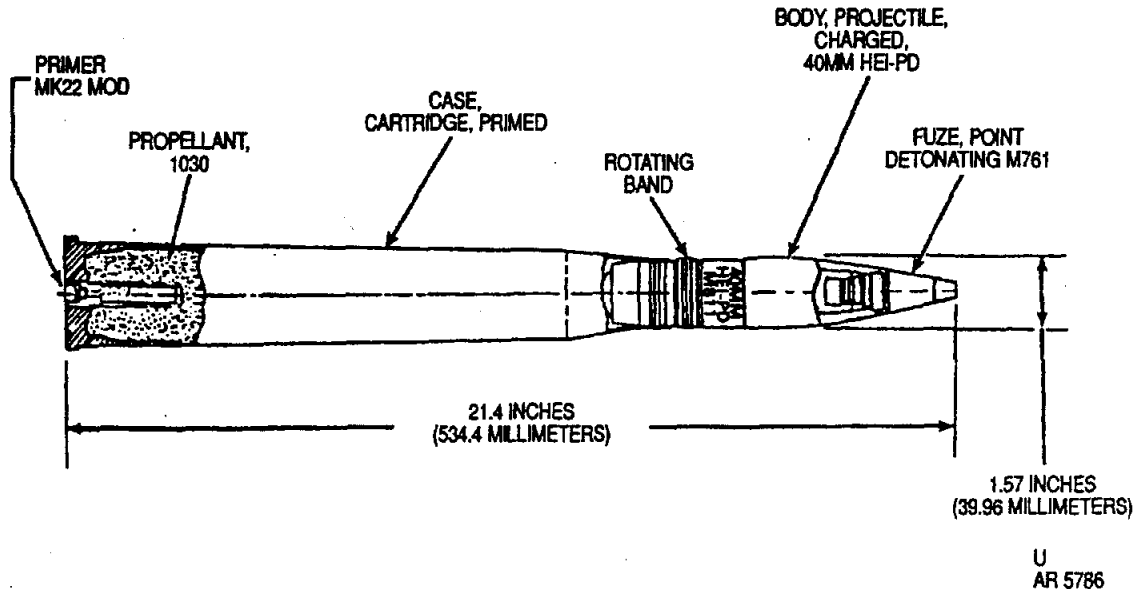
This cartridge is a fixed round of ammunition consisting of an aluminum projectile body with a rotating band and a cartridge case assembly containing the propelling charge and percussion primer. A hollow aluminum ogive is fitted to the front end of the projectile. A steel ball assembly containing a booster charge and a bursting charge is fitted in the rear end of the projectile. A PD fuze assembly is threaded into the front opening of the ball assembly. The projectile assembly is pressfitted into a cartridge case. The case is a hollow bichambered aluminum cylinder with an annealed brass propellant cup assembly fitted into the center of the cartridge base. The cup contains the propelling charge and a percussion primer in the center. It acts as a high-pressure chamber while the hollow cavity in the case, which surrounds the cup,

acts as a low-pressure chamber.

Tabulated Data:

Complete round:	
Type	HE
Weight	0.503 lb
Length	3.894 in.
Weapons used with	M79, M203 40mm grenade launchers (attached to M16 series rifle)
Projectile:	
Body material	Aluminum skirt with steel ball
Color	Olive drab w/yellow markings and yellow ogive
Filler and weight	Comp B, 32 g
Fuze	PD, M551
Propelling charge:	
Cartridge case	M118
Propellant	M9, 330 mg
Primer	M42, FED 100
Performance:	
Maximum range	400 m
Muzzle velocity	76 mps (247 fps)
Arming distance	14 to 27 m

**CARTRIDGE, 40 MILLIMETER: HEI M811 WITH POINT-DETONATING FUZE M761
(FOR SGT YORK)**



Type Classification:

STD MSR O5826003.

Use:

This cartridge is used against low flying aircraft and also ground targets. It is fired from the Sgt York 40mm gun M247.

Description:

The projectile of this cartridge is high-explosive incendiary with a point-detonating delay action fuze. The projectile is alloy steel filled with Octol (165 g). The projectile nose is threaded to receive the fuze. The cartridge case is brass and crimped rigidly to the projectile. The cartridge case contains approximately 500 grams of propellant. The base of the cartridge case contains a percussion primer consisting of a perforated tube containing black powder and a percussion element. The color of the projectile body is painted yellow with black markings and a light red band. The M761D point-detonating fuze has a delay action module, is graze sensitive, and is self-destructing.

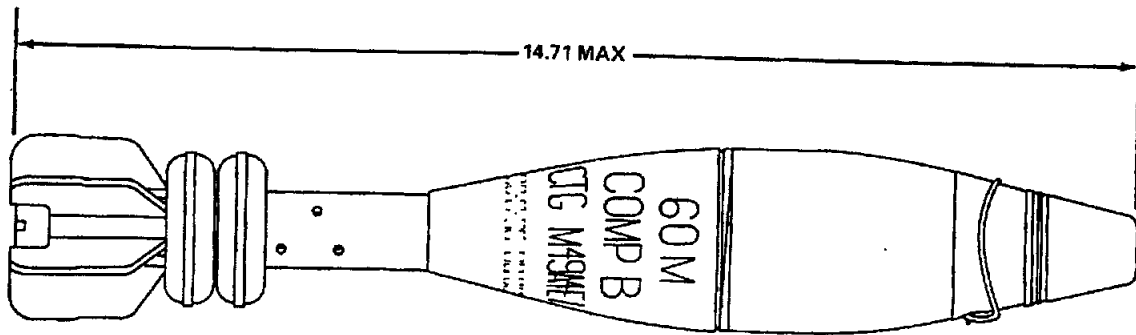
Functioning:

When the firing pin of the weapon strikes the percussion primer, the black powder ignites which, in turn, ignites the propellant. The rapidly expanding gases generated by the burning propellant propels the projectile. Upon impact, the target fuze detonates the high-explosive incendiary charge of the projectile.

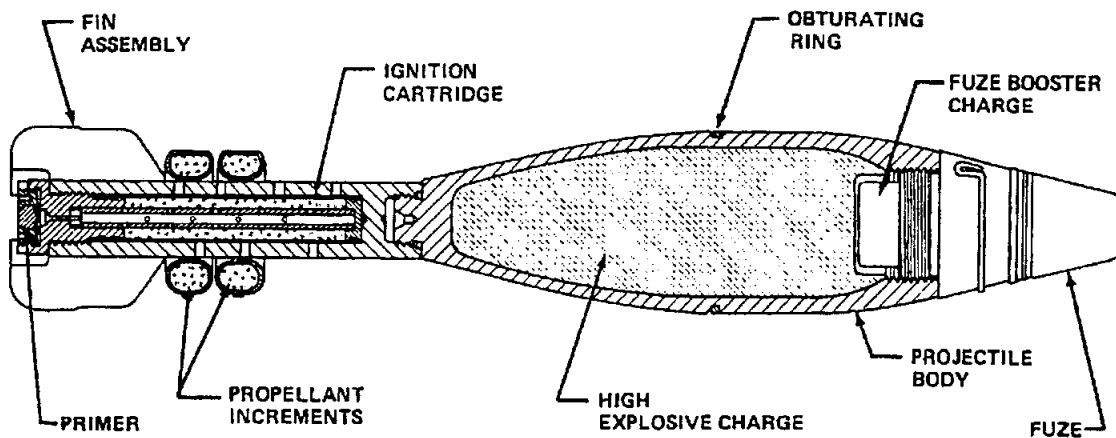
Tabulated Data:

Complete round:	
Type-----	HEI
Weight-----	5.5 lb (2490 g)
Length-----	21 in. (534 mm)
Cannon used -----	M266
Projectile:	
Body material -----	Alloy steel
Color -----	Yellow body w/black markings; 1 light red band
Filler and weight-----	Octol, 165 g
Components:	
Tracer -----	N/A
Fuze-----	M761 PD (delay)

CARTRIDGE, 60 MILLIMETER: HE, M49A5 (M49A4E1)



AR199514



AR199513

Type Classification:

Use:

This cartridge is used against personnel and light materiel, providing both fragmentation and blast effect.

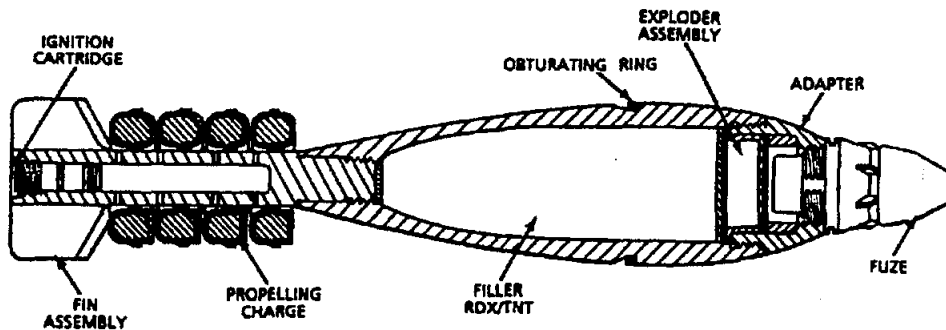
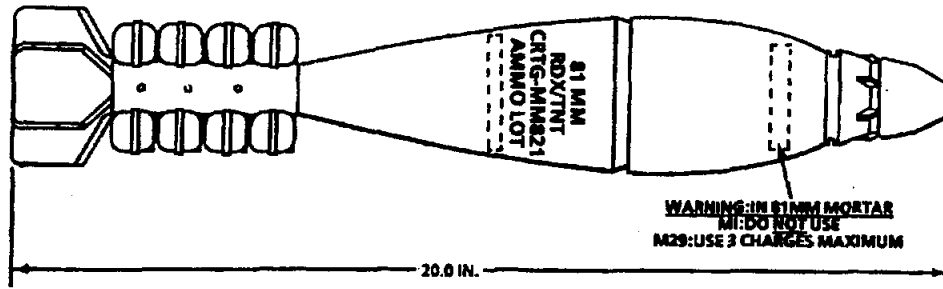
Description:

The complete round consists of a projectile body, a fin assembly, two increments of propellant charge, and an ignition cartridge with a percussion primer. The alloy steel projectile body is internally threaded at the nose to accept the fuze, externally threaded at the base to accept the fin assembly, and grooved to hold the Delrin obturating ring. The body is loaded with Composition B high explosive.

Tabulated Data:

Complete round:	
Type	HE
Weight w/fuze	3.90 lb
Length w/fuze	14.71 in.
Cannon used with	M19
Projectile:	
Body material	Alloy steel
Color	Olive drab w/yellow markings
Filler and weight	Comp B, 0.79 lb
Components:	
Ignition cartridge	M702
Propellant charge	M204
Percussion primer	M35
Fin assembly	M25
Fuze	PD, M935

CARTRIDGE, 81 MILLIMETER: HE, M821



ARD 2536

Type Classification:

Std DA Ltr 7/84.

Use:

This cartridge is a high explosive round developed for use in the M252 improved 81mm mortar system. It is intended for use against personnel and light materiel targets.

Description:

The complete round consists of a fuze, propellant charge, fin assembly, ignition cartridge, and shell body. The shell body, made of Ductile Cast Iron, is loaded with a RDX/TNT filler. The ignition cartridge has a percussion primer and is assembled to the end of the fin assembly. The propelling charge is contained in four horse-shoe felt-fiber containers and assembled around the fin assembly shaft.

Functioning:

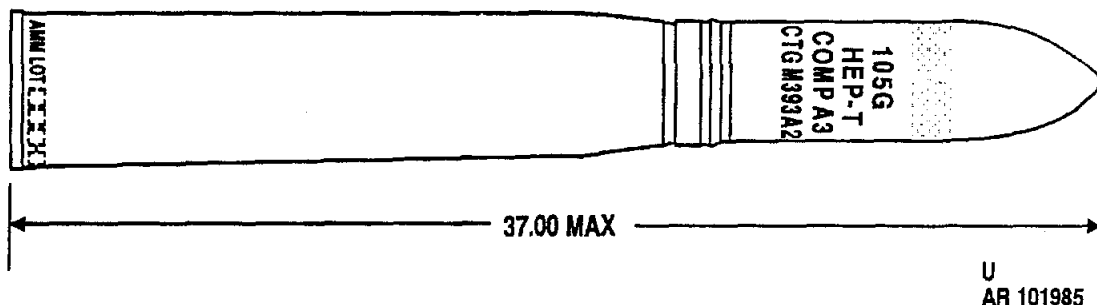
When the cartridge is dropped down the mortar tube, the firing pin at the bottom of the tube initiates the percussion primer and charge in the ignition cartridge. The charge in the ignition cartridge flashes through the holes in the

shaft of the fin assembly and ignites the propelling charge. The gases from the burning propellant expand and propel the cartridge out of the mortar tube. The fuze functions proximity, near surface, on impact, or delay depending on the fuze setting and detonates the projectile.

Tabulated Data:

Complete Round:	
Type	HE
Weight	8.96 lb
Length	20.1 in.
Assembly drawing number ---	9354443
Projectile:	
Body material	Ductile cast iron
Color	Olive drab w/yellow markings
Filler and weight	RDX/TNT, 1.6 lb
Components:	
Ignition cartridge	L33A1
Propellant charge MK5	4 increments (M205 propellant containers w/UK ball propellant)

CARTRIDGE, 105 MILLIMETER: HEP-T, M393A2 AND M393A1



Type Classification:

STD AMCTC 3325 dtd 1965.

Use:

This cartridge is designed for use against armored targets, light materiel, and personnel.

Description:

The cartridge carries a payload of 6.6 pounds of Composition A3, a high-explosive plastic composition. The projectile is a thin-walled cylinder with a relatively short ogive and a flat base. The base of the projectile is fitted with a base-detonating (BD) fuze and a tracer. The projectile is assembled to a brass (or steel) cartridge case fitted with an electric primer and containing a bagged propelling charge.

Functioning:

When the weapon is fired, the electrically initiated primer ignites the propelling charge. The burning propellant ignites the tracer and creates gases which force the projectile out of the gun tube and propels it to the target. Upon impact, the fuze functions initiating the explosive filler.

Difference Between Models:

The M393A1 differs from the M393A2 in that the M393A1 employs the BD fuze M534 while the M392A2 employs the BD fuze M578. The filler weight on the M393A1 is 0.3 pounds less.

Tabulated Data:

Complete round:	
Type-----	HEP-T
Weight-----	45 lb
Length-----	37 in.
Projectile:	
Filler-----	M68
Explosive (393A2)-----	Comp A, 6.6 lb
Explosive (393A1)-----	Comp A, 6.3 lb
Body materiel-----	Steel
Color-----	Olive drab w/ yellow markings and black band
Components:	
Cartridge case-----	M150B1 (steel); M150 (brass)
Propellant-----	M1, 5.9 lb
Primer (electric)-----	M86
Tracer-----	M12
Performance:	
Maximum range-----	9510 m (10,400 yd)
Muzzle velocity-----	2400 m (731.5 mps)
Temperature limits:	
Firing:	
Lower limit-----	-40°F
Upper limit-----	+125°F
Storage:	
Lower limit-----	-80°F (for period not more than 3 days)
Upper limit-----	+160°F (for period not more than 4 hr/day)

APPENDIX C. RADIO FREQUENCY USAGE

Data Communications #1 (Control of Robotech Vehicle)

<u>PARAMETER</u>	<u>TRANSMITTER</u>	<u>RECEIVER</u>
Nomenclature	RF Data Link	Same
Model	CCL901 DP	Same
Manufacturer	COMRAD	Same
Coordinates		
Site Elevation	0m	0m
Frequency Range	905-927 MHz	Same
Frequency Requested	905.150 MHz	905.150 MHz
Frequency Requested	905.350 MHz	905.350 MHz
Frequency Band		
Pulse Repetition Rate	Various	Various
Pulse Duration	Various	Various
RF Power Output	10 mW	10 mW
Type of Emissions	FSK	FSK
Emission Bandwidth	40 KHz	40 KHz
Antenna Type	Dipole	Directional
Antenna Gain	5 dB	5 dB
Antenna Polarization	Omni-directional	Directional
Antenna Azimuth		
Antenna Feed Point Elevation		
Date Frequency Required	28 Oct through 15 Nov	28 Oct through 15 Nov
Proposed Location	YPG, MCD, Kofa Range	YPG, MCD, Kofa Range

Data Communications #2 (Vehicle Computer to Control Station)

<u>PARAMETER</u>	<u>TRANSMITTER</u>	<u>RECEIVER</u>
Nomenclature	RF Data Link	Same
Model	RFM96	Same
Manufacturer	Pacific Crest	Same
Coordinates		
Site Elevation	0m	0m
Frequency Range	415-430 MHz	Same
Frequency Requested		
Frequency Band		
Pulse Repetition Rate	Various	Various
Pulse Duration	Various	Various
RF Power Output	2 W	2 W
Type of Emissions	FSK	FSK
Emission Bandwidth	20 KHz	20 KHz
Antenna Type	Dipole	Directional
Antenna Gain	5 dB	5 dB
Antenna Polarization	Omni-directional	Directional
Antenna Azimuth		
Antenna Feed Point Elevation		
Date Frequency Required	28 Oct through 15 Nov	28 Oct through 15 Nov
Proposed Location	YPG, MCD, Kofa Range	YPG, MCD, Kofa Range

Data Communications #3 (GPS Differential Corrections)

<u>PARAMETER</u>	<u>TRANSMITTER</u>	<u>RECEIVER</u>
Nomenclature	RF Data Link	Same
Model	RFM96	Same
Manufacturer	Pacific Crest	Same
Coordinates		
Site Elevation	0m	0m
Frequency Range	415-430 MHz	Same
Frequency Requested	425 MHz	425 MHz
Frequency Band		
Pulse Repetition Rate	Various	Various
Pulse Duration	Various	Various
RF Power Output	2 W	2 W
Type of Emissions	FSK	FSK
Emission Bandwidth	20 KHz	20 KHz
Antenna Type	Dipole	Directional
Antenna Gain	5 dB	5 dB
Antenna Polarization	Omni-directional	Directional
Antenna Azimuth		
Antenna Feed Point Elevation		
Date Frequency Required	28 Oct through 15 Nov	28 Oct through 15 Nov
Proposed Location	YPG, MCD, Kofa Range	YPG, MCD, Kofa Range

Video Transmitter

<u>PARAMETER</u>	<u>TRANSMITTER</u>	<u>RECEIVER</u>
Nomenclature	Video	Same
Model	T1821/1W	R1821
Manufacturer	HDS	Same
Coordinates		
Site Elevation	0m	0m
Frequency Range		
Frequency Requested	1720 MHz	
Frequency Band		
Pulse Repetition Rate		
Pulse Duration		
RF Power Output	1 W	
Type of Emissions	FM	
Emission Bandwidth	6 KHz	
Antenna Type		
Antenna Gain		
Antenna Polarization	Omni-directional	Directional
Antenna Azimuth		
Antenna Feed Point Elevation		
Date Frequency Required	28 Oct through 15 Nov	28 Oct through 15 Nov
Proposed Location	YPG, MCD, Kofa Range	YPG, MCD, Kofa Range

APPENDIX D. ABBREVIATIONS

CCD	—	Closed Circuit Display
CCV	—	Closed Circuit Video
ESTCP	—	Environmental Security Technology Certification Program
FAR	—	false alarm rate
g	—	gram
GPS	—	Global Positioning System
HE	—	high explosive
lb	—	pound
m	—	meter
m ²	—	square meters
MD	—	metal detector
mm	—	millimeter
PD	—	probability of detection
PFA	—	probability of false alarm
RF	—	radio frequency
SAIC	—	Science Applications International Corporation
TNA	—	thermal neutron activation
UXO	—	unexploded ordnance
YPG	—	U.S. Army Yuma Proving Ground

APPENDIX E. DISTRIBUTION LIST

ADDRESSEE

NO. COPIES

~~COMMANDER~~

~~US ARMY BELVOIR RESEARCH AND DEVELOPMENT CENTER~~

~~NIGHT VISION ELECTRONIC SENSORS DIRECTORATE~~

~~ATTN AMSEL-RD-NV-CD-MD~~

~~FT BELVOIR, VA 22060-5876~~

10221 Burkhead Road Ste. 430

4

SCIENCE APPLICATIONS INTERNATIONAL CORPORATION

ATTN MR G BORGONVI

4161 CAMPUS POINT COURT

SAN DIEGO, CA 92121

2

COMMANDER

US ARMY YUMA PROVING GROUND

ATTN STEYP-MT-EW

ATTN STEYP-MT-A-RL

ATTN STEYP-MT-A-QR

YUMA, AZ 85365

2

1

1

Dr. Jeffery Marjusee

3

ODUSD (ES) / PI

3400 Defense Pentagon

Room 3D768

Washington, DC 20301-3400